Factor XIII-A and Transglutaminase 2 – Novel regulators of adipocyte differentiation and energy metabolism

Vamsee Dhar Myneni

Faculty of Dentistry
McGill University, Montreal, Canada
August, 2015

A thesis submitted to McGill University in partial fulfillment of the requirements of the degree of Doctor of Philosophy in Craniofacial Health Sciences

Table of Contents

ABSTRACT

Obesity is a growing health problem worldwide, and is associated with the development of insulin resistance and type 2 diabetes. Factor XIII-A (FXIII-A) transglutaminase – a protein crosslinking enzyme - was recently identified as a top novel obesity causative gene in white adipose tissue of monozygotic twin pairs discordant for obesity. However, the role of FXIII-A or other transglutaminase enzyme in obesity or function of adipose tissue is not known. The studies in this thesis investigated the role of two transglutaminase family members in adipocyte differentiation and obesity. The work presented here demonstrate that white adipose tissue expresses only FXIII-A and transglutaminase 2 (TG2) of the transglutaminase family. Cell culture data from 3T3-L1 preadipocyte cell line and mouse embryonic fibroblasts showed that FXIII-A is a negative regulator of adipogenesis. In cell cultures, FXIII-A promoted the assembly of plasma fibronectin into preadipocyte extracellular matrix; the assembled plasma fibronectin matrix promoted preadipocyte proliferation, and potentiated the pro-proliferative effects of insulin while suppressing the pro-differentiating insulin signalling. TG2 was also demonstrated as a negative regulator of adipocyte differentiation, by using TG2 deficient mouse embryonic fibroblasts. TG2 inhibited adipogenesis by regulating Pref-1/Dlk1 protein levels, activating Wnt/β-catenin signalling and ROCK kinase activity. Finally, this thesis reports on the metabolic phenotype of FXIII-A knockout mice. FXIII-A deletion protected the mice from developing high-fat diet induced insulin resistance. Improved insulin sensitivity in these mice was seen in epididymal and inguinal adipose tissue, and muscle. Increased insulin sensitivity in obese FXIII-A deficient mice were associated with healthier adipose tissue characterized by reduced macrophage infiltration, increased adipocyte size, and reduced collagen levels. In summary, the finding of this thesis demonstrates that both FXIII-A and TG2 are inhibitors of adipocyte differentiation, and that FXIII-A is an important regulator of insulin sensitivity and energy metabolism. Therapeutic approaches aimed at modulating FXIII-A and TG2 levels or activity in adipose tissue may have great potential in the treatment of obesity and its co-morbidities.

RÉSUME

L'obésité est un problème de santé croissant dans le monde entier associé au développement d'une résistance à l'insuline et au diabète de type 2. Le facteur XIII-A (FXIII-A) transglutaminase - une enzyme de la réticulation les protéines - a récemment été identifié comme un gène causal potentiel de l'obésité en tissu adipeux blanc des paires de jumeaux monozygotes discordants pour l'obésité. Cependant, le rôle de FXIII-A ou de toute autre enzyme transglutaminase dans l'obésité ou la fonction du tissu adipeux ne sont pas connues. Dans cette thèse des étudiés du rôle de deux membres de la famille de la transglutaminase dans la différenciation adipocytaire et l'obésité ont été menées. Il a été démontré que le tissu adipeux blanc exprime seulement le facteur FXIII-A et la transglutaminase 2 (TG2) de la famille des transglutaminases. Les données de culture cellulaire utilisant la lignée cellulaire préadipocytaire 3T3-L1 et de fibroblastes embryonnaires de souris ont montré que FXIII-A est un régulateur négatif de l'adipogenèse. Dans les cultures cellulaires FXIII-A promut l'ensemble de la fibronectine de plasma dans la matrice extracellulaire préadipocyte; la matrice de fibronectine plasmatique assemblé promut la prolifération des préadipocytes et potentialise les effets pro-prolifératifs d'insuline tout en supprimant la signalisation de l'insuline pro-différenciation. En utilisant de fibroblastes embryonnaires de souris déficientes en TG2, il a été démontré que TG2 peut aussi agir comme un régulateur négatif de la différenciation des adipocytes. TG2 inhibe l'adipogenèse par la régulation des niveaux Pref-1 / DLK1, l'activation de la signalisation Wnt / β-caténine et l'activité de la kinase ROCK. Finalement, cette thèse porte sur le phénotype métabolique des souris complètement dépourvu de FXIII-A. La suppression de FXIII-A protège les souris contre le développent d'une résistance à l'insuline induit par une alimentation en matières grasses. Une sensibilité accrue à l'insuline a été observée chez ces souris dans le tissue adipeux épididyme et inguinal, et dans le muscle. La sensibilité accrue à l'insuline dans des souris obeses déficientes en FXIII a été associé à un tissu adipeux plus sain caractérisé une infiltration réduite des macrophages, l'augmentation de la taille des adipocytes, et la diminution des niveaux de collagène. En résumé, les résultats obtenus dans cette thèse démontrent que les deux enzymes FXIII-A et TG2 sont des

modulateurs de la fonction des adipocytes, et que FXIII-A est un régulateur important de la sensibilité à l'insuline et du métabolisme énergétique. Les approches thérapeutiques visant à moduler les taux TG2 et FXIII-A ou l'activité dans le tissu adipeux peuvent avoir un grand potentiel dans le traitement de l'obésité et ses comorbidités.

ACKNOWLEDGEMENTS

I would like to thank my supervisor, Dr. Mari Kaartinen, for being a wonderful mentor. I thank you for providing me your support and giving me opportunities and freedom to independently design, perform and problem-solve my projects. These learning experiences were truly rewarding, and allowed me not only to grow as a critical thinker and scientist, but also as a person and a lifelong learner.

I also thank my co-supervisor, Dr. Belinda Nicolau, and my committee members, Dr. Monzur Murshed, Dr. Dieter P. Reinhardt, Dr. Marie-Claude Rousseau, for their support and guidance.

I thank all the members of Kaartinen lab, both past and present, for their help and support. I would also like to thank Dr. Marc McKee and Dr. Elaine Davis for sharing their laboratory equipment.

I also wish to thank the CIHR Systems Biology Training Program for giving me funding and opportunities to learn cutting edge technologies through workshops and roundtable discussions.

I would like to thank particularly Dr. Valentin an Nelea for the French translation of this thesis abstract.

Finally, I wish to thank my mom and dad for their guidance, sacrifices, endless love and patience. I would like to express my deepest appreciation to my sister who have always been by my side. I dedicate this thesis to my parents.

CONTRIBUTION OF AUTHORS

This thesis includes published paper, paper in press and in preparation manuscript of which the candidate is the primary author. Contributions of all authors are listed as below:

1. **Myneni VD**, Hitomi K, Kaartinen MT. Factor XIII-A transglutaminase acts as a switch between preadipocyte proliferation and differentiation**. Blood. 2014; 124(8):1344-53.**
    - Myneni VD designed and conducted the experiments, analyzed the data and drafted the manuscript.
    - Hitomi K contributed peptide reagents for the study.
    - Kaartinen MT supervised the study, analyzed the data and edited the manuscript.

2. **Myneni VD**, Melino G, Kaartinen MT. Transglutaminase 2-A novel inhibitor of adipogenesis. **Cell Death & Disease.** ***In press.***
    - Myneni VD designed and conducted the experiments, analyzed the data and drafted the manuscript.
    - Melino G provided TG2 knockout mice for the study.
    - Kaartinen MT supervised the study, analyzed the data and edited the manuscript.

3. **Myneni VD** and Kaartinen MT. FXIII-A knockout mice are resistant to high-fat diet induced insulin resistance. ***In preparation.***
    - Myneni VD designed and conducted the experiments, analyzed the data and drafted the manuscript.
    - Kaartinen MT supervised the study, analyzed the data and edited the manuscript.

LIST OF FIGURES

LIST OF ABBREVIATIONS

ASCs	Adipose-derived stem cells
Asp	Aspartate
AT	Adipose tissue
BAT	Brown adipose tissue
C/EBPα	CCAAT/enhancer-binding protein alpha
CatK	Cathepsin K
CatL	Cathepsin L
CatS	Cathepsin S
cFN	Cellular fibronectin
cFXIII-A	Cellular FXIII-A
CLSs	Crown-like structures
Cys	Cysteine
DFAT	Dedifferentiated fat cells
DIO	Diet-induced obesity model
DOC	Deoxycholate detergent
DM	Diabetes Mellitus
ECM	Extracellular matrix
EDA-FN	Extra domains A fibronectin
EDB-FN	Extra domains B fibroncetin
ERK	Extracellular signal-regulated kinase
ES	Embryonic stem cells
FAK	Focal adhesion kinase
FFA	Free fatty acids
FN	Fibronectin
HFD	High-fat diet
His	Histidine
IBMX	3-isobutyl-1-methylxanthine
IL-6	Interleukin 6
IR	Insulin receptor

IRS	Insulin-receptor substrate
LRP5	Lipoprotein receptor related protein 5
MAPK	Mitogen-activated protein kinases
MCP-1	Monocyte chemoattractant protein-1
MEFs	Mouse embryonic fibroblasts
MMPs	Matrix metalloproteinases
MSC	Mesenchymal stem cells
NH_3	Ammonia
PAI-1	Plasminogen activator inhibitor-1
pFN	Plasma fibronectin
PI3K	Phosphatidylinositol-3 kinase
PKB	Protein kinase B
PPARγ	Peroxisome proliferator-activated receptor gamma
SNPs	Single-nucleotide polymorphisms
SVF	Stromal vascular fraction
sWAT	Subcutaneous white adipose tissue
T1DM	Type 1 diabetes mellitus
T2DM	Type 2 diabetes mellitus
TAZ	Transcriptional co-activator with PDZ-binding motif
TCF/LEF	T cell factor/lymphoid enhancing factor
TGs	Transglutaminase
TIMPs	Tissue inhibitors of MMPs
Trp	Tryptophan
UCP1	Uncoupling protein 1
vWAT	Visceral white adipose tissue
WAT	White adipose tissue
YAP	Yes-associated protein

CHAPTER 1 – INTRODUCTION

1.1 Energy balance

The survival of an organism relies on a constant supply of energy. Energy balance or energy homeostasis refers to the physiological system that maintains consistent energy levels by responding to changes in nutrient availability or the use of energy changes. The basic components of energy balance include energy intake, energy expenditure, and energy storage. Energy balance is assessed by assessing body weight or body composition. Energy balance in humans and other mammals follows the law of thermodynamics. The amount of energy stored is determined by the balance between energy intake and energy expenditure.

There are three states of energy balance:
Positive energy balance: when energy intake exceeds energy expenditure, leading to increased energy stores (equivalent to body weight). The consequence of a positive energy balance is increased body mass.

Energy intake > energy expenditure ⇒ weight gain

Negative energy balance: when energy expenditure exceeds energy intake, energy stores are decreased and the consequence is a decrease in body mass.

Energy intake < energy expenditure ⇒ weight loss

Normal energy balance: when energy intake is equal to energy expenditure and the consequence is a stable body mass (Galgani and Ravussin, 2008; Hill et al., 2012; Webber, 2003).

Humans take in energy in the form of carbohydrates, proteins, and fat (Galgani and Ravussin, 2008; Hill et al., 2012). Carbohydrates are the main source of dietary energy. Dietary carbohydrates are converted to glucose, which can be used as energy or stored in the liver as glycogen, or as triglycerides in adipose tissue (AT). The storage of glycogen in liver is very limited; once the liver reaches its limit to store glycogen, excess glucose is converted to triglycerides for storage in AT (Acheson et al., 1988). Proteins constitute about 15% of dietary energy. Amino acids from the proteins are stored as

structural proteins, enzymes, and other cellular proteins. The excess amino acids are converted to glucose via gluconeogenesis, and subsequently used as energy or stored in the form of glycogen (via glycogenesis), or triglycerides (via lipogenesis). The intake of fat is less compared to other nutrients, but fat stores are large. Compared to proteins, fat intake is less than 1% of total fat stores. Fat stores represent the energy buffer of the body, due to the body's limited ability to store carbohydrates and protein as an energy source for long-term use. Of the body's energy, 90% is stored as fat in AT. In other words, fat is the only nutrient which can cause energy imbalance, and the other nutrients have an indirect influence on the energy balance by modulating fat deposition in AT (Galgani and Ravussin, 2008; Hill et al., 2012).

Energy balance is maintained by multiple systems, each sensing nutrition and energy levels, and responding to changes in nutrition and energy levels by changing the fuel availability. Energy balance involves central and peripheral organs. The central organ is the brain; the peripheral organs are the stomach and intestine, liver, muscle, AT, and pancreas. Communication among these organs is essential in maintaining the homeostasis of whole-body energy metabolism (**Figure 1**) (Badman and Flier, 2005).

1.1.1 Central organ

The brain plays a central role in energy intake by regulating eating behavior (appetite) and energy expenditure.The brain collects information on peripheral metabolic status and sends signals that regulate metabolism to the periphery. The hypothalamus in the brain is the primary site for receiving information regarding energy stores and changes in energy availability. The signals from peripheral tissue are sent through nerve signals, nutritional factors (glucose, amino acids, and fatty acids) and hormonal factors (insulin and leptin) (Badman and Flier, 2005; Spiegelman and Flier, 2001; Yamada and Katagiri, 2007).

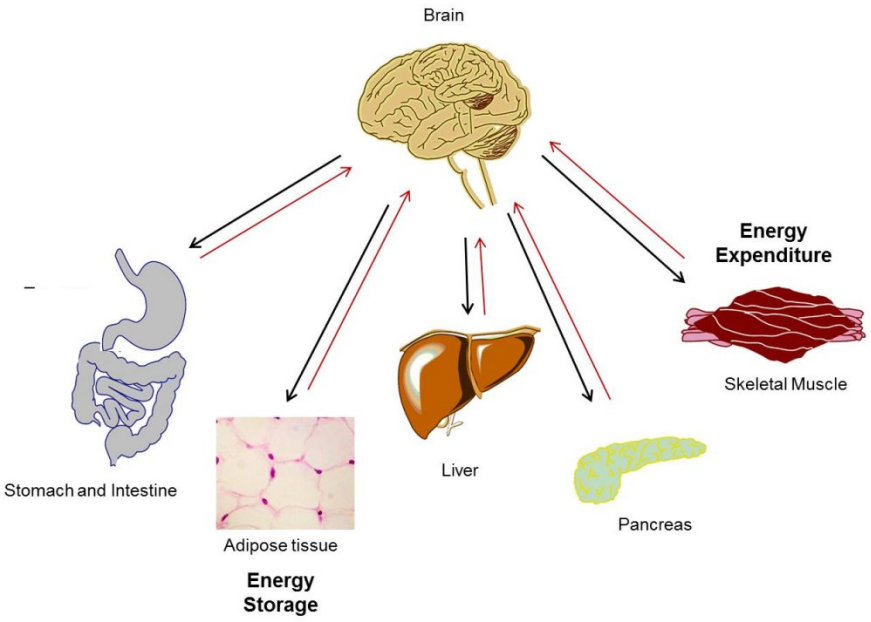

Figure 1: Organs involved in long-term energy balance.
(Adapted from Badman et al (Badman and Flier, 2005))

1.1.2 Peripheral organs

The stomach and intestine are primary sites for food digestion and absorption. The liver plays a major role in glucose, fatty acid and amino acid metabolism. The liver is also the site for gluconeogenesis and is responsible for two-thirds of blood glucose uptake after feeding. Muscle stores three-fourths of glycogen and increases energy expenditure during physical activity.

AT tissue regulates energy metabolism by carefully regulating free fatty acids (FFA) storage and release. In a high caloric state, AT stores circulating FFA in the form of triglycerides. During fasting, FFAs are released for uptake by the liver and muscle (Sethi and Vidal-Puig, 2007; Zimmermann et al., 2009).

The pancreas secretes insulin from islet β-cells, in response to increased circulating glucose levels. Insulin regulates glucose metabolism by stimulating glucose uptake by muscle and adipose tissue and by suppressing glucose production by the liver. Insulin also regulates protein synthesis, FFA uptake and synthesis and inhibits lipolysis in

adipocytes. (Badman and Flier, 2005; Galgani and Ravussin, 2008; Yamada and Katagiri, 2007; Yamada et al., 2008).

1.1.3 Diabetes

Diabetes mellitus (DM) is a broad term used for a group of metabolic disorders characterized by prolonged hyperglycemia, caused by defects in insulin secretion and/or insulin function (American Diabetes, 2010). If insulin is not produced by the β cells in sufficient quantities, or if the body does not respond to the circulating insulin, blood glucose levels increases leading to prediabetes and/or diabetes. Over time, continuous high blood glucose levels cause damage to number of tissues including nerves and blood vessels which leads to complication such as heart disease, stroke, kidney disease, blindness, dental disease, and amputations (American Diabetes, 2010; Kahn et al., 2014).

DM is classified into two different types of diabetes.
Type I (T1DM) accounts for approximately 5% of all diabetes worldwide. T1DM is an autoimmune disorder, where the body's immune system attacks and destroys the β cells. The onset of T1DM usually occurs in childhood and early adulthood (<35 years) and thus T1DM is also known as juvenile diabetes. Genetic and environmental factors contribute to the susceptibility of this diabetes (Atkinson, 2012; van Belle et al., 2011).

Type 2 (T2DM) accounts for approximately 90% of all diagnosed diabetes worldwide. T2DM is characterized by an insufficient synthesis and secretion of insulin, which is secondary to insulin resistance. The incidence of T2DM increases with age, and is normally diagnosed after the fourth decade of life. T2DM is divided into two subgroups, diabetes with obesity and without obesity. In *non-obese T2DM* there is a deficiency in insulin production and release, and also some insulin resistance is observed at the post receptor levels. In *obese T2DM* there is insulin resistance due to alterations in cell insulin receptors, and this is associated with the distribution of abdominal fat (American Diabetes, 2010; Kahn, 1994; Kahn et al., 2014).

1.1.3.1 Insulin signalling pathway

Insulin functions by binding to the insulin receptor (IR) on the cell surface. IR are present in all cells, but the highest concentration of IR is present in cells of major metabolic tissue, such as hepatocytes in the liver, adipocytes in adipose tissue, and myocytes in muscle. IR consist of two α-subunits and two β-subunits; α- and β-subunits are linked to each other by disulphide bonds. α-subunits located outside the cell and β-subunits are transmembrane. Insulin binds to α-subunits, which induces the autophosphorlyation of β-subunits. Upon activation, the receptor phosphorylates several proteins, including insulin receptor substrate proteins (IRS-1 and IRS-2), c-Cbl and Shc. IRS-1/2 regulates the metabolic signalling of insulin and Shc regulates mitogenic signalling of insulin (**Figure 2**).

1.1.3.1.1 Insulin metabolic signalling

Metabolic signaling is predominant in adipocytes, metabolic signalling regulates GLUT4 translocation to the plasma membrane to regulate glucose uptake and protein synthesis (Bryant et al., 2002; Carel et al., 1996). The Phosphorylated IRS-1 activates phosphatidylinositol-3 kinase (PI3K). PI3K in turn activates Akt/PKB and atypical protein kinase (PKC), specifically PKCζ. Akt and PKCζ induce the translocation of intracellular GLUT4 to the plasma membrane (Giorgino et al., 2005; Laviola et al., 2006; Taniguchi et al., 2006; Tsakiridis et al., 1999).

In addition to PI3K signalling, the c-Cbl–CAP pathway also plays a role in insulin stimulated GLUT4 translocation. Activated β-subunits also phosphorylate Cbl. Phosphorylated Cbl associates with CAP, forming a CAP-Cbl complex, which dissociates from IR. This complex along with Crk activates G-protein-TC10. Activated TC10 then regulates GLUT4 translocation to the plasma membrane (Baumann et al., 2000; Chiang et al., 2001; Giorgino et al., 2005). In summary, Akt and PKC essentially control the GLUT 4 translocation to the plasma membrane, which is validated in muscle and adipose tissue. In adipocytes Cbl–CAP pathway has an additional contribution,which requires further studies (Giorgino et al., 2005).

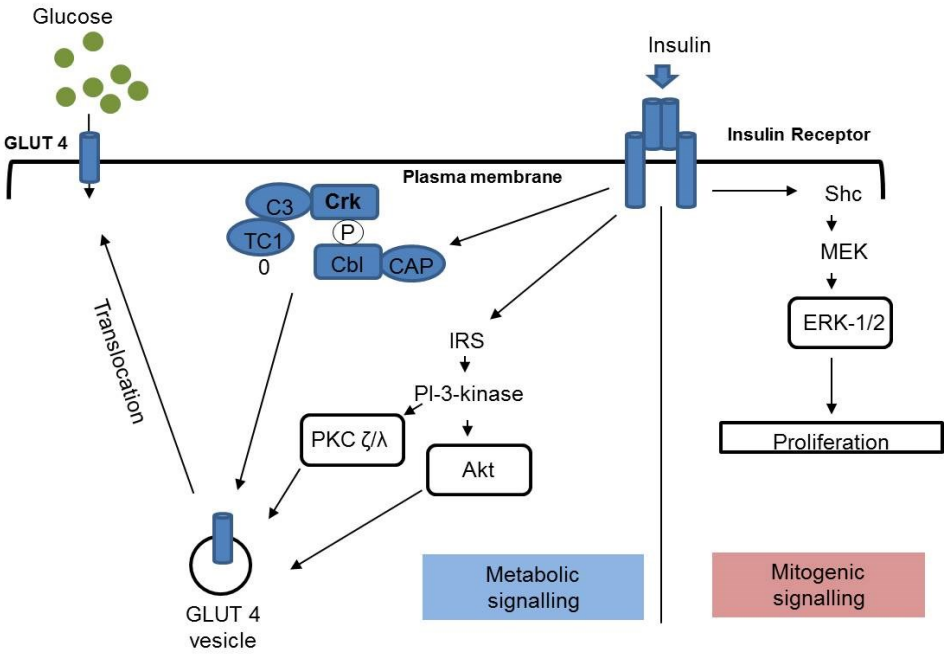

Figure 2: Insulin signalling - Metabolic and mitogenic pathways.

Illustration of key signalling events activated by insulin binding to insulin receptor, leading to metabolic and mitogenic pathway activation (Adapted from (Giorgino et al., 2005) and (Tsakiridis et al., 1999)).

1.1.3.1.2 Insulin mitogenic signalling

Mitogenic signalling is predominant in preadipocytes and in AT precursor cells. Mitogenic signalling is involved in cell proliferation, and the differentiation of cells into adipocytes, which increases the storage capacity of triglycerides in AT. In adipocytes, mitogenic signalling controls gene transcription. Phosphorylated β-subunits recruit Shc protein to phosphorylate Shc, and phosphorylated Shc interacts with Grb2 to recruit Sos (Son of sevenless). Grb2/Sos activates Ras leading to activation of Raf, MEK and ERK. Activated ERK1/2 then translocates to the nucleus to initiate a transcriptional program leading to cell proliferation and differentiation (Carel et al., 1996; Giorgino et al., 2005; Taniguchi et al., 2006).

1.1.4 Obesity

A chronic imbalance in energy homeostasis leads to obesity (Galgani and Ravussin, 2008). Obesity is a global epidemic and it is estimated that by yeas 2030, 1.12 billion individuals will be obese worldwide. Obesity is a significant health problem in developed and developing countries, and the WHO has identified obesity as one of the major emerging chronic diseases of the 21st century (Kelly et al., 2008). In Canada, the prevalence of obesity has increased by 200% since 1985. Currently, one in four adult Canadians is obese, adding up to approximately 6.3 million people, and it is predicted that by 2019, 21% of the Canadian adult population will be obese. The yearly economic burden of obesity is estimated to around $7.1billion (Janz; Twells et al., 2014).

Obesity is defined as an excessive accumulation of fat in AT, to the extent that it affects the overall health of an individual. Body fat in health surveys is measured by using body mass index (BMI)-body weight of a person is divided by the square of a person's height, measured in kg/m^2 and BMI is strongly correlated to the fatness in adults. WHO classifies individuals based on BMI of 18-24.99 (normal), BMI of 25 or more (overweight) and BMI of 30 or more (obese). BMI in the obese range can be subdivided into three classes: Class I – BMI of 30.0 to 34.9; Class II – BMI of 35.0 to 39.9; and Class III – BMI of 40.0 or more . In obesity, fat mass can exceed up to 22% in males, and 32% in females to that of total bodyweight (Cinti, 2002).

Obesity is a major risk factor in developing type 2 diabetes, cardiovascular diseases, hypertension, respiratory diseases, several types of cancers, and osteoarthritis. It also leads to reduced life expectancy (Despres and Lemieux, 2006; Spalding et al., 2008). Obesity is a well-established risk factor for the development of insulin resistance and type 2 diabetes. Insulin resistance is prediabetic condition, characterized by the failure of the liver to suppress glucose production, and decrease in glucose uptake by muscle and AT in response to insulin. Insulin resistance progresses to type 2 diabetes when the increased insulin secretion is not sufficient to prevent hyperglycemia (Borst; Pittas et al., 2004). Association of insulin resistance with visceral obesity, hypertension, dyslipidemia and cardiovascular diseases are termed 'metabolic syndrome' (Despres and Lemieux,

2006). Insulin resistance is the central feature of metabolic syndrome. The WHO definition of metabolic syndrome mandates the presence of insulin resistance. Even if all other criteria were met, the absence of insulin resistance would be considered as not having a metabolic syndrome. To better understand the events in metabolic syndrome, various mouse models are used of which the most widely used is the diet-induced obesity model (Huang, 2009).

1.1.4.1 Diet-induced obesity in mice

The diet-induced obesity model (DIO) are suitable for studying the underlying mechanisms in the development of obesity, insulin resistance and type 2 diabetes, as they show same changes as seen in human obesity. The DIO are useful in understanding cellular events in the excess accumulation of fat and/or excessive dietary fat intake (Muhlhausler, 2009). In this model, healthy non-obese mice are provided with ad libitum access to a high-fat diet (HFD), and mice are maintained on this diet for 8-12 weeks. Feeding a HFD induces increased body weight and mice become obese. Body weight gain during the feeding period is gradual. Fasting blood glucose levels are mild to moderately elevated, and usually accompanied by an increase in fasting plasma insulin levels. The mice also develop glucose intolerance and insulin resistance (Buettner et al., 2007; Surwit et al., 1988).

1.1.5 Therapy for obesity

Currently therapy for obesity can be divided into three categories:

Non-pharmacological method: diet modification, exercise and behavioural modifications. This method is effective only short-term. Regardless of initial weight loss, long-term effectiveness is limited due to relapse in behaviour and compensatory slowing of metabolic rate (Padwal et al., 2004).

Surgical methods: Commonly called bariatric surgery or weight loss surgery. The most commonly used techniques are gastric bypass, sleeve gastrectomy and gastric banding.

The surgical method has the greatest long-term success, but is indicated only in very obese individuals with BMI greater than 40kg/m^2 or with BMI of 35 kg/m^2 with obesity related disorders (Gloy et al., 2013).

Pharmacological methods: also called drug therapy. This therapy is considered for patients with BMI greater than or equal to 30kg/m^2 or BMI of 27kg/m^2 with one or more obesity related disorders. Based on their mechanism of action anti-obesity medications can be divided into three categories. First, drugs that inhibit intestinal fat absorption, Orlistat, the only drug that was FDA approved for long term therapy, which inhibits pancreatic lipase. Second, drugs that suppress appetite, increase thermogenesis, and increase the time of satiety. These drugs act by modifying norepinephrine, dopamine, and serotonin in the central nervous system. Sibutramine is the only drug approved for long term use, which inhibits re-uptake of serotonin and norepinephrine to suppress appetite. Third, drugs that inhibit the endocannabinoid system. Rimonabant, reduces food intake and body weight. Current drugs used in obesity therapy, when used for over a 1 year period, have been shown to reduce a total weight by 1% to 5% only, with serious side effects. The development of new drugs that are safer and, more effective for long term use, with the additional option of weight management are needed (Padwal et al., 2004; Yanovski and Yanovski, 2014).

1.2 Adipose tissue

AT is a specialized loose connective tissue. It is composed of tightly packed adipocytes, preadipocytes, fibroblasts, endothelial cells, pericytes, cells of the innate immune system (macrophages), cells of adaptive immunity (T cells, NK cells and mast cells) and multi-potent stem cells, supported by vascularized loose connective tissue (Armani et al., 2010; Lee et al., 2013a; Schaffler et al., 2005; Wronska and Kmiec, 2012). AT consists of cellular and non-cellular components.

The cellular component are adipocytes, which constitute up to ~90% of adipose tissue by volume and the remaining 10% by stromal vascular fraction (SVF). The size of

adipocytes ranges from 30-150 µm in diameter. Adipocytes contain a large lipid droplet which constitutes 85% of the cell volume, and the remaining 15% is nucleus and cytoplasm displaced to the periphery, giving it a signet-ring shape. Each adipocyte is surrounded by basal lamina and is closely opposed to at least one capillary to support its active metabolism. The SVF contains preadipocytes, endothelial cells, infiltrated monocytes/macrophages and multipotent stem cells. Preadipocytes accounts for 15-50% of the SVF(Brooks JSJ, 1997; Cinti, 2009; Gomillion and Burg, 2006; Tordjman, 2013; Wronska and Kmiec, 2012).

The non-cellular component of AT is made up of extracellular matrix (ECM) proteins. ECM proteins maintain the structural and functional integrity of AT, and protect the cells from mechanical forces. Adipocytes and SVF contribute to the production of ECM components. ECM of AT is comprised of collagen type I, III, IV and type VI, fibronectin, laminins, nidogens, decorin, tenascin C, osteopontin, matrix metalloproteinases, SPARC and many other components. (Divoux and Clement, 2011; Mariman and Wang, 2010; Wronska and Kmiec, 2012).

Adipose tissue can be classified based on functional and biochemical characteristics into white adipose tissue (WAT) and brown adipose tissue (BAT) (**Figure 3**) (Fruhbeck, 2008).

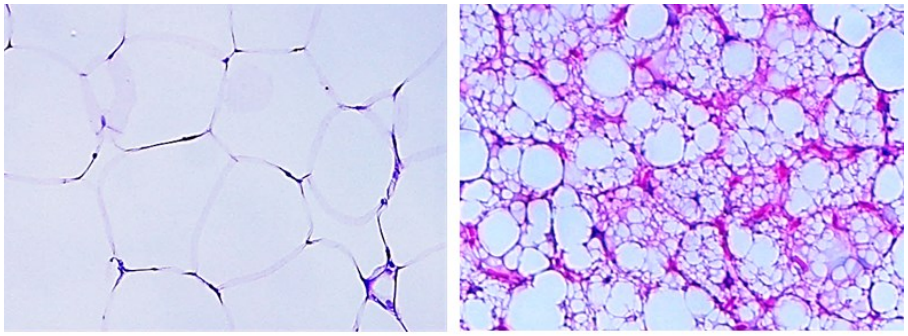

Figure 3: H&E stained sections of WAT and BAT.

1.2.1 White adipose tissue (WAT)

WAT is most abundant adipose tissue. Grossly, WAT is whitish/yellow in color and has a glistening surface. WAT can be subclassified into subcutaneous (sWAT) and visceral (vWAT) depots, based on their anatomical distribution in human and mice. The sWAT depots are present under the skin. vWAT depots are present in the mediastinum and abdominal cavity surrounding internal organs.

In mice, sWAT is subdivided into inguinal and interscapular (**Figure 4**). *Inguinal* deposit is wrapped around the mouse pelvis from back to front on both sides of the mouse. *Interscapular* is distributed on the dorsal side of the forelimbs of mice. vWAT can be subdivided into major and minor depots. Major depots include *Perigonadal* depots. In male mice perigonadal deposit is also called epididymal, present within the peritoneum and in the vicinity of the testis and the epididymis. In females it is called periovarian,surrounding the ovaries, uterus and bladder. The *Mesentric* deposit lines the intestine in the mesentery. *Retroperitoneal* depots are situated behind the kidneys on both sides (Berry et al., 2013; Cinti, 2007; Cinti, 2009; Stephane Gesta, 2012; Wronska and Kmiec, 2012). The minor depots are *paracardial* depots which are located in the mediastinum. *Epicardial* depots are found around the heart. *Epigastric* depots surround the stomach, and *perivascular* depots surround blood vessels (Iozzo, 2011).

sWAT and vWAT depots differ in morphology and physiological function. These differences arise from genetic differences in preadipocyte differentiation programs and epigenetic influences from local environment (Tchkonia et al., 2007; Yamamoto et al., 2010). Functionally, the depots differ in adipokine secretion, tryglyceride synthesis, and rate of lipolysis. Understanding the different depots is important because the development and progression of metabolic disease is associated with changes in fat distribution among the depots more than it's associated with total changes in fat mass (Berry et al., 2013; Stephane Gesta, 2012; Wronska and Kmiec, 2012).

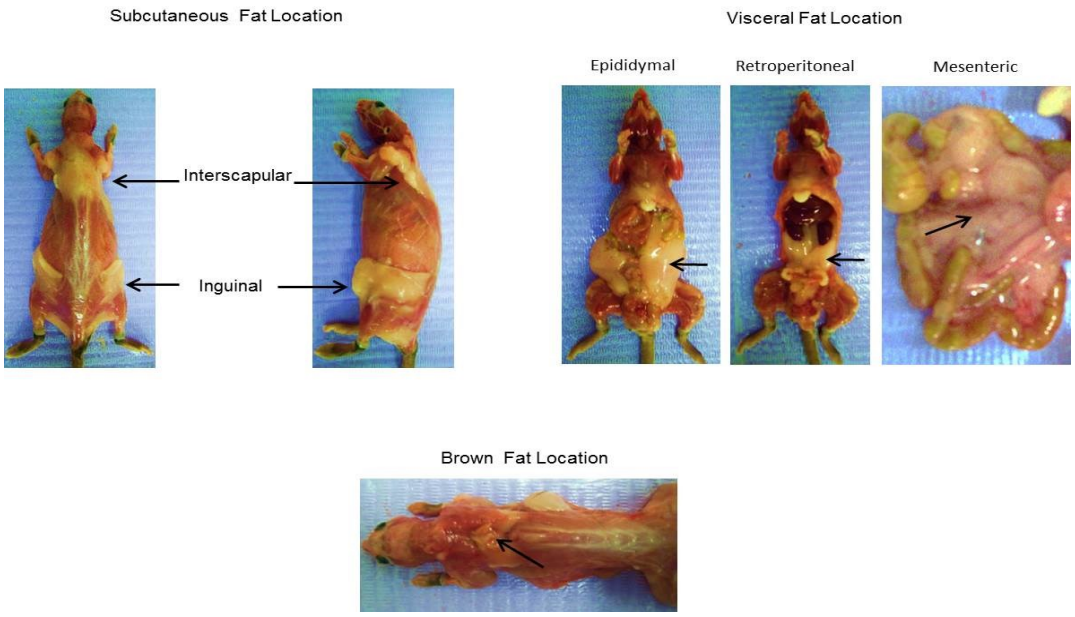

Figure 4: Adipose tissue depots in mice.

The AT organ is made up of subcutaneous depot lying underneath the skin-interscapular and inguinal; visceral-epididymal-associated with the testes; mesenteric-associated with intestines; and retroperitoneal-located behind the kidney.

1.2.2 Brown adipose tissue (BAT)

BAT grossly appears brown due to high content of mitochondria and rich vascularity. Histologically, brown adipocytes contain several small lipid droplets giving it a multilocular appearance compared to white adipocyte. Brown adipocytes are smaller in size with an approximate diameter of 60 µm and constitutes about 50% of the total cells (Cannon and Nedergaard, 2004; Fromme, 2012; Tordjman, 2013). Brown adipocytes are rich in mitochondria, which contain uncoupling protein 1 (UCP1). UCP1 is located in the inner membrane of the mitochondria, and is responsible for the uncoupling of oxidative phosphorylation to generate heat for non-shivering thermogenesis (Cannon and Nedergaard, 2004; Hassan et al., 2012). BAT is most prominent in newborn and in young mammals. BAT is also present in various locations in the body, that can increase

or decrease depending on age, species, environmental factors, and nutritional conditions. In mice, the *interscapular* deposit is the largest BAT deposit and is found between the shoulder blades under the sWAT. BAT may also be found in supraclavicular and axillary regions of the neck, perirenal, in the mediastinum around the major vessels such as aorta and within WAT and skeletal muscle (Gesta et al., 2007; Sacks and Symonds, 2013; Tam et al., 2012).

1.2.3 Adipose tissue function

AT functions as a mechanical cushion, in thermal insulation, storage and release of fat and functions as an endocrine organ (Sethi and Vidal-Puig, 2007; Stephane Gesta, 2012). WAT stores FFA in the form of triglycerides. Adipocytes are the major storage sites for triglycerides. Triglycerides are synthesized from the binding of esterified FFA to a glycerol backbone (Coleman et al., 2000). BAT also stores FFA, but FFA are oxidized to produce heat within the adipocytes, rather than supplying FFA to other tissues (Sethi and Vidal-Puig, 2007; Zimmermann et al., 2009). The break down of triglycerides into FFA and glycerol is called lipolysis. Lipolysis provides adequate energy supply to peripheral tissues during fasting or food deprivation, or during increased energy expenditure (Zechner et al., 2012). AT synthesizes and secretes a wide variety of factors called adipokines. Adipokines can act in an autocrine, paracrine or endocrine manner. Adipokines regulate systemic energy and glucose metabolism by influencing function of the brain, skeletal muscle, liver, pancreas, and heart. Some adipokines mainly produced by adipocytes, which regulate insulin sensitivity are leptin, adiponectin, resistin, visfatin, retinol binding protein-4 (RBP-4) (Antuna-Puente et al., 2008; Kershaw and Flier, 2004).

1.3 Adipogenesis

Adipogenesis is a complex multi-step process which involves the differentiation of precursor cells into fully mature adipocytes through a series of precisely ordered and regulated cellular events. Adipogenesis involves two major phases. The first phase is a

determination phase-during which pluripotent and multipotent mesenchymal stem cells (MSC) are recruited to generate preadipocytes. The second phase is terminal differentiation during which preadipocytes are differentiated to mature adipocytes. The proliferating preadipocytes are permanently growth arrested to become round, lipid filled, and functional mature fat cells. The course of terminal differentiation has been well studied using cell line culture models (Cristancho and Lazar, 2011; Gregoire et al., 1998; Rosen and MacDougald, 2006).

1.3.1 Cell line models of adipogenesis

Cell line culture models are the ideal tool for studying adipogenesis because of homogenous cell population, which allows the cells to remain at the same differentiation stage, which in turn gives a homogeneous response to treatments. When selecting cell model system one must consider getting information regarding proliferation, differentiation and function to ensure relevant results (Armani et al., 2010; Gregoire et al., 1998).

To study adipogenesis, two different cell lines are available: preadipocyte and multipotent stem cell lines. *Preadiocyte cell lines* include 3T3-L1, 3T3-F442A, ST-13 and Ob17 cells. Preadipocyte cell lines are cell lines that are already committed to adipocyte lineage (Armani et al., 2010). The most frequently used preadipocytes cell lines are 3T3-L1 and 3T3-F442A cells. These cells were isolated from the swiss 3T3 cell line, derived from 17-19 days old swiss 3T3 mouse embryo (Green and Kehinde, 1975, 1976; Green and Meuth, 1974). 3T3-F442A cells are at an advanced stage of differentiation compared to 3T3-L1 cells (Gregoire et al., 1998). ST-13 was established from adult primitive mesenchymal cell lines (Yajima et al., 2003). Ob17 cell line derived from epididymal fat pads of ob/ob adult mice (a leptin deficient mouse) (Armani et al., 2010; Negrel et al., 1978).

Multipotent stem cell lines include dedifferentiated fat cells (DFAT), C3H10T1/2, adipose-derived stem cells (ASCs) and embryonic stem cells (ES cells). Multipotent

stem cell lines are cell lines that can be differentiated into a multiple lineage of cells, such as adipocytes, osteoblasts, chondrocytes and myocytes (Armani et al., 2010; Gregoire et al., 1998). Dedifferentiated fat cells (DFAT) are derived from mature adipocytes of fat tissue developed by ceiling culture. In ceiling culture the culture flask is completely filled with media, and the floating adipocytes adhere to the top inner surface of culture plate. In about seven days the adipocytes become fibroblast-like shaped cells with no lipid droplets; these cells are called DFAT. DFAT cells can be differentiated again, not only to adipocytes but also osteoblasts and chondrocytes (Matsumoto et al., 2008; Nobusue et al., 2008; Sugihara et al., 1986; Yagi et al., 2004). C3H10T1/2 cells are derived from 14 to 17 days old C3H mouse embryos; these cells can be differentiated into osteoblasts, chondrocytes, myocytes and adipocytes (Konieczny and Emerson, 1984; Taylor and Jones, 1979). C3H10T1/2 cells require BMP-4 along with adipogenic cocktails to differentiate into adipocytes (Tang et al., 2004). ASCs are multipotent stem cells extracted from adipose tissue; these cells can be differentiated into multiple lineages *in vitro* and *in vivo.* ES cells can be differentiated into various lineages. These cells are used to identify novel regulatory genes that determine the commitment of cells to adipogenesis (Armani et al., 2010; Gregoire et al., 1998).

The cell line described above are mainly murine models. Human cell strains also exist and include liposarcoma-derived human adipocyte cell line, LS14 (Hugo et al., 2006), and cells derived from the stromal cells fraction of subcutaneous adipose tissue of an infant with Simpson-Golabi-Behmel syndrome (SGBS)(Wabitsch et al., 2001). The difference between the human versus murine cell models is that the murine model may not accurately represent the full spectrum of hormonal and metabolic characteristics of human adipocytes. However, given the paucity of suitable human adipocyte cell lines, most investigators have been using murine adipogenic cell lines (Gregoire et al., 1998; Hugo et al., 2006; Wabitsch et al., 2001).

The limitation of cell line models are that the cell lines are aneuploidy and because of this they may not reflect the *in vivo* context. The cell lines are derived from adipose tissue from various species at different stages of development, and from various deposits. The nature of the induction is different for the specific cell culture model. The

supraphysiological concentrations of insulin do not affect the number of differentiated cells but does serve to accelerate lipid accumulation. Due to these limitations the primary cell cultures are useful for validating results obtained in cell lines (Armani et al., 2010; Gregoire et al., 1998).

1.3.2 Differentiation of preadipocytes to adipocytes

The process of adipocyte differentiation is well studied in 3T3-L1 and 3T3-F422A preadipocyte cell lines. *In vitro* preadipocyte cell lines can be differentiated into adipocytes using an induction cocktail containing insulin, dexamethasone, and 3-isobutyl-1-methylxanthine (IBMX) or an agent that elevates cellular cAMP levels. Insulin-, glucocorticoid-, and cAMP- signalling pathways are activated by the inducers, respectively. Preadipocytes are grown to confluence to withdraw from the cell cycle, that is, at the G1 phase of the cell cycle. Differentiation is initiated at this point using the induction cocktail in fetal calf serum containing medium (Gregoire et al., 1998; MacDougald and Lane, 1995; Student et al., 1980; Tang and Lane, 2012). After induction of 16-20 h, growth arrested preadipcytes re-enter the cell cycle and undergo two rounds of cell division, referred as mitotic clonal expansion. Cells exit the cell cycle, become round, accumulate lipids and become fully mature adipocytes (**Figure 4**) (Avram et al., 2007; Cornelius et al., 1994; Gregoire et al., 1998; Tang and Lane, 2012). Adipogenesis is characterized by change in cell shape from a fibroblast-like preadipocytes into spherical lipid filled adipocytes. This morphological transformation is associated with ECM remodelling, changes in cell ECM interactions and cytoskeletal rearrangement. The ECM and cytoskeletal changes induce and promote a cascade of transcriptional factors and cell-cycle proteins which regulate gene expression, leading to the development of mature adipocyte (Cristancho and Lazar, 2011; Gregoire et al., 1998; Rosen et al., 2002; Tang and Lane, 2012).

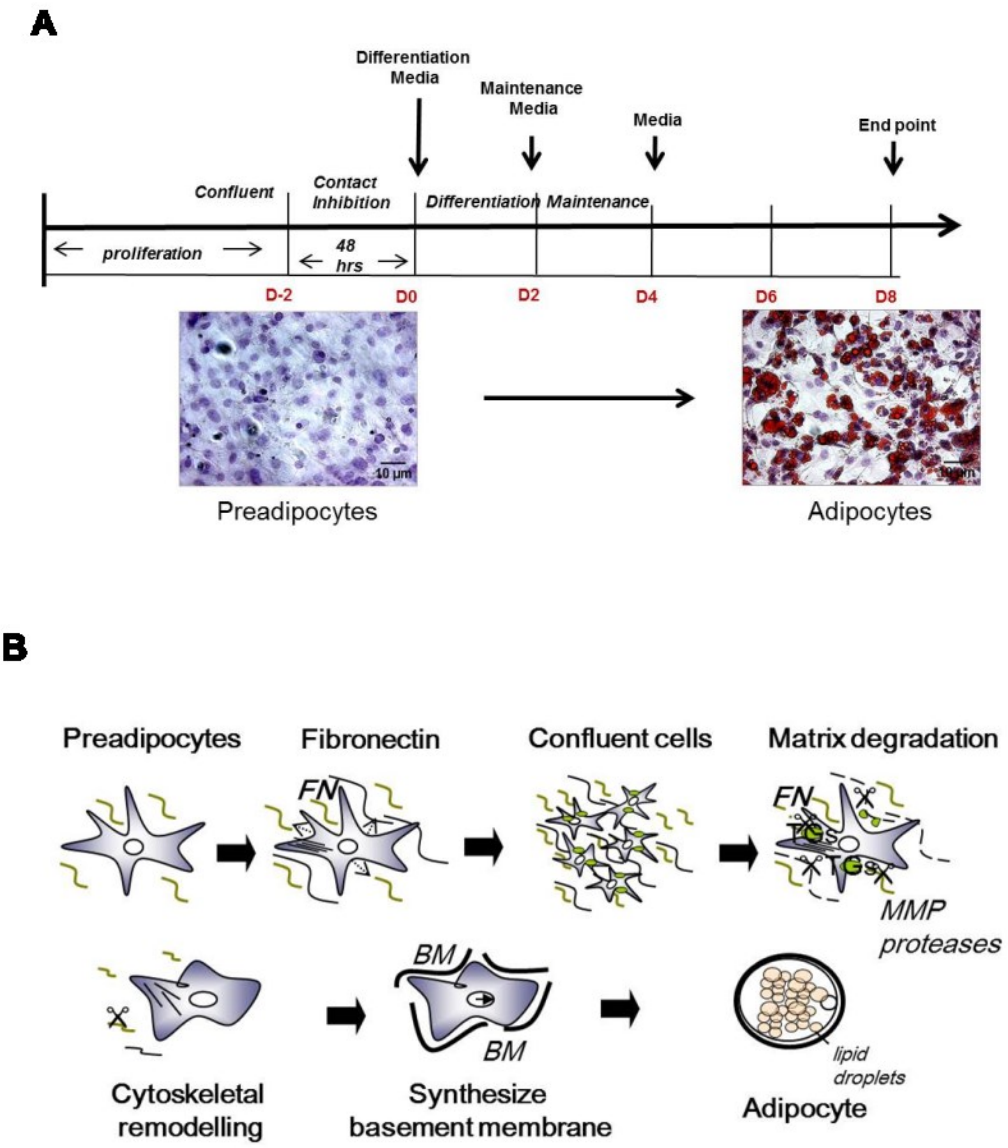

Figure 5: Adipocyte differentiation in culture.

(A) *Schematic of 3T3-L1 cells differentiation in culture. Differentiation media contains IBMX, dexamethasone and insulin. Maintenance media has only insulin. Images depict Oil Red staining of 3T3-L1 preadipocytes and mature adipocytes in culture showing accumulation of lipid (red) in the cells.* ***(B)*** *ECM and cytoskeletal changes during adipocyte differentiation (adapted from (Lilla et al., 2002)).*

1.3.3 Transcriptional factors regulating adipogenesis

The differentiation of preadipocyte into adipocytes involves a network of transcriptional factors. Pro- or anti-adipogenic transcriptional factors coordinate in a sequential manner to induce two key transcription factors: PPARγ (Peroxisome proliferator-activated receptor gamma) and C/EBPα (CCAAT/enhancer-binding protein alpha), which drives terminal adipocyte differentiation (Feve, 2005; Rosen and MacDougald, 2006). The adipogenic cocktail first induces a transient and dramatic induction of C/EBPβ and C/EBPδ(Yeh et al., 1995), which in turn activates PPARγ and C/EBPα (Elberg et al., 2000; Schwarz et al., 1997).

C/EBPβ and C/EBPδ are important for adipogenesis. Mouse embryonic fibroblasts (MEFs) derived from knockout mice of C/EBPβ or C/EBPδ displayed reduced adipogenesis and MEFs of C/EBPβ and C/EBPδ double knockout mice did not differentiate into adipocytes. C/EBPβ and C/EBPδ double knockout mice show reduced WAT, suggesting a synergistic role of C/EBPβ and C/EBPδ during adipogenesis (Tanaka et al., 1997). Over expression of C/EBPβ or C/EBPδ in preadipocyte increased adipogenesis (Darlington et al., 1998; Tanaka et al., 1997). C/EBPβ and C/EBPδ induce PPARγ expression (Feve, 2005; Rosen and MacDougald, 2006).

PPARγ is a member of the nuclear receptor superfamily of ligand-activated transcription factors. PPARγ is the master regulator of adipogenesis and is required for adipogenesis of both WAT and BAT (Kajimura et al., 2008; Tontonoz et al., 1994b). Ectopic expression of *Pparγ* induced differentiation of non adipogenic fibroblasts into adipocytes suggesting that PPARγ alone can induce adipogenesis (Tontonoz et al., 1994b). In mature 3T3-L1 adipocytes, the overexpression of dominant negative mutant of PPARγ caused decreased cell size, lipid accumulation, and reduced expression of key enzymes of lipid metabolism, suggesting that PPARγ is important in maintaining the gene expressions that are characteristic of mature adipocyte (Tamori et al., 2002). PPARγ is expressed as two isoforms: PPARγ1 and PPARγ2 (Fajas et al., 1997; Tontonoz et al., 1994a). PPARγ1 is expressed in many tissues and PPARγ2 is specific to adipocytes

(Mueller et al., 2002). Mice with the AT specific knockout of PPARγ2 show decreased fat pad size, but have substantial fat, suggesting that PPARγ1 can compensate for adipogenic function of PPARγ2 (Zhang et al., 2004). In PPARγ knockout MEFs, ectopic expression of PPARγ1 demonstrated similar adipogenesis to that of PPARγ2, suggesting that PPARγ1 is as efficient as PPARγ2 in inducing adipogenesis (Mueller et al., 2002).

C/EBPα is expressed after PPARγ2 induction (Feve, 2005). C/EBPα is a principal player in WAT formation, but not for BAT (Linhart et al., 2001). PPARγ2 and C/EBPα forms a positive feedback loop, inducing their expression (Gregoire et al., 1998; Rosen and MacDougald, 2006). C/EBPα null mice display reduced PPARγ2 expression (Wu et al., 1999) and PPARγ heterozygous mouse show reduced C/EBPα expression (Barak et al., 1999). C/EBPα deficient MEFs do not undergo adipocyte differentiation, but overexpression of PPARγ was shown to induce adipogenesis (Wu et al., 1999). On the other hand, over expression of C/EBPα in PPARγ null MEFs did not induce adipogenesis, suggesting that PPARγ is the dominant factor of the feedback loop (Rosen et al., 2002). C/EBPα is required to maintain PPARγ expression (Wu et al., 1999). In addition, PPARγ and C/EBPα are also involved in inhibiting proliferation of preadipocytes, which is required for adipocyte differentiation (Holst and Grimaldi, 2002; Porse et al., 2001).

1.3.4 ECM changes during adipogenesis

ECM influences cell adhesion, polarity, migration, proliferation, differentiation, behavior and the survival of cells (Daley et al., 2008). ECM influences differentiation via cell-surface receptors, cell-cell and cell-matrix interactions (Hausman et al., 1996). ECM plays an important role in adipocyte differentiation. ECM components are synthesized and degraded at various stages of differentiation (Ibrahimi et al., 1992; Kubo et al., 2000; Yi et al., 2001). ECM remodelling during adipogenesis is a key event and defines the onset of the differentiation process. ECM remodelling reduces cell-matrix interactions, mediates cytoskeletal rearrangement, and modulates cellular signalling to

influence gene transcription to differentiate to adipocyte (Gregoire et al., 1998). ECM remodelling is characterized by the conversion of preadipocyte fibronectin-rich matrix to a basement membrane (laminin, nidogen/entactin and type-IV collagens) rich matrix of mature adipocyte. Studies done on preadipocyte cell lines have shown that during adipogenesis fibronectin (FN), α5-integrins, type I and III collagens are down regulated and type IV collagen, α6-integrins, laminin, glycosaminoglycans and entactin are up regulated (Avram et al., 2007; Gregoire et al., 1998; Mariman and Wang, 2010).

1.3.4.1 Integrins

Integrins are transmembrane receptors that mediate cell-matrix adhesion and signalling. Integrin expression is differentially regulated during adipogenesis; α5-integrin expression decreases, whereas α6-integrin expression increases as preadipocytes differentiate into adipocytes. This switch of integrins is required for adipocyte differentiation; ectopic expression of α5 integrins promoted preadipocyte proliferation, adhesion and spreading, leading to reduced adipocyte differentiation. In contrast, α6-integrins ectopic expression reduced proliferation of preadipocytes. β1-integrin expression levels do not change during differentiation (Liu et al., 2005), but inhibition of β1-integrin function by ADAM12 promoted cytoskeletal reorganization during early differentiation (Kawaguchi et al., 2003).

1.3.4.2 Fibronectin

During adipogenesis FN is the first ECM component to be synthesized and first to undergo proteolytic degradation. After differentiation is initiated, FN levels increase till day two and then decrease. This was also associated with a decrease in pericellular FN during differentiation (Kubo et al., 2000). FN was shown to inhibit adipocyte differentiation; culturing 3T3-F442A cells on FN inhibited adipogenesis by preventing cytoskeletal remodelling. This inhibitory effect of FN was reversed by treating the cells with cytochalsin D or insulin (Spiegelman and Ginty, 1983). In ST-13 preadipocytes, exogenously added intact FN inhibited adipocyte differentiation; this inhibition was reversed by using RGD-peptide and polyclonal antibody to α5β1 integrin. Intact FN

inhibitory activity depends on RGD-α5β1 integrin interaction. In contrast, thermolysin digest of FN increased adipocyte differentiation. This was inhibited by antibody directed towards the amino-terminal fibrin-binding (Fib 1) domain of FN. Interestingly, purified 24K fragment derived from the Fib 1 domain increased adipogenesis of ST-13 cells, and this study suggests that FN fragments have an opposite effect on adipogenesis compared to intact FN (Fukai et al., 1993). Another protein which inhibits adipocyte differentiation during the early phase is Pref-1 (Hudak and Sul, 2013). Pref-1 interacts with the FN C-terminal domain to inhibit adipogenesis. Knockdown of α5-integrins or treating cells with RGD-peptide prevented the Pref-1 inhibitory effect on adipogenesis (Wang et al., 2010a). After the FN matrix is removed, a laminin and collagen IV organized network of matrix appears. This matrix is remodelled to become the cell surface associated laminin and collagen IV of adipocytes.

1.3.4.3 Collagens

Collagens, which are the main ECM components of connective tissue, are differentially regulated during adipocyte differentiation. During early phase of differentiation collagen type I and III and the C-terminal processing peptide of the collagen decreases, but returns to basal level at the later stage. Production of collagens IV and V gradually increase during differentiation. Collagen VI production initially increases, but decreases later, however, the final levels are still higher compared to the basal levels, i.e., in preadipocyte cultures. Collagen type I, III, V and VI form an extracellular network during midstage and remain throughout the late stage of adipocyte differentiation (Kubo et al., 2000; Mariman and Wang, 2010; Napolitano, 1963). Collagen synthesis during adipogenesis has a biphasic pattern. Inhibition of collagen synthesis in preadipocytes inhibits adipocyte differentiation and triglyceride accumulation, but did not have any effect on adipocytes (Ibrahimi et al., 1992).

1.3.4.4 Proteases

Remodelling of ECM during adipogenesis involves several classes of proteases including serine proteases, metalloproteases and their inhibitors, and cysteine

proteases (Lilla et al., 2002; Mariman and Wang, 2010). The serine proteases involved in adipogenesis are the fibrinolytics system (plasminogen/plasmin). Plasminogen can be activated to plasmin by urokinase, tissue type plasminogen activator, and plasma kallikrein. Plasma kallikrein is the dominant plasminogen activator for adipogenesis in both *in vivo* and *in vitro*. Plasmin promotes adipogenesis by cleaving FN matrix of preadipocytes. Inhibition of plasmin, but not plasminogen activators inhibited adipogenesis (Lilla et al., 2002; Selvarajan et al., 2001). The cysteine proteases, cathepsins, found in adipose tissue are cathepsin S (CatS), cathepsin K (CatK) and cathepsin L (CatL). All three cathepsins promote adipogenesis by degrading FN matrix of preadipocytes. Inhibition of cathepsins in human preadipocytes reduced adipogenesis. CatK and CatL knockout mice showed increased levels of FN and lean phenotype (Taleb et al., 2006; Yang et al., 2008; Yang et al., 2007). Whereas CatS knockout mice show increased adiposity with improved glucose tolerance (Lafarge et al., 2014). Matrix metalloproteinases (MMPs) exert pro- or anti-adipogenic effects depending on their substrates during differentiation. MMP2, MMP9 and MT1-MMP (MMP14) promote adipogenesis and MMP3, MMP11 and MMP19 inhibit adipogenesis (Christiaens et al., 2008; Kumari L. Andarawewa, Springer New York 2008; Lilla et al., 2002). MMPs activity is modulated by their inhibitors-tissues inhibitors of MMPs (TIMPs). Four TIMPs have been detected which are able to inhibit the activities of all the MMPs (Christiaens et al., 2008; Gomez et al., 1997). All TIMPs are modulated during adipocyte differentiation: TIMP-1,-2,-3 levels remain low with TIMP-3 level substantially decreased compared to others. TIMP-3 down regulation is required for adipocyte differentiation (Bernot et al., 2010). The balance between MMPs and TIMPs determines the activity of MMPs (Lilla et al., 2002).

1.3.5 Cytoskeletal remodelling

Cytoskeleton remodelling is an essential step in the morphological transition from fibroblast-like preadipocytes to round adipocytes during adipogenesis. Rearrangement of cytoskeleton proteins during adipogenesis is important for the accumulation of lipid droplets and is a prerequisite for terminal differentiation (Gregoire et al., 1998;

Spiegelman and Farmer, 1982). Significant morphological changes occur during the mitotic clonal expansion phase of differentiation (Tang et al., 2003). Cytoskeleton proteins are actin, tubulin, vimentin.

Cell shape is primarily determined by actin (Jaffe and Hall, 2005). During adipocyte differentiation filamentous (F) actin stress fibers in preadipocytes are rearranged to cortical fibers in adipocytes (Spiegelman and Farmer, 1982; Verstraeten et al., 2011). Formation of actin stress fibers is regulated by RhoA-ROCK signalling (Ridley and Hall, 1992). Disruption of ROCK kinase promotes adipogenesis in preadipocytes and in MSCs. ROCK kinase regulates MSC differentiation into adipocytes or osteoblasts. The activation of ROCK promotes actin stress fiber formation, which inhibits adipogenesis and promotes osteoblast differentiation (McBeath et al., 2004). ROCK kinase was also shown to inhibit adipogenesis in MSCs by promoting the expression of YAP (yes-associated protein) and TAZ (transcriptional co-activator with PDZ-binding motif). Knockdown of YAP and TAZ promotes adipogenesis (Dupont et al., 2011). ROCK knockout MEFs show increased adipogenesis (Noguchi et al., 2007). Disruption of actin stress fibers is required for the induction of PPARγ expression, a major adipogenic transcription factor, during adipocyte differentiation. Downregulation of RhoA-ROCK signalling happens when the preadipocytes are exposed to the adipogenic cocktail, which results in a disruption of actin stress fibers and an increase in globular(G)-actin. Increased G-actin levels bind to MKL1 and prevent its nuclear translocation, leading to the activation of PPARγ (Nobusue et al., 2014).

Vimentin in preadipocytes are extended fibrillar intermediate filaments, which are rearranged into a cage-like structure around lipid droplets in adipocytes with multiple small lipid droplets. In adipocytes with a single large lipid droplet, vimentin is cortically arranged, lining the plasma membrane (Franke et al., 1987; Verstraeten et al., 2011). Vimentin can influence lipid droplet formation, disrupting vimentin during 3T3-L1 cell differentiation inhibited lipid droplet accumulation (Lieber and Evans, 1996). In mature adipocytes, vimentin plays a significant role in lipolysis (Kumar et al., 2007).

Tubulin in preadipocytes is filamentous in arrangement; tubulin is rearranged into a network in between lipid droplets, and under the plasma membrane in adipocytes. Disruption of microtubules increased lipid accumulation in intramuscular preadipocytes (Takenouchi et al., 2004) and enhanced adipogenesis in embryonic stem cells (Feng et al., 2010). Acetylation of α-tubulin initiates tubulin remodelling, allowing lipid droplets to expand (Yang et al., 2013).

1.3.6 Extracellular signalling modulators of adipogenesis

Extracellular and extranuclear factors can also influence adipogenesis in a positive or negative way by activating various signalling pathways. These factors can be hormones, cytokines, growth factors or pharmacological compounds (Feve, 2005; José María Moreno-Navarrete, 2012; Rosen and MacDougald, 2006).

1.3.6.1 Wnt signalling

Wnt proteins act in a paracrine and autocrine manner to regulate cell proliferation and differentiation. Wnt proteins acts through canonical and non-canonical pathways. Canonical signalling converges at β-catenin. When Wnt ligands are absent, cytoplasmic β-catenin is recruited into degradation, binding Wnt ligands to frizzled (FZD) receptors and low density lipoprotein receptor related protein 5 (LRP5) or LRP6 coreceptors leads to inactivation of the degradation complex. The cytoplasmic β-catenin is translocated into the nucleus, binds to T cell factor/lymphoid enhancing factor (TCF/LEF) transcription factors to activate Wnt target genes. Canonical Wnt ligands include Wnt1, Wnt3a, Wnt5b, Wnt7a and Wnt10b. Noncanonical Wnt signalling is β-catenin independent, using various signalling molecules such as MAPK kinase, protein kinase C and calcium/calmodulin dependent protein kinase Iiα. Noncanonical Wnt ligands are Wnt4, Wnt5a and Wnt11 (Christodoulides et al., 2009; Takada et al., 2009). Canonical Wnt signalling inhibits adipocyte differentiation. The inhibition of Wnt signalling in preadipocytes resulted in spontaneous adipocyte differentiation and ectopic expression inhibited adipogenesis (Ross et al., 2000). Canonical Wnt signalling regulates MSC

differentiation by inhibiting adipogenesis (José María Moreno-Navarrete, 2012; Kanazawa et al., 2005; Singh et al., 2006).

1.3.6.2 MAPK pathway

MAPK (Mitogen-activated protein kinase) family members regulate adipocyte differentiation differently. During the proliferative phase ERK1 (Extracellular signal-regulated kinase1) is required for differentiation. Inhibition of ERK in 3T3-L1 cells or in mice inhibits adipogenesis. In contrast, during terminal differentiation ERK1 inhibits adipogenesis (Bost et al., 2005).

1.3.6.3 TGFβ and BMP signalling

TGFβ stimulates preadipocyte proliferation and inhibits adipogenesis. This is mediated through SMAD3, which regulates the transcription of target genes. Blocking endogenous TGFβ or inhibiting SMAD3 increased adipogenesis (Choy and Derynck, 2003; Choy et al., 2000). Transgenic overexpression of TGFβ in mice also impairs adipose tissue development (Clouthier et al., 1997). BMPs can affect the commitment of MSCs to adipogenic lineage; for example, BMP4 promotes adipogenesis of MSCs (Huang et al., 2009). In C3H10T1/2 cells, BMP2 stimulates adipogenesis in low concentrations, but promotes chondrocyte and osteoblast development in high concentration (Wang et al., 1993).

1.3.6.4 Insulin signalling in adipocyte differentiation

Insulin receptor (IR) and downstream signalling components are both important for adipogenesis. Brown preadipocytes cultured from IR knockout mice show reduced adipogenesis which is consistent with adipose tissue specific IR knockout mice showing reduced fat mass (Bluher et al., 2002; Liu et al., 2014). Downstream of IR are insulin-receptor substrate (IRS) proteins. Cells lacking IRS-1 and IRS-3 exhibited severe and moderate defects in adipocyte differentiation, respectively. Cells lacking both IRS-1 and IRS-3 failed to differentiate into adipocytes (Tseng et al., 2004). Downstream of IRS are

phosphatidylinositol-3 kinase (PI3K), AKT1/protein kinase Bα (PKB) or AKT2/PKBβ; inhibition of PI3K or AKT1 or AKT2 inhibits adipogenesis. MEFs of mice deficient in AKT1 and AKT2 did not differentiate into adipocytes, and mice showed a lipoatropic phenotype(Garofalo et al., 2003). Insulin signals also promote adipogenesis by phosphorylating CREB (Klemm et al., 2001), and by promoting the cytoplasmic translocation of Foxo1 and Foxa2 (Nakae et al., 2003).

1.4 Dysregulation of adipose tissue in obesity and metabolic syndrome

During development of obesity AT stores excess fat by increasing cell size (hypertrophy). When the adipocytes reach a critical size and can no longer expand, new adipocytes are generated by recruiting preadipocytes (hyperplasia) (Cinti, 2002; de Ferranti and Mozaffarian, 2008; Martinez-Santibanez and Lumeng, 2014). AT expansion by hypertrophy or hyperplasia depends on fat pad location: in rats, hypertrophy is mainly seen in visceral fat and hyperplasia in subcutaneous fat depots (DiGirolamo et al., 1998). Increased AT mass in obesity leads to hypoxia in the tissues, resulting in adipocyte death, dysregulation of adipokine secretion, and lipid storage and mobilization (Sun et al., 2011).

Adipocyte death stimulates macrophage infiltration into AT, forming crown-like structures (CLSs) around dead adipocytes. CLSs are hallmarks of obese AT and the density of CLSs correlates with insulin resistance and a proinflammatory environment. CLSs are more common in visceral than in subcutaneous AT (Lee et al., 2010; Strissel et al., 2007; Sun et al., 2011). CLSs have M1 macrophages, which take up lipids-to process and prevent lipid release, cellular debris and to generate proinflammatory cytokines(Martinez-Santibanez and Lumeng, 2014). Over-expression diacylglycerol acyltransferase 1 in macrophages increased their capacity for lipid storage, which reduced inflammation and improved the metabolic profile of obese mice (Koliwad et al., 2010).

In parallel to these, deregulation of the ECM levels was also observed. During normal physiological AT expansion, ECM remodelling permits adipocyte expansion and contraction depending on the nutritional demands. The ECM remodelling during physiological AT expansion is dominated by degradation than deposition of ECM. In contrast, during obesity ECM degradation is reduced, with an increase in ECM deposition around adipocytes. This increase in ECM deposition increases stiffness of the microenvironment and prevents adipocyte expansion, which leads to ectopic lipid accumulation in liver and muscle, contributing to the development of metabolic disease and insulin resistance. Thus the appearance of dysfunctional AT is associated with ectopic fat accumulation in other tissues (Martinez-Santibanez and Lumeng, 2014). Increase ECM deposition also reduces adipocyte progenitors cells to differentiate into adipocytes (Chandler et al., 2011). ECM dense regions promote macrophage activation and accumulation; M1 macrophages localized to these areas promote a profibrotic environment (Klingberg et al., 2013). Fibrosis of AT is a hallmark of AT dysfunction and poor metabolic health; fibrosis is more prominent in visceral than subcutaneous AT (Divoux et al., 2010).

Obesity-associated insulin resistance is considered to be due to defective AT expansion and abnormal adipokine secretion. Defective AT expansion leads to impaired lipid storage, which in turn lead to ectopic fat deposit in the liver and muscle, making them insensitive to insulin. In obesity, the inflammatory response in AT modifies the adipokine secretion by adipocytes. The secreted inflammatory adipokines interfere with insulin signaling and metabolic effects within adipocytes, leading to insulin resistance in adipocytes. This insulin resistance contributes to the adipose tissue dysfunction and systemic insulin resistance which occurs in obesity and type 2 diabetes. Hypertrophied adipocytes secrete monocyte chemoattractant protein-1 (MCP-1); MCP-1 increases macrophage infiltration of AT in the obese subjects. The infiltrating macrophages secrete TNFα, which impairs adipocyte differentiation, increases lipolysis and secretion of FFA, leading to insulin resistance. Other adipokines that are overproduced include proinflammatory cytokine-interleukin (IL-6), adipokines that are involved in thrombosis and hypertension, plasminogen activator inhibitor-1 (PAI-1) and angiotensinogen. In

contrast, insulin sensitizing adipokine-adiponectin secretion is decreased (Maury and Brichard, 2010).

1.5 Transglutaminases

Transglutaminase (TGs) (EC 2.3.2.13) was first identified in guinea pig liver extracts in 1957 (Mycek et al., 1959). There are nine members in the TGs family, including TG1-keratinocyte transglutaminase; TG2-tissue transglutaminase; TG3-epidermal transglutaminase; TG4-prostrate transglutaminase; TG5; TG6; TG7; Factor XIII-A; and the non-catalytic erythrocyte band 4.2. The protein structure of all TG family members consists of an N-terminal β-sandwich, an α/β catalytic core, two C-terminal β-barrel domains. FXIII-A and TG1 have an additional N-terminal pro-peptide sequence that is cleaved to generate an active enzyme. The catalytic core consists of cysteine (Cys), histidine (His), and aspartate (Asp) residue, and a conserved tryptophan (Trp) that stabilizes the transition state: all four residues are essential for catalysis (**Figure 6**) (Eckert et al., 2014; Elli et al., 2009; Iismaa et al., 2009).

TGs catalyze the transamidation of specific glutamine residues of one protein, to either lysine residue in a second protein, resulting in the formation of covalent N-γ-glutaminyl-ε-lysyl-isopeptide bond, or to the free amino group of a soluble amine such as polyamine (resulting in covalent bonding of polyamine to glutamine residue). The transamidation reaction is Ca^{2+}-dependent and occurs in two steps; in the first step glutamine residue binds to the Cys residue of the active site in the TG enzyme, forming γ-glutamylthioester; the complex formed is called acylenzyme intermediate. Ammonia (NH_3) is released during this process. In the second step, the lysine residue binds to acylenzyme intermediate and reacts with γ-glutamylthioester to form the isopeptide bond, and regenerating the Cys in the TG enzyme (**Figure 7**) . The covalent isopeptide bond formed is resistant to proteolysis and the crosslinked proteins are also resistant to chemical, enzymatic and physical degradation (Eckert et al., 2014; Griffin et al., 2002; Iismaa et al., 2009).

.

Figure 6: Structure of tranglutaminase enzymes.

Schematic comparison of the protein structure of tranglutaminase family members. Pro, propeptide (adapted from (Lorand and Graham, 2003))

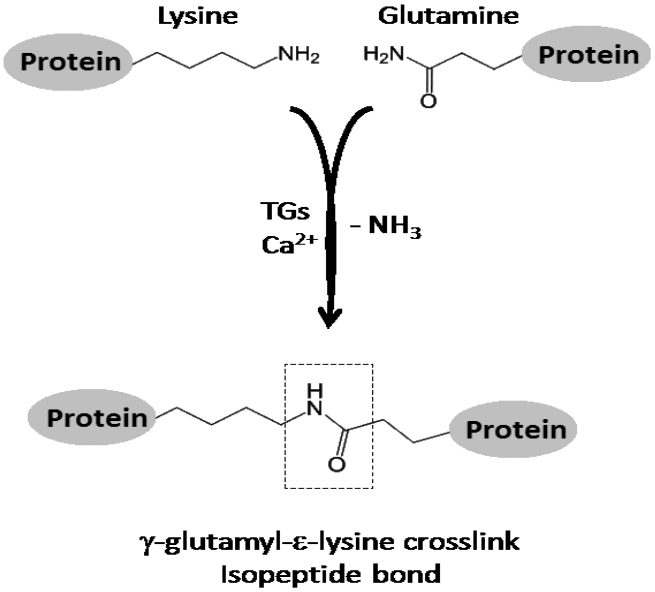

Figure 7: Tranglutaminase activity creates a covalent isopetide bond.

Formation of N-γ-glutaminyl-ε-lysyl-isopeptide bond between the acceptor residue lysine(Lys) on one protein and the donor glutamine(Gln) residue of another protein.

1.5.1 TGs substrates

Substrates for TGs crosslinking function can be divided into proteins and molecules containing primary amino groups. Protein substrates can be divided into protein substrates acting as an acyl donor (glutamine residue) and protein substrates acting as an acyl acceptor (lysine residues). TG substrate protein may also contain both glutamine(s) and lysine(s) as residue. The availability of these residues will dictate the formation of a dimer or a polymer by TGs. TG substrate proteins are present both in extracellular and intracellular compartments. TG substrates in the extracellular space include FN, laminin, collagen, SPARC, osteopontin, nidogen (entactin), and thrombospondin. Also cytoskeletal proteins such as actin, vimentin and tubulin have been reported to act as TG substrates (Facchiano and Facchiano, 2009).

1.5.1.1 FN as a TGs substrate - effects on FN matrix deposition and fibrillogenesis

FN is a ubiquitous ECM glycoprotein. Fibronectin plays a role in cell adhesion, migration, proliferation and differentiation (Schwarzbauer and DeSimone, 2011; Singh et al., 2010). FN is expressed by a wide variety of cell types and is essential during development - FN knockout mice display embryonic lethality (George et al., 1993). FN exists as dimer with two nearly identical ~250 kDa subunits. Monomers are linked together near the C-terminus by disulphide bonds. Each monomer is composed of homologous repeating units which are of three different type: type I, II and III. All the repeating units enable FN to interact with a number of molecules, ECM protein and FN itself (**Figure 8**) (Pankov and Yamada, 2002; Schwarzbauer and DeSimone, 2011). FN has two major forms: plasma FN (pFN) and cellular FN (cFN). pFN is synthesized and secreted by hepatocytes. It circulates in the blood as a soluble, compact and inactive dimer. pFN lacks two alternative spliced type III domains known as extra domains A (EDA) and extra domains B (EDB). cFN is synthesized and secreted by various cell types present in different tissues. cFN can contain variable domains, or EDA and EDB domains. Both pFN and cFN are assembled into a multimeric insoluble form in the tissues through a process called FN fibrillogenesis (Pankov and Yamada, 2002; Schwarzbauer and DeSimone, 2011; Singh et al., 2010).

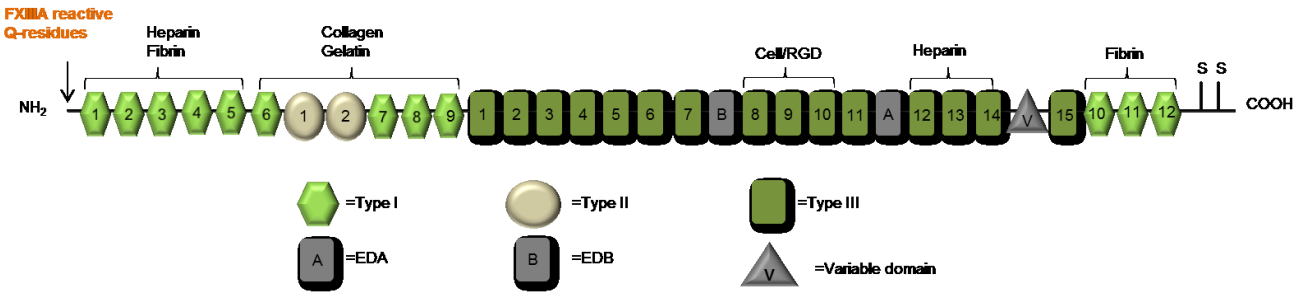

Figure 8: Structure of fibronectin (FN).

(Adapted from (Pankov and Yamada, 2002))

The gold standard assay for FN assembly is the conversion of deoxycholate detergent (DOC) soluble to DOC insoluble; this conversion is an irreversible process that stabilizes FN fibrils into matrix fibrils, to yield a mature fibrillar network. DOC-soluble fraction represents FN binding to receptors on the cell surface and fluorescent microscopy localization indicates that DOC-soluble fraction binding occurs at the edges of the cells and not in the fibrils of the ECM. DOC-Insoluble fraction represents FN incorporated into detergent-insoluble ECM (McKeown-Longo and Mosher, 1985; Singh et al., 2010).

FN matrix is required during development and in adults. During development FN is required for gastrulation, neural crest cell migration, branching morphogenesis of the lungs, kidney, and salivary gland, angiogenesis and vasculogenesis. In adults, FN is required for wound healing. FN also regulates the deposition of other ECM molecules such as fibrinogen, fibulin, collagen, and thrombospondin (Pankov and Yamada, 2002; Schwarzbauer and DeSimone, 2011; To and Midwood, 2011).

FN is a well investigated substrate of TG enzymes, primarily FXIII-A and TG2 and TG activity promotes FN matrix deposition (Hoffmann et al., 2011; Tyrrell et al., 1988). However, the mechanisms how this occurs is not understood. TGs stabilizes the ECM

by enhancing FN matrix formation and the cross-linking of extracellular matrix proteins. N-terminus of FN can be cross-linked by both FXIII-A and TG2, FN lacking N-terminal domain is incapable of assembly. FXIII-A crosslinks FN to FN, FN to fibrin and collagens. TG2 can also bind to gelatin-binding domain of FN, which is adjacent to the N-terminal domain (Hoffmann et al., 2011).

1.5.2 Transglutaminase 2 (TG2)

TG2 (also known as tissue transglutaminase) is the most ubiquitous of the TG family members. TG2, a multi-functional protein, catalyzes the protein crosslinking reaction, serving as a disulphide isomerase, kinase and as a scaffold protein (Belkin, 2011; Eckert et al., 2014). TG2 is expressed in many tissues, including bone, cartilage, kidney, colon, liver, heart, lung, spleen, blood and nervous tissue (Eckert et al., 2014; Fesus and Piacentini, 2002; Iismaa et al., 2009; Siegel and Khosla, 2007; Thomazy and Fesus, 1989). TG2 is expressed by many cell types, like osteoblasts (Al-Jallad et al., 2006), chondrocytes (Long and Ornitz, 2013; Nurminsky et al., 2011), mesenchymal stem cells (MSCs) (Nurminsky et al., 2011; Song et al., 2007), neuronal and glial cells (Eckert et al., 2014; Grosso and Mouradian, 2012; Gundemir et al., 2012), phagocytes, monocytes, neutrophils and T-cells (Akimov and Belkin, 2001b; Eckert et al., 2014; Iismaa et al., 2009; Murtaugh et al., 1983) and pancreatic β-cells (Bernassola et al., 2002). TG2 is implicated in various biological functions including cell differentiation and maturation, cell morphology and adhesion, ECM stabilization, cell death, inflammation, cell migration, and wound healing. TG2 is present in both extracellular and intracellular compartments of the cell. In the intracellular compartment TG2 is mostly cytosolic, but it is also found on the plasma membrane, in the nuclear membrane and in mitochondria. In the extracellular space, TG2 can be found on the cell surface and in the ECM (Eckert et al., 2014; Gundemir et al., 2012; Iismaa et al., 2009).

Extracellular TG2 has a non-enzymatic, or a crosslinking function. TG2 can non-covalently interact with β1-integrin, FN, syndecan-4, growth factor receptors, and ECM proteins. Cell surface TG2 binds to FN and β1-integrin and acts as a bridge to enhance

the interaction of cells with FN. Cell surface TG2 also mediates integrin clustering and potentiates outside-in signaling of integrin, which activates focal adhesion kinase (FAK), Src, and RhoA-ROCK signalling, increasing focal adhesions and actin stress fiber formation. The interaction of cell surface TG2 with syndecan-4 and FN is a parallel adhesive/ signalling function that can be utilized in case of integrin dysregulation. Cell surface TG2 interacts with PDGFR receptors and enhances PDGFR–integrin association by bridging these receptors. This association causes the receptor clustering, increased PDGF binding and upregulated receptor mediated downstream signalling. Binding of extracellular TG2 with LRP5/6 activates the β-catenin pathway by increasing nuclear translocation and inducing Wnt target genes (Belkin, 2011; Eckert et al., 2014; Gundemir et al., 2012; Iismaa et al., 2009). Dysregulation of TG2 function(s) has been implicated in the pathogenesis of celiac disease (Eckert et al., 2014; Iismaa et al., 2009; Klock et al., 2012), diabetes (Bernassola et al., 2002), neurodegenerative disorders such as Huntington's, Alzheimers's and Parkinson's disease (Eckert et al., 2014; Grosso and Mouradian, 2012; Gundemir et al., 2012) as well as inflammatory disorders and cancer (Eckert et al., 2014). Although TG2 is ubiquitous in expression and multiple function TG2 knockout mice did not show any obvious developmental phenotypes, these mice are useful in understanding the role of TG2 in pathology(Eckert et al., 2014; Iismaa et al., 2009).

1.5.3 Factor XIII-A (FXIII-A)

FXIII-A transglutaminase is found in two forms – in circulating plasma FXIII as part of the heterotertrameric coagulation factor FXIII and as cellular FXIII-A (cFXIII-A), which can be found as a monomer (FXIII-A) or a dimer (FXIII-A_2) and in both extracellular and intracellular compartments of the cell. In plasma FXIII-A circulates in an inactive enzyme that is bound to two inhibitory and protective FXIII-B subunits (tetrameric form FXIII-A_2B_2), i.e, FXIII contains of two active A subunits and two B subunits. In plasma all FXIII-A always exists in the complex with FXIII-B, FXIII-B is available 50% more than FXIII-A and can exist in its noncomplexed form. Circulating FXIII-A is predominantly synthesized by cells of bone marrow origin. Cellular FXIII-A is present in

megakaryocytes, monocytes, macrophages, astrocytes, dendritic cells, chondrocytes, osteoblasts and osteocytes (Muszbek et al., 2011).

FXIII-A is a pro-transglutaminase and its activation is dramatically enhanced by thrombin cleavage. This cleavage occurs as part of the coagulation cascade and is directed to rapidly crosslink fibrin in order to increase blood clot stability. FXIII-A can be activated in physiological conditions by thrombin but also by high Ca^{2+} and by Ca^{2+} alone in unphysiological conditions. In physiological conditions thrombin cleaves pro-peptide from each FXIII-A subunit in the tetramer, this thrombin cleaved FXIII-A will still remain inactive in absence of Ca^{2+}. In presence of Ca^{2+} the FXIII-B subunit dissociates, and the FXIII-A conformation changes to give access to the active site for substrates. In unphysiological conditions of very high Ca^{2+} levels (>50mM) FXIII-A can be activated without proteolysis. It is thought that Ca^{2+} induces the dissociation of FXIII-B and the FXIII-A dimer becomes active. Cellular FXIII-A can also be activated by thrombin and Ca^{2+}. Since there is no FXIII-B subunit to inhibit, FXIII-A can be activated by Ca^{2+} alone. In contrast to plasma FXIII-A, low Ca^{2+} concentration is sufficient to bring about the active configuration of the FXIII-A dimer, opening the structure that exposes the active site (Muszbek et al., 2007; Muszbek et al., 2011; Schroeder and Kohler, 2013).

FXIII-A is involved in many different physiological events such as wound healing and angiogenesis, osteoblast differentiation and in infection control and it interacts with complement factors and inflammatory cells (Muszbek et al., 2011). FXIII-A is known to be related to a number of disease states, such as thrombosis, diabetes, and cancer (Muszbek et al., 2011). Deficiency of FXIII-A is an autosomal recessive disorder characterized by bleeding tendency and impaired wound healing. FXIII-A knockout mice display impaired clot retraction, increased incidence of miscarriage and decreased angiogenesis (Kasahara et al., 2010; Koseki-Kuno et al., 2003). In patients with type 2 diabetes and in their relatives FXIII-A and FXIII-B levels are elevated (Eckert et al., 2014; Muszbek et al., 2007; Schroeder and Kohler, 2013).

1.5.3.1 FXIII-A – links to human obesity

A recent genome-wide screen study examined gene expression changes in WAT of monozygotic twin pairs discordant in BMI to seek potentially causative genes for obesity. This study identified F13A1 (which encodes FXIII-A) as the top, potentially causative gene expressed in WAT with the highest association to obesity. The significant association of F13A1 with obesity was further confirmed in a large European ENGAGE consortium study of more than 21,000 unrelated individuals as well as in the GenMets cohort study, which identified 7 single-nucleotide polymorphisms (SNPs) in F13A1 gene associated with BMI (Naukkarinen et al., 2010). These studies strongly imply a link between obesity and FXIII-A in AT. The presence or function of FXIII-A or other members of the TGs family in AT development and function is not known.

1.6 Hypothesis and thesis objectives

Given the recent study that identified F13A1 gene in WAT as a potential causative gene for obesity in humans, and also identified 7 SNPs in F13A1 in unrelated individuals, studies examining the role of transglutaminases and FXIII-A in WAT are warranted. Furthermore, no data is available on the function of FXIII-A or the presence of other members of the TGs family in adipose tissue development and energy metabolism. TG enzymes are expressed in a wide variety of tissues, and play a role in cell differentiation, extracellular matrix stabilization, cytoskeleton regulation and cell signaling. We ***hypothesized*** that **TG enzymes are inhibitors of adipocyte differentiation and regulators of adipose tissue metabolism.**

The ***overall objective*** of this PhD thesis was to determine the role of FXIII-A and other TG enzymes in adipogenesis and whole body energy metabolism. Three studies were conducted with specific objectives:

The first specific objective of the study (Chapter 2) was:

- To identify all the TG family members that are potentially present in adipose tissue and 3T3-L1 preadipocyte cell line.

- To identify whether TGs are enzymatically active in adipose tissue and during adipocyte differentiation.
- To identify which TG family member has a cross-linking function during adipocyte differentiation
- To determine the role of TG activity in the process of adipocyte differentiation
- To determine the role of FXIII-A deficiency on adipocyte differentiation *in vitro* using MEFs.

The second specific objective of the study (Chapter 3) was:

- To determine the role of TG2 in adipocyte differentiation using MEFs *in vitro*.

The third specific objective of the study (Chapter 4) was:

- To characterize the metabolic phenotype of *F13a1* knockout mice on a high-fat diet.

1.7 References

Obesity: preventing and managing the global epidemic. Report of a WHO consultation. World Health Organization technical report series *894*, i-xii, 1-253.

Acheson, K.J., Schutz, Y., Bessard, T., Anantharaman, K., Flatt, J.P., and Jequier, E. (1988). Glycogen storage capacity and de novo lipogenesis during massive carbohydrate overfeeding in man. The American journal of clinical nutrition *48*, 240-247.

Akimov, S.S., and Belkin, A.M. (2001). Cell surface tissue transglutaminase is involved in adhesion and migration of monocytic cells on fibronectin. Blood *98*, 1567-1576.

Al-Jallad, H.F., Nakano, Y., Chen, J.L., McMillan, E., Lefebvre, C., and Kaartinen, M.T. (2006). Transglutaminase activity regulates osteoblast differentiation and matrix mineralization in MC3T3-E1 osteoblast cultures. Matrix biology : journal of the International Society for Matrix Biology *25*, 135-148.

Antuna-Puente, B., Feve, B., Fellahi, S., and Bastard, J.P. (2008). Adipokines: the missing link between insulin resistance and obesity. Diabetes & metabolism *34*, 2-11.

Armani, A., Mammi, C., Marzolla, V., Calanchini, M., Antelmi, A., Rosano, G.M., Fabbri, A., and Caprio, M. (2010). Cellular models for understanding adipogenesis, adipose dysfunction, and obesity. Journal of cellular biochemistry *110*, 564-572.

Avram, M.M., Avram, A.S., and James, W.D. (2007). Subcutaneous fat in normal and diseased states 3. Adipogenesis: from stem cell to fat cell. Journal of the American Academy of Dermatology *56*, 472-492.

Badman, M.K., and Flier, J.S. (2005). The gut and energy balance: visceral allies in the obesity wars. Science *307*, 1909-1914.

Barak, Y., Nelson, M.C., Ong, E.S., Jones, Y.Z., Ruiz-Lozano, P., Chien, K.R., Koder, A., and Evans, R.M. (1999). PPAR gamma is required for placental, cardiac, and adipose tissue development. Molecular cell *4*, 585-595.

Baumann, C.A., Ribon, V., Kanzaki, M., Thurmond, D.C., Mora, S., Shigematsu, S., Bickel, P.E., Pessin, J.E., and Saltiel, A.R. (2000). CAP defines a second signalling pathway required for insulin-stimulated glucose transport. Nature *407*, 202-207.

Belkin, A.M. (2011). Extracellular TG2: emerging functions and regulation. The FEBS journal *278*, 4704-4716.

Bernassola, F., Federici, M., Corazzari, M., Terrinoni, A., Hribal, M.L., De Laurenzi, V., Ranalli, M., Massa, O., Sesti, G., McLean, W.H., et al. (2002). Role of transglutaminase 2 in glucose tolerance: knockout mice studies and a putative mutation in a MODY patient. FASEB journal : official publication of the Federation of American Societies for Experimental Biology *16*, 1371-1378.

Bernot, D., Barruet, E., Poggi, M., Bonardo, B., Alessi, M.C., and Peiretti, F. (2010). Down-regulation of tissue inhibitor of metalloproteinase-3 (TIMP-3) expression is necessary for adipocyte differentiation. The Journal of biological chemistry *285*, 6508-6514.

Berry, D.C., Stenesen, D., Zeve, D., and Graff, J.M. (2013). The developmental origins of adipose tissue. Development (Cambridge, England) *140*, 3939-3949.

Bluher, M., Michael, M.D., Peroni, O.D., Ueki, K., Carter, N., Kahn, B.B., and Kahn, C.R. (2002). Adipose tissue selective insulin receptor knockout protects against obesity and obesity-related glucose intolerance. Developmental cell *3*, 25-38.

Borst, S.E. Adipose Tissue and Insulin Resistance. Nutrition and Health: Adipose Tissue and Adipokines in Health and Disease, 281.

Bost, F., Aouadi, M., Caron, L., and Binetruy, B. (2005). The role of MAPKs in adipocyte differentiation and obesity. Biochimie *87*, 51-56.

Brooks JSJ, P.P. (1997). Histology for Pathologists. Lippincott Williams & Wilkins *2nd ed. New York, NY*, 167–196.

Bryant, N.J., Govers, R., and James, D.E. (2002). Regulated transport of the glucose transporter GLUT4. Nature reviews. Molecular cell biology *3*, 267-277.

Buettner, R., Scholmerich, J., and Bollheimer, L.C. (2007). High-fat diets: modeling the metabolic disorders of human obesity in rodents. Obesity (Silver Spring, Md.) *15*, 798-808.

Cannon, B., and Nedergaard, J. (2004). Brown adipose tissue: function and physiological significance. Physiological reviews *84*, 277-359.

Carel, K., Kummer, J.L., Schubert, C., Leitner, W., Heidenreich, K.A., and Draznin, B. (1996). Insulin stimulates mitogen-activated protein kinase by a Ras-independent pathway in 3T3-L1 adipocytes. The Journal of biological chemistry *271*, 30625-30630.

Chandler, E.M., Berglund, C.M., Lee, J.S., Polacheck, W.J., Gleghorn, J.P., Kirby, B.J., and Fischbach, C. (2011). Stiffness of photocrosslinked RGD-alginate gels regulates adipose progenitor cell behavior. Biotechnology and bioengineering *108*, 1683-1692.

Chiang, S.H., Baumann, C.A., Kanzaki, M., Thurmond, D.C., Watson, R.T., Neudauer, C.L., Macara, I.G., Pessin, J.E., and Saltiel, A.R. (2001). Insulin-stimulated GLUT4 translocation requires the CAP-dependent activation of TC10. Nature *410*, 944-948.

Choy, L., and Derynck, R. (2003). Transforming growth factor-beta inhibits adipocyte differentiation by Smad3 interacting with CCAAT/enhancer-binding protein (C/EBP) and repressing C/EBP transactivation function. The Journal of biological chemistry *278*, 9609-9619.

Choy, L., Skillington, J., and Derynck, R. (2000). Roles of autocrine TGF-beta receptor and Smad signaling in adipocyte differentiation. The Journal of cell biology *149*, 667-682.

Christiaens, V., Scroyen, I., and Lijnen, H.R. (2008). Role of proteolysis in development of murine adipose tissue. Thrombosis and haemostasis *99*, 290-294.

Christodoulides, C., Lagathu, C., Sethi, J.K., and Vidal-Puig, A. (2009). Adipogenesis and WNT signalling. Trends in endocrinology and metabolism: TEM *20*, 16-24.

Cinti, S. (2002). Adipocyte differentiation and transdifferentiation: plasticity of the adipose organ. Journal of endocrinological investigation *25*, 823-835.

Cinti, S. (2007). The Adipose Organ. Springer "Adipose Tissue and Adipokines in Health and Disease", 3-19.

Cinti, S. (2009). Transdifferentiation properties of adipocytes in the adipose organ. American journal of physiology. Endocrinology and metabolism *297*, E977-986.

Clouthier, D.E., Comerford, S.A., and Hammer, R.E. (1997). Hepatic fibrosis, glomerulosclerosis, and a lipodystrophy-like syndrome in PEPCK-TGF-beta1 transgenic mice. The Journal of clinical investigation *100*, 2697-2713.

Coleman, R.A., Lewin, T.M., and Muoio, D.M. (2000). Physiological and nutritional regulation of enzymes of triacylglycerol synthesis. Annual review of nutrition *20*, 77-103.

Cornelius, P., MacDougald, O.A., and Lane, M.D. (1994). Regulation of adipocyte development. Annual review of nutrition *14*, 99-129.

Cristancho, A.G., and Lazar, M.A. (2011). Forming functional fat: a growing understanding of adipocyte differentiation. Nature reviews. Molecular cell biology *12*, 722-734.

Daley, W.P., Peters, S.B., and Larsen, M. (2008). Extracellular matrix dynamics in development and regenerative medicine. Journal of cell science *121*, 255-264.

Darlington, G.J., Ross, S.E., and MacDougald, O.A. (1998). The role of C/EBP genes in adipocyte differentiation. The Journal of biological chemistry *273*, 30057-30060.

de Ferranti, S., and Mozaffarian, D. (2008). The perfect storm: obesity, adipocyte dysfunction, and metabolic consequences. Clinical chemistry *54*, 945-955.

Despres, J.P., and Lemieux, I. (2006). Abdominal obesity and metabolic syndrome. Nature *444*, 881-887.

DiGirolamo, M., Fine, J.B., Tagra, K., and Rossmanith, R. (1998). Qualitative regional differences in adipose tissue growth and cellularity in male Wistar rats fed ad libitum. The American journal of physiology *274*, R1460-1467.

Divoux, A., and Clement, K. (2011). Architecture and the extracellular matrix: the still unappreciated components of the adipose tissue. Obesity reviews : an official journal of the International Association for the Study of Obesity *12*, e494-503.

Divoux, A., Tordjman, J., Lacasa, D., Veyrie, N., Hugol, D., Aissat, A., Basdevant, A., Guerre-Millo, M., Poitou, C., Zucker, J.D., et al. (2010). Fibrosis in human adipose tissue: composition, distribution, and link with lipid metabolism and fat mass loss. Diabetes *59*, 2817-2825.

Dupont, S., Morsut, L., Aragona, M., Enzo, E., Giulitti, S., Cordenonsi, M., Zanconato, F., Le Digabel, J., Forcato, M., Bicciato, S., et al. (2011). Role of YAP/TAZ in mechanotransduction. Nature *474*, 179-183.

Eckert, R.L., Kaartinen, M.T., Nurminskaya, M., Belkin, A.M., Colak, G., Johnson, G.V., and Mehta, K. (2014). Transglutaminase regulation of cell function. Physiological reviews *94*, 383-417.

Elberg, G., Gimble, J.M., and Tsai, S.Y. (2000). Modulation of the murine peroxisome proliferator-activated receptor gamma 2 promoter activity by CCAAT/enhancer-binding proteins. The Journal of biological chemistry *275*, 27815-27822.

Elli, L., Bergamini, C.M., Bardella, M.T., and Schuppan, D. (2009). Transglutaminases in inflammation and fibrosis of the gastrointestinal tract and the liver. Digestive and liver disease : official journal of the Italian Society of Gastroenterology and the Italian Association for the Study of the Liver *41*, 541-550.

Facchiano, A., and Facchiano, F. (2009). Transglutaminases and their substrates in biology and human diseases: 50 years of growing. Amino acids *36*, 599-614.

Fajas, L., Auboeuf, D., Raspe, E., Schoonjans, K., Lefebvre, A.M., Saladin, R., Najib, J., Laville, M., Fruchart, J.C., Deeb, S., et al. (1997). The organization, promoter analysis, and expression of the human PPARgamma gene. The Journal of biological chemistry *272*, 18779-18789.

Feng, T., Szabo, E., Dziak, E., and Opas, M. (2010). Cytoskeletal disassembly and cell rounding promotes adipogenesis from ES cells. Stem cell reviews *6*, 74-85.

Fesus, L., and Piacentini, M. (2002). Transglutaminase 2: an enigmatic enzyme with diverse functions. Trends in biochemical sciences *27*, 534-539.

Feve, B. (2005). Adipogenesis: cellular and molecular aspects. Best practice & research. Clinical endocrinology & metabolism *19*, 483-499.

Franke, W.W., Hergt, M., and Grund, C. (1987). Rearrangement of the vimentin cytoskeleton during adipose conversion: formation of an intermediate filament cage around lipid globules. Cell *49*, 131-141.

Fromme, M.K.a.T. (2012). Brown Adipose Tissue. Springer "Adipose Tissue Biology", 39-69.

Fruhbeck, G. (2008). Overview of adipose tissue and its role in obesity and metabolic disorders. Methods in molecular biology (Clifton, N.J.) *456*, 1-22.

Fukai, F., Iso, T., Sekiguchi, K., Miyatake, N., Tsugita, A., and Katayama, T. (1993). An amino-terminal fibronectin fragment stimulates the differentiation of ST-13 preadipocytes. Biochemistry *32*, 5746-5751.

Galgani, J., and Ravussin, E. (2008). Energy metabolism, fuel selection and body weight regulation. International journal of obesity (2005) *32 Suppl 7*, S109-119.

Garofalo, R.S., Orena, S.J., Rafidi, K., Torchia, A.J., Stock, J.L., Hildebrandt, A.L., Coskran, T., Black, S.C., Brees, D.J., Wicks, J.R., et al. (2003). Severe diabetes, age-dependent loss of adipose tissue, and mild growth deficiency in mice lacking Akt2/PKB beta. The Journal of clinical investigation *112*, 197-208.

George, E.L., Georges-Labouesse, E.N., Patel-King, R.S., Rayburn, H., and Hynes, R.O. (1993). Defects in mesoderm, neural tube and vascular development in mouse embryos lacking fibronectin. Development (Cambridge, England) *119*, 1079-1091.

Gesta, S., Tseng, Y.H., and Kahn, C.R. (2007). Developmental origin of fat: tracking obesity to its source. Cell *131*, 242-256.

Giorgino, F., Laviola, L., and Eriksson, J.W. (2005). Regional differences of insulin action in adipose tissue: insights from in vivo and in vitro studies. Acta physiologica Scandinavica *183*, 13-30.

Gloy, V.L., Briel, M., Bhatt, D.L., Kashyap, S.R., Schauer, P.R., Mingrone, G., Bucher, H.C., and Nordmann, A.J. (2013). Bariatric surgery versus non-surgical treatment for obesity: a systematic review and meta-analysis of randomised controlled trials. BMJ (Clinical research ed.) *347*, f5934.

Gomez, D.E., Alonso, D.F., Yoshiji, H., and Thorgeirsson, U.P. (1997). Tissue inhibitors of metalloproteinases: structure, regulation and biological functions. European journal of cell biology *74*, 111-122.

Gomillion, C.T., and Burg, K.J. (2006). Stem cells and adipose tissue engineering. Biomaterials *27*, 6052-6063.

Green, H., and Kehinde, O. (1975). An established preadipose cell line and its differentiation in culture. II. Factors affecting the adipose conversion. Cell *5*, 19-27.

Green, H., and Kehinde, O. (1976). Spontaneous heritable changes leading to increased adipose conversion in 3T3 cells. Cell *7*, 105-113.

Green, H., and Meuth, M. (1974). An established pre-adipose cell line and its differentiation in culture. Cell *3*, 127-133.

Gregoire, F.M., Smas, C.M., and Sul, H.S. (1998). Understanding adipocyte differentiation. Physiological reviews *78*, 783-809.

Griffin, M., Casadio, R., and Bergamini, C.M. (2002). Transglutaminases: nature's biological glues. The Biochemical journal *368*, 377-396.

Grosso, H., and Mouradian, M.M. (2012). Transglutaminase 2: biology, relevance to neurodegenerative diseases and therapeutic implications. Pharmacology & therapeutics *133*, 392-410.

Gundemir, S., Colak, G., Tucholski, J., and Johnson, G.V. (2012). Transglutaminase 2: a molecular Swiss army knife. Biochimica et biophysica acta *1823*, 406-419.

Hassan, M., Latif, N., and Yacoub, M. (2012). Adipose tissue: friend or foe? Nature reviews. Cardiology *9*, 689-702.

Hausman, G.J., Wright, J.T., and Richardson, R.L. (1996). The influence of extracellular matrix substrata on preadipocyte development in serum-free cultures of stromal-vascular cells. Journal of animal science *74*, 2117-2128.

Hill, J.O., Wyatt, H.R., and Peters, J.C. (2012). Energy balance and obesity. Circulation *126*, 126-132.

Hoffmann, B.R., Annis, D.S., and Mosher, D.F. (2011). Reactivity of the N-terminal region of fibronectin protein to transglutaminase 2 and factor XIIIA. The Journal of biological chemistry *286*, 32220-32230.

Holst, D., and Grimaldi, P.A. (2002). New factors in the regulation of adipose differentiation and metabolism. Current opinion in lipidology *13*, 241-245.

Huang, H., Song, T.J., Li, X., Hu, L., He, Q., Liu, M., Lane, M.D., and Tang, Q.Q. (2009). BMP signaling pathway is required for commitment of C3H10T1/2 pluripotent stem cells to the adipocyte lineage. Proceedings of the National Academy of Sciences of the United States of America *106*, 12670-12675.

Huang, P.L. (2009). A comprehensive definition for metabolic syndrome. Disease models & mechanisms *2*, 231-237.

Hudak, C.S., and Sul, H.S. (2013). Pref-1, a gatekeeper of adipogenesis. Frontiers in endocrinology *4*, 79.

Ibrahimi, A., Bonino, F., Bardon, S., Ailhaud, G., and Dani, C. (1992). Essential role of collagens for terminal differentiation of preadipocytes. Biochemical and biophysical research communications *187*, 1314-1322.

Iismaa, S.E., Mearns, B.M., Lorand, L., and Graham, R.M. (2009). Transglutaminases and disease: lessons from genetically engineered mouse models and inherited disorders. Physiological reviews *89*, 991-1023.

Iozzo, P. (2011). Myocardial, perivascular, and epicardial fat. Diabetes care *34 Suppl 2*, S371-379.

Jaffe, A.B., and Hall, A. (2005). Rho GTPases: biochemistry and biology. Annual review of cell and developmental biology *21*, 247-269.

Janz, T.N.a.T. Adjusting the scales: Obesity in the Canadian population after correcting for respondent bias. Statistics Canada, 82-624-X.

José María Moreno-Navarrete, J.M.F.-R. (2012). Adipocyte Differentiation. Springer "Adipose Tissue Biology", 17-38.

Kajimura, S., Seale, P., Tomaru, T., Erdjument-Bromage, H., Cooper, M.P., Ruas, J.L., Chin, S., Tempst, P., Lazar, M.A., and Spiegelman, B.M. (2008). Regulation of the

brown and white fat gene programs through a PRDM16/CtBP transcriptional complex. Genes & development *22*, 1397-1409.

Kanazawa, A., Tsukada, S., Kamiyama, M., Yanagimoto, T., Nakajima, M., and Maeda, S. (2005). Wnt5b partially inhibits canonical Wnt/beta-catenin signaling pathway and promotes adipogenesis in 3T3-L1 preadipocytes. Biochemical and biophysical research communications *330*, 505-510.

Kasahara, K., Souri, M., Kaneda, M., Miki, T., Yamamoto, N., and Ichinose, A. (2010). Impaired clot retraction in factor XIII A subunit-deficient mice. Blood *115*, 1277-1279.

Kawaguchi, N., Sundberg, C., Kveiborg, M., Moghadaszadeh, B., Asmar, M., Dietrich, N., Thodeti, C.K., Nielsen, F.C., Moller, P., Mercurio, A.M., et al. (2003). ADAM12 induces actin cytoskeleton and extracellular matrix reorganization during early adipocyte differentiation by regulating beta1 integrin function. Journal of cell science *116*, 3893-3904.

Kelly, T., Yang, W., Chen, C.S., Reynolds, K., and He, J. (2008). Global burden of obesity in 2005 and projections to 2030. International journal of obesity (2005) *32*, 1431-1437.

Kershaw, E.E., and Flier, J.S. (2004). Adipose tissue as an endocrine organ. The Journal of clinical endocrinology and metabolism *89*, 2548-2556.

Klemm, D.J., Leitner, J.W., Watson, P., Nesterova, A., Reusch, J.E., Goalstone, M.L., and Draznin, B. (2001). Insulin-induced adipocyte differentiation. Activation of CREB rescues adipogenesis from the arrest caused by inhibition of prenylation. The Journal of biological chemistry *276*, 28430-28435.

Klingberg, F., Hinz, B., and White, E.S. (2013). The myofibroblast matrix: implications for tissue repair and fibrosis. The Journal of pathology *229*, 298-309.

Klock, C., Diraimondo, T.R., and Khosla, C. (2012). Role of transglutaminase 2 in celiac disease pathogenesis. Seminars in immunopathology *34*, 513-522.

Koliwad, S.K., Streeper, R.S., Monetti, M., Cornelissen, I., Chan, L., Terayama, K., Naylor, S., Rao, M., Hubbard, B., and Farese, R.V., Jr. (2010). DGAT1-dependent triacylglycerol storage by macrophages protects mice from diet-induced insulin resistance and inflammation. The Journal of clinical investigation *120*, 756-767.

Konieczny, S.F., and Emerson, C.P., Jr. (1984). 5-Azacytidine induction of stable mesodermal stem cell lineages from 10T1/2 cells: evidence for regulatory genes controlling determination. Cell *38*, 791-800.

Koseki-Kuno, S., Yamakawa, M., Dickneite, G., and Ichinose, A. (2003). Factor XIII A subunit-deficient mice developed severe uterine bleeding events and subsequent spontaneous miscarriages. Blood *102*, 4410-4412.

Kubo, Y., Kaidzu, S., Nakajima, I., Takenouchi, K., and Nakamura, F. (2000). Organization of extracellular matrix components during differentiation of adipocytes in long-term culture. In vitro cellular & developmental biology. Animal *36*, 38-44.

Kumar, N., Robidoux, J., Daniel, K.W., Guzman, G., Floering, L.M., and Collins, S. (2007). Requirement of vimentin filament assembly for beta3-adrenergic receptor activation of ERK MAP kinase and lipolysis. The Journal of biological chemistry *282*, 9244-9250.

Kumari L. Andarawewa, M.-C.R. (Springer New York 2008). New Insights into MMP function in Adipogenesis. The Cancer Degradome, 361-372.

Lafarge, J.C., Pini, M., Pelloux, V., Orasanu, G., Hartmann, G., Venteclef, N., Sulpice, T., Shi, G.P., Clement, K., and Guerre-Millo, M. (2014). Cathepsin S inhibition lowers blood glucose levels in mice. Diabetologia *57*, 1674-1683.

Laviola, L., Perrini, S., Cignarelli, A., and Giorgino, F. (2006). Insulin signalling in human adipose tissue. Archives of physiology and biochemistry *112*, 82-88.

Lee, M.J., Wu, Y., and Fried, S.K. (2010). Adipose tissue remodeling in pathophysiology of obesity. Current opinion in clinical nutrition and metabolic care *13*, 371-376.

Lee, M.J., Wu, Y., and Fried, S.K. (2013). Adipose tissue heterogeneity: implication of depot differences in adipose tissue for obesity complications. Molecular aspects of medicine *34*, 1-11.

Lieber, J.G., and Evans, R.M. (1996). Disruption of the vimentin intermediate filament system during adipose conversion of 3T3-L1 cells inhibits lipid droplet accumulation. Journal of cell science *109 (Pt 13)*, 3047-3058.

Lilla, J., Stickens, D., and Werb, Z. (2002). Metalloproteases and adipogenesis: a weighty subject. The American journal of pathology *160*, 1551-1554.

Linhart, H.G., Ishimura-Oka, K., DeMayo, F., Kibe, T., Repka, D., Poindexter, B., Bick, R.J., and Darlington, G.J. (2001). C/EBPalpha is required for differentiation of white, but not brown, adipose tissue. Proceedings of the National Academy of Sciences of the United States of America *98*, 12532-12537.

Liu, J., DeYoung, S.M., Zhang, M., Zhang, M., Cheng, A., and Saltiel, A.R. (2005). Changes in integrin expression during adipocyte differentiation. Cell metabolism *2*, 165-177.

Liu, X., Magee, D., Wang, C., McMurphy, T., Slater, A., During, M., and Cao, L. (2014). Adipose tissue insulin receptor knockdown via a new primate-derived hybrid recombinant AAV serotype. Molecular therapy. Methods & clinical development *1*.

Long, F., and Ornitz, D.M. (2013). Development of the endochondral skeleton. Cold Spring Harbor perspectives in biology *5*, a008334.

Lorand, L., and Graham, R.M. (2003). Transglutaminases: crosslinking enzymes with pleiotropic functions. Nature reviews. Molecular cell biology *4*, 140-156.

MacDougald, O.A., and Lane, M.D. (1995). Transcriptional regulation of gene expression during adipocyte differentiation. Annual review of biochemistry *64*, 345-373.

Mariman, E.C., and Wang, P. (2010). Adipocyte extracellular matrix composition, dynamics and role in obesity. Cellular and molecular life sciences : CMLS *67*, 1277-1292.

Martinez-Santibanez, G., and Lumeng, C.N. (2014). Macrophages and the regulation of adipose tissue remodeling. Annual review of nutrition *34*, 57-76.

Matsumoto, T., Kano, K., Kondo, D., Fukuda, N., Iribe, Y., Tanaka, N., Matsubara, Y., Sakuma, T., Satomi, A., Otaki, M., et al. (2008). Mature adipocyte-derived dedifferentiated fat cells exhibit multilineage potential. Journal of cellular physiology *215*, 210-222.

Maury, E., and Brichard, S.M. (2010). Adipokine dysregulation, adipose tissue inflammation and metabolic syndrome. Molecular and cellular endocrinology *314*, 1-16.

McBeath, R., Pirone, D.M., Nelson, C.M., Bhadriraju, K., and Chen, C.S. (2004). Cell shape, cytoskeletal tension, and RhoA regulate stem cell lineage commitment. Developmental cell *6*, 483-495.

McKeown-Longo, P.J., and Mosher, D.F. (1985). Interaction of the 70,000-mol-wt amino-terminal fragment of fibronectin with the matrix-assembly receptor of fibroblasts. The Journal of cell biology *100*, 364-374.

Mueller, E., Drori, S., Aiyer, A., Yie, J., Sarraf, P., Chen, H., Hauser, S., Rosen, E.D., Ge, K., Roeder, R.G., et al. (2002). Genetic analysis of adipogenesis through peroxisome proliferator-activated receptor gamma isoforms. The Journal of biological chemistry *277*, 41925-41930.

Muhlhausler, B.S. (2009). Nutritional models of type 2 diabetes mellitus. Methods in molecular biology (Clifton, N.J.) *560*, 19-36.

Murtaugh, M.P., Mehta, K., Johnson, J., Myers, M., Juliano, R.L., and Davies, P.J. (1983). Induction of tissue transglutaminase in mouse peritoneal macrophages. The Journal of biological chemistry *258*, 11074-11081.

Muszbek, L., Ariens, R.A., and Ichinose, A. (2007). Factor XIII: recommended terms and abbreviations. Journal of thrombosis and haemostasis : JTH *5*, 181-183.

Muszbek, L., Bereczky, Z., Bagoly, Z., Komaromi, I., and Katona, E. (2011). Factor XIII: a coagulation factor with multiple plasmatic and cellular functions. Physiological reviews *91*, 931-972.

Mycek, M.J., Clarke, D.D., Neidle, A., and Waelsch, H. (1959). Amine incorporation into insulin as catalyzed by transglutaminase. Archives of biochemistry and biophysics *84*, 528-540.

Nakae, J., Kitamura, T., Kitamura, Y., Biggs, W.H., 3rd, Arden, K.C., and Accili, D. (2003). The forkhead transcription factor Foxo1 regulates adipocyte differentiation. Developmental cell *4*, 119-129.

Napolitano, L. (1963). THE DIFFERENTIATION OF WHITE ADIPOSE CELLS. AN ELECTRON MICROSCOPE STUDY. The Journal of cell biology *18*, 663-679.

Naukkarinen, J., Surakka, I., Pietilainen, K.H., Rissanen, A., Salomaa, V., Ripatti, S., Yki-Jarvinen, H., van Duijn, C.M., Wichmann, H.E., Kaprio, J., et al. (2010). Use of genome-wide expression data to mine the "Gray Zone" of GWA studies leads to novel candidate obesity genes. PLoS genetics *6*, e1000976.

Negrel, R., Grimaldi, P., and Ailhaud, G. (1978). Establishment of preadipocyte clonal line from epididymal fat pad of ob/ob mouse that responds to insulin and to lipolytic hormones. Proceedings of the National Academy of Sciences of the United States of America *75*, 6054-6058.

Nobusue, H., Endo, T., and Kano, K. (2008). Establishment of a preadipocyte cell line derived from mature adipocytes of GFP transgenic mice and formation of adipose tissue. Cell and tissue research *332*, 435-446.

Nobusue, H., Onishi, N., Shimizu, T., Sugihara, E., Oki, Y., Sumikawa, Y., Chiyoda, T., Akashi, K., Saya, H., and Kano, K. (2014). Regulation of MKL1 via actin cytoskeleton dynamics drives adipocyte differentiation. Nature communications *5*, 3368.

Noguchi, M., Hosoda, K., Fujikura, J., Fujimoto, M., Iwakura, H., Tomita, T., Ishii, T., Arai, N., Hirata, M., Ebihara, K., et al. (2007). Genetic and pharmacological inhibition of Rho-associated kinase II enhances adipogenesis. The Journal of biological chemistry *282*, 29574-29583.

Nurminsky, D., Shanmugasundaram, S., Deasey, S., Michaud, C., Allen, S., Hendig, D., Dastjerdi, A., Francis-West, P., and Nurminskaya, M. (2011). Transglutaminase 2 regulates early chondrogenesis and glycosaminoglycan synthesis. Mechanisms of development *128*, 234-245.

Padwal, R., Li, S.K., and Lau, D.C. (2004). Long-term pharmacotherapy for obesity and overweight. The Cochrane database of systematic reviews, Cd004094.

Pankov, R., and Yamada, K.M. (2002). Fibronectin at a glance. Journal of cell science *115*, 3861-3863.

Pittas, A.G., Joseph, N.A., and Greenberg, A.S. (2004). Adipocytokines and insulin resistance. The Journal of clinical endocrinology and metabolism *89*, 447-452.

Porse, B.T., Pedersen, T.A., Xu, X., Lindberg, B., Wewer, U.M., Friis-Hansen, L., and Nerlov, C. (2001). E2F repression by C/EBPalpha is required for adipogenesis and granulopoiesis in vivo. Cell *107*, 247-258.

Ridley, A.J., and Hall, A. (1992). The small GTP-binding protein rho regulates the assembly of focal adhesions and actin stress fibers in response to growth factors. Cell *70*, 389-399.

Rosen, E.D., Hsu, C.H., Wang, X., Sakai, S., Freeman, M.W., Gonzalez, F.J., and Spiegelman, B.M. (2002). C/EBPalpha induces adipogenesis through PPARgamma: a unified pathway. Genes & development *16*, 22-26.

Rosen, E.D., and MacDougald, O.A. (2006). Adipocyte differentiation from the inside out. Nature reviews. Molecular cell biology *7*, 885-896.

Ross, S.E., Hemati, N., Longo, K.A., Bennett, C.N., Lucas, P.C., Erickson, R.L., and MacDougald, O.A. (2000). Inhibition of adipogenesis by Wnt signaling. Science *289*, 950-953.

Sacks, H., and Symonds, M.E. (2013). Anatomical locations of human brown adipose tissue: functional relevance and implications in obesity and type 2 diabetes. Diabetes *62*, 1783-1790.

Schaffler, A., Scholmerich, J., and Buchler, C. (2005). Mechanisms of disease: adipocytokines and visceral adipose tissue--emerging role in intestinal and mesenteric diseases. Nature clinical practice. Gastroenterology & hepatology *2*, 103-111.

Schroeder, V., and Kohler, H.P. (2013). New developments in the area of factor XIII. Journal of thrombosis and haemostasis : JTH *11*, 234-244.

Schwarz, E.J., Reginato, M.J., Shao, D., Krakow, S.L., and Lazar, M.A. (1997). Retinoic acid blocks adipogenesis by inhibiting C/EBPbeta-mediated transcription. Molecular and cellular biology *17*, 1552-1561.

Schwarzbauer, J.E., and DeSimone, D.W. (2011). Fibronectins, their fibrillogenesis, and in vivo functions. Cold Spring Harbor perspectives in biology *3*.

Selvarajan, S., Lund, L.R., Takeuchi, T., Craik, C.S., and Werb, Z. (2001). A plasma kallikrein-dependent plasminogen cascade required for adipocyte differentiation. Nature cell biology *3*, 267-275.

Sethi, J.K., and Vidal-Puig, A.J. (2007). Thematic review series: adipocyte biology. Adipose tissue function and plasticity orchestrate nutritional adaptation. Journal of lipid research *48*, 1253-1262.

Siegel, M., and Khosla, C. (2007). Transglutaminase 2 inhibitors and their therapeutic role in disease states. Pharmacology & therapeutics *115*, 232-245.

Singh, P., Carraher, C., and Schwarzbauer, J.E. (2010). Assembly of fibronectin extracellular matrix. Annual review of cell and developmental biology *26*, 397-419.

Singh, R., Artaza, J.N., Taylor, W.E., Braga, M., Yuan, X., Gonzalez-Cadavid, N.F., and Bhasin, S. (2006). Testosterone inhibits adipogenic differentiation in 3T3-L1 cells: nuclear translocation of androgen receptor complex with beta-catenin and T-cell factor 4 may bypass canonical Wnt signaling to down-regulate adipogenic transcription factors. Endocrinology *147*, 141-154.

Song, H., Chang, W., Lim, S., Seo, H.S., Shim, C.Y., Park, S., Yoo, K.J., Kim, B.S., Min, B.H., Lee, H., et al. (2007). Tissue transglutaminase is essential for integrin-mediated survival of bone marrow-derived mesenchymal stem cells. Stem cells (Dayton, Ohio) *25*, 1431-1438.

Spalding, K.L., Arner, E., Westermark, P.O., Bernard, S., Buchholz, B.A., Bergmann, O., Blomqvist, L., Hoffstedt, J., Naslund, E., Britton, T., et al. (2008). Dynamics of fat cell turnover in humans. Nature *453*, 783-787.

Spiegelman, B.M., and Farmer, S.R. (1982). Decreases in tubulin and actin gene expression prior to morphological differentiation of 3T3 adipocytes. Cell *29*, 53-60.

Spiegelman, B.M., and Flier, J.S. (2001). Obesity and the regulation of energy balance. Cell *104*, 531-543.

Spiegelman, B.M., and Ginty, C.A. (1983). Fibronectin modulation of cell shape and lipogenic gene expression in 3T3-adipocytes. Cell *35*, 657-666.

Stephane Gesta, C.R.K. (2012). White Adipose Tissue. Springer "Adipose Tissue Biology", 71-121.

Strissel, K.J., Stancheva, Z., Miyoshi, H., Perfield, J.W., 2nd, DeFuria, J., Jick, Z., Greenberg, A.S., and Obin, M.S. (2007). Adipocyte death, adipose tissue remodeling, and obesity complications. Diabetes *56*, 2910-2918.

Student, A.K., Hsu, R.Y., and Lane, M.D. (1980). Induction of fatty acid synthetase synthesis in differentiating 3T3-L1 preadipocytes. The Journal of biological chemistry *255*, 4745-4750.

Sugihara, H., Yonemitsu, N., Miyabara, S., and Yun, K. (1986). Primary cultures of unilocular fat cells: characteristics of growth in vitro and changes in differentiation properties. Differentiation; research in biological diversity *31*, 42-49.

Sun, K., Kusminski, C.M., and Scherer, P.E. (2011). Adipose tissue remodeling and obesity. The Journal of clinical investigation *121*, 2094-2101.

Surwit, R.S., Kuhn, C.M., Cochrane, C., McCubbin, J.A., and Feinglos, M.N. (1988). Diet-induced type II diabetes in C57BL/6J mice. Diabetes *37*, 1163-1167.

Takada, I., Kouzmenko, A.P., and Kato, S. (2009). Wnt and PPARgamma signaling in osteoblastogenesis and adipogenesis. Nature reviews. Rheumatology *5*, 442-447.

Takenouchi, T., Miyashita, N., Ozutsumi, K., Rose, M.T., and Aso, H. (2004). Role of caveolin-1 and cytoskeletal proteins, actin and vimentin, in adipogenesis of bovine intramuscular preadipocyte cells. Cell biology international *28*, 615-623.

Taleb, S., Cancello, R., Clement, K., and Lacasa, D. (2006). Cathepsin s promotes human preadipocyte differentiation: possible involvement of fibronectin degradation. Endocrinology *147*, 4950-4959.

Tam, C.S., Lecoultre, V., and Ravussin, E. (2012). Brown adipose tissue: mechanisms and potential therapeutic targets. Circulation *125*, 2782-2791.

Tamori, Y., Masugi, J., Nishino, N., and Kasuga, M. (2002). Role of peroxisome proliferator-activated receptor-gamma in maintenance of the characteristics of mature 3T3-L1 adipocytes. Diabetes *51*, 2045-2055.

Tanaka, T., Yoshida, N., Kishimoto, T., and Akira, S. (1997). Defective adipocyte differentiation in mice lacking the C/EBPbeta and/or C/EBPdelta gene. The EMBO journal *16*, 7432-7443.

Tang, Q.Q., and Lane, M.D. (2012). Adipogenesis: from stem cell to adipocyte. Annual review of biochemistry *81*, 715-736.

Tang, Q.Q., Otto, T.C., and Lane, M.D. (2003). Mitotic clonal expansion: a synchronous process required for adipogenesis. Proceedings of the National Academy of Sciences of the United States of America *100*, 44-49.

Tang, Q.Q., Otto, T.C., and Lane, M.D. (2004). Commitment of C3H10T1/2 pluripotent stem cells to the adipocyte lineage. Proceedings of the National Academy of Sciences of the United States of America *101*, 9607-9611.

Taniguchi, C.M., Emanuelli, B., and Kahn, C.R. (2006). Critical nodes in signalling pathways: insights into insulin action. Nature reviews. Molecular cell biology *7*, 85-96.

Taylor, S.M., and Jones, P.A. (1979). Multiple new phenotypes induced in 10T1/2 and 3T3 cells treated with 5-azacytidine. Cell *17*, 771-779.

Tchkonia, T., Lenburg, M., Thomou, T., Giorgadze, N., Frampton, G., Pirtskhalava, T., Cartwright, A., Cartwright, M., Flanagan, J., Karagiannides, I., et al. (2007). Identification of depot-specific human fat cell progenitors through distinct expression profiles and developmental gene patterns. American journal of physiology. Endocrinology and metabolism *292*, E298-307.

Thomazy, V., and Fesus, L. (1989). Differential expression of tissue transglutaminase in human cells. An immunohistochemical study. Cell and tissue research *255*, 215-224.

To, W.S., and Midwood, K.S. (2011). Plasma and cellular fibronectin: distinct and independent functions during tissue repair. Fibrogenesis & tissue repair *4*, 21.

Tontonoz, P., Hu, E., Graves, R.A., Budavari, A.I., and Spiegelman, B.M. (1994a). mPPAR gamma 2: tissue-specific regulator of an adipocyte enhancer. Genes & development *8*, 1224-1234.

Tontonoz, P., Hu, E., and Spiegelman, B.M. (1994b). Stimulation of adipogenesis in fibroblasts by PPAR gamma 2, a lipid-activated transcription factor. Cell *79*, 1147-1156.

Tordjman, J. (2013). Histology of Adipose Tissue. Physiology and Physiopathology of Adipose Tissue *Springer*, pp 67-75.

Tsakiridis, T., Tong, P., Matthews, B., Tsiani, E., Bilan, P.J., Klip, A., and Downey, G.P. (1999). Role of the actin cytoskeleton in insulin action. Microscopy research and technique *47*, 79-92.

Tseng, Y.H., Kriauciunas, K.M., Kokkotou, E., and Kahn, C.R. (2004). Differential roles of insulin receptor substrates in brown adipocyte differentiation. Molecular and cellular biology *24*, 1918-1929.

Twells, L.K., Gregory, D.M., Reddigan, J., and Midodzi, W.K. (2014). Current and predicted prevalence of obesity in Canada: a trend analysis. CMAJ open *2*, E18-26.

Tyrrell, D.J., Sale, W.S., and Slife, C.W. (1988). Fibronectin is a component of the sodium dodecyl sulfate-insoluble transglutaminase substrate. The Journal of biological chemistry *263*, 8464-8469.

Verstraeten, V.L., Renes, J., Ramaekers, F.C., Kamps, M., Kuijpers, H.J., Verheyen, F., Wabitsch, M., Steijlen, P.M., van Steensel, M.A., and Broers, J.L. (2011). Reorganization of the nuclear lamina and cytoskeleton in adipogenesis. Histochemistry and cell biology *135*, 251-261.

Wang, E.A., Israel, D.I., Kelly, S., and Luxenberg, D.P. (1993). Bone morphogenetic protein-2 causes commitment and differentiation in C3H10T1/2 and 3T3 cells. Growth factors (Chur, Switzerland) *9*, 57-71.

Wang, Y., Zhao, L., Smas, C., and Sul, H.S. (2010). Pref-1 interacts with fibronectin to inhibit adipocyte differentiation. Molecular and cellular biology *30*, 3480-3492.

Webber, J. (2003). Energy balance in obesity. The Proceedings of the Nutrition Society *62*, 539-543.

Wronska, A., and Kmiec, Z. (2012). Structural and biochemical characteristics of various white adipose tissue depots. Acta physiologica (Oxford, England) *205*, 194-208.

Wu, Z., Rosen, E.D., Brun, R., Hauser, S., Adelmant, G., Troy, A.E., McKeon, C., Darlington, G.J., and Spiegelman, B.M. (1999). Cross-regulation of C/EBP alpha and

PPAR gamma controls the transcriptional pathway of adipogenesis and insulin sensitivity. Molecular cell *3*, 151-158.

Yagi, K., Kondo, D., Okazaki, Y., and Kano, K. (2004). A novel preadipocyte cell line established from mouse adult mature adipocytes. Biochemical and biophysical research communications *321*, 967-974.

Yamada, T., and Katagiri, H. (2007). Avenues of communication between the brain and tissues/organs involved in energy homeostasis. Endocrine journal *54*, 497-505.

Yamada, T., Oka, Y., and Katagiri, H. (2008). Inter-organ metabolic communication involved in energy homeostasis: potential therapeutic targets for obesity and metabolic syndrome. Pharmacology & therapeutics *117*, 188-198.

Yamamoto, Y., Gesta, S., Lee, K.Y., Tran, T.T., Saadatirad, P., and Kahn, C.R. (2010). Adipose depots possess unique developmental gene signatures. Obesity (Silver Spring, Md.) *18*, 872-878.

Yang, M., Sun, J., Zhang, T., Liu, J., Zhang, J., Shi, M.A., Darakhshan, F., Guerre-Millo, M., Clement, K., Gelb, B.D., et al. (2008). Deficiency and inhibition of cathepsin K reduce body weight gain and increase glucose metabolism in mice. Arteriosclerosis, thrombosis, and vascular biology *28*, 2202-2208.

Yang, M., Zhang, Y., Pan, J., Sun, J., Liu, J., Libby, P., Sukhova, G.K., Doria, A., Katunuma, N., Peroni, O.D., et al. (2007). Cathepsin L activity controls adipogenesis and glucose tolerance. Nature cell biology *9*, 970-977.

Yang, W., Guo, X., Thein, S., Xu, F., Sugii, S., Baas, P.W., Radda, G.K., and Han, W. (2013). Regulation of adipogenesis by cytoskeleton remodelling is facilitated by acetyltransferase MEC-17-dependent acetylation of alpha-tubulin. The Biochemical journal *449*, 605-612.

Yanovski, S.Z., and Yanovski, J.A. (2014). Long-term drug treatment for obesity: a systematic and clinical review. Jama *311*, 74-86.

Yeh, W.C., Cao, Z., Classon, M., and McKnight, S.L. (1995). Cascade regulation of terminal adipocyte differentiation by three members of the C/EBP family of leucine zipper proteins. Genes & development *9*, 168-181.

Yi, T., Choi, H.M., Park, R.W., Sohn, K.Y., and Kim, I.S. (2001). Transcriptional repression of type I procollagen genes during adipocyte differentiation. Experimental & molecular medicine *33*, 269-275.

Zechner, R., Zimmermann, R., Eichmann, T.O., Kohlwein, S.D., Haemmerle, G., Lass, A., and Madeo, F. (2012). FAT SIGNALS--lipases and lipolysis in lipid metabolism and signaling. Cell metabolism *15*, 279-291.

Zhang, J., Fu, M., Cui, T., Xiong, C., Xu, K., Zhong, W., Xiao, Y., Floyd, D., Liang, J., Li, E., et al. (2004). Selective disruption of PPARgamma 2 impairs the development of adipose tissue and insulin sensitivity. Proceedings of the National Academy of Sciences of the United States of America *101*, 10703-10708.

Zimmermann, R., Lass, A., Haemmerle, G., and Zechner, R. (2009). Fate of fat: the role of adipose triglyceride lipase in lipolysis. Biochimica et biophysica acta *1791*, 494-500.

CHAPTER 2 - Factor XIII-A transglutaminase acts as a switch between preadipocyte proliferation and differentiation

2.1 Preamble

The *F13A1* gene has recently been identified as the top novel obesity-linked factor in human WAT, through obese-lean twin investigations and through large European cohort studies. The potential mechanism by which a coagulation factor – Factor XIII-A – could be linked to obesity or adipogenesis is unknown. This study demonstrates a mechanism that now links FXIII-A and adipogenesis. In this study, we used 3T3-L1 cells and MEF extracted from FXIII-A wild type and knockout mice. Firstly, we show a completely novel finding that FXIII-A is expressed and active in preadipocytes. Secondly, we show that FXIII-A function in preadipocytes is to promote the proliferation by stabilizing pFN into preadipocyte extracellular matrix. The assembled pFN matrix inhibits adipogenesis and alters insulin sensitivity.

Impact in brief:

- This is the first report demonstrating transglutaminase activity in adipose tissue and during adipogenesis, with FXIII-A being identified as the main enzyme responsible for the crosslinking activity.
- This is the first report linking liver-derived plasma fibronectin to adipose tissue function, which is an exciting new link between liver, plasma and energy metabolism.
- This is the first report showing the function and mechanism of action of FXIII-A in preadipocytes and how it might be linked to obesity in humans.

The study presented in this chapter was originally published in ***Blood***. 2014; 124(8):1344-53.

Factor XIII-A transglutaminase acts as switch between preadipocyte proliferation and differentiation

Vamsee D. Myneni[1], Kyotaka Hitomi[2], Mari T. Kaartinen[1,3]

[1]Division of Biomedical Sciences, Faculty of Dentistry, McGill University, Montreal, Quebec, Canada

[2]Department of Basic Medical Sciences, Graduate School of Pharmaceutical Sciences, Nagoya University, Chikusa, Nagoya, Japan

[3]Division of Experimental Medicine, Department of Medicine, Faculty of Medicine, McGill University, Montreal, Quebec, Canada

Key Points

1. Preadipocytes produce Factor XIII-A which acts as a negative regulator of adipogenesis by increasing plasma fibronectin matrix assembly.
2. Factor XIII-A and plasma fibronectin matrix promote preadipocyte proliferation and pro-proliferative effects of insulin.

2.2 Abstract

Factor XIII-A transglutaminase was recently identified as a potential causative obesity gene in human white adipose tissue. Here, we have examined the role of transglutaminase activity and the role of protein crosslinking in adipogenesis. Mouse white adipose tissue and preadipocytes showed abundant transglutaminase activity arising from Factor XIII-A. Factor XIII-A was localized to the cell surface and acted as a negative regulator of adipogenesis by promoting assembly of fibronectin from plasma into preadipocyte extracellular matrix. This modulated cytoskeletal dynamics and maintained the preadipocyte state. Factor XIII-A-assembled plasma fibronectin matrix promoted preadipocyte proliferation and potentiated the pro-proliferative effects of insulin while supressing the pro-differentiating insulin signalling. FXIII-A-deficient

mouse embryonic fibroblasts showed increased lipid accumulation and decreased proliferation, as well as decreased pFN assembly into extracellular matrix. Thus, FXIII-A serves as a preadipocyte-bound proliferation/differentiation switch that mediates effects of hepatocyte-produced circulating plasma fibronectin.

2.3 Introduction

Obesity, which is characterized by abnormally high fat accumulation in adipose tissue and in other organs, has a heritability range of 65-80%(Christakis and Fowler, 2007; Malis et al., 2005) and is a risk factor for thrombosis and many severe chronic illnesses, including type 2 diabetes, coronary heart disease, arthritis, and cancer(Gesta et al., 2007; Van Gaal et al., 2006). Obesity is also associated with the hypercoagulable state caused by increased production of liver-derived clotting factors occurring as a reaction to increased circulating lipids and inflammatory cytokines caused by dysfunctioning adipose tissue(Kaye et al., 2012; Mertens and Van Gaal, 2002; Nagai et al., 2008; Poirier et al., 2006; Rosito et al., 2004). A recent genome-wide screen study examined gene expression changes linked to body mass index (BMI) from white adipose tissue (WAT) of monozygotic twin pairs discordant in BMI to seek potentially causative genes (versus reactive genes) for obesity. The study identified *F13A1* (which encodes for Factor XIII-A [FXIII-A] coagulation factor) as the top, potentially causative gene expressed in WAT with the high association to obesity(Naukkarinen et al., 2010). The significant association of *F13A1* with obesity was further confirmed in a large European ENGAGE consortium study of more than 21,000 unrelated individuals as well as in the GenMets cohort study which identified 7 SNPs in *F13A1* gene associated with (BMI)[10]. These studies strongly suggest that the link between obesity and FXIII-A may differ from the link between obesity and other clotting factors in that FXIII-A may be produced by WAT and functioning in adipogenesis.

FXIII-A is a transglutaminase enzyme that stabilizes the fibrin network as the last step of the blood coagulation cascade(Ariens et al., 2000; Muszbek et al., 2011). Circulating FXIII-A exists as a dimer which is bound to an inhibitory dimeric FXIII-B subunit.

Together they form the heterotetrameric FXIII clotting factor(Muszbek et al., 2011). In contrast to most of the other clotting factors, the source of circulating FXIII-A is considered to be predominantly cells of bone marrow origin such as megakaryocytes(Poon et al., 1989; Wolpl et al., 1987). In addition to being found in plasma, FXIII-A is also found in tissues and is synthesized by various cells including macrophages, chondrocytes, osteoblasts and osteocytes, where it is found in the cytosol, nucleus and on the plasma membrane or cell surface, and in the extracellular matrix(Muszbek et al., 2011). Cellular FXIII-A activity has been shown to regulate fibroblast adhesion(Ueki et al., 1996), megakaryocyte morphology, platelet maturation(Malara et al., 2011), proliferation and migration of monocytes, macrophages and fibroblasts(Cordell et al., 2010)'(Dardik et al., 2007), and to regulate extracellular matrix synthesis and stabilization required for differentiation of cells of mesenchymal origin(Al-Jallad et al., 2006; Cui et al., 2014; Nurminskaya and Kaartinen, 2006; Nurminskaya et al., 1998). FXIII-A, as a member of the transglutaminase (TG) family, catalyzes a Ca^{2+}-dependent acyl-transfer reaction between polypeptide-bound glutamine residues and lysine residues resulting in a covalent γ-(glutamyl)-ε-lysyl bond (isopeptide crosslink / bond) that can induce the formation of multimeric protein networks, change conformation, structure, solubility, biochemical stability and cell-adhesion properties of substrate proteins(Eckert et al., 2014; Greenberg et al., 1991; Iismaa et al., 2009; Kaartinen et al., 1999; Lorand and Graham, 2003; Nelea et al., 2008; Wang et al., 2014). In addition to fibrin, a major extracellular substrate for FXIII-A is fibronectin (FN)(Mosher and Schad, 1979).

FN is an extracellular glycoprotein capable of regulating various cellular functions, including proliferation and differentiation(Singh et al., 2010; Sottile and Hocking, 2002; Sottile et al., 1998). FN is found in human and mouse WAT and in preadipocyte cultures(Lee et al., 2013b; Spiegelman and Ginty, 1983; Wang et al., 2010a), where its role is associated with inhibition of adipogenesis(Spiegelman and Ginty, 1983; Wang et al., 2010a). In the physiological setting, FN exists as two pools – as cellular FN synthesized by tissue-resident cells, and as plasma FN (pFN) produced by the liver(Singh et al., 2010). pFN has recently been shown to accumulate from the

circulation into several tissues (liver, brain, testis, heart, lungs and bone)(Bentmann et al., 2010; Moretti et al., 2007), and to contribute to the majority of the FN extracellular matrix associated with several cell types(Malara et al., 2011; Singh et al., 2010; Sottile and Hocking, 2002; Sottile et al., 1998). FXIII-A has been shown to increase FN matrix accumulation in fibroblasts(Barry and Mosher, 1988).

Given the association between the FXIII-A and obesity and its potential presence in WAT, our aim here was to explore the role of TG activity and FXIII-A in adipogenesis. Here we provide the first report demonstrating that differentiating preadipocytes have abundant TG activity which derives from FXIII-A. Our studies using 3T3-L1 preadipocytes as well as normal and *F13a1*-deficient mouse embryonic fibroblasts show that FXIII-A is located on the cell surface, where it exerts its effects via promoting soluble pFN assembly into extracellular matrix of preadipocytes. This maintains focal adhesions, promotes proliferation, and potentiates pro-proliferative effects of insulin while acting as an antagonist for adipocyte differentiation and lipid accumulation. Our work suggests a novel function for FXIII-A and circulating pFN in energy metabolism.

2.4 Materials and methods

Proteins, peptides and antibodies

Human coagulation FXIII was purchased from EMD Millipore (Billerica, MA, USA). Bovine plasma fibronectin and transglutaminase 2 from guinea pig liver were purchased from Sigma-Aldrich (St. Louis, MO, USA). Rabbit anti-human Factor XIII-A (ab97636) antibody was from Abcam (Cambridge, MA, USA), and mouse anti-human FXIII-A (A-4) was from Santa Cruz Biotechnology (Santa Cruz, CA, USA). Rabbit anti-mouse FXIII-A (675-688 peptide sequence) (polyclonal antibody) was designed and generated by GenScript corporation (Piscataway, NJ, USA)(Al-Jallad et al., 2011). Rabbit anti-dansyl antibody was from Life Technologies (Grand Island, NY, USA). Mouse anti-isopeptide antibody [81D1C2] (ab422), and mouse anti-human vinculin [SPM227] antibody were from Abcam (Cambridge, MA, USA). Mouse anti-human fibronectin antibody (EP5) was from Santa Cruz Biotechnology (Santa Cruz, CA, USA). Antibodies against rabbit anti-

Akt (pan), rabbit anti- phospho-Akt (Ser^{473})(D9E), rabbit anti-ERK1/2, rabbit anti-phospho-ERK1/2, rabbit anti-PPARγ were purchased from Cell Signalling Technology Inc. (Beverly, MA, USA). Mouse anti-EDA-FN (FN-3E2) and rabbit anti-actin antibody were obtained from Sigma-Aldrich (St Louis, MO, USA). Rabbit anti-fibronectin antibody, human recombinant MYPT1 (654-880) and rabbit anti-phospho-MYPT1 (Thr696) (used in the ROCK assay) were from EMD Millipore (Billerica, MA, USA). Horseradish peroxidase-conjugated anti-rabbit IgG was purchased from Cell Signalling Technology Inc. (Beverly, MA, USA). Horseradish peroxidase-conjugated goat anti-rabbit IgM was purchased from Santa Cruz Biotechnology (Santa Cruz, CA, USA). Horseradish peroxidase-conjugated anti-mouse, and anti-rabbit IgG, were from Jackson ImmunoResearch Inc. (West Grove, PA, USA), and Neutravidin HRP, Neutravidin agarose beads, Alexa Fluor® 488 and 596, and Alexa Fluor® 568-phalloidin were from Life Technologies (Grand Island, NY, USA). Biotin-F11 (DQMMLPWPAVAL) and biotin-F11QN (DNMMLPWPAVAL) peptides were synthesised by Biologica Co. (Nagoya, Japan) and by BIOMATIK Corporation (Cambridge, Ontario, Canada).

Reagents

Dulbecco's modified Eagle's medium (DMEM) and 0.5 mg/ml Trypsin and 0.2 mg/ml EDTA from ATCC (Cedarlane, Burlington, ON, Canada). Newborn calf serum was from HyClone via Thermo Fisher Scientific Inc (Rockford, IL, USA). Fetal bone serum and penicillin-streptomycin were from Gibco (Burlington, ON, Canada). Oil Red O, IGEPAL CA-630, dexamethasone, insulin, 3-Isobutyl-1-methylxanthine (IBMX), 3,3′,5,5′-Tetramethylbenzidine (TMB), monodansyl cadaverin were from Sigma-Aldrich (St Louis, MO, USA). Y-27632, troglitazone, LY294002, PPP and HNMPA-(AM)3 were purchased from Santa Cruz Biotechnology (Santa Cruz, CA, USA). Sulfo-NHS-LC-biotin and 5-(biotinamido)pentylamine (BPA), Disuccinimidyl suberate (DSS) cross-linker, protein G plus agarose beads were purchased from Pierce (Rockford, IL, USA). NC9 was synthesized by Gene Tech Inc (Indianapolis, IN, USA). The ECL kit was from Zmtech Scientifique (Montreal, QC, Canada). All other reagents unless otherwise specified were purchased from Sigma-Aldrich or Fisher Scientific.

Animals

F13a1-/- mice were a generous gift from Dr. Gerhardt Dickneite (Aventis Behring GMBH, Germany)(Lauer et al., 2002). Wild type (WT) mice were purchased from Jackson Laboratories (Bar Harbor, Maine, USA). Mice were kept under a normal diurnal cycle in a temperature-controlled room and fed with standard chow. Animal procedures (WAT extraction and MEF isolation) and study protocols were approved by the McGill University Animal Care Committee.

Preadipocyte cell culture, differentiation and Oil Red O staining

3T3-L1 cells (ATCC, Manassas, VA, USA) were maintained in DMEM containing 10% calf serum, 100 U/ml penicillin G, and 100 µg/ml streptomycin. Differentiation into adipocytes was induced 2 days post-confluency with 10% fetal bovine serum (FBS), 1 µM dexamethasone (DEX), 0.5 mM isobutyl-1-methylzanthine (IBMX), and 1 µg/ml insulin (INS), and is referred to as differentiation media (DM). After 2 days, the DM was replaced with maintenance medium which includes 10% FBS and 1 µg/ml insulin. After 2 days, the maintenance medium was replaced with medium containing 10% FBS, with the endpoint of the experiment being day 8. On day 8, intracellular triglyceride was stained by Oil Red O and quantified; cells were counterstained with hematoxylin and photographed with a light microscope as described previously(Bennett et al., 2002). Treatments included: NC9 and NC10 (20-40 µM), PI3-kinase inhibitor LY294002 (10 µM), biotin-F11 (DQMMLPWPAVAL) and biotin-F11QN (DNMMLPWPAVAL) peptides (50 µM), PPP (10 µM) and HNMPA-AM3 (10 µM).

Mouse embryonic fibroblast culture, differentiation and Oil Red O staining

Mouse embryonic fibroblasts (MEFs) were prepared from 13.5-day *F13a1*+/+ and *F13a1*-/- mouse(Lauer et al., 2002) embryos isolated according to a previously published protocol(Xu, 2005). MEFs were maintained and differentiated in DMEM containing 10% FBS. Post-confluent cells were differentiated into adipocytes with 10% FBS, 1 µM dexamethasone, 0.5 mM isobutyl-1-methylzanthine, 1 µg/ml insulin, and 10 µM troglitazone for 2 days. After 2 days, media was replaced with maintenance medium which includes 10% FBS and 1 µg/ml insulin and 10 µM troglitazone. On day 4,

maintenance media was replaced with medium containing 10% FBS and cells were cultured in this until the end of the experiment, being day 8. On day 8, intracellular triglycerides were stained by Oil Red O and quantified; cells were counterstained with hematoxylin and photographed with a light microscope as described previously(Bennett et al., 2002). Concentrations of used compounds were the same as for 3T3-L1 cells.

Immunohistochemistry, whole-mount staining and immunofluorescence microscopy

For immunohistochemistry, mouse WAT was fixed with 10% neutral-buffered formalin, and embedded in paraffin for histology. Deparaffinized sections were antigen-retrieved with citrate buffer (pH 6) for 15 min. Sections were peroxidase-blocked using 3% H_2O_2, and blocked for 20 min in blocking buffer (1% BSA, 2% goat serum, 0.1% Triton X-100 in PBS). Incubations with primary antibody were done overnight at 4°C. Bound primary antibodies were detected with horseradish peroxidase-conjugated secondary antibody and visualized with 3, 3′-diaminobenzidine (DAB) as the substrate. Sections were counterstained with hematoxylin. For whole-mount staining, mouse WAT was fixed in 10% neutral-buffered formalin. Fixed tissue was cut with a scalpel into 5 mm × 5 mm pieces, and blocked with 3% BSA, 0.3% Triton X-100, in PBS for 12-24 h at 4°C. Incubated with primary antibodies was done overnight at 4°C. Alexa Fluor®-conjugated secondary antibodies were incubated for 1 h at room temperature and nuclei were stained with DAPI(Koh et al., 2009). Antibody omission and isotype specific immunoglobulins were used as controls. For immunofluorescence microscopy, cells were grown in 8-well Nunc Lab-Tek® II glass chamber slides (Fisher Scientific) as indicated above. At the endpoint, cells were fixed with 3.7% formaldehyde for 30 min at room temperature or with 1% formaldehyde for 15 min at room temperature (for optimal cell-surface protein staining). Staining was done as previously described(Al-Jallad et al., 2006).

***In vitro*, *in situ* and *ECM/cell surface* transglutaminase activity assays**

In vitro TG activity of protein extracts was determined from different fat locations of WAT. WAT was collected from 6-8-week-old mice, and WAT was extracted with lysis

buffer containing 50 mM Tris-HCl (pH 8.0), 135 mM NaCl, 1% TritonX-100, 1 mM EDTA**,** 1 mM sodium orthovanadate and EDTA-free protease inhibitor cocktail (Roche Diagnostics). *In vitro* activity was determined using BPA and analyzed in microplates as described for *in situ* TG activity assay(Kaartinen et al., 2002). *In situ* TG activity was measured as described previously with some modifications(Zhang et al., 1998). Briefly, 2 mM 5-(biotinamido)pentylamine (BPA) was incubated overnight during adipocyte differentiation. At the indicated timepoint, cells were extracted with extraction buffer 50 mM Tris-HCl (pH 8.0), 135 mM NaCl, 1% Triton X-100, 1 mM EDTA**,** 1 mM sodium orthovanadate and EDTA-free protease inhibitor cocktail. Assays were done in 96-well plates (Nunc Immune Module, MaxiSorp) where 25 µg of protein extract in 50 µl of extraction buffer was incubated overnight at 4°C. Blocking was with 3% BSA, 0.1% Tween 20 in PBS for 1 h at room temperature. Wells were incubated with Neutravidin HRP for 1 h at room temperature. The peroxidase reaction was conducted in the dark in TMB (3,3',5,5'–Tetramethylbenzidine. The reaction was stopped by addition of 2 M H_2SO_4 and OD was quantified at a wavelength of 450 nm. *ECM and cell surface* TG activity was measured by an assay measuring incorporation of 5-(biotinamido)pentylamine into FN as done previously with some minor modifications(Verderio et al., 1999). Briefly, 96-well plates were coated with 10 µg/ml of bovine pFN, cells were plated at a density of 60,000 cells/cm^2 in serum-free DM in the presence of 0.1 mM BPA, with or without NC9. Cells were incubated for 2 h. After 2 h, wells were washed with 10 mM EDTA in PBS, and attached cells were removed with 0.1% DOC in PBS containing 3 mM EDTA, leaving the BPA-incorporated FN layer attached to the wells. Wells were blocked with 1% BSA in PBS (blocking buffer) for 30 min. Wells were incubated for 1 h at room temperature with Neutravidin-HRP in blocking buffer. Peroxidase activity was revealed by TMB, and the reaction was stopped with 2 M H_2SO_4. Optical density (OD) was measured at a wavelength of 450 nm using a microplate reader.

Transglutaminase substrate labelling using monodansyl cadaverine (MDC)

35-mm plates were coated with 10 µg/ml of bovine pFN, and cells were plated at a density of 60,000 cells/cm^2 in serum-free DM in the presence of 0.1 mM MDC. Cells

were incubated for 2 h. After 2 h, wells were washed with PBS and total cell lysate was prepared with extraction buffer 50 mM Tris-HCl (pH 8.0), 135 mM NaCl, 1% Triton X-100, 1 mM EDTA**,** 1 mM sodium orthovanadate and EDTA-free protease inhibitor cocktail. 30 µg of total cell extract was used for Western blotting and 300 µg for immunoprecipitation.

Cell surface biotinylation

3T3-L1 cells were cultured on 5 µg/ml plasma FN-coated plates for 2 h in serum-free DM in the presence or absence of NC9. After 2hr cells were incubated with 0.5 mg/mL sulfo-NHS-SS-biotin in PBS for 30 min at 4°C. Reactions were quenched with 50 mM Tris-HCl. Cells were lysed with 1% SDS, boiled for 5 min at 95°C, and centrifuged at 15,000 rpm for 15 minutes at room temperature. The extracts were diluted with buffer containing 50 mM Tris, pH 7.5, 100 mM NaCl, 1% Triton X-100, and 1 mM EDTA (dilution buffer), and lysates were then incubated with Neutravidin-agarose beads at 4°C overnight. The beads were washed in dilution buffer and captured protein material was released from the beads by heating at 95°C in SDS-PAGE sample buffer, followed by Western blot analysis of the material.

Biotinylation of plasma fibronectin and detection by ELISA

Biotinylation of plasma fibronectin (bpFN) was prepared as described previously(Pankov and Yamada, 2004), and 20 µg/ml was used in the cell culture experiments. A FN sandwich ELISA was done using FN monoclonal (EP5) antibody to capture FN from the total cell lysate or media. Captured FN was detected by using polyclonal FN antibody or using Neutravidin HRP for bpFN. Peroxidase activity was revealed using TMB, and the reaction was stopped with 2 M H_2SO_4. OD measured at a wavelength of 450 nm using a microplate reader.

Protein extractions, immunoprecipitation, Western blotting

Total cell lysates were prepared using lysis buffer containing 50 mM Tris-HCl (pH 8.0), 135 mM NaCl, 1% TritonX-100, 1 mM EDTA**,** 1 mM sodium orthovanadate and EDTA-free protease inhibitor cocktail (Roche Diagnostics). Extracts were centrifuged at 16,000

g for 20 min at 4°C. Cytoplasmic and cytoskeletal preparations were performed following the manufacturers' instructions using the ProteoExtract Subcellular Proteome Extraction Kit (S-PEK) (EMD Biosciences). Deoxycholate (DOC)-soluble and DOC-insoluble matrix extracts (SDS-soluble) were prepared as described previously(Pankov and Yamada, 2004). For immunoprecipitation of MDC, cell lysates were incubated with anti-dansyl antibody for 2 h on a rocker at 4°C. After 2 hr, a 50% slurry of protein A agarose beads was added and incubated with the samples overnight at 4°C to capture the immunocomplexes. Beads were washed with lysis buffer and re-suspended in Laemmli sample buffer, boiled and analyzed by Western blotting.

Immunoprecipitation of dansyl (NC9)-labelled material was done by covalently crosslinking the dansyl antibody and control IgG to protein G agarose beads as previously described with some modifications(Gordon et al., 2010). Briefly, protein G plus agarose beads were first noncovalently complexed with dansyl antibody. Unbound antibody was washed with PBS, and antibody-bound beads were re-suspended in 1 mM disuccinimidyl suberate (DSS) cross-linker, and the crosslinking reaction was performed for 1 hr at room temperature. Excess DSS was removed by washing the resin with Tris-buffered saline (TBS) (50 mM Tris, 150 mM NaCl, pH 7.2), and with 0.1 M glycine (pH 2.8) to remove free antibody. Cell lysate was prepared with ice-cold cell lysis buffer (20 mM Tris, 150 mM NaCl, 5 mM EDTA, 0.5% (wt/vol) sodium deoxycholate, and 0.5% (vol/vol) Triton X-100, pH 7.5) supplemented with 1 mM phenylmethylsulfonyl fluoride, 1 mM sodium vanadate and EDTA-free protease inhibitor cocktail (Roche Diagnostics) and incubated for 30 min on ice. The lysate was further disrupted by passage through a 25G syringe needle and centrifuged at 15,000 *g* for 15 min at 4°C, and the supernatants were transferred to a clean microcentrifuge tube and pre-cleared with protein G plus agarose beads at 4°C for 30 min. To precipitate immunocomplexes, 50 µl of antibody-protein G plus agarose complex was added and incubated over night at 4°C. Beads were washed three times with lysis buffer and eluted in 0.1 M glycine (pH 2.8), and were neutralized by addition of Tris-HCl (pH 9.2). Samples were denatured by addition of sample buffer followed by boiling for 5 min, and analyzed by Western blotting. Western blot analysis and Coomassie staining was done as described previously(Al-Jallad et al.,

2011; Al-Jallad et al., 2006). Quantification of bands was done using Image J (v1.34i, NIH).

Cell proliferation assay

Proliferation experiments were done in 96-well plates or in 60-mm plates. 3T3-L1 cells or mouse embryonic fibroblasts (MEFs) were serum-starved for 20 h after which $3x10^5$ cells/ml cells were plated and stimulated with the indicated media for 24 h followed by analysis using the MTT assay (Thiazolyl Blue Tetrazolium Bromide) as previously described(Al-Jallad et al., 2006).

Platelet-rich plasma (PRP) and plasma collection

Blood from mice was collected into tubes with 3.8% sodium citrate in a ratio of 1 part anticoagulant to 9 parts blood. Platelet-rich plasma (PRP) was obtained by centrifugation at 800*g* for 5 minutes as previously described(Kasahara et al., 2010), followed by platelet collection and protein extraction as previously described(Jayo et al., 2009). Plasma was collected in EDTA-containing tubes.

***In-vitro* human FXIII activation:**

FXIII was activated as previously published(Bagoly et al., 2008), briefly 25µg/ml of FXIII in 50mM HEPES, 100mM NaCl buffer (pH 7.4) with 2.5mM $CaCl_2$ and 10U/ml thrombin for 45min at 37^0C. After 45 min NC9 was added to the samples and incubated for another 15min at 37^0C, then the reaction was stopped by adding loading buffer and western blotted as described.

ROCK kinase activity assay

ROCK kinase activity in cell extracts was measured by a microplate *in vitro* kinase assay using human recombinant MYPT1(654-880) as substrate. Cell lysates were prepared with buffer (50 mM Tris-HCl, pH 7.5, 150 mM NaCl, 1 mM 2-glycerophosphate, 1% Triton X-100, 1 mM EDTA,1 mM EGTA, 1 mM Na_3VO_4, and EDTA-free protease inhibitor cocktail. Cell lysates were centrifuged at 14,000 rpm for 10 min and the supernatant was used for the assay. Plates (96-wells) were coated with

recombinant MYPT1 (2 µg/ml in 20 mM Tris, pH 8.5) overnight at 4°C. 5 µg of cell lysate was diluted in kinase buffer (25 mM Tris, pH 7.5, 10 mM $MgCl_2$, 5 mM β glycerophosphate, 0.1 mM Na_3VO_4, 1 mM DTT and 200 µM ATP) and incubated at 30°C for 30 min. Wells were washed and incubated with anti-phospho-MYPT1 (Thr696) for 1 h at 30°C. Wells were washed and incubated with HRP-conjugated secondary antibody for 1 h at 30°C. Peroxidase activity was revealed using TMB, and the reaction was stopped with 2 M H_2SO_4. OD measured at a wavelength of 450 nm using a microplate reader. Active ROCK II was used as a positive control.

Cell adhesion assay

Cell culture dishes (96-well plates) were coated with bovine plasma FN diluted in PBS, and incubated overnight at 4°C. Plates were blocked with 1% BSA in PBS at 37°C for 1 h. The amount of FN adsorbed onto the surface was confirmed with reverse curve fit of FN ELISA(Asthagiri et al., 2000). Cell adhesion assays were done using crystal violet as previously described(Humphries, 2001).

RT-PCR

RNA was isolated from 3T3-L1 cells using RNeasy spin columns (Qiagen). RNA was treated with DNase (New England Biolabs, Ipswich, MA, USA), and PCR was performed with SuperScript™III One-Step RT-PCR System with Platinum® Taq DNA Polymerase (Invitrogen). PCR products were analyzed by 2% agarose gel electrophoresis. Primers used were previously described, for the TGs(Al-Jallad et al., 2006), and for PPARγ2 and C/EBPα(Tanabe et al., 2004)

Statistical analysis

"n" refers to the number of times the experiments were repeated, each experiment was done in duplicates or triplicates. Error bars represent standard error of the mean (SEM). Statistical significance was assessed by unpaired ANOVA followed by Tukey's *post hoc* testing or by student's T-test using OriginPro8.0 software and Microsoft Excel respectively. *P* values are as follows: *p>0.05, **p>0.01, ***p>0.001.

2.5 Results

TG activity is present in mouse WAT, differentiating 3T3-L1 preadipocytes, and arises from FXIII-A

To investigate the role of TG activity in adipogenesis, we first examined the presence of ε-(γ-glutamyl) lysine crosslinks (isopeptide bonds) − indicative of TG activity − in mouse WAT. Immunohistochemistry demonstrated an abundance of isopeptide bonds at the periphery of adipocytes and adipose tissue stroma (**Figure 1A**). Assessment of TG activity using the BPA incorporation assay in extracts of different mouse WAT depots showed that TG activity was present in epididymal, mesentric, perirenal/retroperitoneal, inguinal, and subcutaneous WAT depots *in vivo* (**Figure 1B**). mRNA analysis of TG family members – TG1-TG7 and Factor XIII-A – in mouse WAT and in the 3T3-L1 cell line showed only *Tgm2* and *F13a1* expression (**Figure 1C).** Both enzymes were also detected by whole-mount immunofluorescence microscopy of mouse WAT (**Figure 1D**). 3T3-L1 cell line is commonly used to study adipogenesis *in vitro*, this cell line is derived from mouse embryonic fibroblasts (MEF) that can differentiate into lipid-storing adipocytes upon stimulation with differentiation medium (DM)(containing insulin, IBMX and dexamethasone). Analyses of TG expression during adipocyte differentiation of 3T3-L1 cells showed that *Tgm2* mRNA levels did not change during differentiation, whereas *F13a1* mRNA responded to differentiation medium (DM) by an initial decrease at day 1, followed by an increase at day 2, and finally gradually decreasing as the cells began to accumulate lipids (**Figure 1E**).

To determine whether TG activity was present during adipocyte differentiation, we assessed TG activity *in situ* by using 5-(biotinamido)pentylamine (BPA) incorporation assay in differentiating 3T3-L1 cells treated with DM. A dramatic and significant induction of TG activity on day 1 and 2 was observed (8-fold and 10-fold increases, respectively, compared to day 0), and this was followed by a gradual decrease in activity as the cells matured into adipocytes (**Figure 2A**). To examine which of the two TGs were active during cell differentiation, NC9 – a TG inhibitor containing a dansyl probe – was used to detect activity. NC9 incorporates irreversibly into active TG enzymes, including TG2(Caron et al., 2012) and FXIII-A(Al-Jallad et al., 2011). Here we

further demonstrate that NC9 incorporates into thrombin activated FXIII-A *in vitro* (**Figure S1A,B**), but not into nonactivated FXIII-A as shown by dansyl detection after Western blotting (WB) (**Figure S1B**). Immunofluorescence staining of cells treated with NC9 for dansyl shows co-localization with FXIII-A at the cell periphery (**Figure 2B**). No co-localization with TG2 was observed in the cells (**Figure S2**). This suggests that preadipocyte TG activity arises from FXIII-A and that TG2 may not be active as a transglutaminase or not in its open active conformation in these cells. WB detection of dansyl in cell-surface preparations of preadipocytes showed strong dansyl incorporation mostly into a protein band above 150 kDa and in lesser extend into a protein band between 50-75 kDa (**Figure 2C**). Immunoprecipitation of NC9 dansyl with dansyl antibody and detection with FXIII-A antibody demonstrated that the high molecular weight (HMW) protein is FXIII-A (**Figure 2D**). HMW FXIII-A was also detected in 3T3-L1 extracts and MEFs where it was induced upon differentiation treatment that also induced TG activity (**Figure 2E**). Since neither of the observed MWs correspond to the MW of circulating FXIII-A monomer (83 kDa), we used two anti-human FXIII-A antibodies (A-4 and ab976362) to detect mouse preadipocyte FXIII-A together with human FXIII-A as a positive control. **Figure S1A** shows Coomassie Blue staining of the nonactivated and thrombin-activated human FXIII which runs at about 75 kDa. A HMW band was seen in the gels above 150 kDa upon thrombin activation and in the WBs using the two anti-human FXIII-A antibodies (**Figure 2F,G**). This HMW FXIII-A band is likely a dimer. Comparing human FXIII-A to mouse platelet rich plasma (mPRP) and 3T3-L1 extracts showed that the mouse preparations had a FXIII-A protein of smaller MW than human FXIII-A (**Figure 2F**). Another human FXIII-A antibody (**Figure 2G**) detected two FXIII-A bands in mPRP at 75 kDa and between 50-75 kDa, strongly suggesting that mouse platelets also have a smaller MW FXIII-A. Incubation of mouse platelet extracts and mouse plasma with NC9 *in vitro* showed its clear incorporation into a band between 50-75 kDa that corresponds to the smaller, monomer FXIII-A found in preadipocytes (**Figure 2H).** The fact that ultimately two FXIII-A forms are detected in platelets suggests that the smaller form may be proteolytically cleaved from the full length FXIII-A. Collectively, these results suggest that preadipocyte FXIII-A may be a

cleaved form that complexes/dimerizes and gets activated at the cell surface of preadipocytes.

FXIII-A acts as an antagonist for adipogenesis

Given the high level of FXIII-A activity during adipocyte differentiation, we asked if the activity is required for cell differentiation. As shown in **Figure 3A**, NC9 significantly and in a concentration-dependent manner increased lipid accumulation and lipid droplet size in adipocytes. Control compound NC10, lacking the warhead acryloyl group did not have an effect on adipogenesis (**Figure S3).** NC9 was most efficient in promoting lipid accumulation when given to 3T3-L1 cells between days 0 to 4, which enhanced lipid accumulation to the same extent as a full 8-day treatment. A significant increase in lipid accumulation was also seen when the inhibitor was given between days 0 and 2, and a decrease in lipid accumulation was observed in treatments occurring during days 4-8 (**Figure 3B**). Similar results were observed with mouse embryonic fibroblasts (MEFs), whose differentiation into adipocytes was promoted by NC9 in both a dose- and time-dependent manner (**Figure S4**). WB analysis and quantification of the adipogenic transcription factor PPARγ showed a significant increase in NC9-treated cells (1.5-fold) when compared to the control (**Figure 3C,D**). Analysis of PI3K/Akt signalling – the main regulator of PPARγ expression(Aubin et al., 2005; Kim and Chen, 2004) – showed significant changes: *i*) Akt phosphorylation was increased (1.5-fold) on day 1 following NC9 treatment (**Figure 3E,F)**, and *ii*) LY294002 − a PI3K inhibitor − reversed the increase in differentiation caused by NC9 (**Figure 3G)**. Since inhibition of FXIII-A activity stimulated PI3K/Akt signalling, we differentiated cells with partial hormonal stimulation (DEX and IBMX only, no insulin) in the presence and absence of NC9. Remarkably, inhibition of FXIII-A activity induced differentiation at a level similar to insulin stimulation (**Figure 3H**). Collectively, these data strongly suggest that preadipocyte FXIII-A acts as an antagonist during the early phase of adipogenesis. No FXIII-A was detected in fetal bovine serum used in the preadipocyte cultures (**Figure S5**) and thus its contribution to the observed effects can be excluded.

FXIII-A activity promotes actin dynamics and focal adhesion formation in preadipocytes by crosslinking fibronectin

In the search of mechanisms for how preadipocyte FXIII-A inhibits adipogenesis and the P13K/Akt pathway, we considered that TG activity has been linked with cell-matrix interactions(Zemskov et al., 2006), and that during adipocyte differentiation preadipocytes undergo a major morphological change where the transition from fibroblast-like (preadipocytes) cells to rounded (adipocyte) cells is associated with extensive cytoskeletal and matrix remodelling(Cristancho and Lazar, 2011; Croissandeau et al., 2002; Feng et al., 2010; Meyers et al., 2005). Examination of cytoskeletal dynamics in NC9-treated preadipocytes plated on fibronectin under serum-free conditions showed that the inhibitor dramatically reduced actin stress fiber formation, and increased cortical actin assembly, compared to control cells. This was also associated with reduced focal adhesion assembly as seen by a lack of vinculin co-localization with actin stress fibres (**Figure 4A**). WB analysis of subcellular fractions of these cells showed redistribution of vinculin from the cytoskeleton to the cytosol upon NC9 treatment (**Figure S6A**). Furthermore, NC9 also reduced preadipocyte adhesion (**Figure S6B**), and ROCK kinase activity (**Figure S6C**), necessary for the maintenance of actin stress fibres and focal adhesions(Amano et al., 2010; Noguchi et al., 2007; Sit and Manser, 2011). The dansyl group of NC9 was detected on the cell periphery of preadipocytes by immunofluorescence microscopy which was associated with reduction of actin stress fibers and rounding of the cells (**Figure 4B**). These results show that FXIII-A on the cell surface of preadipocytes promotes cell adhesion, actin stress fiber formation and focal adhesion assembly. To examine FXIII-A substrates in these cultures, we conducted *in situ* labelling of preadipocytes with monodansylcadaverine (MDC) which incorporates covalently into TG-reactive Q residues of TG substrate proteins. MDC was found in protein(s) having a molecular weight of 250 kDa (**Figure 4C**), which corresponds to FN (monomer). FN is one of the major extracellular FXIII-A substrates also linked to cytoskeletal dynamics(Corbett et al., 1997; Hoffmann et al., 2011; Mosher, 1978). To examine whether the FXIII-A activity crosslinks (and labels) extracellular FN in preadipocyte cultures, MDC-labelled cells were immunoprecipitated using dansyl antibody and detected with FN antibody – this showed that the coated FN

is a TG substrate in these cultures (**Figure 4C**). The effect of NC9 on FN labelling in the cultures was examined by an *in situ* TG activity assay, where BPA incorporation by the cells onto coated FN was quantified(Verderio et al., 1999). NC9 decreased the amount of BPA incorporated into FN outside the cells by 50% compared to the DM-treated preadipocyte control (**Figure 4D**). In summary, these results confirmed that FXIII-A activity is predominantly found at the cell surface of preadipocytes, and that FN is a major crosslinking substrate in the extracellular compartment.

FXIII-A activity is required for plasma FN matrix assembly and preadipocyte proliferation

We next investigated the function of FXIII-A activity with regard to the role of FN in preadipocytes. ELISA analysis of FN levels in cell layers showed increased levels of FN associated with initiation of differentiation, reaching a maximum by day 2; by day 4, FN levels decreased to the day 0 level (**Figure 5A**). This pattern was similar to the pattern of TG activity in the cultures as shown in **Figure 2A**. FN can be assembled into the cell layers as extracellular matrix from two pools of FN – from circulating plasma FN (pFN) made by hepatocytes in liver (present in the serum used in cell cultures) and from cellular FN (cFN) synthesized by tissue-resident cells(Moretti et al., 2007; Singh et al., 2010). Both forms can be found as DOC-soluble and DOC-insoluble matrix. To investigate whether both pFN and cFN were substrates for FXIII-A activity, cell cultures were labelled with BPA, and the labelled material was affinity-purified and detected with FN antibody (detects all FN) and EDA-FN (cFN) antibody. Detection in this way showed labelling of only total FN but not cFN (EDA-FN), suggesting that only pFN is a substrate for TG activity (**Figure 5B**). To further confirm that FXIII-A in preadipocytes crosslinks pFN, we used a FXIII-A-specific substrate peptide – bF11 – which is a biotinylated peptide containing a reactive glutamine (Q) residue(Sugimura et al., 2006); this peptide is capable of incorporating into substrates only when FXIII-A is active. Cells were labelled with bF11 or control F11QN (where the Q is replaced by asparagine [N]) for 24 h and pulled down with Neutravidin beads. WB showed clear detection of total FN with bF11 but not with control bF11QN. NC9 blocked FN labelling by bF11 (**Figure 5C**). To further demonstrate that FXIII-A promotes pFN incorporation into matrix in preadipocyte

cultures, cells were given exogenous biotinylated pFN (bpFN) in a 'pulse/chase' experiment. Fluorescence microscopy of the bpFN matrix network showed that FXIII-A inhibition decreased FN assembly in preadipocyte cultures (**Figure 5D**). Levels of bpFN were analyzed from media and from DOC-soluble and DOC-insoluble extracts after 24 h incubation. These data show *i*) a significantly higher level of bpFN retained in the media in NC9-treated cultures (**Figure 5E**), *ii*) intracellular FN (icFN) levels, analyzed from trypsinized cells, which showed no change upon NC9 treatment demonstrating that FN production was neither increased or decreased (**Figure 5F**), and *iii*) significantly lower bpFN levels in both DOC-soluble and DOC-insoluble matrix by NC9 treatment (**Figure 5G,H).** These data suggest that FXIII-A activity on the preadipocyte surface is specifically directed towards assembling a soluble form of pFN into preadipocyte extracellular matrix. Adding recombinant, soluble FXIII-A (activated) to the 3T3-L1 cultures, along with bpFN, did not result in organized fibrillogenesis but rather aggregated bpFN resulting in an increase in lipid accumulation (data not shown). This suggests that soluble FXIII-A may not promote bpFN fibrillogenesis in preadipocyte cultures.

After initiation of differentiation, 3T3-L1 cells undergo mitotic clonal expansion for 48 to 72 h, which coincides with the increased FXIII-A activity (**Figure 2A**) and increased levels of FN in cell layers. Thus, we hypothesized that FXIII-A activity regulates pFN matrix assembly to promote preadipocyte proliferation. Proliferation was assessed by plating cells under serum-free conditions on pFN-coated plates or by supplementing the media with pFN. Proliferation assays showed that both ways of exposing the cells to pFN increased preadipocyte proliferation in a concentration-dependent manner (**Figure 6A**). A blocking antibody against EDA-FN further increased preadipocyte proliferation, suggesting that pFN and EDA-FN may have opposing functions in preadipocytes (**Figure 6B).** Cell proliferation can be induced by FN and by soluble mitogens such as insulin(Asthagiri et al., 2000). Since insulin was a component of the differentiation media for preadipocytes, we examined the combined effects of insulin and pFN on preadipocyte proliferation. The analyses showed a significant 4-fold increase in proliferation by insulin-pFN treatment compared to pFN treatment alone, demonstrating

a synergistic effect. The pro-proliferative effect was dependent on FXIII-A activity since NC9 significantly attenuated these effects for both the pFN treatment alone and the insulin-pFN treatment combination (**Figure 6C**). It is known that insulin mediates cell proliferation via activating the MAPK/Erk pathway(Pages et al., 1993). Analysis of Erk phosphorylation levels in pFN- and insulin-treated preadipocytes showed that NC9 decreased the sustained Erk phosphorylation in these cells in both serum and serum-free conditions (**Figure S7**). To examine whether insulin effects are mediated through the insulin-like growth factor receptor (IGFR) or through the insulin receptor (IR), we inhibited both receptors and assessed cell proliferation. As seen in **Figure 6D**, only the IR inhibitor (HNMPA-(AM)3 was able to decrease the combined pro-proliferative effects of pFN and insulin. Inhibition of IGFR with its specific inhibitor PPP had an opposite effect and promoted cell proliferation. These results indicate that FXIII-A-mediated assembly of pFN is required for proliferation of preadipocytes and can potentiate the pro-proliferative effects of insulin.

F13a1-/- MEFs show reduced cell adhesion, proliferation and increased adipogenesis

To confirm the role of FXIII-A in adipocyte function, we examined the ability of *F13a1*-/- MEFs to proliferate and to differentiate into adipocytes. Compared to *F13a1*+/+ cells, *F13a1*-/- MEFs exhibited a 30% increase in lipid accumulation (**Figure 7A and Figure S8A**) and decreased cell adhesion to pFN (**Figure S8B**). mRNA expression of *F13a1* and *Tgm2* were not altered during differentiation of *F13a1*+/+ MEFs (**Figure S8C**). *F13a1*-/- MEFs also showed a significant decrease in their ability to proliferate and a decreased response to the proliferative effects of exogenous pFN supplemented into the serum-free media. The *F13a1*-/- MEFs also showed an overall reduced proliferative response to insulin with or without exogenous pFN (**Figure 7B**). Fluorescence microscopy of bpFN in MEFs showed that *F13a1*-/- cells assembled bpFN poorly into the fibrillar matrix as compared to *F13a1*+/+ cells (**Figure 7C)**. These data show that pFN constitutes the majority of the total FN extracellular matrix in preadipocytes/MEFs and requires FXIII-A for its assembly.

2.6 Discussion

Recent genome-wide association studies of human WAT identified *F13A1* as a potentially causative gene for obesity(Naukkarinen et al., 2010), suggesting that FXIII-A may be linked to adipose tissue function. In our study, we provide the first set of evidence showing that WAT has abundant FXIII-A activity and how FXIII-A can be linked to adipogenesis. FXIII-A enzyme was localized to the preadipocyte surface where it assisted in assembling pFN into the matrix to promote cell proliferation and to potentiate the pro-proliferative effects of insulin. This antagonized the pro-differentiating effects of insulin on preadipocytes (**Figure 7 D, E**). FXIII-A, jointly with pFN, maintained preadipocytes in an undifferentiated state by modulating cytoskeletal dynamics. Thus, we conclude that FXIII-A acts as a negative regulator of adipogenesis. Our study also demonstrated that preadipocytes express TG2; however, TG activity probe and inhibitor NC9 did not covalently incorporate into TG2 based on immunofluorescence data indicating that it is not active as a TG enzyme. However, since its function has been strongly linked to cytoskeletal dynamics(Zemskov et al., 2006) it may also contribute to maintenance of the cytoskeleton of preadipocytes/adipocytes via mechanism that does not involve its TG activity.

Preadipocyte differentiation into lipid-accumulating mature adipocytes is part of normal adipose tissue function and is critical for storage and elimination of lipids from the circulation. Preadipocyte proliferation is required for adipose tissue expansion to accommodate the increased requirement for energy storage in obesity. Failure to accumulate lipids or to expand adipose tissue results in increased circulating fatty acids and their ectopic storage in non-metabolic tissues which is a major contributor to the development of insulin resistance(Bays et al., 2008; Gregoire et al., 1998; Poulos et al., 2010; Rosen and MacDougald, 2006; Waki and Tontonoz, 2007). Our results show that FXIII-A, jointly with pFN, increases preadipocyte proliferation, but inhibits lipid accumulation. The role of FN as a negative regulator of adipogenesis *in vitro* has been demonstrated in mouse and human preadipocytes where it inhibits lipid accumulation by blocking the morphological and cytoskeletal changes necessary for lipid accumulation(Croissandeau et al., 2002; Hudak and Sul, 2013; Selvarajan et al., 2001;

Taleb et al., 2006; Wang et al., 2010a). Our work is the first to demonstrate that pFN, synthesized by hepatocytes in liver, contributes to adipogenesis. This adds to the list of tissues (liver, brain, testis, heart, lungs and bone(Bentmann et al., 2010; Moretti et al., 2007)) and cell types that have been shown to accumulate pFN for their function(Sottile and Hocking, 2002; Sottile et al., 1998). Furthermore, while FN matrix is clearly an important component of WAT and preadipocyte cultures, its actual function has remained elusive. Our work shows that preadipocytes use pFN matrix for proliferation, and that this matrix sensitizes the cells for the pro-proliferative effects of insulin. Vascularization of WAT is critical for adipose tissue expansion during increased need for energy storage; it is likely that pFN is one of the circulating factors that can regulate this tissue expansion.

The transition of preadipocytes from a proliferation phase to a differentiation phase is reflected by changes in cell morphology accompanied by major remodelling of extracellular matrix components. While preadipocytes themselves regulate synthesis and degradation of collagen and laminin matrices(Lilla et al., 2002), the pFN matrix accumulation appears to be regulated by the presence of FXIII-A in the cells. pFN levels in preadipocyte cultures follow the pattern of *F13a1* mRNA and enzyme activity, and a decrease in FN matrix was associated with decreased *F13a1* mRNA levels by the cells. Thus, FXIII-A regulation in preadipocytes may be part of the transition between the proliferative and differentiation states (**Figure 7A**). The preadipocyte FXIII-A is found on the cell surface mostly as a complex form. Similar HMW FXIII-A was found to form upon activation of human FXIII *in vitro* suggesting that preadipocyte cell surface FXIII-A may be a covalent, active dimer. Whether this preadipocyte FXIII-A requires further proteolytic activation remains unknown; however, it is possible that the observed dimerization/complexation, together increased Ca^{2+} levels, and binding to substrate in the extracellular space, suffices to induce activity. Of interest is also the observation that preadipocytes produce mostly FXIII-A monomer of lower MW. This form is also found in platelets which produce two forms as per to our antibody detection data. Thus, it is possible that this smaller monomer FXIII-A, in both platelets and adipocytes, is a

proteolytically cleaved form arising from the full length FXIII-A, and that the cleavage process could be linked to mechanisms on how FXIII-A is anchored to the cell surface.

FXIII-A deficiency in humans results in a rare blood-clotting defect(Ariens et al., 2002). There are no reports of energy metabolism dysregulation or BMI-linked abnormalities in FXIII-A-deficient patients; however, circulating FXIII-A levels are increased in type 2 diabetics(Mansfield et al., 2000). Thus, it is possible that obesity-linked *F13A1* SNPs in WAT discovered in the ENGAGE study(Naukkarinen et al., 2010) may have effects on FXIII-A function only locally in adipose tissue, while having no effects on coagulation or other cellular processes. Indeed, a specific regulation, modification and function of FXIII-A in WAT is supported by the observation that the Finnish twins discordant in BMI and having altered FXIII-A expression in WAT, have normal FXIII-A levels in blood(Kaye et al., 2012). Similarly, the FXIII-A Val34Leu polymorphism – which results in increased enzyme activation – has a protective effect against coronary artery disease(Muszbek et al., 2011; Muszbek et al., 2010), but is not linked to obesity(Naukkarinen et al., 2010). In conclusion, our study shows the presence and relevance of FXIII-A in adipose tissue and preadipocytes, suggesting a mechanism by which FXIII-A might be linked to obesity and weight gain. Elucidating the full metabolic phenotype of *F13a1*-/- mice, and understanding how FXIII-A is modulated, processed, secreted and anchored to the cell surface in adipocytes in the normal versus the obese state, can provide valuable information how to regulate adipose tissue health.

2.7 Acknowledgements

We would like to thank Aisha Mousa for assistance. This study was supported by grants to MTK from the Canadian Institutes of Health Research (CIHR) and the CIHR Institute of Genetics. KH was supported by a Grant-in-Aid for Scientific Research (B) (No. 23380200) from JSPS, Japan (KH). VDM received stipends from Faculty of Dentistry and the CIHR Systems Biology Training Program.

Conflict of interest

The authors declare no competing financial interest.

2.8 References

Al-Jallad, H.F., Myneni, V.D., Piercy-Kotb, S.A., Chabot, N., Mulani, A., Keillor, J.W., and Kaartinen, M.T. (2011). Plasma membrane factor XIIIA transglutaminase activity regulates osteoblast matrix secretion and deposition by affecting microtubule dynamics. PloS one *6*, e15893.

Al-Jallad, H.F., Nakano, Y., Chen, J.L., McMillan, E., Lefebvre, C., and Kaartinen, M.T. (2006). Transglutaminase activity regulates osteoblast differentiation and matrix mineralization in MC3T3-E1 osteoblast cultures. Matrix biology : journal of the International Society for Matrix Biology *25*, 135-148.

Amano, M., Nakayama, M., and Kaibuchi, K. (2010). Rho-kinase/ROCK: A key regulator of the cytoskeleton and cell polarity. Cytoskeleton (Hoboken, N.J.) *67*, 545-554.

Ariens, R.A., Lai, T.S., Weisel, J.W., Greenberg, C.S., and Grant, P.J. (2002). Role of factor XIII in fibrin clot formation and effects of genetic polymorphisms. Blood *100*, 743-754.

Ariens, R.A., Philippou, H., Nagaswami, C., Weisel, J.W., Lane, D.A., and Grant, P.J. (2000). The factor XIII V34L polymorphism accelerates thrombin activation of factor XIII and affects cross-linked fibrin structure. Blood *96*, 988-995.

Asthagiri, A.R., Reinhart, C.A., Horwitz, A.F., and Lauffenburger, D.A. (2000). The role of transient ERK2 signals in fibronectin- and insulin-mediated DNA synthesis. Journal of cell science *113 Pt 24*, 4499-4510.

Aubin, D., Gagnon, A., and Sorisky, A. (2005). Phosphoinositide 3-kinase is required for human adipocyte differentiation in culture. International journal of obesity (2005) *29*, 1006-1009.

Bagoly, Z., Fazakas, F., Komaromi, I., Haramura, G., Toth, E., and Muszbek, L. (2008). Cleavage of factor XIII by human neutrophil elastase results in a novel active truncated form of factor XIII A subunit. Thrombosis and haemostasis *99*, 668-674.

Barry, E.L., and Mosher, D.F. (1988). Factor XIII cross-linking of fibronectin at cellular matrix assembly sites. The Journal of biological chemistry *263*, 10464-10469.

Bays, H.E., Gonzalez-Campoy, J.M., Bray, G.A., Kitabchi, A.E., Bergman, D.A., Schorr, A.B., Rodbard, H.W., and Henry, R.R. (2008). Pathogenic potential of adipose tissue and metabolic consequences of adipocyte hypertrophy and increased visceral adiposity. Expert review of cardiovascular therapy *6*, 343-368.

Bennett, C.N., Ross, S.E., Longo, K.A., Bajnok, L., Hemati, N., Johnson, K.W., Harrison, S.D., and MacDougald, O.A. (2002). Regulation of Wnt signaling during adipogenesis. The Journal of biological chemistry *277*, 30998-31004.

Bentmann, A., Kawelke, N., Moss, D., Zentgraf, H., Bala, Y., Berger, I., Gasser, J.A., and Nakchbandi, I.A. (2010). Circulating fibronectin affects bone matrix, whereas osteoblast fibronectin modulates osteoblast function. Journal of bone and mineral research : the official journal of the American Society for Bone and Mineral Research *25*, 706-715.

Caron, N.S., Munsie, L.N., Keillor, J.W., and Truant, R. (2012). Using FLIM-FRET to measure conformational changes of transglutaminase type 2 in live cells. PloS one *7*, e44159.

Christakis, N.A., and Fowler, J.H. (2007). The spread of obesity in a large social network over 32 years. The New England journal of medicine *357*, 370-379.

Corbett, S.A., Lee, L., Wilson, C.L., and Schwarzbauer, J.E. (1997). Covalent cross-linking of fibronectin to fibrin is required for maximal cell adhesion to a fibronectin-fibrin matrix. The Journal of biological chemistry *272*, 24999-25005.

Cordell, P.A., Kile, B.T., Standeven, K.F., Josefsson, E.C., Pease, R.J., and Grant, P.J. (2010). Association of coagulation factor XIII-A with Golgi proteins within monocyte-macrophages: implications for subcellular trafficking and secretion. Blood *115*, 2674-2681.

Cristancho, A.G., and Lazar, M.A. (2011). Forming functional fat: a growing understanding of adipocyte differentiation. Nature reviews. Molecular cell biology *12*, 722-734.

Croissandeau, G., Chretien, M., and Mbikay, M. (2002). Involvement of matrix metalloproteinases in the adipose conversion of 3T3-L1 preadipocytes. The Biochemical journal *364*, 739-746.

Cui, C., Wang, S., Myneni, V.D., Hitomi, K., and Kaartinen, M.T. (2014). Transglutaminase activity arising from Factor XIIIA is required for stabilization and conversion of plasma fibronectin into matrix in osteoblast cultures. Bone *59*, 127-138.

Dardik, R., Krapp, T., Rosenthal, E., Loscalzo, J., and Inbal, A. (2007). Effect of FXIII on monocyte and fibroblast function. Cellular physiology and biochemistry : international journal of experimental cellular physiology, biochemistry, and pharmacology *19*, 113-120.

Eckert, R.L., Kaartinen, M.T., Nurminskaya, M., Belkin, A.M., Colak, G., Johnson, G.V., and Mehta, K. (2014). Transglutaminase regulation of cell function. Physiological reviews *94*, 383-417.

Feng, T., Szabo, E., Dziak, E., and Opas, M. (2010). Cytoskeletal disassembly and cell rounding promotes adipogenesis from ES cells. Stem cell reviews *6*, 74-85.

Gesta, S., Tseng, Y.H., and Kahn, C.R. (2007). Developmental origin of fat: tracking obesity to its source. Cell *131*, 242-256.

Gordon, J.A., Hassan, M.Q., Saini, S., Montecino, M., van Wijnen, A.J., Stein, G.S., Stein, J.L., and Lian, J.B. (2010). Pbx1 represses osteoblastogenesis by blocking Hoxa10-mediated recruitment of chromatin remodeling factors. Molecular and cellular biology *30*, 3531-3541.

Greenberg, C.S., Birckbichler, P.J., and Rice, R.H. (1991). Transglutaminases: multifunctional cross-linking enzymes that stabilize tissues. FASEB journal : official publication of the Federation of American Societies for Experimental Biology *5*, 3071-3077.

Gregoire, F.M., Smas, C.M., and Sul, H.S. (1998). Understanding adipocyte differentiation. Physiological reviews *78*, 783-809.

Hoffmann, B.R., Annis, D.S., and Mosher, D.F. (2011). Reactivity of the N-terminal region of fibronectin protein to transglutaminase 2 and factor XIIIA. The Journal of biological chemistry *286*, 32220-32230.

Hudak, C.S., and Sul, H.S. (2013). Pref-1, a gatekeeper of adipogenesis. Frontiers in endocrinology *4*, 79.

Humphries, M.J. (2001). Cell-substrate adhesion assays. Current protocols in cell biology / editorial board, Juan S. Bonifacino ... [et al.] *Chapter 9*, Unit 9.1.

Iismaa, S.E., Mearns, B.M., Lorand, L., and Graham, R.M. (2009). Transglutaminases and disease: lessons from genetically engineered mouse models and inherited disorders. Physiological reviews *89*, 991-1023.

Jayo, A., Conde, I., Lastres, P., Jimenez-Yuste, V., and Gonzalez-Manchon, C. (2009). New insights into the expression and role of platelet factor XIII-A. Journal of thrombosis and haemostasis : JTH *7*, 1184-1191.

Kaartinen, M.T., El-Maadawy, S., Rasanen, N.H., and McKee, M.D. (2002). Tissue transglutaminase and its substrates in bone. Journal of bone and mineral research : the official journal of the American Society for Bone and Mineral Research *17*, 2161-2173.

Kaartinen, M.T., Pirhonen, A., Linnala-Kankkunen, A., and Maenpaa, P.H. (1999). Cross-linking of osteopontin by tissue transglutaminase increases its collagen binding properties. The Journal of biological chemistry *274*, 1729-1735.

Kasahara, K., Souri, M., Kaneda, M., Miki, T., Yamamoto, N., and Ichinose, A. (2010). Impaired clot retraction in factor XIII A subunit-deficient mice. Blood *115*, 1277-1279.

Kaye, S.M., Pietilainen, K.H., Kotronen, A., Joutsi-Korhonen, L., Kaprio, J., Yki-Jarvinen, H., Silveira, A., Hamsten, A., Lassila, R., and Rissanen, A. (2012). Obesity-related derangements of coagulation and fibrinolysis: a study of obesity-discordant monozygotic twin pairs. Obesity (Silver Spring, Md.) *20*, 88-94.

Kim, J.E., and Chen, J. (2004). regulation of peroxisome proliferator-activated receptor-gamma activity by mammalian target of rapamycin and amino acids in adipogenesis. Diabetes *53*, 2748-2756.

Koh, Y.J., Park, B.H., Park, J.H., Han, J., Lee, I.K., Park, J.W., and Koh, G.Y. (2009). Activation of PPAR gamma induces profound multilocularization of adipocytes in adult mouse white adipose tissues. Experimental & molecular medicine *41*, 880-895.

Lauer, P., Metzner, H.J., Zettlmeissl, G., Li, M., Smith, A.G., Lathe, R., and Dickneite, G. (2002). Targeted inactivation of the mouse locus encoding coagulation factor XIII-A: hemostatic abnormalities in mutant mice and characterization of the coagulation deficit. Thrombosis and haemostasis *88*, 967-974.

Lee, S.H., Park, H.S., Lee, J.A., Song, Y.S., Jang, Y.J., Kim, J.H., Lee, Y.J., and Heo, Y. (2013). Fibronectin gene expression in human adipose tissue and its associations with obesity-related genes and metabolic parameters. Obesity surgery *23*, 554-560.

Lilla, J., Stickens, D., and Werb, Z. (2002). Metalloproteases and adipogenesis: a weighty subject. The American journal of pathology *160*, 1551-1554.

Lorand, L., and Graham, R.M. (2003). Transglutaminases: crosslinking enzymes with pleiotropic functions. Nature reviews. Molecular cell biology *4*, 140-156.

Malara, A., Gruppi, C., Rebuzzini, P., Visai, L., Perotti, C., Moratti, R., Balduini, C., Tira, M.E., and Balduini, A. (2011). Megakaryocyte-matrix interaction within bone marrow: new roles for fibronectin and factor XIII-A. Blood *117*, 2476-2483.

Malis, C., Rasmussen, E.L., Poulsen, P., Petersen, I., Christensen, K., Beck-Nielsen, H., Astrup, A., and Vaag, A.A. (2005). Total and regional fat distribution is strongly influenced by genetic factors in young and elderly twins. Obesity research *13*, 2139-2145.

Mansfield, M.W., Kohler, H.P., Ariens, R.A., McCormack, L.J., and Grant, P.J. (2000). Circulating levels of coagulation factor XIII in subjects with type 2 diabetes and in their first-degree relatives. Diabetes care *23*, 703-705.

Mertens, I., and Van Gaal, L.F. (2002). Obesity, haemostasis and the fibrinolytic system. Obesity reviews : an official journal of the International Association for the Study of Obesity *3*, 85-101.

Meyers, V.E., Zayzafoon, M., Douglas, J.T., and McDonald, J.M. (2005). RhoA and cytoskeletal disruption mediate reduced osteoblastogenesis and enhanced adipogenesis of human mesenchymal stem cells in modeled microgravity. Journal of

bone and mineral research : the official journal of the American Society for Bone and Mineral Research *20*, 1858-1866.

Moretti, F.A., Chauhan, A.K., Iaconcig, A., Porro, F., Baralle, F.E., and Muro, A.F. (2007). A major fraction of fibronectin present in the extracellular matrix of tissues is plasma-derived. The Journal of biological chemistry *282*, 28057-28062.

Mosher, D.F. (1978). Cross-linking of plasma and cellular fibronectin by plasma transglutaminase. Annals of the New York Academy of Sciences *312*, 38-42.

Mosher, D.F., and Schad, P.E. (1979). Cross-linking of fibronectin to collagen by blood coagulation Factor XIIIa. The Journal of clinical investigation *64*, 781-787.

Muszbek, L., Bereczky, Z., Bagoly, Z., Komaromi, I., and Katona, E. (2011). Factor XIII: a coagulation factor with multiple plasmatic and cellular functions. Physiological reviews *91*, 931-972.

Muszbek, L., Bereczky, Z., Bagoly, Z., Shemirani, A.H., and Katona, E. (2010). Factor XIII and atherothrombotic diseases. Seminars in thrombosis and hemostasis *36*, 18-33.

Nagai, N., Hoylaerts, M.F., Cleuren, A.C., Van Vlijmen, B.J., and Lijnen, H.R. (2008). Obesity promotes injury induced femoral artery thrombosis in mice. Thrombosis research *122*, 549-555.

Naukkarinen, J., Surakka, I., Pietilainen, K.H., Rissanen, A., Salomaa, V., Ripatti, S., Yki-Jarvinen, H., van Duijn, C.M., Wichmann, H.E., Kaprio, J., et al. (2010). Use of genome-wide expression data to mine the "Gray Zone" of GWA studies leads to novel candidate obesity genes. PLoS genetics *6*, e1000976.

Nelea, V., Nakano, Y., and Kaartinen, M.T. (2008). Size distribution and molecular associations of plasma fibronectin and fibronectin crosslinked by transglutaminase 2. The protein journal *27*, 223-233.

Noguchi, M., Hosoda, K., Fujikura, J., Fujimoto, M., Iwakura, H., Tomita, T., Ishii, T., Arai, N., Hirata, M., Ebihara, K., et al. (2007). Genetic and pharmacological inhibition of Rho-associated kinase II enhances adipogenesis. The Journal of biological chemistry *282*, 29574-29583.

Nurminskaya, M., and Kaartinen, M.T. (2006). Transglutaminases in mineralized tissues. Frontiers in bioscience : a journal and virtual library *11*, 1591-1606.

Nurminskaya, M., Magee, C., Nurminsky, D., and Linsenmayer, T.F. (1998). Plasma transglutaminase in hypertrophic chondrocytes: expression and cell-specific intracellular activation produce cell death and externalization. The Journal of cell biology *142*, 1135-1144.

Pages, G., Lenormand, P., L'Allemain, G., Chambard, J.C., Meloche, S., and Pouyssegur, J. (1993). Mitogen-activated protein kinases p42mapk and p44mapk are

required for fibroblast proliferation. Proceedings of the National Academy of Sciences of the United States of America *90*, 8319-8323.

Pankov, R., and Yamada, K.M. (2004). Non-radioactive quantification of fibronectin matrix assembly. Current protocols in cell biology / editorial board, Juan S. Bonifacino ... [et al.] *Chapter 10*, Unit 10.13.

Poirier, P., Giles, T.D., Bray, G.A., Hong, Y., Stern, J.S., Pi-Sunyer, F.X., and Eckel, R.H. (2006). Obesity and cardiovascular disease: pathophysiology, evaluation, and effect of weight loss. Arteriosclerosis, thrombosis, and vascular biology *26*, 968-976.

Poon, M.C., Russell, J.A., Low, S., Sinclair, G.D., Jones, A.R., Blahey, W., Ruether, B.A., and Hoar, D.I. (1989). Hemopoietic origin of factor XIII A subunits in platelets, monocytes, and plasma. Evidence from bone marrow transplantation studies. The Journal of clinical investigation 84, 787-792.

Poulos, S.P., Hausman, D.B., and Hausman, G.J. (2010). The development and endocrine functions of adipose tissue. Molecular and cellular endocrinology 323, 20-34.

Rosen, E.D., and MacDougald, O.A. (2006). Adipocyte differentiation from the inside out. Nature reviews. Molecular cell biology 7, 885-896.

Rosito, G.A., D'Agostino, R.B., Massaro, J., Lipinska, I., Mittleman, M.A., Sutherland, P., Wilson, P.W., Levy, D., Muller, J.E., and Tofler, G.H. (2004). Association between obesity and a prothrombotic state: the Framingham Offspring Study. Thrombosis and haemostasis 91, 683-689.

Selvarajan, S., Lund, L.R., Takeuchi, T., Craik, C.S., and Werb, Z. (2001). A plasma kallikrein-dependent plasminogen cascade required for adipocyte differentiation. Nature cell biology 3, 267-275.

Singh, P., Carraher, C., and Schwarzbauer, J.E. (2010). Assembly of fibronectin extracellular matrix. Annual review of cell and developmental biology 26, 397-419.

Sit, S.T., and Manser, E. (2011). Rho GTPases and their role in organizing the actin cytoskeleton. Journal of cell science 124, 679-683.

Sottile, J., and Hocking, D.C. (2002). Fibronectin polymerization regulates the composition and stability of extracellular matrix fibrils and cell-matrix adhesions. Molecular biology of the cell 13, 3546-3559.

Sottile, J., Hocking, D.C., and Swiatek, P.J. (1998). Fibronectin matrix assembly enhances adhesion-dependent cell growth. Journal of cell science 111 (Pt 19), 2933-2943.

Spiegelman, B.M., and Ginty, C.A. (1983). Fibronectin modulation of cell shape and lipogenic gene expression in 3T3-adipocytes. Cell 35, 657-666.

Sugimura, Y., Hosono, M., Wada, F., Yoshimura, T., Maki, M., and Hitomi, K. (2006). Screening for the preferred substrate sequence of transglutaminase using a phage-displayed peptide library: identification of peptide substrates for TGASE 2 and Factor XIIIA. The Journal of biological chemistry 281, 17699-17706.

Taleb, S., Cancello, R., Clement, K., and Lacasa, D. (2006). Cathepsin s promotes human preadipocyte differentiation: possible involvement of fibronectin degradation. Endocrinology 147, 4950-4959.

Tanabe, Y., Koga, M., Saito, M., Matsunaga, Y., and Nakayama, K. (2004). Inhibition of adipocyte differentiation by mechanical stretching through ERK-mediated downregulation of PPARgamma2. Journal of cell science 117, 3605-3614.

Ueki, S., Takagi, J., and Saito, Y. (1996). Dual functions of transglutaminase in novel cell adhesion. Journal of cell science 109 (Pt 11), 2727-2735.

Van Gaal, L.F., Mertens, I.L., and De Block, C.E. (2006). Mechanisms linking obesity with cardiovascular disease. Nature 444, 875-880.

Verderio, E., Gaudry, C., Gross, S., Smith, C., Downes, S., and Griffin, M. (1999). Regulation of cell surface tissue transglutaminase: effects on matrix storage of latent transforming growth factor-beta binding protein-1. The journal of histochemistry and cytochemistry : official journal of the Histochemistry Society 47, 1417-1432.

Waki, H., and Tontonoz, P. (2007). Endocrine functions of adipose tissue. Annual review of pathology 2, 31-56.

Wang, S., Cui, C., Hitomi, K., and Kaartinen, M.T. (2014). Detyrosinated Glu-tubulin is a substrate for cellular Factor XIIIA transglutaminase in differentiating osteoblasts. Amino acids.

Wang, Y., Zhao, L., Smas, C., and Sul, H.S. (2010). Pref-1 interacts with fibronectin to inhibit adipocyte differentiation. Molecular and cellular biology *30*, 3480-3492.

Wolpl, A., Lattke, H., Board, P.G., Arnold, R., Schmeiser, T., Kubanek, B., Robin-Winn, M., Pichelmayr, R., and Goldmann, S.F. (1987). Coagulation factor XIII A and B subunits in bone marrow and liver transplantation. Transplantation *43*, 151-153.

Xu, J. (2005). Preparation, culture, and immortalization of mouse embryonic fibroblasts. Current protocols in molecular biology / edited by Frederick M. Ausubel ... [et al.] *Chapter 28*, Unit 28.21.

Zemskov, E.A., Janiak, A., Hang, J., Waghray, A., and Belkin, A.M. (2006). The role of tissue transglutaminase in cell-matrix interactions. Frontiers in bioscience : a journal and virtual library *11*, 1057-1076.

Zhang, J., Lesort, M., Guttmann, R.P., and Johnson, G.V. (1998). Modulation of the in situ activity of tissue transglutaminase by calcium and GTP. The Journal of biological chemistry *273*, 2288-2295.

2.9 Figures

Figure 1

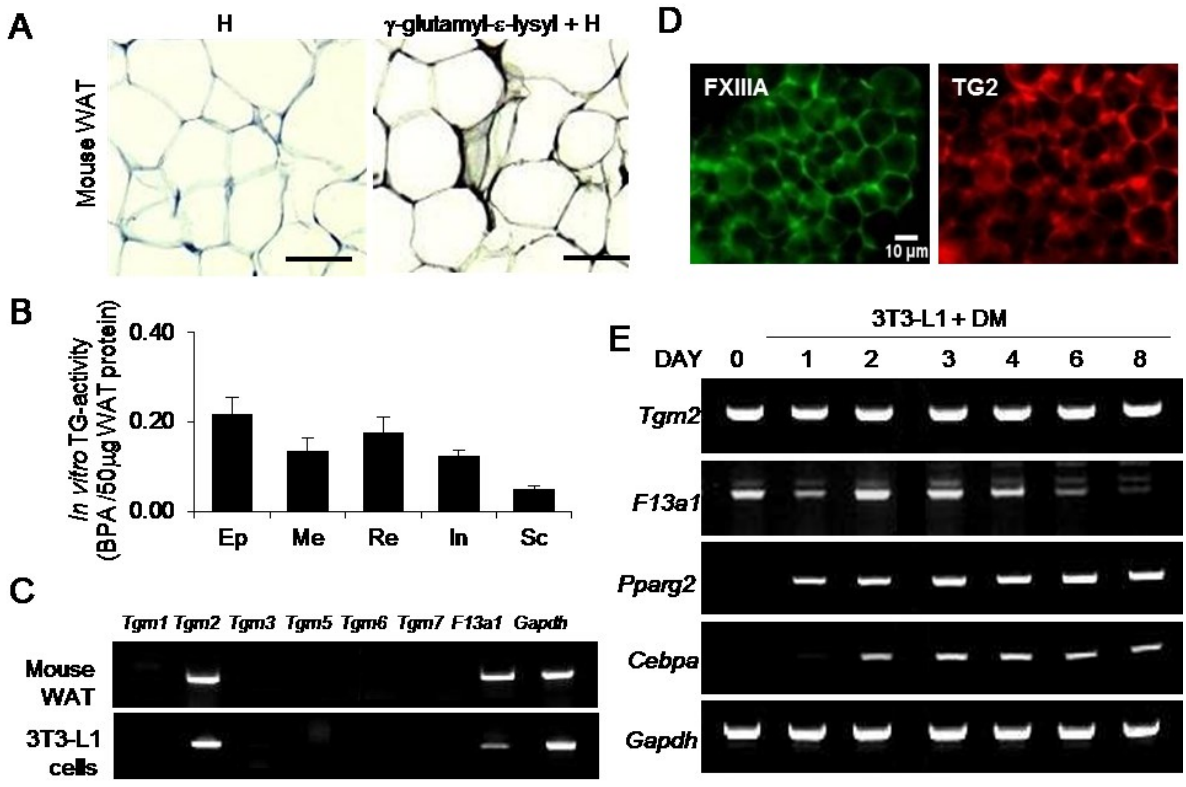

Figure 1. Presence of TG activity, FXIII-A and TG2 in mouse white adipose tissue (WAT) and in differentiating 3T3-L1 preadipocytes. **(A)** Immunohistochemical visualization of γ-glutamyl-ε-lysyl bonds (isopeptide bonds) in WAT showing abundant staining in the extracellular compartment. Epididymal fat pad tissue was obtained from 8-week-old mice. Specimens were counterstained with haematoxylin (H). n=2, Scale bar equals 100 µm. **(B)** *In vitro* TG activity of protein extracts of different WAT fat depots of 6- to 8-week-old male mice. Protein extracts of Epididymal (Ep), Mesenteric (Me), Perirenal/retroperitoneal (Re), Inguinal (In), and Subcutaneous (Sc) fat pads were assessed by microplate 5-(biotinamido)pentylamine (BPA) incorporation assay (n=2). **(C)** RT-PCR analysis of TG enzyme family members in mouse WAT and 3T3-L1 preadipocytes. Only *Tgm2* and *F13a1* are expressed (n=3). **(D)** Whole-mount

immunofluorescence staining of mouse WAT showing the presence of TG2 (red) and FXIII-A (green) in the tissue. Epididymal fat pads of 2 mice were used; Scale bar equals 10 μm. **(E)** RT-PCR analyses of *Tgm2* and *F13a1* during 3T3-L1 preadipocyte differentiation to adipocytes, showing different expression patterns for the two TGs during adipogenesis. *Tgm2* levels remain constant while *F13a1* levels are high at the early phase of adipogenesis followed by a gradual decrease as the cells mature to adipocytes. *Pparg2* and *Cbpa* are adipocyte differentiation markers. *Gapdh* was used as internal control. DM; differentiation medium (n=3).

Figure 2

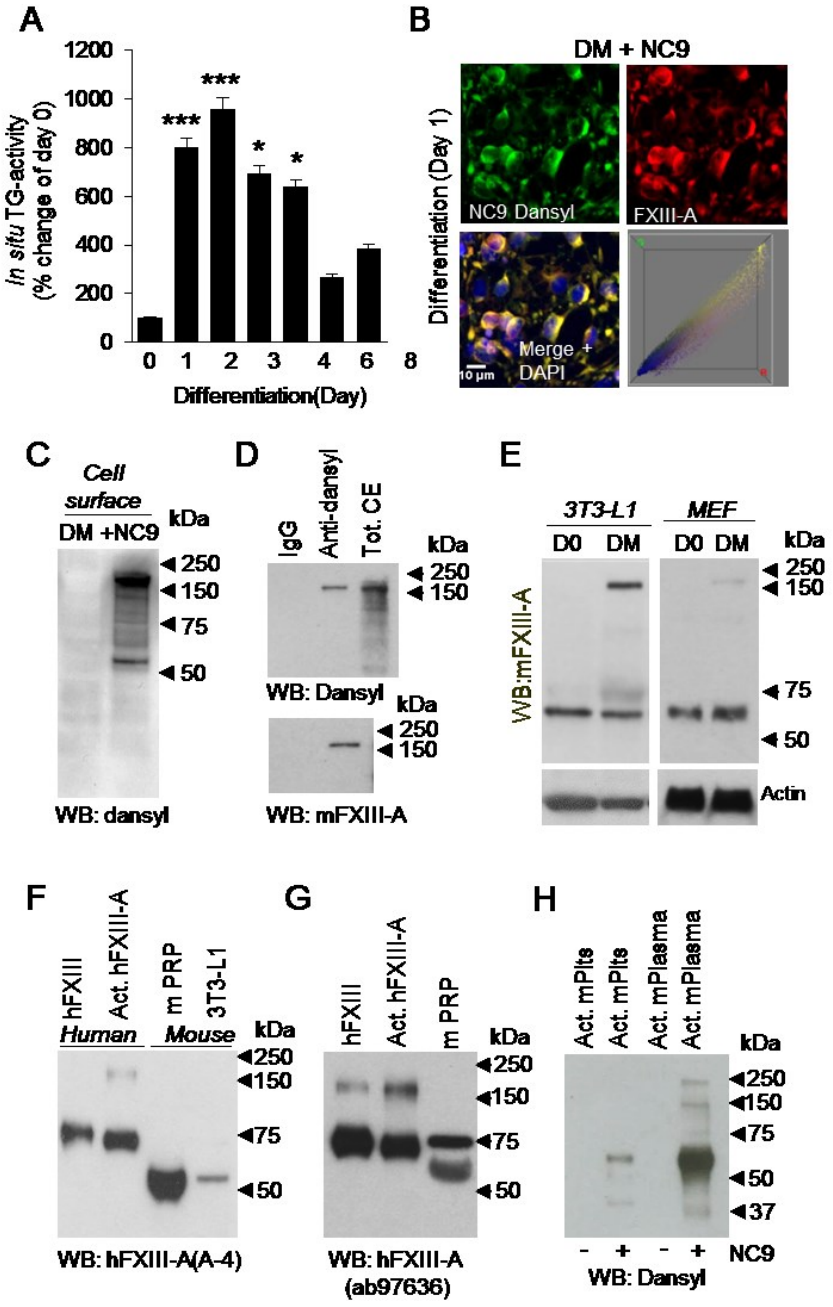

Figure 2. TG activity in preadipocytes arises from FXIII-A. (A) *In situ* assessment of TG activity during differentiation of 3T3-L1 preadipocytes shows a significant increase upon induction of differentiation until day 2, which is followed by a gradual decrease as

cells begin to accumulate lipids. TG activity was assessed by 5-(biotinamido)pentylamine (BPA) incorporation assay.n=3, analysis was done using ANOVA *p<0.05; ***p<0.001. Error bars represent SEM. **(B)** Immunofluorescence tracking of TG activity using NC9 which incorporates irreversibly into the active TG enzyme. Immunofluorescence microscopy shows co-localization (merge, yellow) of NC9-dansyl (green) and FXIII-A (red) identifying FXIII-A as the active TG enzyme in preadipocytes. Nuclei are visualized with DAPI (blue). Color correlation distribution, constructed using the Color Inspector 3D plug-in of Image J, shows the extent correlation of co-localization. n=2, Scale bar equals 10 μm. **(C)** TG activity is located on the cell surface. Cell-surface biotinylated samples were affinity purified using Neutravidin beads and subsequently detected with dansyl antibody which showed a major band between 150 kDa and 250 kDa and a weaker band between 75 kDa and 50 kDa (n=3). **(D)** Immunoprecipitation of NC9-labeled material with anti-dansyl antibody and detection with anti-mouse FXIII-A antibody positively identified the active TG enzyme to be FXIII-A (running between 150 kDa and 250 kDa) (n=5). **(E)** WB detection of FXIII-A in 3T3-L1 preadipocytes and mouse embryonic fibroblasts (MEFs) before (D0) and after induction of differentiation (DM)(Day 1) using anti-mouse FXIII-A antibody. High-molecular weight FXIII-A was observed at day 1 of differentiation (n=3)**.** **(F)** WB detection of nonactivated human FXIII (hFXIII), activated human FXIII (Act.hFXIII), mouse platelet rich plasma (mPRP) and 3T3-L1 cell extract using anti-human FXIII-A antibody (A-4). WB shows human and mouse FXIII-A at different molecular weights, with mouse FXIII-A being smaller (n=3). **(G)** WB detection of nonactivated human FXIII (hFXIII), activated human FXIII (Act.hFXIII), and mouse platelet rich plasma (mPRP) using anti-human FXIII-A antibody (ab97636). WB shows detection of two FXIII-A bands in mPRP, one at 75 kDa and a smaller band between 50 kDa and 75 kDa (n=3). **(H)** A smaller FXIII-A band is active as a TG enzyme. Mouse platelet lysate (mPlts) and mouse plasma (mPlasma) were activated with thrombin and Ca^{2+} for 1 h at 37°C and further incubated with NC9. Dansyl incorporation into the active enzyme was visualized by WB detection of dansyl. Dansyl was found to be integrated into a band between 50 kDa and 75 kDa which represents the smaller form of FXIII-A (n=3).

Figure 3

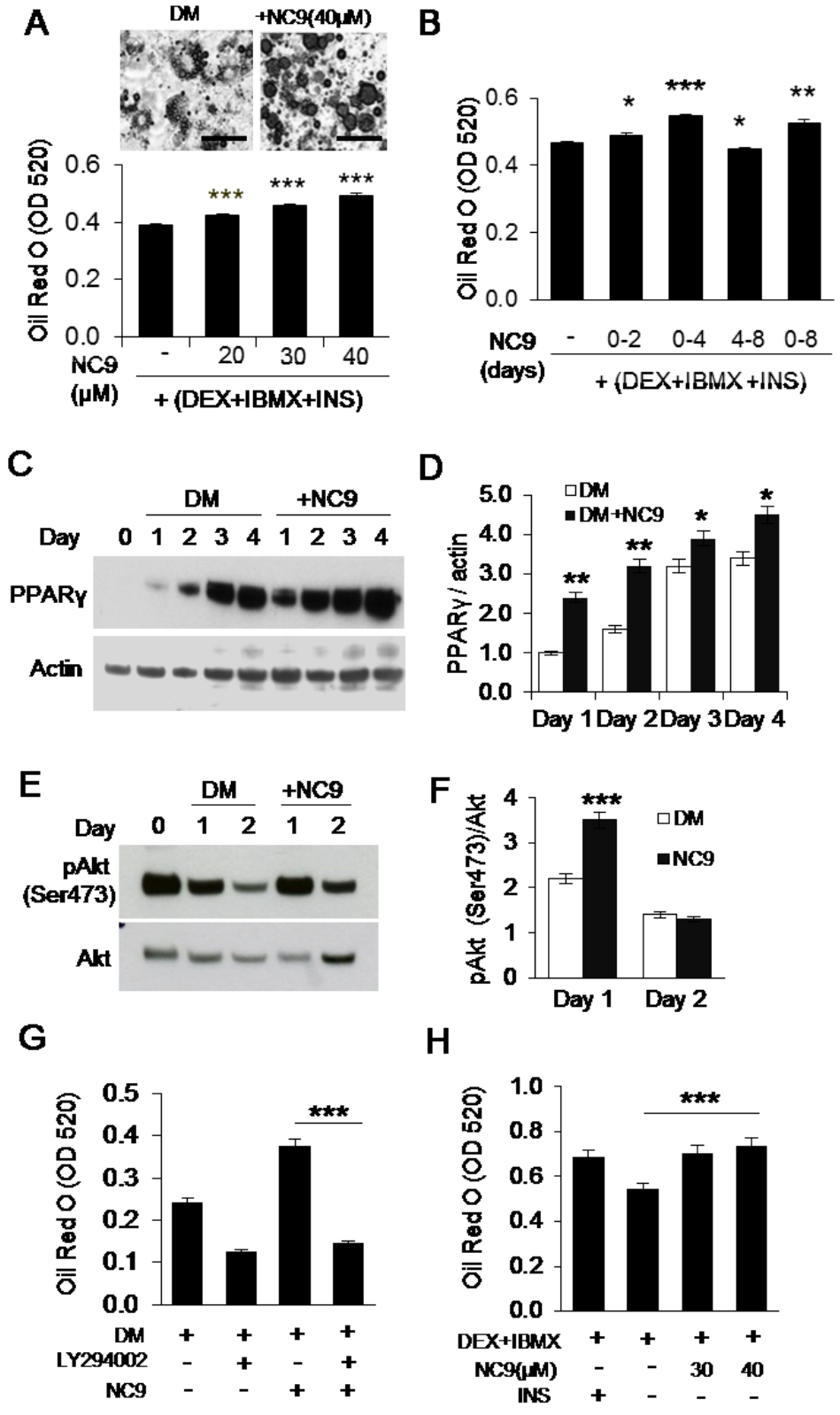
A
DM
+NC9(40μM)
Oil Red O (OD 520)
0.6
0.4
0.2
0.0
***
***
***
NC9 (μM)
-
20
30
40
+ (DEX+IBMX+INS)
B
Oil Red O (OD 520)
0.6
0.4
0.2
0.0
*
***
*
**
NC9 (days)
-
0-2
0-4
4-8
0-8
+ (DEX+IBMX+INS)
C
DM
+NC9
Day
0 1 2 3 4 1 2 3 4
PPARγ
Actin
D
DM
DM+NC9
PPARγ / actin
5.0
4.0
3.0
2.0
1.0
0.0
**
**
*
*
Day 1 Day 2 Day 3 Day 4
E
DM
+NC9
Day
0 1 2 1 2
pAkt (Ser473)
Akt
F
pAkt (Ser473)/Akt
4
3
2
1
0
***
DM
NC9
Day 1
Day 2
G
Oil Red O (OD 520)
0.5
0.4
0.3
0.2
0.1
0.0
***
DM + + + +
LY294002 - + - +
NC9 - - + +
H
Oil Red O (OD 520)
1.0
0.8
0.6
0.4
0.2
0.0
***
DEX+IBMX + + + +
NC9(μM) - - 30 40
INS + - - -

Figure 3. Inhibition of FXIII-A TG activity increases adipocyte differentiation and lipid accumulation. **(A)** Inhibition of TG activity with the irreversible TG inhibitor NC9 increases lipid accumulation in a concentration-dependent manner as assessed by quantification of Oil Red O staining of 3T3-L1 cultures on day 8 of differentiation. Images show the increased size of lipid droplets in Oil Red O-stained cells. **(B)** Inhibition of TG activity during different stages of 3T3-L1 culture shows that TG activity has its most prominent inhibitory effect on lipid accumulation when given during days 0-4. **(C, D)** WB analysis and quantification of PPARγ expression (normalized to actin) during adipocyte differentiation shows increased expression (and thus accelerated differentiation) of NC9-treated cells. **(E, F)** WB analysis, and quantification of Akt phosphorylation at Ser473, shows that inhibition of TG activity significantly increases Akt activation. **(G)** The PI3K pathway inhibitor LY294002 used from day 0-4 reversed the NC9-mediated increase in adipogenesis; the graph shows quantification of Oil Red staining of the cultures on day 8. **(H)** Inhibition of TG activity with NC9 between days 0-4 can function in a similar manner as insulin in differentiation media to promote preadipocyte differentiation; the graph shows quantification of Oil Red O-stained cultures on day 8. All error bars represent SEM. (n=3) *p<0.05; **p<0.01; ***p<0.001.

Figure 4

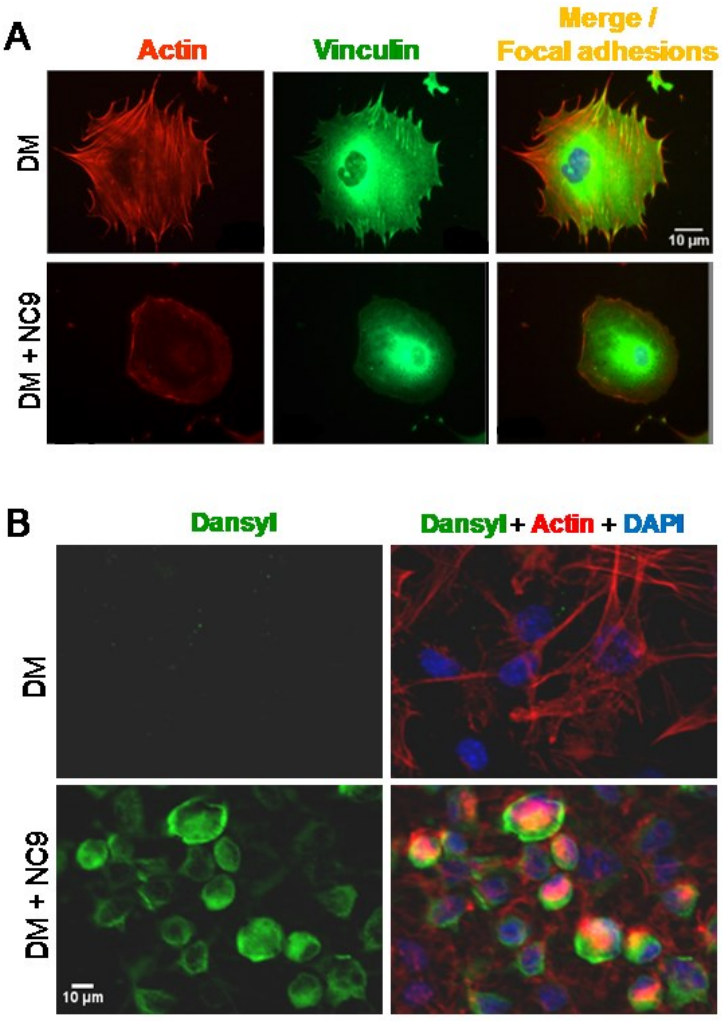
A
Actin
Vinculin
Merge / Focal adhesions
DM
DM + NC9
10 µm
B
Dansyl
Dansyl + Actin + DAPI
DM
DM + NC9
10 µm
C
DM
DM +MDC
250▶ kDa
Actin
MDC - + +
IgG + + -
IP: Dansyl
WB: FN
D
BPA labeled FN / tot FN
0.4
0.3
0.2
0.1
0.0
***
DMSO + + +
BPA + + +
PreAdipc. + + +
DM - + +
NC9 - - +

Figure 4. FXIII-A activity regulates cytoskeletal dynamics – FN is a major extracellular substrate of FXIII-A. **(A)** Immunofluorescence microscopy of cell morphology and cytoskeletal elements of preadipocytes upon inhibition of FXIII-A activity with NC9. Inhibition attenuates actin stress fiber formation, promotes cortical actin assembly and reduces focal adhesion formation (actin and vinculin co-localization). F-actin (red), vinculin (green) and focal adhesions (merge, yellow). n=3, Scale bar equals 10 μm. **(B)** Immunofluorescence microscopy of the dansyl group of NC9 (green) shows its incorporation into FXIII-A enzyme at the periphery of preadipocytes which is accompanied by disappearance of the actin stress fibers seen in control cells. Actin (red) and DAPI (blue). n=3, Scale bar equals 10 μm. **(C)** WB analysis of monodansylcadaverine (MDC)-labeled preadipocyte extracts, blotted for dansyl demonstrates that the substrate probe labels a 250 kDa protein(s) in preadipocyte cultures. Immunoprecipitation with dansyl antibody followed by detection with FN antibody shows the labeled substrate is FN, n=3. **(D)** *In situ* extracellular TG activity assay, *i.e.,* analysis of 5-(biotinamido)pentylamine (BPA) incorporation into coated FN by cellular TG activity. Biotin detection with Neutravidin was performed after all cells were removed. NC9 reduces BPA incorporation into coated FN, (n=4) ***$p<0.001$. Error bars represent SEM.

Figure 5

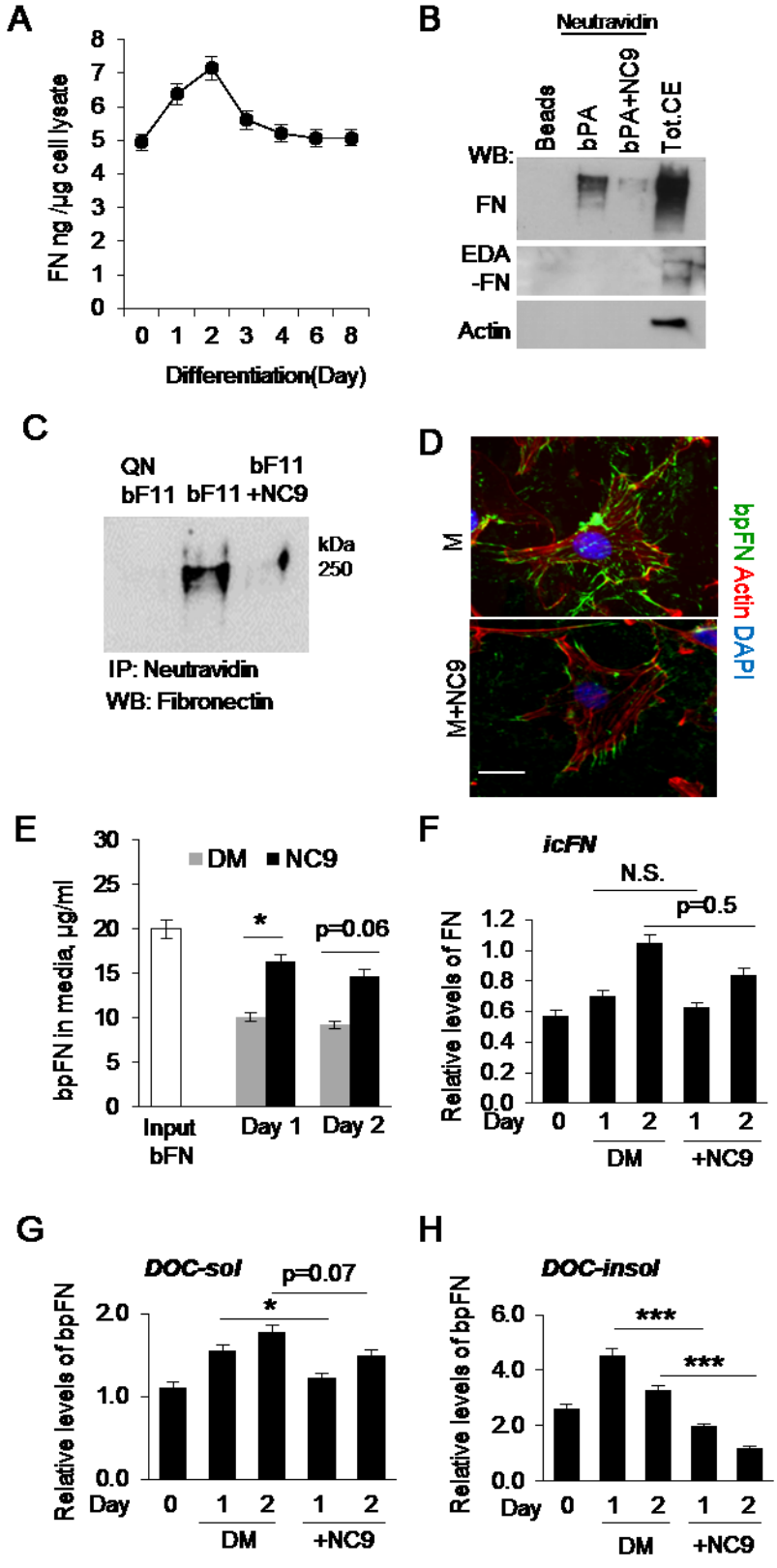
A
FN ng /μg cell lysate
Differentiation(Day)
B
Neutravidin
Beads
bPA
bPA+NC9
Tot.CE
WB:
FN
EDA -FN
Actin
C
QN bF11
bF11 bF11 +NC9
kDa
250
IP: Neutravidin
WB: Fibronectin
D
M
M+NC9
bpFN Actin DAPI
E
DM NC9
bpFN in media, μg/ml
*
p=0.06
Input bFN
Day 1
Day 2
F
icFN
N.S.
p=0.5
Relative levels of FN
Day
DM
+NC9
G
DOC-sol
p=0.07
*
Relative levels of bpFN
H
DOC-insol
***
***

Figure 5. Plasma FN is a substrate for FXIII-A activity. (A) FN detection in total cell protein extracts by ELISA during differentiation of preadipocytes to adipocytes over 8 days. FN levels increase in preadipocyte layers during early differentiation and peak at day 2. **(B)** Affinity-purified preadipocyte culture extracts labelled with 5-(biotinamido)pentylamine (BPA) shows its incorporation into total FN but not into cFN (EDA-FN), thus demonstrating that cFN/EDA-FN is not a TG substrate and suggesting that pFN is the main crosslinking target in preadipocytes. Total cell extract (Tot.CE) was used as positive control. **(C)** The FXIII-A-specific substrate peptide – bF11 – was able to pull down FN demonstrating that it acts as a specific FXIII-A substrate in preadipocytes. NC9 blocks bF11-mediated FN labeling. The control peptide bF11QN shows no labeling. **(D)** Immunofluorescence microscopy of biotinylated plasma FN (bpFN) (green) in preadipocytes (actin, red) treated with basic cell culture media (M) (serum-free conditions). Inhibition of TG activity by NC9 decreased bpFN matrix levels (green) in preadipocytes. Nuclei are stained with DAPI (blue). **(E)** Analysis of exogenous bpFN levels in media using ELISA after 24 h incubation with preadipocytes during differentiation shows a significant increase in media upon NC9 treatment at day 1, indicating that less pFN is incorporating as extracellular matrix. **(F)** Quantification of intracellular FN levels analyzed from trypsinized cells shows no change in FN levels in cells upon NC9 treatment. **(G, H)** Assembly of pFN into preadipocyte extracellular matrix is impaired by NC9 treatment. Exogenous bpFN was given to the cells for 24 h followed by its detection prepared with DOC (DOC-sol) and SDS-containing (DOC-insol) buffers. Quantification was done after WB and detection of biotin. All error bars represent SEM. (n=3) *$p<0.05$; **$p<0.01$; ***$p<0.001$.

Figure 6

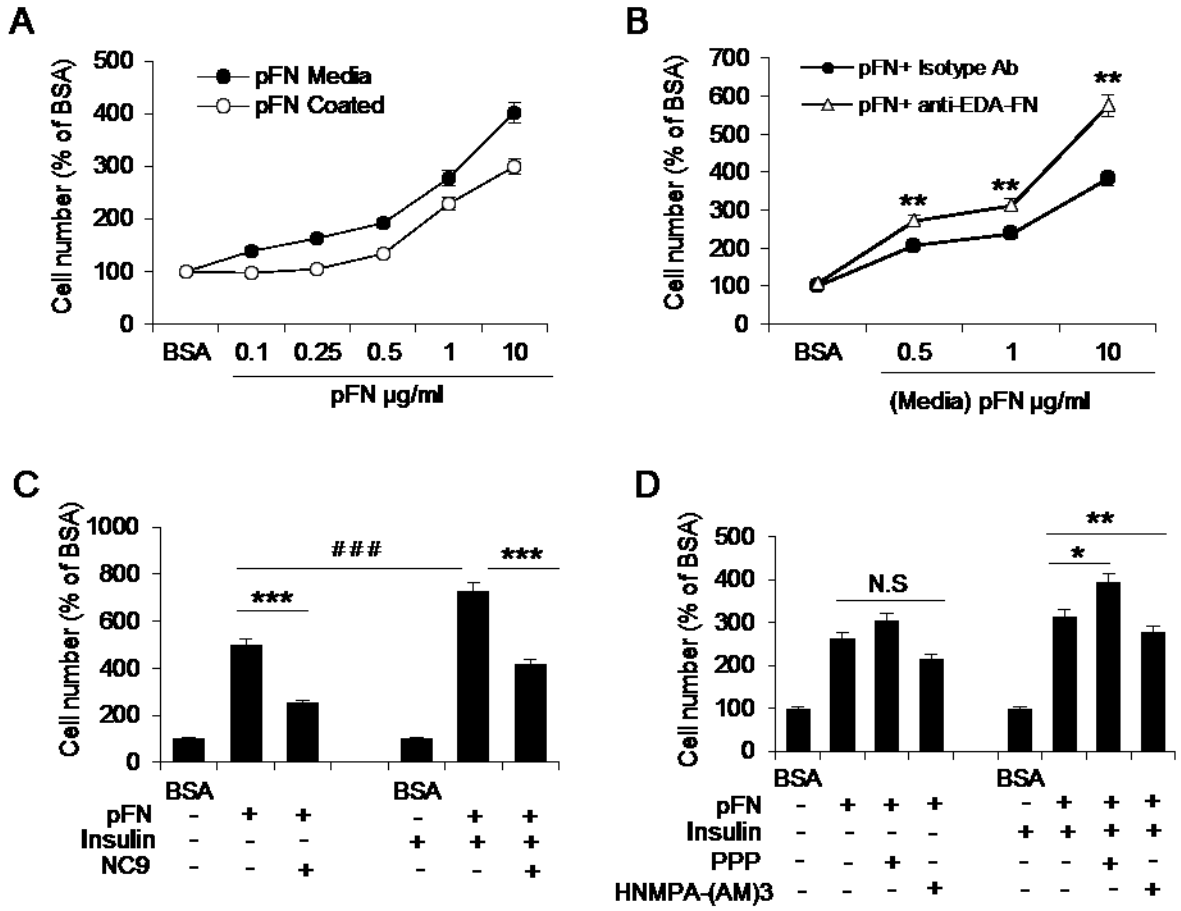

Figure 6. FXIII-A activity regulates proliferation of preadipocytes by promoting plasma FN (pFN) assembly into preadipocyte extracellular matrix. (A) Exogenous pFN immobilized onto culture plates (white circles) or added to media (black circles) under serum-free conditions promotes preadipocyte proliferation in a concentration-dependent manner (n=4). **(B)** Blocking antibody towards EDA-FN (white triangle) further increased pFN-mediated preadipocyte proliferation suggesting that the two forms of FN have opposing functions. Control treatment; isotype antibody (black circles). n=3, **p<0.01. **(C)** Media supplemented with pFN potentiates the pro-proliferative effect of insulin on preadipocytes under serum-free conditions. The combined effect of pFN and insulin on preadipocyte proliferation is inhibited by NC9. n=3, *** or ### p<0.001 **(D)**

The pro-proliferative effect of insulin on preadipocytes under serum-free conditions is mediated by the insulin receptor (IR) and not by the insulin-like growth factor receptor (IGFR), as demonstrated by the ability of respective receptor inhibitors to block the effect. Only the IR inhibitor (HNMPA-(AM)3, 10 μM) reduced proliferation caused by combined pFN and insulin treatment; addition of the IGFR inhibitor (PPP, 10 μM) had the opposite effect. Pro-proliferative effects of pFN alone were not mediated by either IR or IGFR. n=3, *$p<0.05$; **$p<0.01$; N.S- not significant. Error bars represent SEM.

Figure 7

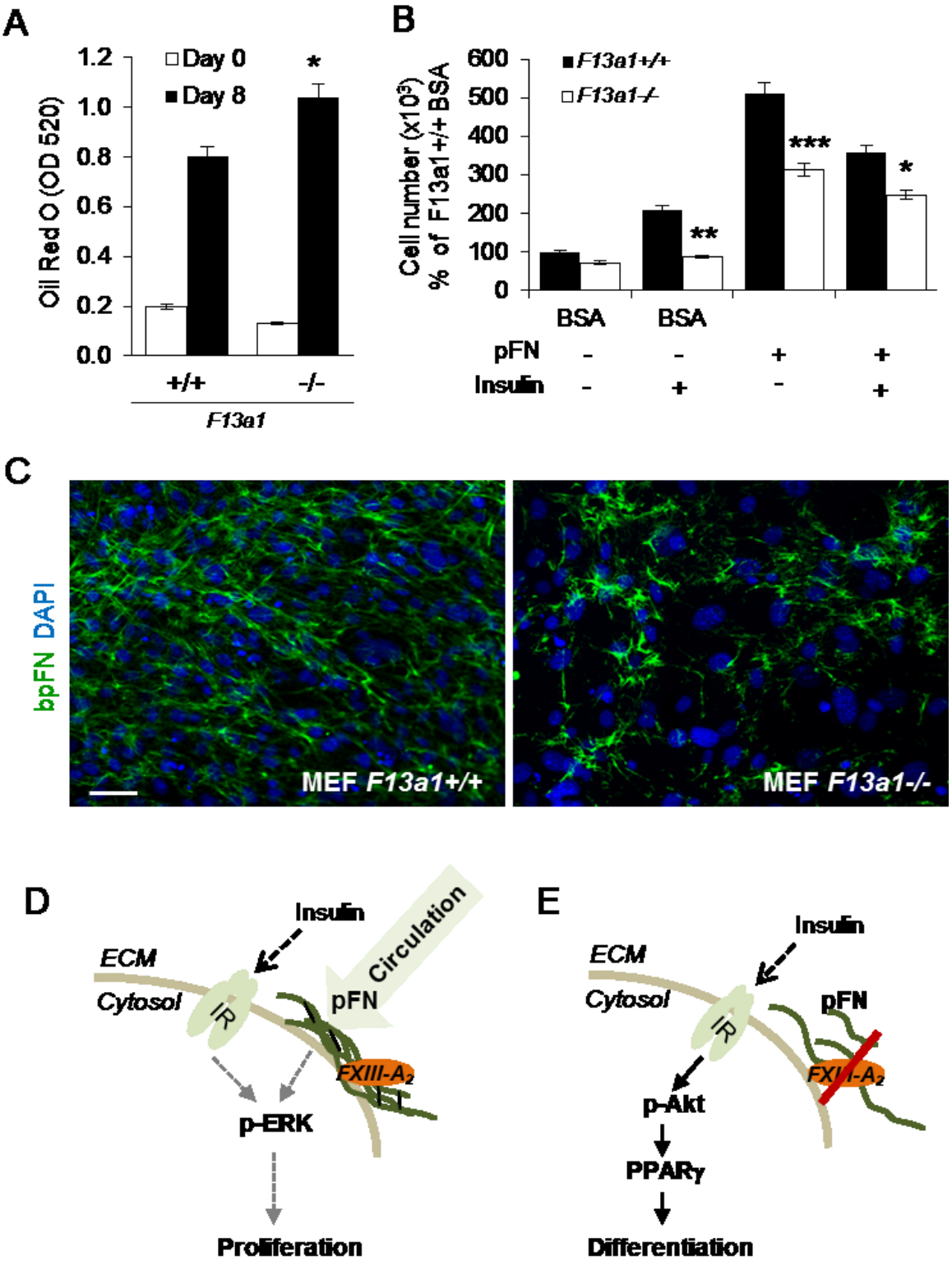
A
Oil Red O (OD 520)
1.2
1.0
0.8
0.6
0.4
0.2
0.0
Day 0
Day 8
*
+/+
-/-
F13a1
B
Cell number (x10³)
% of F13a1+/+ BSA
600
500
400
300
200
100
0
F13a1+/+
F13a1-/-
**
***
*
BSA
BSA
pFN - - + +
Insulin - + - +
C
bpFN DAPI
MEF F13a1+/+
MEF F13a1-/-
D
Insulin
Circulation
ECM
Cytosol
IR
pFN
FXIII-A2
p-ERK
Proliferation
E
Insulin
ECM
Cytosol
IR
pFN
FXIII-A2
p-Akt
PPARγ
Differentiation

Figure 7. *F13a1*-/- MEFs show increased adipogenesis, decreased proliferation, and a defect in plasma FN (pFN) matrix assembly. **(A)** *F13a1*-/- MEFs accumulate significantly more lipids in 8 days when subjected to adipogenic differentiation. Lipid accumulation was visualized and quantified by Oil Red O staining on day 8 of differentiation. n=3, *p<0.05. **(B)** *F13a1*-/- MEFs show a significantly poorer response to the pro-proliferative effect of exogenous pFN given alone to cells or in combination with insulin. n=3, *p<0.05; **p<0.01; ***p<0.001. Error bars represent SEM. **(C)** pFN assembly is impaired in *F13a1*-/- MEF cultures compared to *F13a1*+/+ cultures as assessed by incorporation of exogenous biotinylated plasma FN (bpFN) (green) into extracellular matrix on day 1 of differentiation. Nuclei are stained in blue (DAPI). n=2, Scale bar equals 100 μm. **(D)** Proposed mechanism for the role of FXIII-A in predipocytes. FXIII-A acts on the cell surface of preadipocytes where it promotes liver-derived, circulating pFN assembly into preadipocyte extracellular matrix. pFN matrix promotes cell proliferation and potentiates the pro-proliferative effects of insulin via the insulin receptor (IR) and activation of the Erk pathway. **(E)** In the absence of FXIII-A transglutaminase activity, pFN assembly is reduced, which switches insulin signaling to activation of the Akt pathway resulting in increased PPAR expression and adipocyte differentiation. Thus, the extent of FXIII-A-mediated pFN assembly in preadipocytes and adipocytes can modulate the mitogenic and metabolic effects of insulin.

Supplemental data

Figure S1

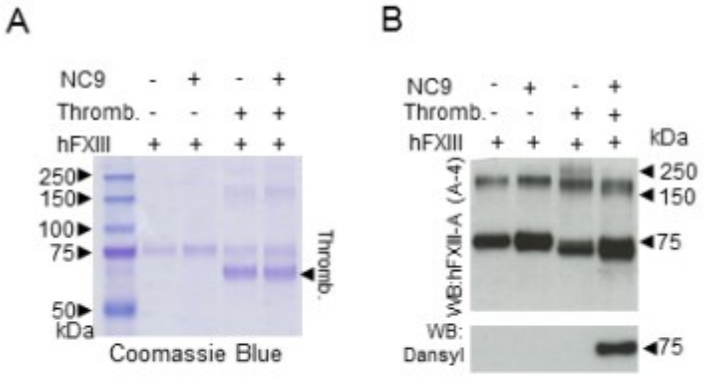

Figure S1. NC9 incorporates only into active FXIII-A (A) Coomassie Blue staining of human FXIII (25µg/ml) ($FXIIIA_2B_2$ heterotetramer) nonactivated and activated for 45min with thrombin (10U/ml) and 2.5 mM $CaCl_2$ at 37°C, inactivated with NC9 for additional 15 min at 37°C. FXIIIA runs with a 75 kDa protein marker (marker from Bio-Rad). Upon activation, a high-molecular weight FXIII-A (150-250 kDa) is observed. **(B)** WB detection of same samples as above. Detection was done using anti-human FXIII-A (A-4) antibody. The dansyl group of NC9 was also detected. The blot shows FXIII-A at 75 kDa and between 150-250 kDa. Dansyl is only detected in samples that were activated with thrombin (n=3).

Supplemental data

Figure S2

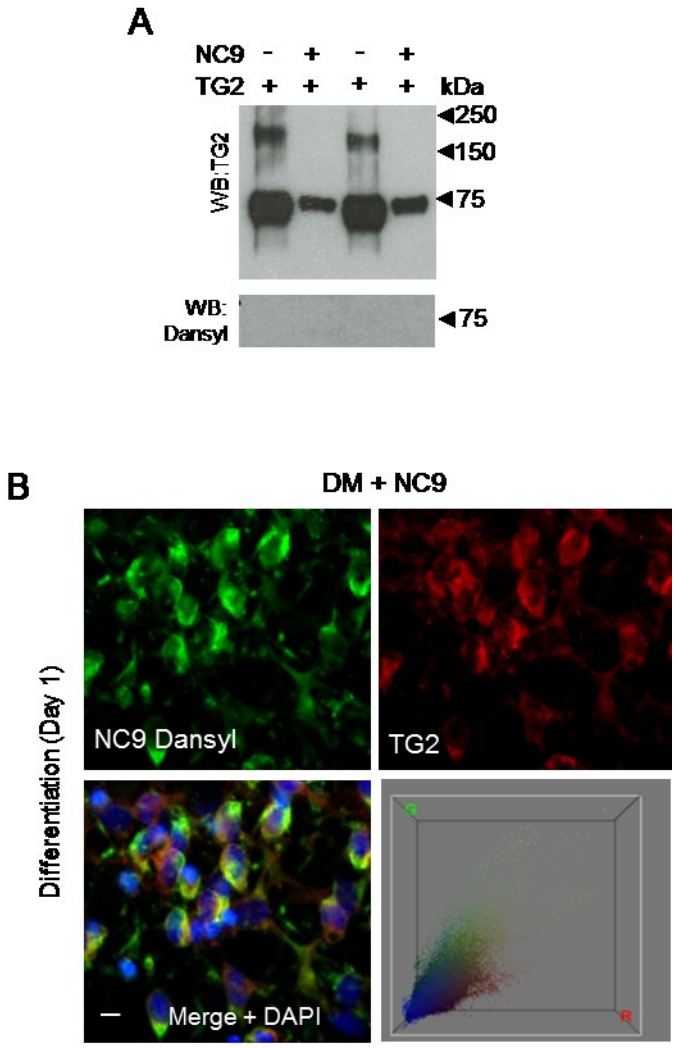

Figure S2. TG2 does not co-localize with NC9. Tracking of the dansyl group of the irreversible TG inhibitor NC9 by immunofluorescence microscopy shows dansyl (green) and TG2 (red) without co-localization (merge). This shows that TG2 is not an active TG enzyme in preadipocytes. Nuclei are visualized with DAPI (blue). Color correlation distribution was constructed using the Color Inspector 3D plug-in of Image J and shows no correlation. n=2, Scale bar equals 10 μm.

Supplemental data

Figure S3

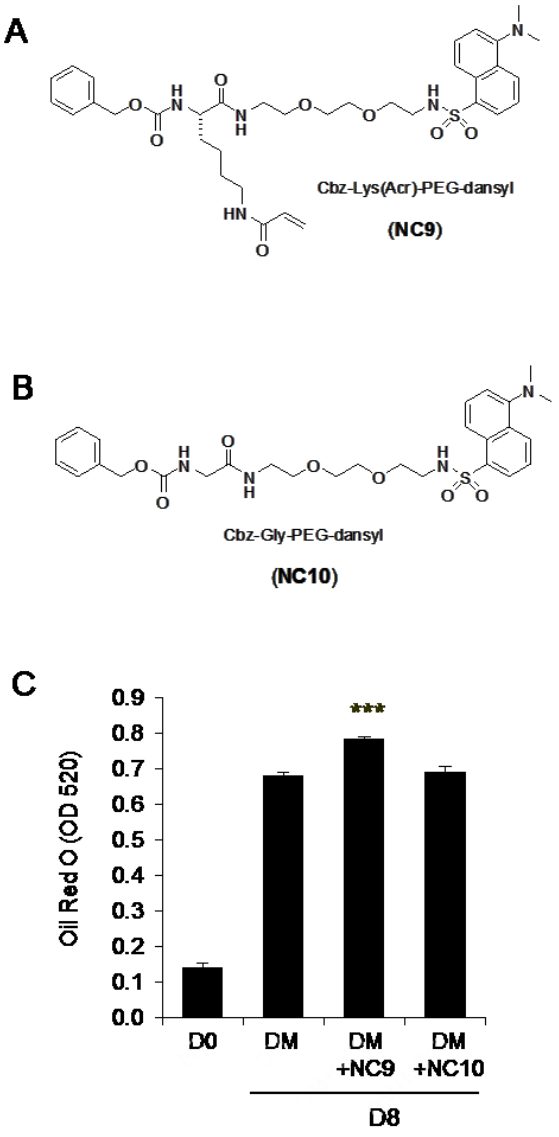

Figure S3. NC10, an inactive control compound for NC9, does not increase lipid accumulation during adipocyte differentiation. (A) Structure of NC9, an irreversible TG inhibitor. **(B)** Structure of NC10. **(C)** Quantification of Oil Red O staining of 3T3-L1 preadipocyte cultures differentiated into adipocytes on day 8 in presence of NC9 (40 μM) and NC10 (40 μM) showing no increase in lipid accumulation after NC10 treatment. n=3, *** $p<0.001$. Error bars represent SEM.

Supplemental data

Figure S4

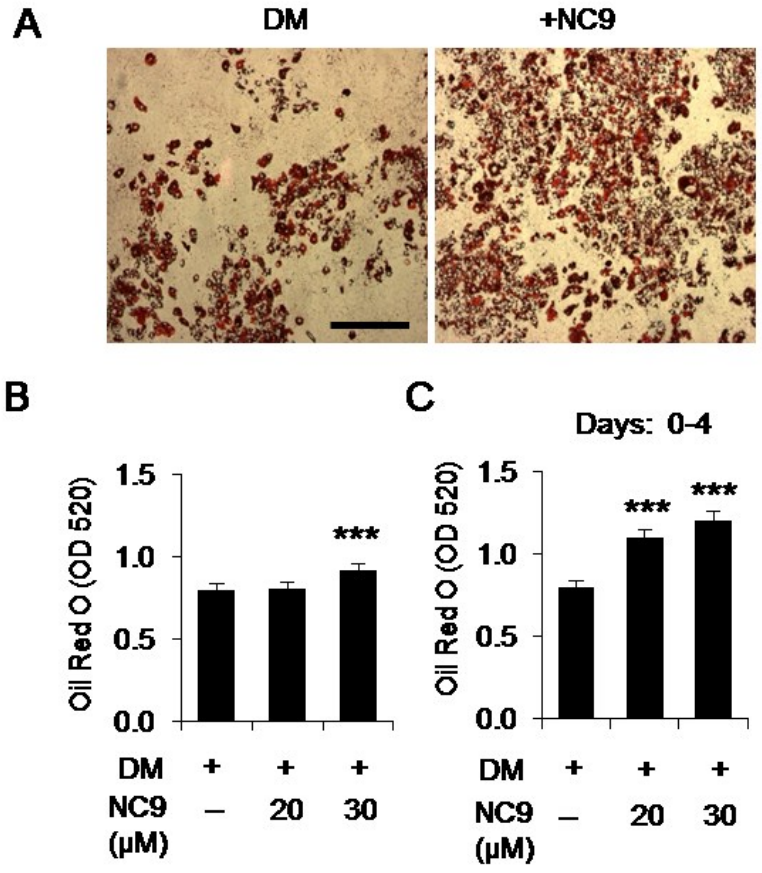

Figure S4. Inhibition of TG activity and FXIII-A with NC9 promotes adipocyte differentiation of mouse embryonic fibroblasts (MEFs). **(A)** Light microscopic images of Oil Red O staining of MEF cells treated with NC9 showing an increase in lipid accumulation compared to the control cells. Scale bar equals 100 μm. **(B)** Quantification of Oil Red O staining of NC9-treated cultures shows a significant increase in lipid accumulation in the presence of a 30 μM concentration of NC9. **(C)** Inhibition of TG activity in MEF cultures between days 0-4 promotes adipogenesis. Differentiation media (DM) contains troglitazone, IBMX, insulin, dexamethasone. n=3, *** $p<0.001$. Error bars represent SEM.

Supplemental data

Figure S5

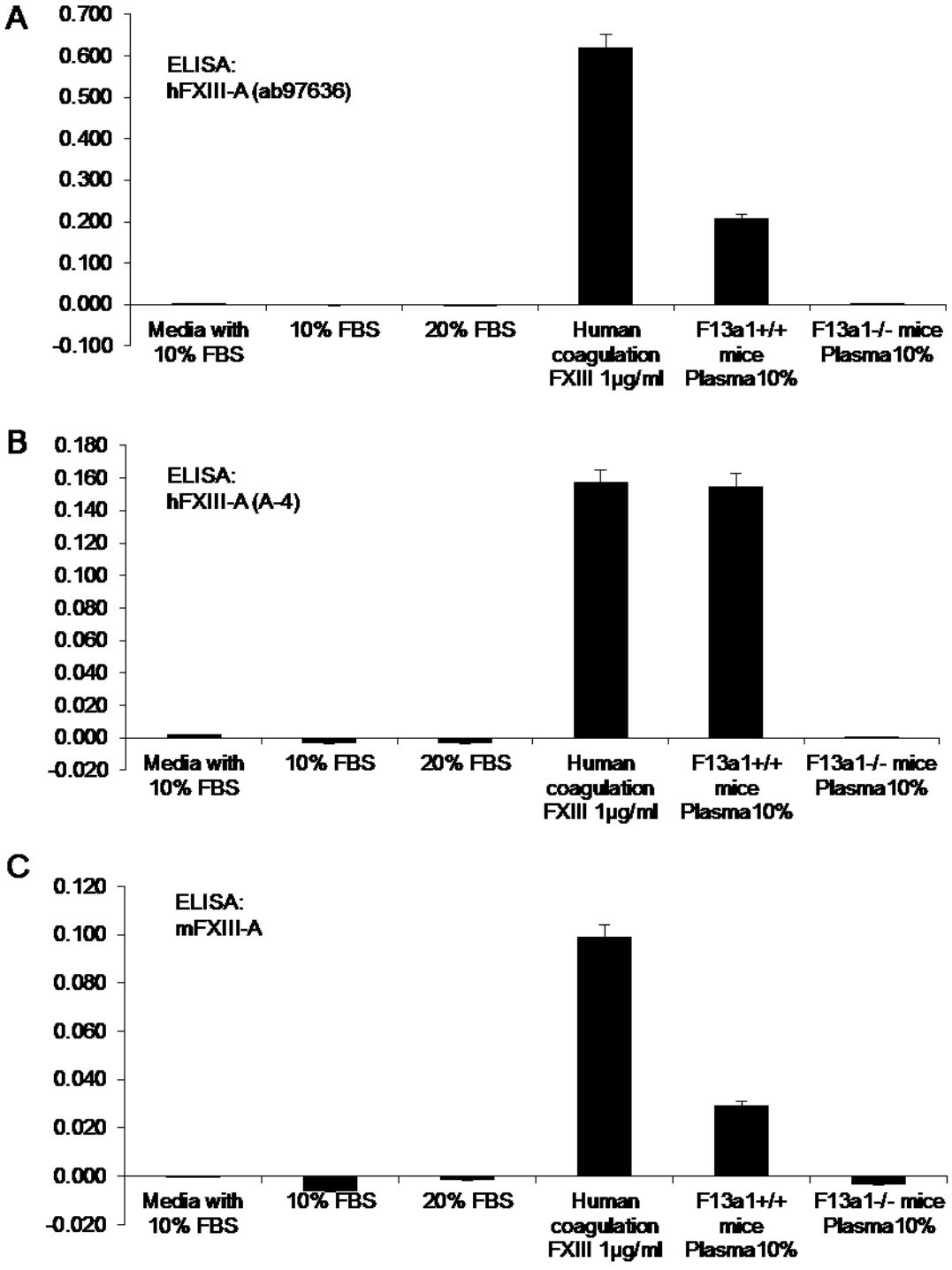

Figure S5. FXIII-A detection in fetal bovine serum (FBS) used for cell culture. The presence of FXIII-A was detected by adsorption ELISA assay using three different FXIII-A antibodies. Samples analyzed were: media with 10% FBS, 10% FBS, 20% FBS. Positive controls were human FXIII (1 µg/ml), *F13a1*+/+ mouse plasma (10%). *F13a1*-/- plasma (10%) was used as a negative control. **(A)** ELISA with anti-FXIII-A antibody (ab97636). **(B)** ELISA with anti-FXIII-A (A-4) (sc-271122). **(C)** ELISA with anti-FXIII-A antibody 675-688 peptide sequence. No FXIII-A was detected by any of the tested FXIII-A antibodies (n=3).

Supplemental data

Figure S6

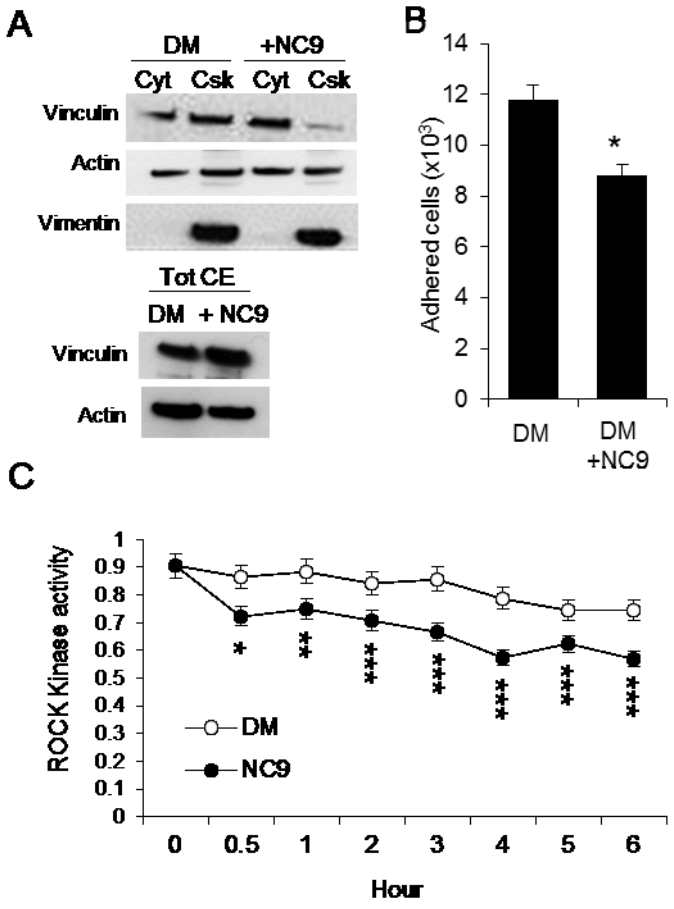

Figure S6. FXIII-A TG activity regulates cytoskeletal dynamics of preadipocytes. **(A)** Vinculin localization in cytosolic and cytoskeletal protein fractions of control and NC9-treated cells demonstrating redistribution of vinculin from the cytoskeleton (Csk) to the cytosol (Cyt) in preadipocytes treated with NC9. Total levels of vinculin are not altered by NC9 (n=3). **(B)** Inhibition of TG activity reduces preadipocyte adhesion to FN. n=5, *p<0.05. **(C)** ROCK kinase activity was assessed by an ELISA assay in control cells treated with differentiation media (DM-white circles) and DM+NC9-treated cells (black circles). Inhibition of TG activity by NC9 significantly reduces ROCK kinase activity in preadipocytes. n=3, *p<0.05; **p<0.01; ***p<0.001. All error bars represent SEM.

Supplemental data

Figure S7

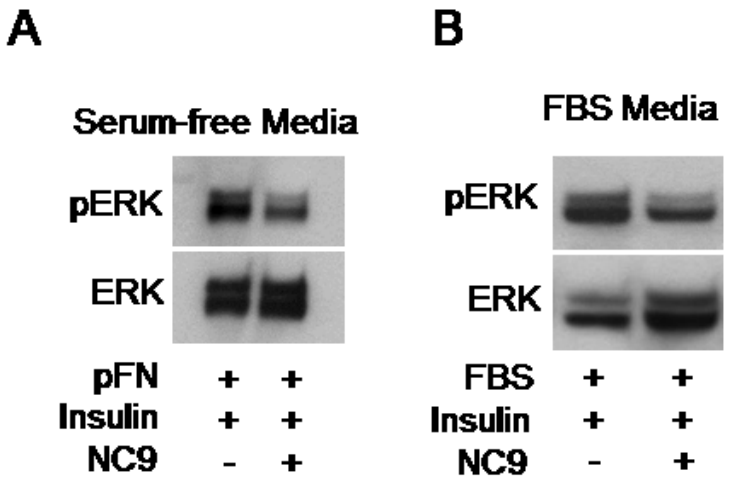

Figure S7. Inhibition of TG activity with NC9 reduces Erk phosphorylation. (A,B) Erk phosphorylation (Thr202/Tyr204), which is maintained by pFN and insulin in preadipocyte cultures, was decreased by NC9 in both serum and serum-free media (n=2).

Supplemental data

Figure S8

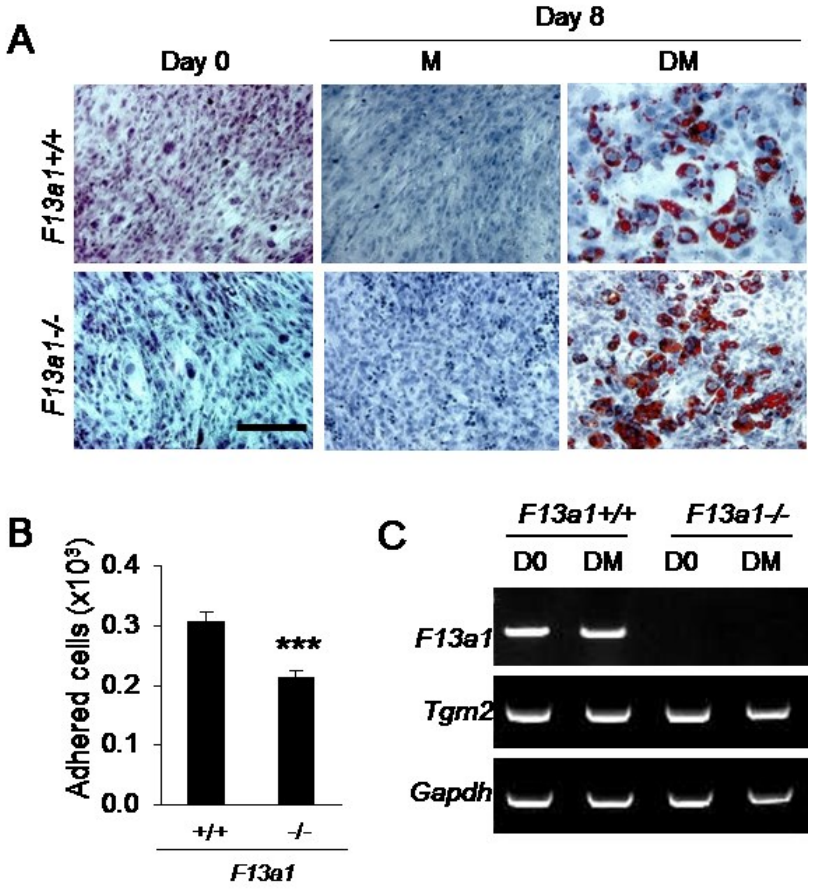

Figure S8. *F13a1*-/- MEFs show increased adipogenesis and reduced cell adhesion and no change in *Tgm2* expression. **(A)** Oil Red O staining of *F13a1*-/- and *F13a1*+/+ MEFs on day 0 and on day 8 of cells treated with medium only (M) or with adipogenic differentiation media (DM). Counter-staining was done with hematoxylin (n=3). **(B)** *F13a1*-/- MEFs show reduced adhesion to coated pFN compared to *F13a1*+/+ MEFs. n=3, ***p<0.001. Error bars represent SEM. **(C)** RT-PCR analysis for *Tgm2* and *F13a1* on day 0 and day 1 of MEFs from *F13a1*+/+ and *F13a1*-/-. *Tgm2* mRNA was not altered in *F13a1*-/- MEF. *Gapdh* was used as internal control (n=2).

CHAPTER 3 - Tranglutaminase 2 - A novel inhibitor of adipogenesis

3.1 Preamble

We have identified two transglutaminase FXIII-A and TG2 in adipose tissue. FXIII-A acts an inhibitor of adipogenesis by promoting pFN assembly into preadipocyte matrix, which promotes cell proliferation but inhibits differentiation. TG2 function in adipogenesis is not known. In this paper, we demonstrate for the first time that TG2 inhibits adipogenesis by using MEFs extracted from TG2 wild type (*Tgm2+/+*) and TG2 null mice (*Tgm2-/-*). First, we showed that *Tgm2-/-* MEFs displayed accelerated and increased adipogenesis. Second, we showed that Pref-1 protein levels, Wnt/β-catenin nuclear translocation and ROCK kinase activity are downregulated, and Akt signaling is upregulated in *Tgm2-/-* MEFs. Third, the extracellular TG2 inhibits adipogenesis by upregulating Wnt/β-catenin nuclear translocation, and recovering Pref-1 protein levels.

Impact in brief:

- This is the first report demonstrating TG2 function in adipogenesis.
- We show that TG2 is an inhibitor of adipogenesis, and that effects arise mainly from extracellular TG2.
- This is a first report showing that Pref-1 potein levels can be modulated by extracellular TG2.

The study presented in this chapter is an article is ***in press*** the journal ***Cell Death & Disease.***

Tranglutaminase 2 - A novel inhibitor of adipogenesis

Vamsee D. Myneni[1], Melino G[2] and Kaartinen MT [1,3*]

[1]Faculty of Dentistry, McGill University, Montreal, QC, Canada. [2] Department Experimental Medicine & Surgery, University of Rome Tor Vergata, Rome, Italy. [3]Division of Experimental Medicine, Department of Medicine, Faculty of Medicine, McGill University, Montreal, QC.

3.2 Abstract

Differentiation of preadipocytes to lipid storing adipocytes involves extracellular signalling pathways, matrix remodelling and cytoskeletal changes. A number of factors have been implicated in maintaining the preadipocyte state and preventing their differentiation to adipocytes. We have previously reported that a multifunctional and protein crosslinking enzyme, transglutaminase 2 (TG2) is present in white adipose tissue (WAT). In this study, we have investigated TG2 function during adipocyte differentiation. We show that TG2 deficient mouse embryonic fibroblasts (*Tgm2-/-* MEFs) display increased and accelerated lipid accumulation due to increased expression of major adipogenic transcription factors, *PPARγ* and *C/EBPα*. Examination of Pref-1/Dlk1, an early negative regulator of adipogenesis, showed that the Pref-1/Dlk1 protein was completely absent in *Tgm2*-/- MEFs during early differentiation. Similarly, *Tgm2*-/- MEFs displayed defective canonical Wnt/β-catenin signalling with reduced β-catenin nuclear translocation. TG2 deficiency also resulted in reduced ROCK kinase activity, actin stress fiber formation, and increased Akt phosphorylation in MEFs, but did not alter fibronectin matrix levels or solubility. TG2 protein levels were unaltered during adipogenic differentiation, and was found predominantly in the extracellular compartment of MEFs and mouse WAT. Addition of exogenous TG2 to *Tgm2*+/+ and *Tgm2*-/- MEFs significantly inhibited lipid accumulation, reduced expression of *PPARγ* and *C/EBPα*, promoted the nuclear accumulation of β-catenin, and recovered Pref-1/Dlk1 protein levels. Our study identifies TG2 as a novel a negative regulator of adipogenesis.

3.3 Introduction

The prevalence of obesity is steadily increasing globally and is recognized as a major risk factor for diabetes, heart disease and certain cancers (Kahn et al., 2006; Spalding et al., 2008; Van Gaal et al., 2006). During excess energy intake adipose tissue expands to store extra lipids. This expansion initially occurs via an increasing the size of existing adipocytes (hypertrophy) which is followed by an increase in adipocyte number via proliferation of preadipocytes (hyperplasia) and their differentiation into mature adipocytes (adipogenesis)(Spalding et al., 2008). Impaired adipogenesis and adipose tissue function are associated with the development of metabolic complications in obesity, such as the development of type 2 diabetes (Tchoukalova et al., 2007; Virtue and Vidal-Puig, 2008).

Adipogenesis involves conversion of spindle-shaped preadipocytes to round lipid filled adipocytes, this morphological change requires conversion of filamentous actin to cortical actin (Kanzaki and Pessin, 2001; Spiegelman and Ginty, 1983) which is associated with remodeling of extracellular matrix (ECM) fibronectin (FN) matrix to laminin rich matrix. Adipogenesis is regulated by various factors that can either promote or inhibit adipogenesis. Many of these factors regulate ECM components and cytoskeletal tension, some of the factors or proteins which maintain preadipocyte state and act as inhibitors during early phase of adipogenesis include Wnt/β-catenin signalling, Pref-1/Dlk1, RhoA and ROCK kinases. These factors are amongst those which determine whether preadipocytes will be in quiescence, or undergo proliferation and differentiate to adipocytes (Cristancho and Lazar, 2011; Feve, 2005).

In our previous work we have identified two members of transglutaminase (TG) enzyme family, Factor XIII-A (FXIII-A) and transglutaminase 2 (TG2), in white adipose tissue (WAT)(Myneni et al., 2014). TGs are enzymes with ability to form isopeptide bonds between glutamine residue of one protein to a lysine residue of another protein by transamidation reaction (Eckert et al., 2014; Gundemir et al., 2012; Iismaa et al., 2009). TGs can also have functions that do not involve their transamidase activity (Eckert et al., 2014). In our recent work, we have shown that FXIII-A is responsible for the

transamidase/crosslinking activity during adipocyte differentiation. In 3T3-L1 adipocyte and mouse embryonic fibroblasts (MEFs) cultures, FXIII-A crosslinking activity increased plasma FN assembly into preadipocyte matrix which promoted preadipocyte proliferation. Inhibition of TG activity of FXIII-A in these cultures resulted in increased adipocyte differentiation (Myneni et al., 2014). The role of TG2 in adipogenesis remained unaddressed.

TG2 is the most ubiquitous of the TG family members and expressed in many tissues such as bone, cartilage, kidney, colon, liver, heart, lung, spleen, blood and nervous tissue (Eckert et al., 2014; Fesus and Piacentini, 2002; Iismaa et al., 2009; Siegel and Khosla, 2007; Thomazy and Fesus, 1989). TG2 is expressed by many cell types such as osteoblasts (Al-Jallad et al., 2006), chondrocytes (Long and Ornitz, 2013; Nurminsky et al., 2011), mesenchymal stem cells (MSCs) (Nurminsky et al., 2011; Song et al., 2007), neuronal and glial cells (Eckert et al., 2014; Grosso and Mouradian, 2012; Gundemir et al., 2012), phagocytes, monocytes, neutrophils and T-cells (Akimov and Belkin, 2001b; Eckert et al., 2014; Iismaa et al., 2009; Murtaugh et al., 1983) and pancreatic β-cells (Bernassola et al., 2002). TG2 has been implicated in various biological functions including cell differentiation and maturation, cell morphology and adhesion, ECM stabilization, cell death, inflammation, cell migration and wound healing (Eckert et al., 2014; Gundemir et al., 2012; Iismaa et al., 2009). TG2 is present in both extracellular and intracellular compartments of the cell. In the extracellular compartment, TG2 can be found on the cell surface and in the ECM. In the intracellular compartment, TG2 is mostly cytosolic but also found on the plasma membrane, in the nuclear membrane and in mitochondria (Belkin, 2011; Eckert et al., 2014; Gundemir et al., 2012; Iismaa et al., 2009). Dysregulation of TG2 function(s) has been implicated in pathogenesis of celiac disease (Eckert et al., 2014; Iismaa et al., 2009; Klock et al., 2012), diabetes (Bernassola et al., 2002), neurodegenerative disorders such as Huntington's, Alzheimers's and Parkinson's disease (Eckert et al., 2014; Grosso and Mouradian, 2012; Gundemir et al., 2012) as well as inflammatory disorders and cancer (Eckert et al., 2014).

In this study, we have used MEFs from TG2 wild-type (*Tgm2*+/+) and TG2 deficient mice (*Tgm2*-/-) to address the potential role of TG2 during adipocyte differentiation. We report that TG2 deficiency results in accelerated and increased adipogenesis in MEFs due to increased expression of adipogenic transcription factors PPARγ and C/EBPα. We further examined the role of TG2 in several anti-adipogenic pathways and demonstrate that TG2 regulates adipogenesis via multiple factors – these include Pref-1/Dlk1 expression and modulation of Wnt/β-catenin signaling, ROCK kinase activity and Akt signalling.

3.4 Materials and methods

Animals

Tgm2-/- mice were described before (De Laurenzi and Melino, 2001). Wild type (WT) mice were purchased from Jackson Laboratories (Bar Harbor, Maine, USA). Mice were kept under a normal diurnal cycle in a temperature-controlled room and fed with standard chow. Animal procedures (WAT extraction and MEF isolation) and study protocols were approved by the McGill University Animal Care Committee.

Antibodies and proteins

Antibodies against rabbit anti-Akt (pan), rabbit anti- phospho-Akt (Ser^{473})(D9E), rabbit anti-PPARγ, rabbit anti-histone, rabbit anti-Pref-1 were purchased from Cell Signalling Technology Inc. (Beverly, MA, USA). Rabbit anti-actin, mouse anti-tubulin antibodies were obtained from Sigma-Aldrich (St Louis, MO, USA). Rabbit anti-fibronectin antibody, human recombinant MYPT1 (654-880) and rabbit anti-phospho-MYPT1 (Thr696) were from EMD Millipore (Billerica, MA, USA). Rabbit anti-C/EBPα purchased from Santa Cruz Biotechnology (Santa Cruz, CA, USA). Rabbit anti-β-catenin purchased from Abcam (Cambridge, MA,USA). Mouse monoclonal TG2 Ab-3 antibody (Clones CUB 7402+TG100) was from Fisher Scientific (Fremont, CA, USA). Horseradish peroxidase-conjugated anti-rabbit IgG was purchased from Cell Signalling Technology Inc. (Beverly, MA, USA). Horseradish peroxidase-conjugated goat anti-rabbit IgM was purchased from Santa Cruz Biotechnology (Santa Cruz, CA,

USA). Horseradish peroxidase-conjugated anti-mouse, and anti-rabbit IgG were from Jackson ImmunoResearch Inc. (West Grove, PA, USA). Alexa Fluor® 488 and 596, Alexa Fluor® 568-phalloidin and Bodipy 493/503 were from Life Technologies (Grand Island, NY, USA).

Reagents

Dulbecco's modified Eagle's medium (DMEM) and 0.5 mg/ml trypsin and 0.2 mg/ml EDTA from ATCC (Cedarlane, ON, Canada). Fetal bovine serum (FBS) and penicillin-streptomycin were from Gibco (Burlington, ON, Canada). Oil Red O, IGEPAL CA-630, dexamethasone, insulin, 3-Isobutyl-1-methylxanthine (IBMX), 3,3′,5,5′-Tetramethylbenzidine (TMB) were from Sigma-Aldrich (St Louis, MO, USA). Troglitazone were purchased from Santa Cruz Biotechnology (Santa Cruz, CA, USA). Sulfo-NHS-LC-biotin and 5-(biotinamido)pentylamine were purchased from Pierce (Rockford, IL, USA). ECL kit was from Zmtech Scientifique (Montreal, QC, Canada). All other reagents unless otherwise specified were purchased from Sigma-Aldrich or Fisher Scientific.

MEF cell culture and differentiation

Mouse embryonic fibroblasts (MEFs) were prepared from 13.5 days *Tgm2*$^{+/+}$ and *Tgm2*$^{-/-}$ mouse embryos, MEFs isolation, culture and staining with Oil Red O was done according to previously published protocol (Myneni et al., 2014). MEFs were differentiated into adipocytes with 10% FBS, 1μM dexamethasone, 0.5mM isobutyl-1-methylzanthine, 1μg/ml insulin, and 10μM troglitazone for 2 days. On day 2, media were replaced with maintenance medium which includes 10% FBS and 1μg/ml insulin and 10μM troglitazone. On day 4, maintenance media were replaced with medium containing 10% FBS and cells were cultured in this until the end of the experiment, i.e., day 8. Intracellular triglyceride was stained with Oil Red O and quantified; cells were counterstained with haematoxylin and photographed with a light microscope.

Whole mount staining, immunofluorescence and histology

For whole-mount staining, mouse WAT from *Tgm2*+/+ mice was fixed in 10% neutral-buffered formalin. Fixed tissue was cut with a scalpel to 5 mm × 5 mm sections, and blocked with 3% BSA, 0.3% Triton X-100, in PBS for 12-24h at 4°C. Tissue pieces were incubated with primary antibodies overnight at 4°C which was followed by incubation with Alexa Fluor®-conjugated secondary antibodies for 1 h at room temperature. Nuclei were stained with DAPI. Antibody omission and isotype specific immunoglobulins were used as controls (Myneni et al., 2014). For histology, mouse epididymal fat pad from *Tgm2*+/+ and *Tgm2*-/- mice were fixed in 10% neutral-buffered formalin and paraffin embedded and stained with eosin and hematoxylin (Myneni et al., 2014). For immunofluorescence, cells were grown in 8-well Nunc Lab-Tek® II glass chamber slides (Fisher Scientific). Cells were fixed with 10% neutral-buffered formalin for 30 min at room temperature or with 1% formaldehyde for 15 min at room temperature (for optimal cell-surface protein staining). Staining was done as previously described (Myneni et al., 2014). Quantification was done with Image J (v1.34i, NIH).

Protein extraction and western blotting

The total cell lysate was prepared with lysis buffer containing 20 mM Tris-HCl, pH 7.5, 5 mM EDTA, 150 mM NaCl, 0.5% DOC, 0.5% Triton X-100, 1 mM PMSF, and 1 mM orthovanadate and protease inhibitor cocktail (Sigma). Cell lysates were incubated on ice for 30 min with occasional vortexing and then centrifuged for 15 min at 15,000 x *g* at 4 °C. Nuclear and cytosolic fractions were prepared as previously described (Rosner and Hengstschlager, 2008). Deoxycholate (DOC)-soluble and DOC-insoluble FN matrix extracts were prepared as described previously (Pankov and Yamada, 2004). Western blotting and quantification of bands with Image J (v1.34i, NIH) was done as previously described (Myneni et al., 2014).

Cell surface biotinylation

Cell surface biotinylation was done for *Tgm2*+/+ MEFs as previously described (Myneni et al., 2014).

RT-PCR and Real time PCR

mRNA was isolated using Trizol method. RNA was treated with DNase (New England Biolabs, Ipswich, MA, USA), and PCR was performed with SuperScript™III One-Step RT-PCR System with Platinum® Taq DNA Polymerase (Invitrogen). PCR products were analyzed by 1.5% agarose gel electrophoresis. Primers used were previously described *Pref-1*(Han et al., 2002), EDA, EDB (Han et al., 2005), *Fn*, *Gapdh* (Al-Jallad et al., 2006), *Pparγ2* and *Cebpα* (Tanabe et al., 2004). Real-time PCR was performed on a ABIHT7900 RT-PCR machine using the comparative C_T method in triplicate using the TaqMan Universal Master Mix II. Expression levels of *Pparγ2* (Mm 01184322_m1, *Cebpα* (Mm 514283_s1) and normalized to *Rn18S* (Mm 03928990_g1).

***In situ* transglutaminase activity assay**

In situ transglutaminase activity assay was done by giving 2mM 5-(biotinamido)pentylamine to the cells during differentiation. At the indicated time point, total cell extracts were prepared with 50mM Tris-HCl (pH 8.0), 135mM NaCl, and 1% Triton X-100, 1mM EDTA**,** 1mM sodium orthovanadate and EDTA-free protease inhibitor cocktail. To see the basal level of TG activity under these conditions, biotinamidopentylamine (BPA) was added to the cultures on day -1 (i.e. 1 day after the cells are confluent). The total cell lysate was extracted on day 0, i.e. 24 hr after the BPA was added, but before adipogenic treatment was started. The value obtained by microplate TG-activity assay from cell lysate without BPA was subtracted from the value of cell lysate containing BPA, and the resulting value was considered TG-activity on day 0. Microplate assay to detect biotin was done as previously described (Myneni et al., 2014).

ROCK kinase activity

ROCK kinase activity was determined by using microplate *in vitro* kinase assay as previously described (Myneni et al., 2014). Cell lysate was prepared with 50mM Tris-HCl, pH 7.5, 150mM NaCl, 1mM 2-glycerophosphate, 1% Triton X-100, 1mM EDTA, 1mM EGTA, 1mM Na_3VO_4, and EDTA-free protease inhibitors cocktail.

Statistical analysis

All values are expressed as standard error of the mean (SEM) of three independent experiments. Statistical significance was assessed by student's T-test. *P* values are as follows: *p>0.05, **p>0.01, ***p>0.001.

3.5 Results

Tgm2-/- MEFs show increased and accelerated adipocyte differentiation

Our previous work identified two TG enzymes, FXIII-A and TG2, in mouse WAT and in the 3T3-L1 preadipocyte cell line, and identified FXIII-A as a regulator of preadipocyte proliferation (Myneni et al., 2014). In this study, we examined the role of TG2 in adipogenesis by using TG2 deficient and wild-type MEFs as a model, and examined *Tgm2*+/+ and *Tgm2*-/- MEFs capacity to differentiate into adipocytes under adipogenic conditions. Oil Red O staining for lipid and quantification on day 8 of adipogenesis, shows a 1.5-fold increase in adipose conversion in *Tgm2*-/- MEFs compared to *Tgm2*+/+ cells (**Figure 1A,B**). Increased adipogenesis was associated with an increase in mRNA expression levels of main adipogenesis transcription factors, *Pparγ* and *Cebpα; Tgm2*-/- MEFs showing a 1.8-fold and 1.5-fold increase, respectively compared to *Tgm2*+/+ MEFs on day 8 (**Figure 1C**). The increase in the transcription factor mRNA in *Tgm2*-/- MEFs was also associated with an increase in PPARγ protein levels and increased production of its downstream target GLUT4 (**Figure 1D**).

Time course analysis of lipid droplet accumulation in cells during early differentiation on days 0, 3 and 5, show that *Tgm2*-/- MEFs accumulate lipids earlier on day 3 compared to *Tgm2*+/+ MEFs that show lipids on day 4-5 (**Figure 2A**). Accelerated adipogenesis was associated with an increase in mRNA expression levels of *Ppar*γ and *Cebp*α*; Tgm2*-/- MEFs showing a 5-fold and 4-fold increase, respectively compared to *Tgm2*+/+ MEFs on day 3 (**Figure 2B**). Increase in mRNA expression was also accompanied by significantly increased PPARγ and C/EBPα positive nuclei in *Tgm2*-/- MEFs compared to *Tgm2*+/+ MEFs on day 3 indicative of their increased nuclear translocation and thus activation (**Figure 2C,D**). Western blot analysis of PPARγ and C/EBPα show that both

are upregulated in *Tgm2*-/- MEFs compared to *Tgm2*+/+ MEFs. PPARγ was detected in *Tgm2*-/- MEFs but not *Tgm2*+/+ MEFs on day 3, and PPARγ was detected in *Tgm2*+/+ MEFs by day 4 supporting the accelerated adipogenesis seen in *Tgm2*-/- MEFs (**Figure 2E**). These results indicate that TG2 is a negative regulator of adipogenesis.

TG2 is critical for Pref-1 protein expression

Due to the accelerated adipogenesis in *Tgm2*-/- MEFs, we examined Pref-1/Dlk-1 expression levels in these cells. Pref-1 inhibits adipogenesis during the early phase of differentiation, and Pref-1 downregulation coincides with upregulation of C/EBPα and PPARγ (Hudak and Sul, 2013; Kim et al., 2007; Wang et al., 2006). Examination of Pref-1 protein levels in total cell lysate reveals a dramatic loss of Pref-1 protein in *Tgm2*-/- MEFs compared to *Tgm2*+/+ MEFs. Only very low levels are detected at day 3 of adipogenesis (**Figure 3A)**. mRNA expression of *Pref-1* (**Figure 3B,C**) on day 0 was significantly lower in *Tgm2*-/- MEFs, but no significant difference was observed between *Tgm2*-/- and *Tgm2*+/+ MEFs after the initiation of adipocyte differentiation. However, this similar mRNA expression did not result in an increase in Pref-1 protein expression suggesting that TG2 regulates mainly Pref-1 protein production.

TG2 is required for β-catenin nuclear translocation

Due to the links of TG2 to canonical Wnt/β-catenin signaling (Faverman et al., 2008) and its inhibitory role in adipogenesis, and PPARγ and C/EBPα expression (Christodoulides et al., 2009; Ross et al., 2000), we examined canonical Wnt/β-catenin pathway to see if it is affected in *Tgm2*-/- MEFs. Examination of β-catenin nuclear translocation – a hallmark of Wnt signalling activation in cells – show that *Tgm2*-/- MEFs have significantly decreased β-catenin levels in the nucleus and increased in cytosol compared to *Tgm2*+/+ cells (**Fig. 4A,B**). Total β-catenin levels were not altered (**Fig. 4C**). These results indicate that TG2 inhibits early phase of adipogenesis by regulating Pref-1 production and β-catenin signaling.

TG2 is predominantly extracellular during early adipogenesis

To gain mechanistic insight into the inhibitory effect of TG2 during adipogenesis, we examined the TG2 protein levels, *in situ* TG-activity and cellular localization in *Tgm2*+/+ MEFs during the course of differentiation and its location in WAT. **Figure 5A**, shows that TG2 total protein levels did not markedly change during adipogenesis. TG-activity, measured *in situ* by growing the MEFs with 5-(biotinamido)pentylamine, showed no significant change in *Tgm2*-/- MEFs compared to *Tgm2*+/+ MEFs during early adipocyte differentiation, suggesting that the lack of TG-activity is not the cause of inhibitory effects seen in *Tgm2*-/- MEFs (**Figure 5B**). It has been shown that in airway epithelial cell lines, TG2 crosslinks PPARγ to a higher molecular weight form between 72-250 kDa, which contributes to change in the monomer (55 kDa) levels (Maiuri et al., 2008). Western blot analysis for PPARγ after reduced and nonreduced SDS-PAGE condition of total day 8 cell lysate in showed no higher molecular weight products of PPARγ (**Figure S1**) demonstrating that crosslinking is not involved in its regulation. Cell surface biotinylation experiments (**Figure 5C**) and immunofluoresence staining (**Figure 5D**) of TG2 in *Tgm2*+/+ MEFs that were not permeabilized by Triton-X100 shows that TG2 is found in the extracellular space and increased cell surface expression on days 1 of differentiation. Whole-mount immunofluorescence staining of mouse epididymal WAT confirms that TG2 is mainly present in the extracellular space of adipose tissue (**Figure 5E**).

Exogenous TG2 inhibits adipogenesis and increases β-catenin nuclear translocation, and Pref-1 protein expression

To investigate if extracellular TG2 regulates adipogenesis, exogenous TG2 enzyme (ExoTG2) was added to *Tgm2*+/+ and *Tgm2*-/- MEF cultures during differentiation. The addition of ExoTG2 caused a significant decrease in lipid accumulation in both *Tgm2*+/+ and *Tgm2*-/- MEFs (**Figure 6A,B**). Lipid accumulation was reduced by 23-35% in *Tgm2*+/+ MEFs and 16-29% in *Tgm2*-/- MEFs with concentrations ranging from 0.5-5 µg/ml. Reduced adipogenesis by ExoTG2 was also associated with reduced *Ppar*γ and *Cebp*α expression in *Tgm2*+/+ and *Tgm2*-/- MEFs (**Figure 6C; Figure S2A,B**). The total β-catenin levels were not altered by ExoTG2 compared to controls (**Figure 6D**), but

significantly increased nuclear β-catenin in *Tgm2-/-* MEFs (**Figure 6E,F**). *Pref-1* mRNA expression was not altered by ExoTG2 in *Tgm2-/-* MEFs (**Figure 6G; Figure S2C**). However, ExoTG2 completely recovered the Pref-1 protein levels in *Tgm2-/-* MEFs (**Figure 6H**). These results suggest that extracellular TG2 inhibits adipogenesis and regulates Pref-1 protein production, but not mRNA expression.

Tgm2-/- MEFs show decreased ROCK kinase activity and increased Akt phosphorylation – no changes in FN matrix levels

In search other potential anti-adipogenic pathways that TG2 may regulate we considered the facts that adipogenesis involves major cytoskeletal changes to accommodate to lipid storage. Given the function of TG2 in regulating actin cytoskeleton via RhoA-ROCK signaling (Janiak et al., 2006) and the role of ROCK as an inhibitor of adipogenesis (Noguchi et al., 2007) we analyzed ROCK activity during early differentiation. Data shows a moderate but significant downregulation of ROCK activity in *Tgm2-/-* MEFs on day 1 and day 2 (**Figure 7A**). Examination of actin stress fibers, that are regulated by ROCK kinase (Amano et al., 2010), by immunofluorescence show reduced F-actin network in *Tgm2-/-* MEFs compared to *Tgm2+/+* MEFs (**Figure 7B**). It is known that inhibition of ROCK enhances Akt signalling, which plays a crucial promoting role in adipocyte differentiation and PPARγ regulation (Aubin et al., 2005; Kim and Chen, 2004; Noguchi et al., 2007). **Figure 7C,D** shows a significant upregulation of Akt phosphorylation on day 3 in *Tgm2-/-* MEFs compared to *Tgm2+/+* MEFs. The effect of TG2 deficiency on cytoskeleton is not mediated by FN matrix levels as *Tgm2-/-* MEFs assembled normal FN matrix and showed no changes in the amounts of FN in DOC-soluble or DOC-insoluble fractions (**Figure S3**). mRNA expression of total and cellular FN (EDA-FN or EDB-FN) were also not altered (**Fig. S4**). This data suggests that TG2 modulation of actin cytoskeleton and Akt signalling also contributes to increased adipogenesis.

Tgm2-/- mice adipose tissue display increased adipocyte number

To see how an increase in adipogenesis in *Tgm2-/-* MEFs *in vitro* translates to adipose tissue in mice, epididymal fat pad of *Tgm2-/-* and *Tgm2+/+* mice was used to assess

adipocyte size and number *in vivo*. **Figure 8A,B** show that the adipocyte size is significantly reduced in *Tgm2-/-* mice compared to *Tgm2+/+* mice. However, adipocyte number is significantly increased in *Tgm2-/-* mice compared to *Tgm2+/+* mice (**Figure 8C**). The increase in adipocyte number in *Tgm2*-/- mice suggest increased proliferation of precursor cells and/or preadipocytes (hyperplasia), and their differentiation into mature adipocytes (adipogenesis).

3.6 Discussion

Our previous work identified two members of TG family, FXIII-A and TG2, in WAT and demonstrated that FXIII-A can regulate adipocyte proliferation via promoting plasma FN matrix assembly which inhibits adipogenesis (Myneni et al., 2014). In this study, we have examined the role of TG2 in adipogenesis and report for the first time that TG2 also acts as an inhibitor of adipocyte differentiation. We show that *Tgm2*-/- MEFs display accelerated and enhanced adipogenesis which is associated with downregulation of multiple anti-adipogenic signaling pathways that jointly lead to increased expression and activation of master transcription factors of adipogenesis, *Pparγ* and *Cebpα*, and increased lipid accumulation in the cells. The pathways identified in this study are; regulation of Pref-1 protein levels, β-catenin signaling and modulation of ROCK-mediated cytoskeletal tension and Akt signaling.

The identification of TG2 in as an anti-adipogenic factor is not entirely unexpected as TG2 has been implicated in regulation of number of pathways in multiple location in cells (Eckert et al., 2014). Our report shows for the first time that in MEFs *Tgm2* deficiency dramatically reduces *Pref-1* protein expression. Pref-1 is an major inhibitor of adipocyte differentiation and a factor whose expression is highest during early differentiation and then gradually disappears as the cells differentiate into adipocytes (Smas and Sul, 1993) (Hudak and Sul, 2013). Pref-1 protein mediates its effects on adipocyte differentiation by directly binding to FN, which activates integrin signaling to engage the MAPK/ERK pathway. This induces Sox9 expression which inhibits adipocyte differentiation (Wang et al., 2006; Wang et al., 2010a). *Pref-1* knockout mice

have increased adipose tissue mass, pre- and postnatal growth retardation and skeletal abnormalities (Moon et al., 2002) and conversely *Pref-1* overexpressing mice have reduced adipose tissue mass, impaired glucose tolerance and reduced insulin sensitivity(Lee et al., 2003; Villena et al., 2008). Other effects of Pref-1 protein are also mediated by Sox9 which promotes chondrogenic commitment of MSCs, but inhibits chondrocyte maturation and osteoblast differentiation(Wang and Sul, 2009). Linked with Pref-1 function in chondrocyte maturation, TG2 has been shown to regulate the transition into the prehypertrophic stage during chondrocyte maturation. Premature, forced expression of TG2 accelerated progression towards prehypertrophy and it was shown that extracellular TG2 can increase Sox9 expression (Nurminsky et al., 2011). Based on our work, it is highly possible that the effects of TG2 on chondrocytes may also be mediated via Pref-1. TG2 is also expressed by osteoblasts where it is located on the cell surface(Al-Jallad et al., 2006). TG2 knockout mice do not show any chondrogenic or osteogenic abnormalities during development or postnatally(De Laurenzi and Melino, 2001), which is likely due to compensatory function from upregulation of FXIII-A and TGFβ1(Tarantino et al., 2009). It is possible that TG2, jointly with other TG enzymes and Pref-1, may act as an upstream regulators of mesenchymal stem cell differentiation into the different lineages, particularly into chondrocytes, osteoblasts and adipocytes.

In addition to Pref-1, we reported here that TG2 regulates β-catenin nuclear translocation in preadipocytes. Canonical Wnt signalling is a crucial pathway that regulates lineage determination of MSCs. In preadipocytes, Wnt signaling maintains preadipocytes in undifferentiated state by inhibiting PPARγ and C/EBPα (Ross et al., 2000). During early phase of adipogenesis PPARγ suppresses Wnt signalling by increasing β-catenin degradation and PPARγ upregulation coincides with decreased total and nuclear β-catenin levels, suggesting a reciprocal relation between Wnt and PPARγ (Girnun et al., 2002; Liu et al., 2006; Moldes et al., 2003). Here we report that *Tgm2*-/- cells display increase in *Pparγ* and *Cebpα* mRNA expression and reduced β-catenin nuclear accumulation during the early phase of adipogenesis. When exogenous TG2 was added, a significant decrease in lipid accumulation was seen and this was

associated with an increase in nuclear accumulation of β-catenin as well as decreased *Pparγ* and *Cebpα* mRNA expression. Interestingly, *Pref-1* was shown to be a Wnt target gene and was, in fact, shown to be downregulated by TCF/β-catenin complex in fetal lung epithelial cells and MEFs (Galceran et al., 2004; Paul et al., 2015; Weng et al., 2009). Furthermore, Pref-1 can act as a noncanonical Notch ligand and inhibit Notch signalling and, in turn, Wnt/β-catenin signalling is negatively regulated by Notch (Andersen et al., 2012). This crosstalk between Notch and Wnt signalling may be one of the regulatory mechanism for Pref-1 production. We are currently exploring the mechanisms how TG2 affects the Pref-1 protein regulation.

It is well documented that canonical Wnt signalling inhibits adipogenesis and promotes osteogenesis in MSCs (Takada et al., 2009). Canonical Wnt signalling can also inhibit adipogenesis in lineage committed preadipocytes (Ross et al., 2000). Furthermore, canonical Wnt receptor LRP6 knockout MEFs show increased adipogenesis (Kawai et al., 2007). In smooth muscle cells, extracellular TG2 regulates canonical Wnt signalling and β-catenin nuclear translocation which promotes calcification of the cell cultures system. This effect in smooth muscle cells is mediated by extracellular TG2 binding to LRP5/6 on the smooth muscle cell surface and this reported interaction does not require transamidation activity (Faverman et al., 2008). In this study, we show that extracellular TG2 activates canonical Wnt signalling contributing to the inhibitory effect on adipogenesis. While we did not address the exact mechanism how exogenous extracellular TG2 here regulates β-catenin nuclear translocation, it is plausible that the mechanism is the same as in smooth muscle cells. It is also possible that the exogenous TG2 promotes β-catenin release from the plasma membrane E-cadherin to the cytosol and from there to nucleus. This concept is supported by the observation that exogenous TG2 addition caused an increase in cytosolic and nuclear pools of β-catenin without affecting the total β-catenin levels in protein extracts.

Consistent with previous work on the role of TG2 in maintaining cytoskeletal tension, we also report here that *Tgm2*-deficient MEFs have decreased ROCK kinase activity and decreased actin stress fibers, which also contributes to increased adipogenesis.

Adipogenesis is characterized by change in cell shape, from spindle shaped preadipocytes to round adipocytes and this transition is partly determined by the cytoskeletal tension. During adipogenesis filamentous actin from stress fibers is rearranged to cortical pattern and down regulation of ROCK kinase disrupts actin stress fibers (McBeath et al., 2004; Spiegelman and Ginty, 1983). Inhibition of ROCK kinase was shown to promote adipogenesis and Akt signaling (Lee et al., 2009; Noguchi et al., 2007) and conversely activating ROCK kinase inhibits adipogenesis (McBeath et al., 2004). TG2 was reported to activate ROCK via two pathways - retinoic acid-induced TG2 enzymatic activity was reported to activate ROCK kinase by intracellular TG2 (Singh et al., 2001) and cell surface TG2 was reported to amplify integrin mediated signalling to activate ROCK kinase in a non-enzymatic manner (Janiak et al., 2006). ECM quantity and quality is a major regulator of cytoskeleton (Chiquet et al., 2009) and it is known that cell surface TG2 cooperates with α5β1 integrins to enhance FN-integrin binding which is required for FN assembly.

TG2 has been suggested to stabilize ECM in a number of studies and factors such as TGFβ - an inhibitor of adipogenesis - was shown to increase cell surface expression of TG2 and increase FN assembly (Akimov and Belkin, 2001a). FN matrix itself is a major inhibitor of adipogenesis and must be decreased for the preadipocytes to allow differentiation towards mature adipocytes. However, in our study, we show that the absence of TG2 does not affect FN matrix levels or solubility in preadipocytes which strongly suggests that TG2 is not involved in FN matrix assembly and that cytoskeletal alterations in *Tgm2*-/- MEFs are not mediated by ECM itself, but likely via cell surface TG2 and the manner cells adhere to ECM. Indeed, *Tgm2*-/- deficient fibroblasts have been demonstrated to have an adhesion defect (Telci et al., 2008; Wang et al., 2010b). Moreover, the data strongly suggest that TG2 is not involved in MEF matrix assembly and does not appear to participate in MEF extracellular transamidation/crosslinking events. This is also supported by the fact that *Tgm2*-/- and *Tgm2*+/+ MEFs had similar levels of TG activity – this activity likely deriving from FXIII-A. Interestingly, both TG2 and FXIII-A act as negative regulators of adipogenesis and thus they may have a complementary effect on adipogenesis.

Increased fat mass in obesity is associated with an increase in adipocyte cell size and/or adipocyte number which are reactions to expand adipose tissue upon need to increase energy storage (Spalding et al., 2008). Defects in this expansion are linked to obesity-linked comorbidities such as development of type 2 diabetes (Tchoukalova et al., 2007; Virtue and Vidal-Puig, 2008). In this work, we have identified a new factor, TG2 that maintains preadipocyte state and thus acts as a negative regulator of adipogenesis. It is thus likely that regulation of TG2 in preadipocytes is tightly controlled to balance proliferation and differentiation. Further understanding of TG2 and its role and regulation in metabolic disorders would aid the development of new therapies to maintain healthy energy metabolism.

3.7 Acknowledgements

We would like to thank Aisha Mousa for assistance. This study was supported by grants to MTK from the Canadian Institutes of Health Research (CIHR), and the CIHR Institute of Genetics. VDM received stipends from Faculty of Dentistry and the CIHR Systems Biology Training Program.

Conflict of interest

The authors declare no conflict of interest.

3.8 References

Akimov, S.S., and Belkin, A.M. (2001a). Cell-surface transglutaminase promotes fibronectin assembly via interaction with the gelatin-binding domain of fibronectin: a role in TGFbeta-dependent matrix deposition. Journal of cell science *114*, 2989-3000.

Akimov, S.S., and Belkin, A.M. (2001b). Cell surface tissue transglutaminase is involved in adhesion and migration of monocytic cells on fibronectin. Blood *98*, 1567-1576.

Al-Jallad, H.F., Nakano, Y., Chen, J.L., McMillan, E., Lefebvre, C., and Kaartinen, M.T. (2006). Transglutaminase activity regulates osteoblast differentiation and matrix mineralization in MC3T3-E1 osteoblast cultures. Matrix biology : journal of the International Society for Matrix Biology *25*, 135-148.

Amano, M., Nakayama, M., and Kaibuchi, K. (2010). Rho-kinase/ROCK: A key regulator of the cytoskeleton and cell polarity. Cytoskeleton (Hoboken, N.J.) *67*, 545-554.

Andersen, P., Uosaki, H., Shenje, L.T., and Kwon, C. (2012). Non-canonical Notch signaling: emerging role and mechanism. Trends in cell biology *22*, 257-265.

Aubin, D., Gagnon, A., and Sorisky, A. (2005). Phosphoinositide 3-kinase is required for human adipocyte differentiation in culture. International journal of obesity (2005) *29*, 1006-1009.

Belkin, A.M. (2011). Extracellular TG2: emerging functions and regulation. The FEBS journal *278*, 4704-4716.

Bernassola, F., Federici, M., Corazzari, M., Terrinoni, A., Hribal, M.L., De Laurenzi, V., Ranalli, M., Massa, O., Sesti, G., McLean, W.H., et al. (2002). Role of transglutaminase 2 in glucose tolerance: knockout mice studies and a putative mutation in a MODY patient. FASEB journal : official publication of the Federation of American Societies for Experimental Biology *16*, 1371-1378.

Chiquet, M., Gelman, L., Lutz, R., and Maier, S. (2009). From mechanotransduction to extracellular matrix gene expression in fibroblasts. Biochimica et biophysica acta *1793*, 911-920.

Christodoulides, C., Lagathu, C., Sethi, J.K., and Vidal-Puig, A. (2009). Adipogenesis and WNT signalling. Trends in endocrinology and metabolism: TEM *20*, 16-24.

Cristancho, A.G., and Lazar, M.A. (2011). Forming functional fat: a growing understanding of adipocyte differentiation. Nature reviews. Molecular cell biology *12*, 722-734.

De Laurenzi, V., and Melino, G. (2001). Gene disruption of tissue transglutaminase. Molecular and cellular biology *21*, 148-155.

Eckert, R.L., Kaartinen, M.T., Nurminskaya, M., Belkin, A.M., Colak, G., Johnson, G.V., and Mehta, K. (2014). Transglutaminase regulation of cell function. Physiological reviews *94*, 383-417.

Faverman, L., Mikhaylova, L., Malmquist, J., and Nurminskaya, M. (2008). Extracellular transglutaminase 2 activates beta-catenin signaling in calcifying vascular smooth muscle cells. FEBS letters *582*, 1552-1557.

Fesus, L., and Piacentini, M. (2002). Transglutaminase 2: an enigmatic enzyme with diverse functions. Trends in biochemical sciences *27*, 534-539.

Feve, B. (2005). Adipogenesis: cellular and molecular aspects. Best practice & research. Clinical endocrinology & metabolism *19*, 483-499.

Galceran, J., Sustmann, C., Hsu, S.C., Folberth, S., and Grosschedl, R. (2004). LEF1-mediated regulation of Delta-like1 links Wnt and Notch signaling in somitogenesis. Genes & development *18*, 2718-2723.

Girnun, G.D., Smith, W.M., Drori, S., Sarraf, P., Mueller, E., Eng, C., Nambiar, P., Rosenberg, D.W., Bronson, R.T., Edelmann, W., et al. (2002). APC-dependent suppression of colon carcinogenesis by PPARgamma. Proceedings of the National Academy of Sciences of the United States of America *99*, 13771-13776.

Grosso, H., and Mouradian, M.M. (2012). Transglutaminase 2: biology, relevance to neurodegenerative diseases and therapeutic implications. Pharmacology & therapeutics *133*, 392-410.

Gundemir, S., Colak, G., Tucholski, J., and Johnson, G.V. (2012). Transglutaminase 2: a molecular Swiss army knife. Biochimica et biophysica acta *1823*, 406-419.

Han, F., Adams, C.S., Tao, Z., Williams, C.J., Zaka, R., Tuan, R.S., Norton, P.A., and Hickok, N.J. (2005). Transforming growth factor-beta1 (TGF-beta1) regulates ATDC5 chondrogenic differentiation and fibronectin isoform expression. Journal of cellular biochemistry *95*, 750-762.

Han, J., Farmer, S.R., Kirkland, J.L., Corkey, B.E., Yoon, R., Pirtskhalava, T., Ido, Y., and Guo, W. (2002). Octanoate attenuates adipogenesis in 3T3-L1 preadipocytes. J Nutr *132*, 904-910.

Hudak, C.S., and Sul, H.S. (2013). Pref-1, a gatekeeper of adipogenesis. Frontiers in endocrinology *4*, 79.

Iismaa, S.E., Mearns, B.M., Lorand, L., and Graham, R.M. (2009). Transglutaminases and disease: lessons from genetically engineered mouse models and inherited disorders. Physiological reviews *89*, 991-1023.

Janiak, A., Zemskov, E.A., and Belkin, A.M. (2006). Cell surface transglutaminase promotes RhoA activation via integrin clustering and suppression of the Src-p190RhoGAP signaling pathway. Molecular biology of the cell *17*, 1606-1619.

Kahn, S.E., Hull, R.L., and Utzschneider, K.M. (2006). Mechanisms linking obesity to insulin resistance and type 2 diabetes. Nature *444*, 840-846.

Kanzaki, M., and Pessin, J.E. (2001). Insulin-stimulated GLUT4 translocation in adipocytes is dependent upon cortical actin remodeling. The Journal of biological chemistry *276*, 42436-42444.

Kawai, M., Mushiake, S., Bessho, K., Murakami, M., Namba, N., Kokubu, C., Michigami, T., and Ozono, K. (2007). Wnt/Lrp/beta-catenin signaling suppresses adipogenesis by inhibiting mutual activation of PPARgamma and C/EBPalpha. Biochemical and biophysical research communications *363*, 276-282.

Kim, J.E., and Chen, J. (2004). regulation of peroxisome proliferator-activated receptor-gamma activity by mammalian target of rapamycin and amino acids in adipogenesis. Diabetes *53*, 2748-2756.

Kim, K.A., Kim, J.H., Wang, Y., and Sul, H.S. (2007). Pref-1 (preadipocyte factor 1) activates the MEK/extracellular signal-regulated kinase pathway to inhibit adipocyte differentiation. Molecular and cellular biology *27*, 2294-2308.

Klock, C., Diraimondo, T.R., and Khosla, C. (2012). Role of transglutaminase 2 in celiac disease pathogenesis. Seminars in immunopathology *34*, 513-522.

Koh, Y.J., Park, B.H., Park, J.H., Han, J., Lee, I.K., Park, J.W., and Koh, G.Y. (2009). Activation of PPAR gamma induces profound multilocularization of adipocytes in adult mouse white adipose tissues. Experimental & molecular medicine *41*, 880-895.

Lee, D.H., Shi, J., Jeoung, N.H., Kim, M.S., Zabolotny, J.M., Lee, S.W., White, M.F., Wei, L., and Kim, Y.B. (2009). Targeted disruption of ROCK1 causes insulin resistance in vivo. The Journal of biological chemistry *284*, 11776-11780.

Lee, K., Villena, J.A., Moon, Y.S., Kim, K.H., Lee, S., Kang, C., and Sul, H.S. (2003). Inhibition of adipogenesis and development of glucose intolerance by soluble preadipocyte factor-1 (Pref-1). The Journal of clinical investigation *111*, 453-461.

Liu, J., Wang, H., Zuo, Y., and Farmer, S.R. (2006). Functional interaction between peroxisome proliferator-activated receptor gamma and beta-catenin. Molecular and cellular biology *26*, 5827-5837.

Long, F., and Ornitz, D.M. (2013). Development of the endochondral skeleton. Cold Spring Harbor perspectives in biology *5*, a008334.

McBeath, R., Pirone, D.M., Nelson, C.M., Bhadriraju, K., and Chen, C.S. (2004). Cell shape, cytoskeletal tension, and RhoA regulate stem cell lineage commitment. Developmental cell *6*, 483-495.

Moldes, M., Zuo, Y., Morrison, R.F., Silva, D., Park, B.H., Liu, J., and Farmer, S.R. (2003). Peroxisome-proliferator-activated receptor gamma suppresses Wnt/beta-catenin signalling during adipogenesis. The Biochemical journal *376*, 607-613.

Moon, Y.S., Smas, C.M., Lee, K., Villena, J.A., Kim, K.H., Yun, E.J., and Sul, H.S. (2002). Mice lacking paternally expressed Pref-1/Dlk1 display growth retardation and accelerated adiposity. Molecular and cellular biology *22*, 5585-5592.

Murtaugh, M.P., Mehta, K., Johnson, J., Myers, M., Juliano, R.L., and Davies, P.J. (1983). Induction of tissue transglutaminase in mouse peritoneal macrophages. The Journal of biological chemistry *258*, 11074-11081.

Myneni, V.D., Hitomi, K., and Kaartinen, M.T. (2014). Factor XIII-A transglutaminase acts as a switch between preadipocyte proliferation and differentiation. Blood *124*, 1344-1353.

Noguchi, M., Hosoda, K., Fujikura, J., Fujimoto, M., Iwakura, H., Tomita, T., Ishii, T., Arai, N., Hirata, M., Ebihara, K., et al. (2007). Genetic and pharmacological inhibition of Rho-associated kinase II enhances adipogenesis. The Journal of biological chemistry *282*, 29574-29583.

Nurminsky, D., Shanmugasundaram, S., Deasey, S., Michaud, C., Allen, S., Hendig, D., Dastjerdi, A., Francis-West, P., and Nurminskaya, M. (2011). Transglutaminase 2 regulates early chondrogenesis and glycosaminoglycan synthesis. Mechanisms of development *128*, 234-245.

Pankov, R., and Yamada, K.M. (2004). Non-radioactive quantification of fibronectin matrix assembly. Current protocols in cell biology / editorial board, Juan S. Bonifacino ... [et al.] *Chapter 10*, Unit 10.13.

Paul, C., Sardet, C., and Fabbrizio, E. (2015). The Wnt-target gene Dlk-1 is regulated by the Prmt5-associated factor Copr5 during adipogenic conversion. Biology open.

Rosner, M., and Hengstschlager, M. (2008). Cytoplasmic and nuclear distribution of the protein complexes mTORC1 and mTORC2: rapamycin triggers dephosphorylation and delocalization of the mTORC2 components rictor and sin1. Human molecular genetics *17*, 2934-2948.

Ross, S.E., Hemati, N., Longo, K.A., Bennett, C.N., Lucas, P.C., Erickson, R.L., and MacDougald, O.A. (2000). Inhibition of adipogenesis by Wnt signaling. Science *289*, 950-953.

Siegel, M., and Khosla, C. (2007). Transglutaminase 2 inhibitors and their therapeutic role in disease states. Pharmacology & therapeutics *115*, 232-245.

Singh, U.S., Kunar, M.T., Kao, Y.L., and Baker, K.M. (2001). Role of transglutaminase II in retinoic acid-induced activation of RhoA-associated kinase-2. The EMBO journal *20*, 2413-2423.

Smas, C.M., and Sul, H.S. (1993). Pref-1, a protein containing EGF-like repeats, inhibits adipocyte differentiation. Cell *73*, 725-734.

Song, H., Chang, W., Lim, S., Seo, H.S., Shim, C.Y., Park, S., Yoo, K.J., Kim, B.S., Min, B.H., Lee, H., et al. (2007). Tissue transglutaminase is essential for integrin-mediated survival of bone marrow-derived mesenchymal stem cells. Stem cells (Dayton, Ohio) *25*, 1431-1438.

Spalding, K.L., Arner, E., Westermark, P.O., Bernard, S., Buchholz, B.A., Bergmann, O., Blomqvist, L., Hoffstedt, J., Naslund, E., Britton, T., et al. (2008). Dynamics of fat cell turnover in humans. Nature *453*, 783-787.

Spiegelman, B.M., and Ginty, C.A. (1983). Fibronectin modulation of cell shape and lipogenic gene expression in 3T3-adipocytes. Cell *35*, 657-666.

Takada, I., Kouzmenko, A.P., and Kato, S. (2009). Wnt and PPARgamma signaling in osteoblastogenesis and adipogenesis. Nature reviews. Rheumatology *5*, 442-447.

Tanabe, Y., Koga, M., Saito, M., Matsunaga, Y., and Nakayama, K. (2004). Inhibition of adipocyte differentiation by mechanical stretching through ERK-mediated downregulation of PPARgamma2. Journal of cell science *117*, 3605-3614.

Tarantino, U., Oliva, F., Taurisano, G., Orlandi, A., Pietroni, V., Candi, E., Melino, G., and Maffulli, N. (2009). FXIIIA and TGF-beta over-expression produces normal musculo-skeletal phenotype in TG2-/- mice. Amino acids *36*, 679-684.

Tchoukalova, Y., Koutsari, C., and Jensen, M. (2007). Committed subcutaneous preadipocytes are reduced in human obesity. Diabetologia *50*, 151-157.

Telci, D., Wang, Z., Li, X., Verderio, E.A., Humphries, M.J., Baccarini, M., Basaga, H., and Griffin, M. (2008). Fibronectin-tissue transglutaminase matrix rescues RGD-impaired cell adhesion through syndecan-4 and beta1 integrin co-signaling. The Journal of biological chemistry *283*, 20937-20947.

Thomazy, V., and Fesus, L. (1989). Differential expression of tissue transglutaminase in human cells. An immunohistochemical study. Cell and tissue research *255*, 215-224.

Van Gaal, L.F., Mertens, I.L., and De Block, C.E. (2006). Mechanisms linking obesity with cardiovascular disease. Nature *444*, 875-880.

Villena, J.A., Choi, C.S., Wang, Y., Kim, S., Hwang, Y.J., Kim, Y.B., Cline, G., Shulman, G.I., and Sul, H.S. (2008). Resistance to high-fat diet-induced obesity but exacerbated insulin resistance in mice overexpressing preadipocyte factor-1 (Pref-1): a new model of partial lipodystrophy. Diabetes *57*, 3258-3266.

Virtue, S., and Vidal-Puig, A. (2008). It's not how fat you are, it's what you do with it that counts. PLoS biology *6*, e237.

Wang, Y., Kim, K.A., Kim, J.H., and Sul, H.S. (2006). Pref-1, a preadipocyte secreted factor that inhibits adipogenesis. J Nutr *136*, 2953-2956.

Wang, Y., and Sul, H.S. (2009). Pref-1 regulates mesenchymal cell commitment and differentiation through Sox9. Cell metabolism *9*, 287-302.

Wang, Y., Zhao, L., Smas, C., and Sul, H.S. (2010a). Pref-1 interacts with fibronectin to inhibit adipocyte differentiation. Molecular and cellular biology *30*, 3480-3492.

Wang, Z., Collighan, R.J., Gross, S.R., Danen, E.H., Orend, G., Telci, D., and Griffin, M. (2010b). RGD-independent cell adhesion via a tissue transglutaminase-fibronectin

matrix promotes fibronectin fibril deposition and requires syndecan-4/2 alpha5beta1 integrin co-signaling. The Journal of biological chemistry *285*, 40212-40229.

Weng, T., Gao, L., Bhaskaran, M., Guo, Y., Gou, D., Narayanaperumal, J., Chintagari, N.R., Zhang, K., and Liu, L. (2009). Pleiotrophin regulates lung epithelial cell proliferation and differentiation during fetal lung development via beta-catenin and Dlk1. The Journal of biological chemistry *284*, 28021-28032.

3.9 Figures

Fig.1

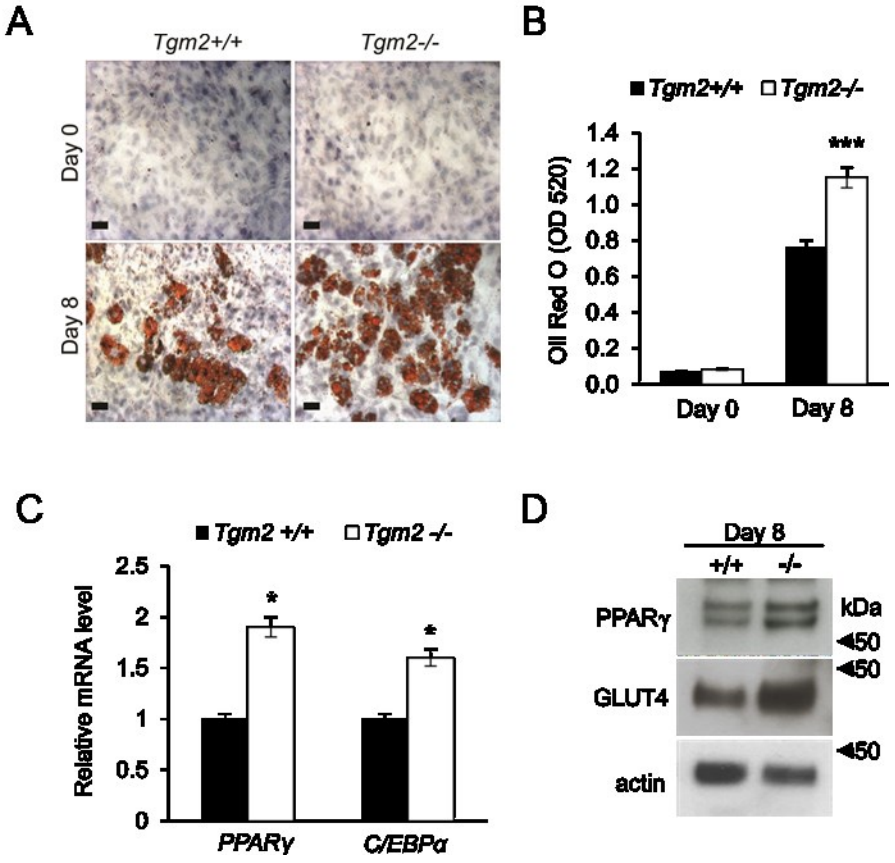

Fig. 1. *Tgm2-/-* MEFs show enhanced adipogenesis. (A) *Tgm2+/+* and *Tgm2-/-* MEFs were subjected to adipogenic differentiation and their ability to accumulate lipids was assessed on day 0 and day 8 by Oil Red O staining. Cells were counter stained with hematoxylin. Increases lipids are visible in *Tgm2-/-* MEFs on day 8. Scale bar equals 70 µm. **(B)** Quantification of Oil Red O cultures on day 0 and 8 show significantly increases lipid accumulation to *Tgm2-/-* MEFs compared to *Tgm2+/+* MEFs. Results are mean values ± SEM (n=3). ***p<0.001. **(C)** mRNA expression analysis of *Pparγ* and

Cebpα from *Tgm2+/+* and *Tgm2-/-* MEFs on day 8 shows a significant increase in *Tgm2-/-* MEFs. The relative quantity of mRNA expression was normalized to 18S. Error bars ± SD (n=3), *p<0.05. **(D)** Western blot analysis of total cell lysate of *Tgm2-/-* and *Tgm2+/+* MEFs on day 8, show increased PPARγ protein and its downstream target gene GLUT4 in *Tgm2-/-* MEFs; actin used as loading control.

Fig.2

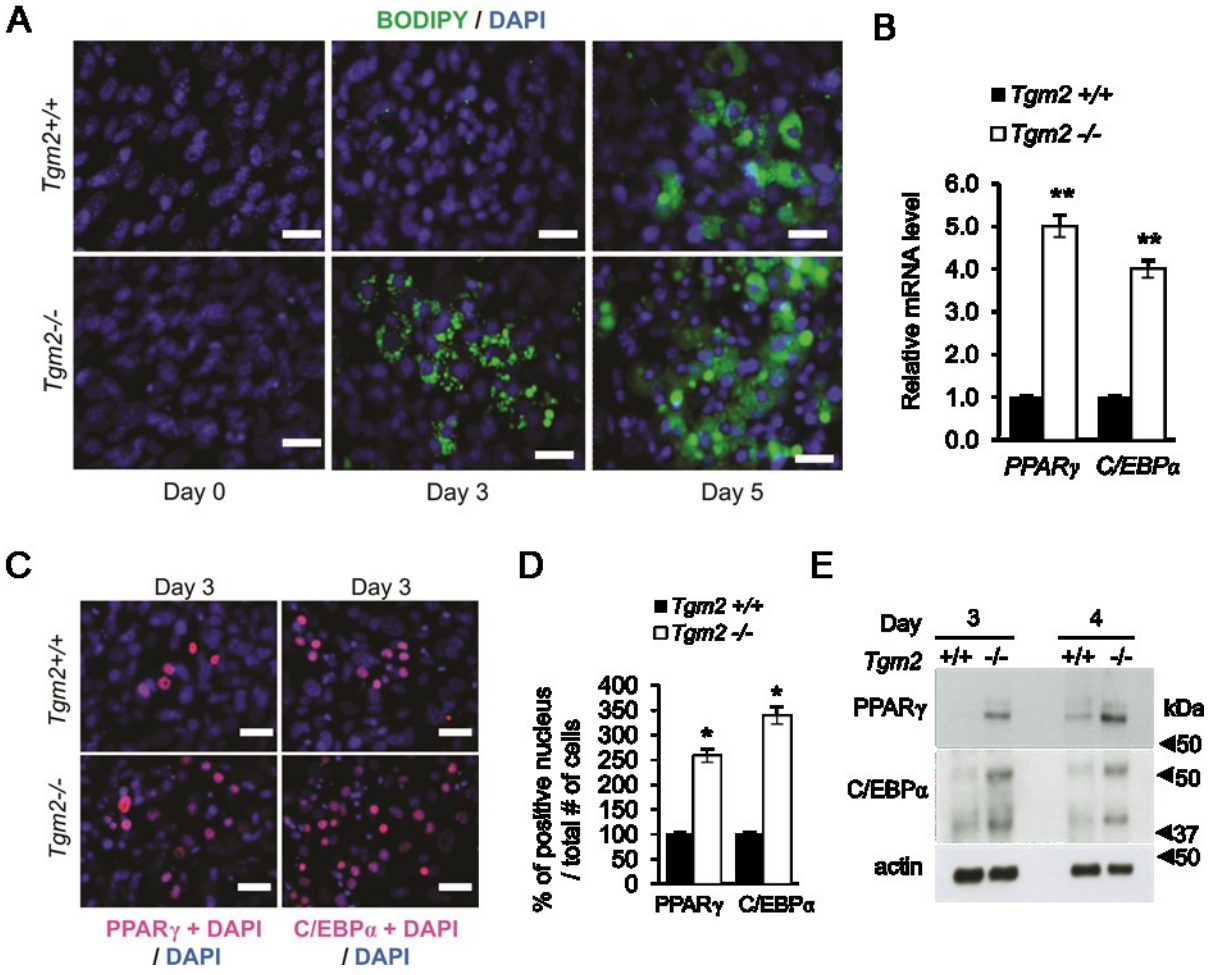

Fig. 2. *Tgm2-/-* MEFs show accelerated adipogenesis. (A) Immunofluorescence staining for lipid with Bodipy 493/503 (green) during differentiation of *Tgm2+/+* and *Tgm2-/-* MEFs. Lipid accumulation is visible on day 3 in *Tgm2-/-* MEFs compared to *Tgm2+/+* MEFs which show lipids only on day 4-5 onwards. Nuclei were visualized with DAPI (blue). Scale bar equals 50 µm. **(B)** mRNA expression of *Pparγ* and *Cebpα* from *Tgm2+/+* and *Tgm2-/-* MEFs on day 3, show a significant increase in *Tgm2-/-* MEFs. The relative quantity of mRNA expression was normalized to 18S. Error bars ± SD (n=3), **p<0.01. **(C)** Nuclear translocation of PPARγ and C/EBPα (colocalization with

DAPI in pink) in *Tgm2+/+* and *Tgm2-/-* MEFs on day 3 show increased activation of transcription factors. Nuclei stained with DAPI (blue). Scale bar equals 50 μm. **(D)** Quantification of PPARγ and C/EBPα positive nucleus per total number of cells in *Tgm2+/+* and *Tgm2-/-* MEFs on day 3 shows a dramatic and significant increase in *Tgm2-/-* MEFs. Error bars ± SEM (n=3), *p<0.05. **(E)** Western blot analysis of PPARγ and C/EBPα in total cell lysates on day 3 and 4 show increased PPARγ and C/EBPα protein levels in *Tgm2*-/- MEFs; actin used as loading control.

Fig.3

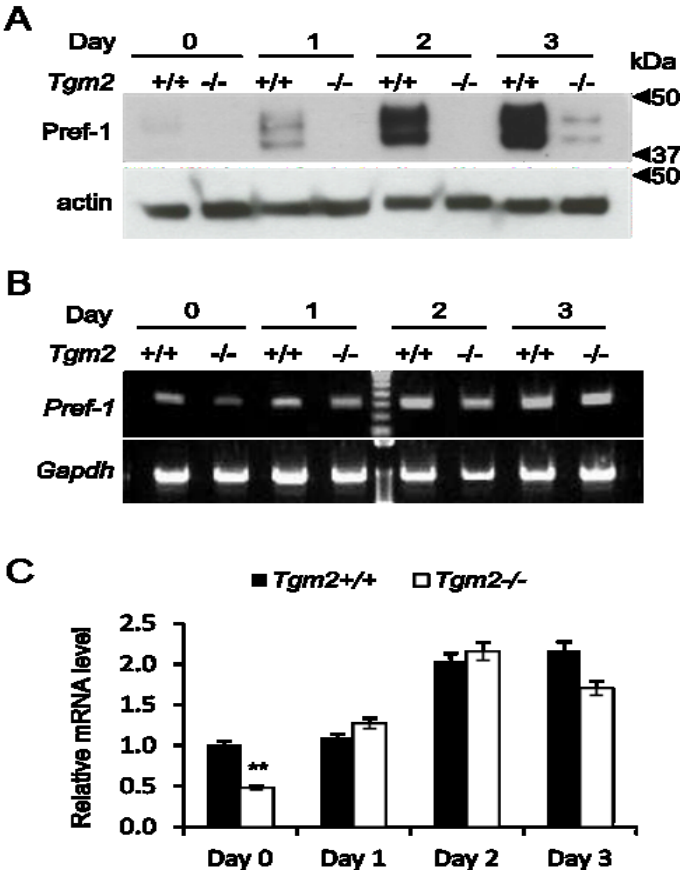

Fig. 3. Pref-1 protein and mRNA production is compromised in *Tgm2-/-* MEFs.

(A) Western blot analysis of Pref-1 in total cell lysates of *Tgm2*-/- and *Tgm2*+/+ MEFs during early differentiation on days 0-3 show almost complete absence of the protein. Actin was used as loading control. **(B)** mRNA expression of *Pref-1* by RT-PCR in the cells shows that on day 1 Pref-1 mRNA is lower in *Tgm2*-/- compared to *Tgm2*+/+ MEFs, however, on day 3 the difference is no longer observed. This mRNA does not appear to translate into protein as per Western blot analysis. *Gapdh* used as loading control. **(C)** Quantification of mRNA expression of Pref-1in panel B, shows significantly reduced of Pref-1 on day 0 in *Tgm2*-/- compared to *Tgm2*+/+ MEFs. Pref-1 expression was similar in both *Tgm2*-/- and *Tgm2*+/+ MEFs after initiation of differentiation (day 1). Error bars ± SEM (n=3), **p<0.01.

Fig.4

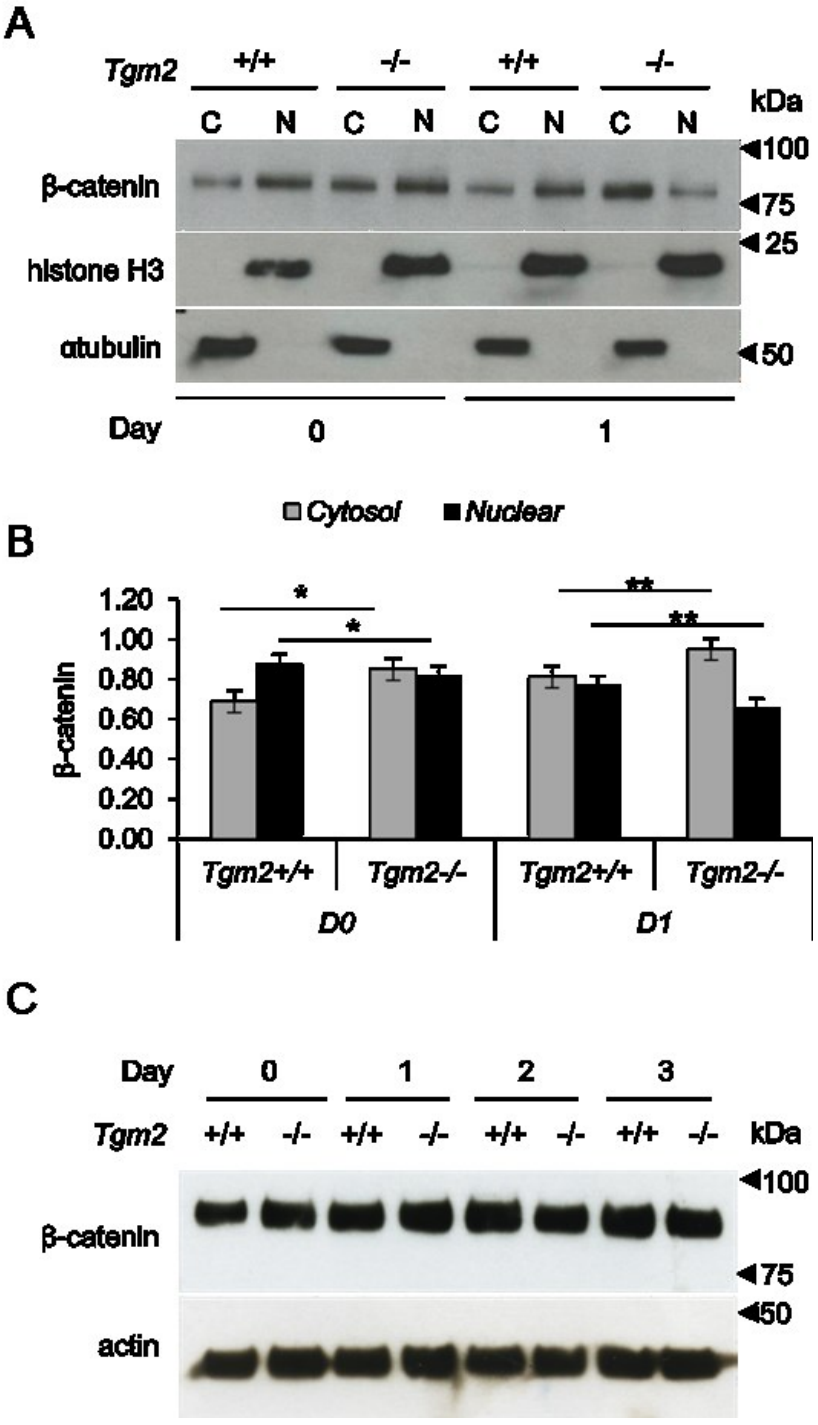
A
Tgm2
+/+
-/-
+/+
-/-
kDa
C N C N C N C N
β-catenin
histone H3
αtubulin
100
75
25
50
Day
0
1
Cytosol
Nuclear
B
β-catenin
1.20
1.00
0.80
0.60
0.40
0.20
0.00
*
*
**
**
Tgm2+/+
Tgm2-/-
Tgm2+/+
Tgm2-/-
D0
D1
C
Day
0
1
2
3
Tgm2
+/+ -/- +/+ -/- +/+ -/- +/+ -/-
kDa
β-catenin
actin
100
75
50

Fig. 4. *Tgm2-/-* MEFs show decreased β-catenin nuclear translocation. (A) Western blot analysis of β-catenin levels in cytosol (C) and nuclear (N) fractions of *Tgm2+/+* and *Tgm2-/-* MEFs on day 0 and day 1. α-Tubulin and histone H3 were used as cytosolic and nuclear loading controls, respectively. **(B)** Quantification of Western blots shows significantly reduced nuclear translocation of β-catenin in *Tgm2-/-* MEFs compared to control cells before (day 0) and after initiation of differentiation (day 1). Error bars ± SEM (n=3), *p<0.05; **p<0.01. **(C)** Western blot analysis for β-catenin levels in total cell lysates of *Tgm2+/+* and *Tgm2-/-* MEFs from day 0-3 show no changes;actin used as a loading control.

Fig.5

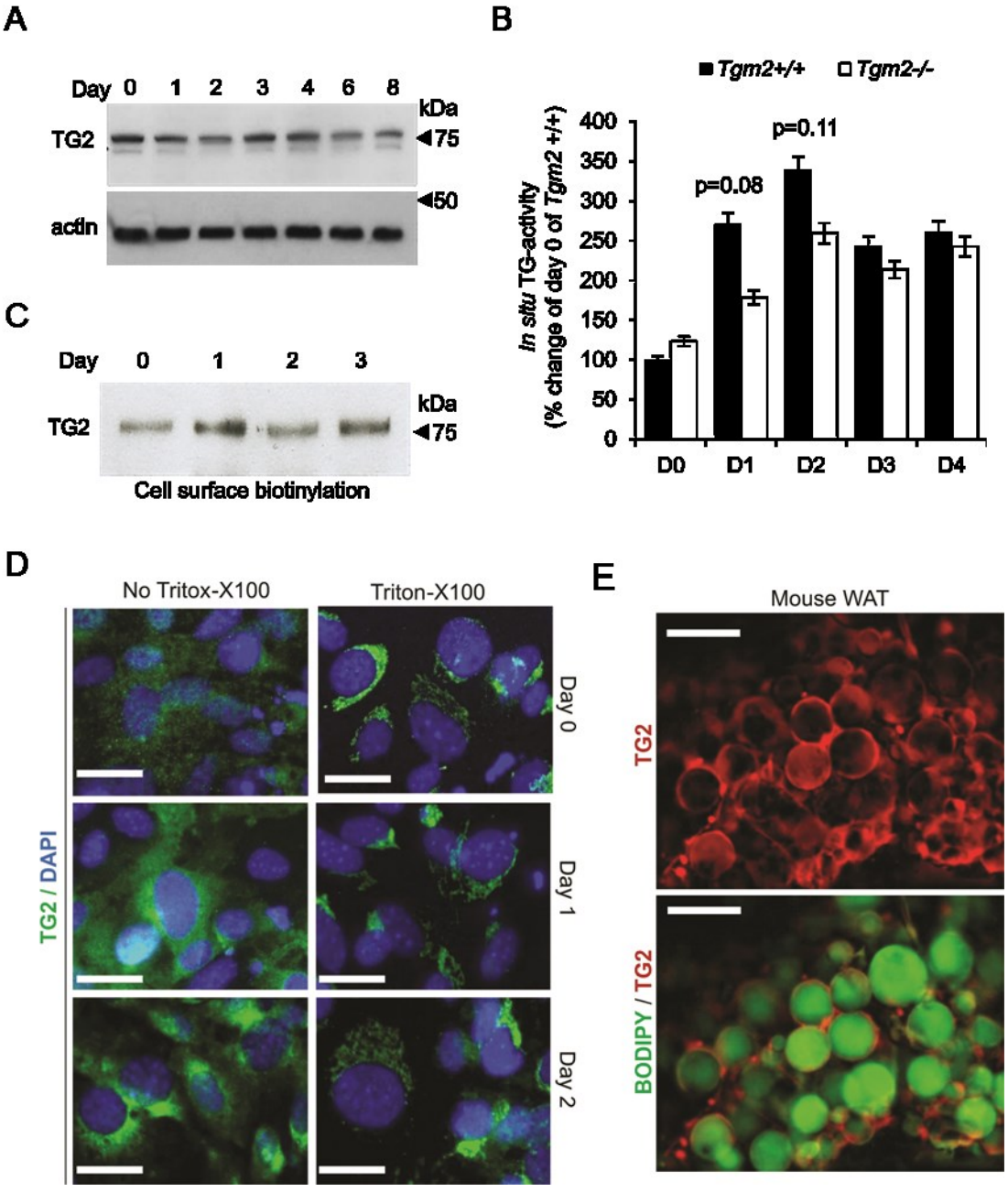
A
Day 0 1 2 3 4 6 8
kDa
TG2
75
actin
50
B
Tgm2+/+
Tgm2-/-
In situ TG-activity
(% change of day 0 of Tgm2 +/+)
400
350
300
250
200
150
100
50
0
p=0.11
p=0.08
D0 D1 D2 D3 D4
C
Day 0 1 2 3
kDa
TG2
75
Cell surface biotinylation
D
No Tritox-X100
Triton-X100
TG2 / DAPI
Day 0
Day 1
Day 2
E
Mouse WAT
TG2
BODIPY / TG2

Fig. 5. TG2 levels and location during early adipogenesis and in WAT. (A) Western blot analysis of total cell lysate from *Tgm2+/+* MEFs during adipocyte differentiation. TG2 levels remain constant with no major fluctuations during differentiation. Actin used as loading control. **(B)** Transamidase activity in *Tgm2*-/- and *Tgm2*+/+ MEFs during adipogenesis was assessed *in situ* using 5-(biotinamido) pentylamine as an activity probe. Graph displayed is biotin detection in cells and the activity is normalized to TG-activity on day 0 of *Tgm2+/+* MEFs (set for 100%). Results are mean values ± SEM (n=3). **(C)** Western blot analysis of cell surface biotinylated protein extract for TG2 protein levels in *Tgm2+/+* MEFs during adipocyte differentiation. TG2 levels on cell surface increase with initiation of differentiation (day1). **(D)** Immunofluorescence staining of TG2 (green) during early differentiation of *Tgm2+/+* MEFs. Nuclei were stained with DAPI (blue). Cells not treated with Triton-X100 show the extracellular distribution of TG2; Triton X-100 permeabilized cells show the intracellular distribution; Scale bar equals 100 μm. **(E)** Immunofluorescence staining of whole mount mouse white adipose tissue (WAT) showing distribution of TG2 (red) and lipids (Bodipy 493/503, green) in the tissue; TG2 is mainly extracellular; Scale bar equals 50 μm.

Fig.6

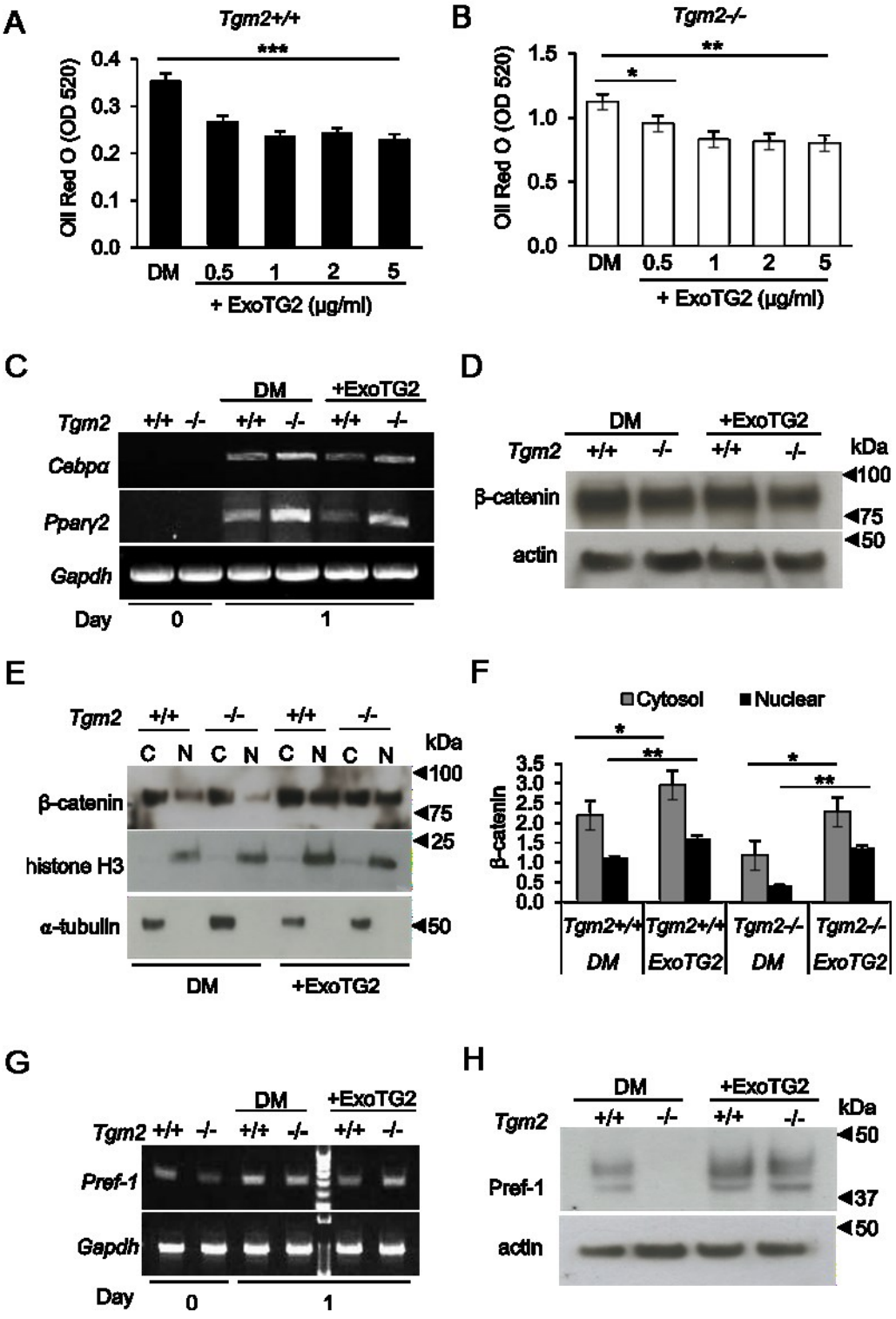
A
Tgm2+/+
***
Oil Red O (OD 520)
0.4
0.3
0.2
0.1
0.0
DM
0.5
1
2
5
+ ExoTG2 (μg/ml)
B
Tgm2-/-
**
*
Oil Red O (OD 520)
1.5
1.0
0.5
0.0
DM
0.5
1
2
5
+ ExoTG2 (μg/ml)
C
DM
+ExoTG2
Tgm2
+/+
-/-
+/+
-/-
+/+
-/-
Cebpα
Pparγ2
Gapdh
Day
0
1
D
DM
+ExoTG2
Tgm2
+/+
-/-
+/+
-/-
kDa
β-catenin
actin
100
75
50
E
Tgm2
+/+
-/-
+/+
-/-
C
N
C
N
C
N
C
N
kDa
β-catenin
histone H3
α-tubulin
100
75
25
50
DM
+ExoTG2
F
Cytosol
Nuclear
*
**
*
**
β-catenin
3.5
3.0
2.5
2.0
1.5
1.0
0.5
0.0
Tgm2+/+ DM
Tgm2+/+ ExoTG2
Tgm2-/- DM
Tgm2-/- ExoTG2
G
DM
+ExoTG2
Tgm2
+/+
-/-
+/+
-/-
+/+
-/-
Pref-1
Gapdh
Day
0
1
H
DM
+ExoTG2
Tgm2
+/+
-/-
+/+
-/-
kDa
Pref-1
actin
50
37
50

Fig. 6. Exogenous, extracellular TG2 inhibits adipogenesis and activates β-catenin signaling and recovers Pref-1 protein levels (A,B) *Tgm2+/+* and *Tgm2-/-* MEF cultures were treated with increasing concentrations (0.5 – 5 μg/ml) of exogenous TG2 (ExoTG2) from day 0 to day 8. Graphs show quantification of Oil Red O staining on day 8. Exogenous TG2 was able to reduce lipid accumulation in a significant manner in both *Tgm2+/+* and *Tgm2-/-* MEFs. Results are mean values ± SEM (n=3). ***p<0.001. *p<0.05; **p<0.01. **(C)** mRNA expression of *Pparγ* and *Cebpα* in *Tgm2+/+* and *Tgm2-/-* MEFs on day 0 and day 1 with or without ExoTG2 (5 μg/ml); DM-differentiation medium. A reduced expression was observed with ExoTG2. **(D)** Western blot analysis of total β-catenin levels in the total cell lysate of *Tgm2+/+* and *Tgm2-/-* MEFs on day 1 with or without ExoTG2 (5 μg/ml) show no difference; actin used as a loading control. **(E,F)** Western blot analysis and quantification of β-catenin levels in cytosolic (C) and nuclear (N) fractions of *Tgm2+/+* and *Tgm2-/-* MEFs on day 1 with or without ExoTG2 (5 μg/ml). Normalization was done with loading controls α-tubulin and histone H3. *Tgm2-/-* MEFs show significantly increased levels of β-catenin in the nucleus. Error bars ± SEM (n=3), *p<0.05; **p<0.01. **(G)** mRNA expression of *Pref-1* in *Tgm2+/+* and *Tgm2-/-* MEFs on day 0 and day 1 with or without ExoTG2 (5 μg/ml). **(H)** Western blot analysis of total cell lysate for Pref-1 in *Tgm2+/+* and *Tgm2-/-* MEFs on day 1 with or without ExoTG2 (5 μg/ml). ExoTG2 treatment recovered Pref-1 protein levels in *Tgm2-/-* MEFs.

Fig.7

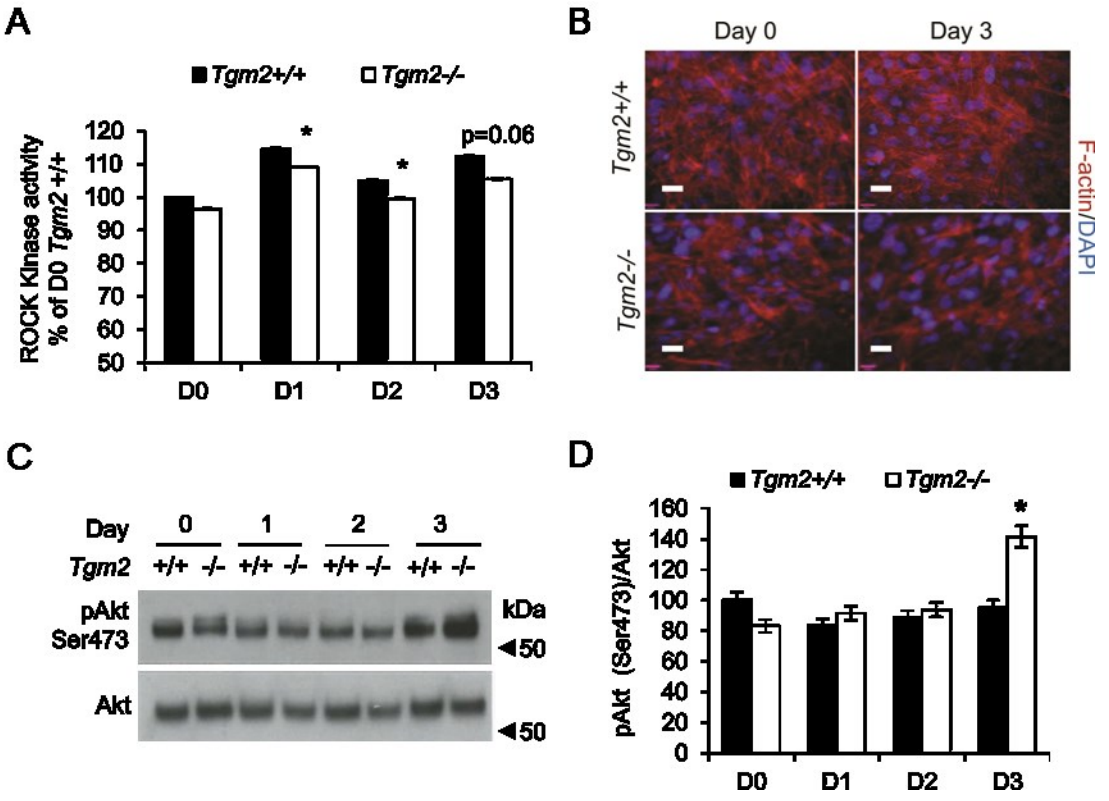

Fig. 7. *Tgm2-/-* MEFs display reduced ROCK kinase activity, actin fibers and increased Akt phosphorylation. (A) Microplate ROCK kinase activity of *Tgm2+/+* and *Tgm2-/-* MEFs in total cell lysate during differentiation show moderate but significant decrease in *Tgm2-/-* cells on days 1 and 2. Error bars ± SEM (n=3), *p<0.05. **(B)** Immunofluorescence staining of of *Tgm2+/+* and *Tgm2-/-* MEFs for F-actin on day 0 and day 3. A decrease in actin stress fibers is observed. Nuclei are stained with DAPI (blue). Scale bar 200µm. **(C,D)** Western blot analysis and quantification of pAkt (Ser473) and total Akt in MEF cell lysates from day 0-3. An increase in Akt phosphorylation is seen on day 3 in *Tgm2-/-* MEFs compared to *Tgm2+/+* MEFs. Results are mean values ± SEM (n=3), *p<0.05.

Fig.8

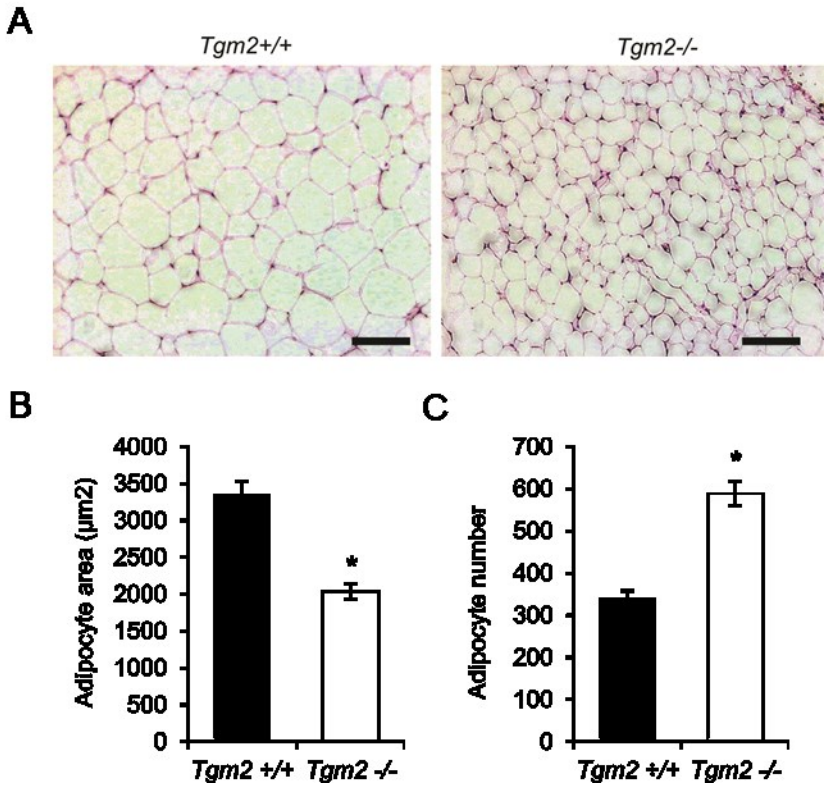

Fig. 8. Increased adipocyte number in *Tgm2-/-* mouse WAT. (A) H&E stained sections of epididymal fat pads from *Tgm2-/-* and *Tgm2+/+* mice at 24 weeks of age. **(B)** Average adipocyte area, shows a significant decrease in the adipocyte area in *Tgm2-/-* compared to *Tgm2+/+* mice. **(C)** Average adipocyte number was significantly increased in *Tgm2-/-* mice compared to *Tgm2+/+.* Results are mean values ± SEM (n=3), *p<0.05. Scale bar equals 100 µm.

Fig. S1

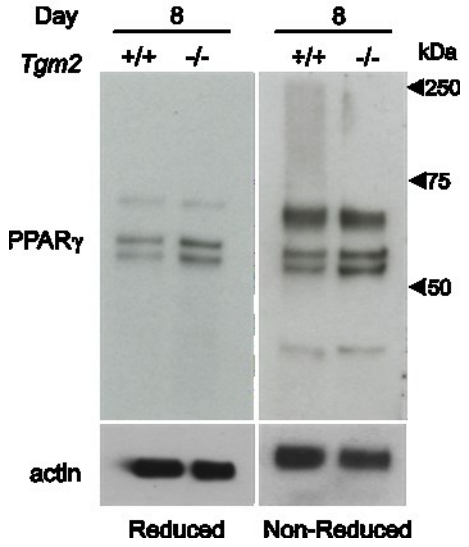

Fig. S1. PPARγ is not found in high molecular weight forms in MEFs and thus not crosslinked by TG2 during adipocyte differentiation. Western blot analysis of total cell lysate on day 8 in both reduced and non-reduced conditions for PPARγ protein, higher molecular weight products expected to be found at molecular weights between 75 to 250 kDa. No higher molecular weight products were observed in either condition.

Fig. S2

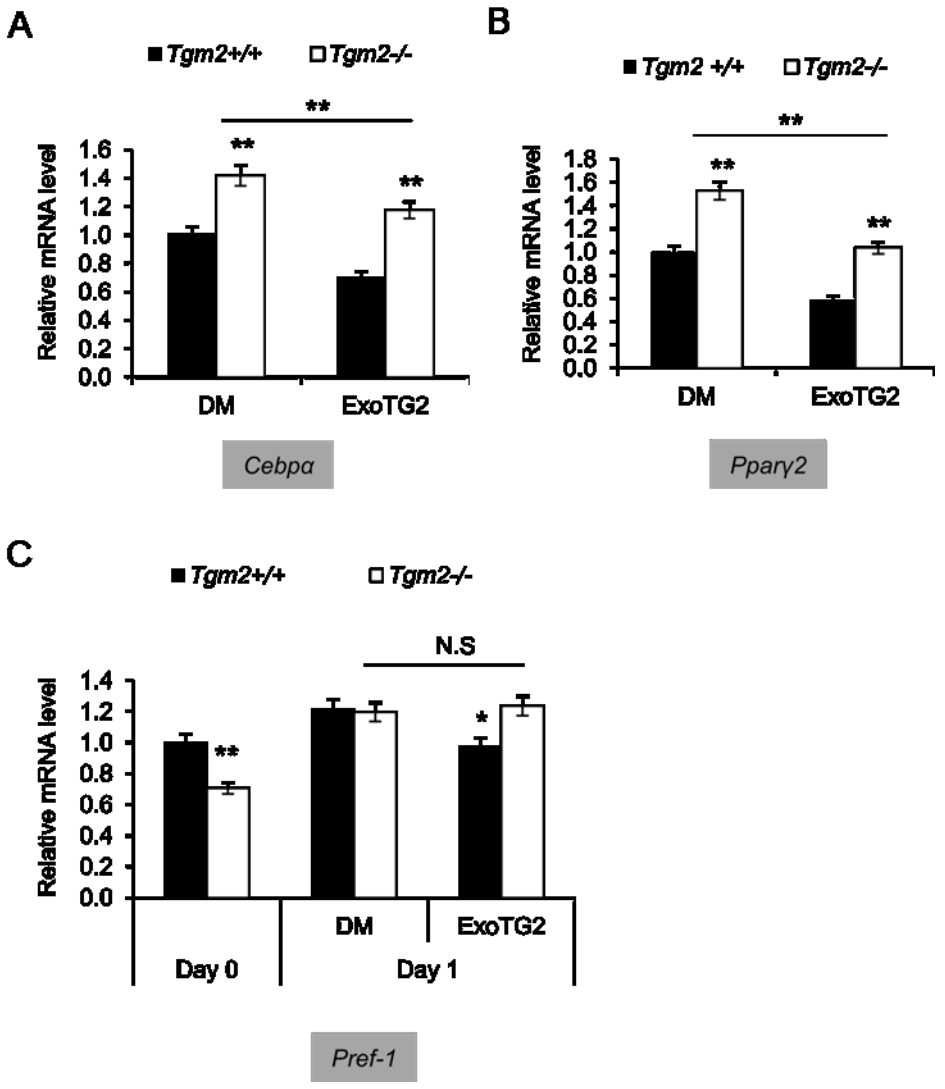

Fig. S2. Extracellular TG2 down regulates mRNA expression of *Pparγ* and *Cebpα*. **(A,B)** Quantification of mRNA analyses from **Fig 6C** for *Pparγ* and *Cebpα* and normalized to *Gapdh*, show significant reduction in *Pparγ* and *Cebpα* in both *Tgm2*-/- and *Tgm2*+/+ MEFs. Error bars ± SEM; N.S-Not Significant; *p<0.05; **p<0.01. **(C)** Quantification of mRNA analyses from **Fig 6G** for *Pref-1* normalized to *Gapdh*, shows no difference in *Tgm2*-/- MEFs, but surprisingly show a significant reduction in *Tgm2+/+* MEFs.

Fig. S3

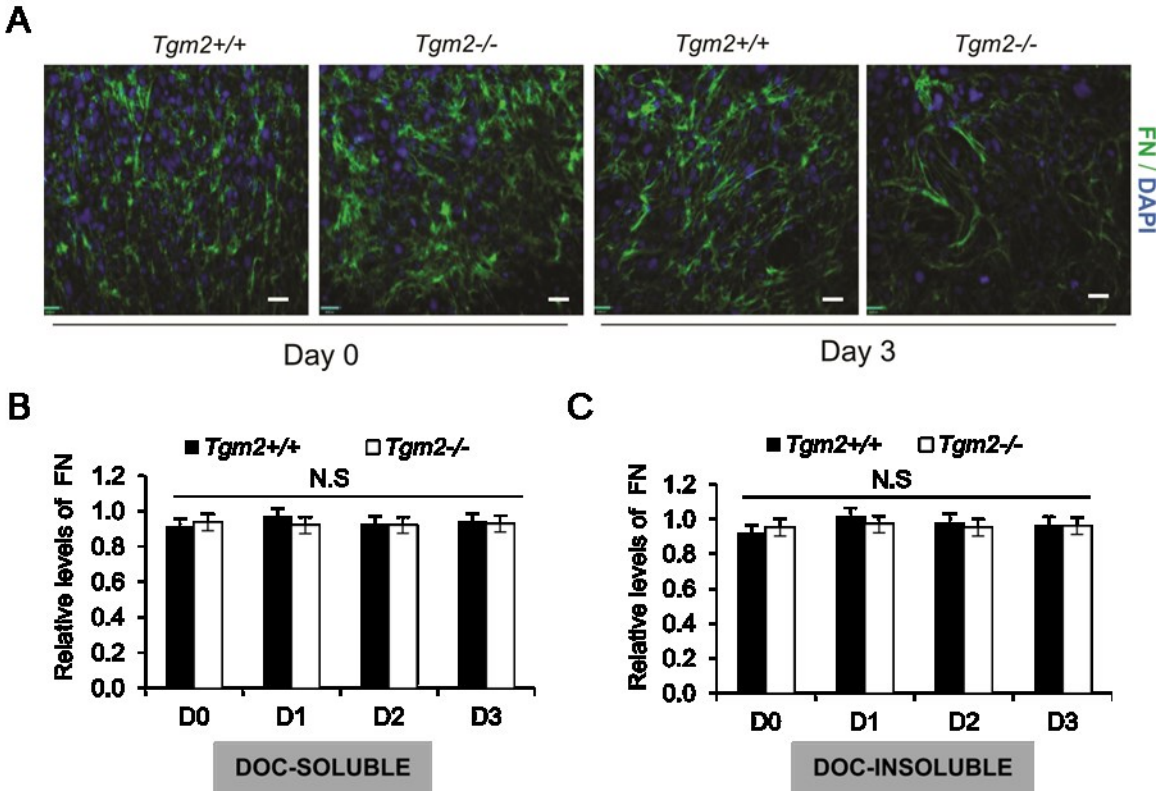

Fig. S3. FN levels were not altered in *Tgm2-/-* MEFs. (A) Immunofluorescence staining for FN in *Tgm2+/+* and *Tgm2-/-* MEFs on day 0 and day 3. No major change was observed in FN matrix levels. Scale bar equals 200µm. **(B)** Quantification of FN in deoxycholate (DOC)-soluble and DOC-insoluble fractions after Western blotting, shows no changes in FN solubility. Quantification of FN Western blots was done by normalizing to loading controls. Actin was used for DOC-soluble and vimentin for DOC-insoluble fractions. N.S-Not Significant; Error bars ± SEM (n=3).

Fig. S4

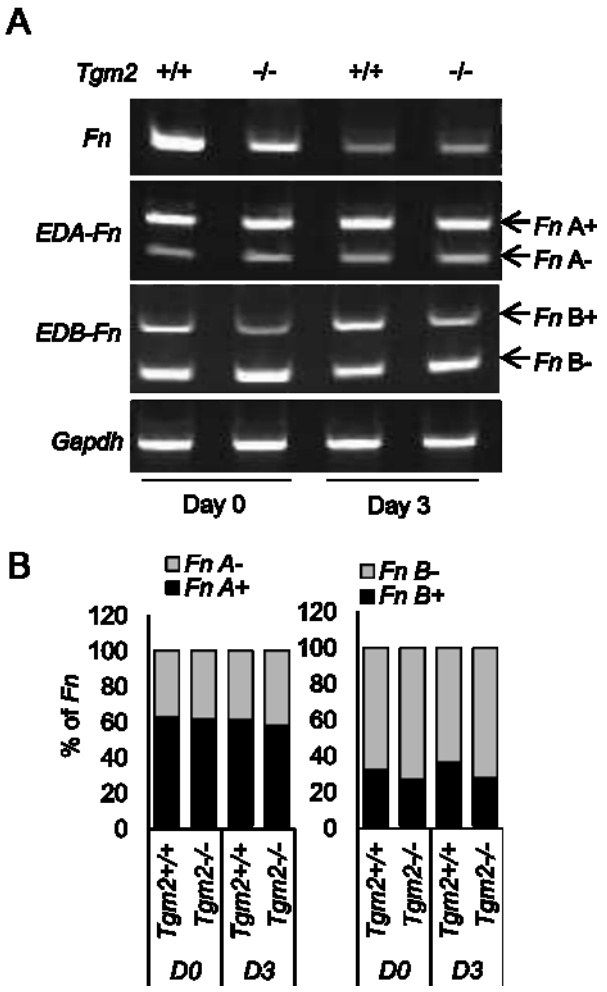

Fig. S4. *Fn* and cellular *Fn* expression did not change in *Tgm2-/-* MEFs. (A) mRNA expression of *Fn* and *EDA-Fn* and *EDB-Fn* in *Tgm2+/+* and *Tgm2-/-* MEFs on day 0 and day 3. On day 0, a decrease in *Fn* expression is seen in *Tgm2-/-* cells, however, the difference disappears on day 3. *EDA-Fn* and *EDB-Fn* shows no changes. **(B)** Quantification of RT-PCR of *EDA-Fn* and *EDB-Fn* expressed as percentage of *Fn* on day 0 and day 3. No changes are seen.

CHAPTER 4 - Factor XIII-A knockout mice are resistant to high-fat diet induced insulin resistance

4.1 Preamble

The *F13A1* gene has recently been identified as the top novel obesity-linked gene in human white adipose tissue through obese-lean twin investigations. Our previous study has shown that FXIII-A is an inhibitor of adipocyte differentiation *in vitro*. In this study, we report the metabolic phenotype of FXIII-A deficient mice on an obesogenic, high fat diet. Firstly, we show that *F13a1-/-* mice are resistant to fat mass gain compared to *F13a1+/+* mice on high fat diet. Secondly, we show that *F13a1-/-* mice are resistant to high fat diet induced insulin resistance. Increase in insulin sensitivity in *F13a1-/-* mice is seen in AT and skeletal muscle. improved insulin sensitivity of AT is associated with reduced macrophage infiltration, reduced collagen levels and increase in adipocyte size in AT.

Impact in brief:

- This is the first report demonstrating a metabolic phenotype of *F13a1-/-* mice, and the first report to show a role for FXIII-A in AT *in vivo*.
- We demonstrate a role for FXIII-A in regulating insulin sensitivity in AT and muscle, by showing that that *F13a1-/-* mice are resistant to diet induced insulin resistance.
- *F13a1-/-* mice exhibit characteristics of metabolically healthy obesity, indicating that FXIII-A have a role in the development of insulin resistance and subsequent metabolic syndrome.

The study presented in this chapter is ***in preparation*** to be submitted to ***Blood***.

Factor XIII-A knockout mice are resistant to high-fat diet induced insulin resistance

Vamsee D. Myneni[1] and Kaartinen MT [1,2]

[1]Faculty of Dentistry, McGill University, Montreal, QC, Canada, [2]Division of Experimental Medicine, Department of Medicine, Faculty of Medicine, McGill University, Montreal, QC.

4.2 Abstract

Obesity is a worldwide epidemic and is associated with the development of insulin resistance and prediabetes. Recent genome wide association studies have identified *F13A1* gene as a top and potentially causative gene for obesity in human white AT, *F13A1* encodes Factor XIII-A. FXIII-A is a plasma transglutaminase that participates in the final stage of the coagulation cascade, and is also expressed by various cell types participating in tissue homeostasis. Our previous work showed that FXIII-A regulates adipocyte differentiation by modulating plasma fibronectin assembly and insulin signalling in preadipocyte cultures. However, the role of FXIII-A in the development of obesity and metabolic disturbances *in vivo* is not known. In this study, we examined the metabolic phenotype of FXIII-A deficient mice and their propensity to become obese and prediabetic on an obesogenic diet. Male *F13a1-/-* and *F13a1+/+* wild type littermate controls were fed on a high fat diet (HFD) for 16 weeks. On this diet, *F13a1*-/- and *F13a1*+/+ mice gained similar body weight, however, the *F13a1*-/- mice were resistant to fat mass gain. FXIII-A deletion also protected the mice from diet-induced insulin resistance. Improved insulin sensitivity was attributed to increased sensitivity in epididymal, inguinal AT, and muscle, but not in liver. The AT of *F13a1*-/- mice had reduced macrophage infiltration, increased adipocyte size, reduced collagen and fibronectin levels. The mice also showed reduced circulating triglycerides and decrease in liver fat all of which suggests that *F13a1-/-* mice exhibit characteristics of metabolically healthy obesity.

4.3 Introduction

Obesity is a global epidemic and a major risk factor for development of insulin resistance, type 2 diabetes, cardiovascular diseases, hypertension, respiratory diseases, several types of cancers and osteoarthritis leading to reduced life expectancy (Borst; Despres and Lemieux, 2006; Pittas et al., 2004; Spalding et al., 2008). It is estimated that 65-80% of obesity is linked to genetic predisposition. Many genome wide association studies have identified several novel genes that contribute to the development of obesity and related comorbidities (Maes et al., 1997; Visscher et al., 2012). One recent study using monozygotic twin pairs discordant in obesity identified *F13A1* in white AT (WAT) as a potential causative gene for obesity. The significant association of *F13A1* with obesity was confirmed in a large European ENGAGE consortium study of more than 21,000 unrelated individuals, and identified seven SNPs in *F13A1* gene associated with body mass index (BMI) in the GenMets cohort study (Naukkarinen et al., 2010). One of the identified SNP of *F13A1* (rs7766109) was shown to be associated with BMI and insulin resistance in polycystic ovary syndrome (Schweighofer et al., 2012).

F13A1 encodes for Factor XIII-A (FXIII-A)(mouse gene; *F13a1*), which is part of the heterotetrameric FXIII blood clotting factor composed of two FXIII-A subunits and two carrier FXIII-B subunits. FXIII-A is released from its the inhibitory FXIII-B subunits during activation of the coagulation cascade and acts to stabilize the fibrin network (Ariens et al., 2000; Muszbek et al., 2011). FXIII-A belongs to transglutaminase enzyme family, which are capable of modifying protein bound glutamine residues via transamidation reaction. The best characterized modification is the formation of covalent N-glutamyl-ε-lysyl crosslinks, i.e., isopeptide bonds between substrate proteins such as fibrin and fibronectin (FN) (Muszbek et al., 2011). The circulating FXIII-A is considered to be produced by cells of bone marrow origin, such as megakaryocytes (Poon et al., 1989; Wolpl et al., 1987), however, many cell types and tissues have now been reported to produce this enzyme. In addition to being found in plasma, FXIII-A is synthesized by monocytes, macrophages, chondrocytes, osteoblasts, osteocytes and preadipocytes (Muszbek et al., 2011; Myneni et al., 2014) and its role has been linked to many

different physiological events such as wound healing and angiogenesis (Dardik et al., 2006b), osteoblast differentiation (Al-Jallad et al., 2011; Al-Jallad et al., 2006) and monocyte/macrophage migration and phagocytosis (Sarvary et al., 2004). In our previous work, we examined the role of transglutaminase activity in mouse WAT and identified FXIII-A as the active transglutaminase enzyme in 3T3-L1 preadipocyte cell line and in mouse embryonic fibroblasts. We demonstrated that FXIII-A can regulate insulin signaling via promoting plasma fibronectin assembly to preadipocyte matrix. Inhibition of transglutaminase activity and elimination of FXIII-A during adipogenesis *in vitro* promotes pro-differentiating signals of insulin and augmented adipocyte differentiation.

FXIII-A knockout mice display clotting defects, increased incidence of miscarriage (Koseki-Kuno et al., 2003) and decreased angiogenesis (Dardik et al., 2006a), impaired wound healing (Inbal et al., 2005), and resistance to developing arthritis (Raghu et al., 2015). The genetic obesity studies in humans and our previous work in preadipocytes and WAT suggest a potentially important role for FXIII-A in metabolism. In this study, we report on the metabolic phenotype of *F13a1*-/- mice on HFD. We report that absence of FXIII-A results in decreased AT in both subcutaneous and visceral fat depots on HFD. *F13a1*-/- mice on HFD show resistance to diet-induced insulin resistance and exhibit several signs of 'metabolically healthy obesity' such as increased adipocyte size, decreased collagen and fibronectin levels in AT, reduced macrophage infiltration to AT, reduced circulating triglycerides and decrease in liver fat compared to its wild type counterpart. Our study demonstrates for the first time that FXIII-A can improve general metabolic health, and as an important factor that regulates insulin sensitivity in obesity.

4.4 Materials and methods

Antibodies and reagents

Antibodies against rabbit anti-Akt (pan), rabbit anti- phospho-Akt (Ser^{473})(D9E), were purchased from Cell Signalling Technology Inc. (Beverly, MA, USA). Rabbit anti-fibronectin antibody was from EMD Millipore (Billerica, MA, USA). Mouse anti-

fibronectin (EP5) purchased from Santa Cruz Biotechnology (Santa Cruz, CA, USA). Horseradish peroxidase-conjugated anti-mouse, and anti-rabbit IgG were from Jackson ImmunoResearch Inc. (West Grove, PA, USA). Glucose was measured by using The One Touch UltraMini glucometer. Novo rapid insulin was purchased from Novo Nordisk Canada (Mississauga,ON, Canada). All other reagents were purchased from Sigma or Fisher Scientific unless otherwise notes.

Animals

F13a1-/- mice were kindly provided by Dr. Gerhardt Dickneite (Aventis Behring GMBH, Germany)(Lauer et al., 2002). Wild type mice obtained from Jacksons laboratories and used for breeding. All mice were maintained in 12 h light/12-h dark cycle. Mice have ad libitum access to water and food. All male mice were fed with standard chow diet till 4 weeks of age. At 4 weeks of age, male *F13a1-/-* and *F13a1+/+* were fed with either chow or high fat diet (HFD) (containing 60% Kcal from fat) (Harlan Laboratories) until the mice were 20 weeks old. Weight gain was monitored by weighing mice weekly. At the end of the study, mice were sacrificed and plasma, AT, muscle, liver was harvested and used for various analyses. All the experiments involving mice were approved by the animal care committee of McGill University.

Glucose tolerance test (GTT) and insulin tolerance test (ITT)

Glucose and insulin tolerance tests were done on mice at 18 weeks on a chow or HFD, after 6hr of fasting. For glucose tolerance test, Interperitonal injection of glucose (1g/kg body weight) was done and blood glucose level was measured using glucometer at 0, 15, 30, 60, 120 minutes after glucose injection. For insulin tolerance test, interperitonal injection insulin (0.5U/Kg body weight) was done and blood glucose levels were measured at 0, 30, 60, 90, 120 minutes after insulin injection. Area under the curve was calculated as previously described (Ferron et al., 2010).

***In vivo* insulin signalling**

Mice were fasted for 6hr, and injected intraperitoneally with human insulin or saline at a dose of 2.5 U/kg body weight. Mice were sacrificed at 10 min postinjection and tissues

were homogenized in buffer containing 100mMTris (pH 7.4), 1% Triton X-100, 10mM EDTA, 100mM sodium fluoride, 2mM phenylmethylsulfonyl fluoride, 5mM sodium orthovanadate, and protease inhibitor cocktail. The protein lysate was analyzed by Western blotting as previously described. The blots were probed with anti-phospho-Akt (S473) and anti-total-Akt. Densitometric analysis of the bands was done by using Image J.

Histology and immunohistochemistry

ATs and liver were fixed in 10% neutral buffered formalin (NBF) overnight at RT and were embedded in paraffin, sectioned and stained with hematoxylin and eosin-stain by standard method. For quantification of adipocyte size, tissue sections from epididymal AT from 20-week-old mice were stained with H&E. Image J software was used to measure adipocyte area, the percentage of adipocytes in each 100-μm^2 area and the average adipocyte area (in μm^2). Adipocyte size was measured from four mice/genotype (>500 cells/genotype). Immunohistochemistry of fat pads for macrophages was done using F4/80 as a marker as previously described (Myneni et al., 2014).

Collagen and fibronectin quantification

Tissue collagen content was determined by sircol assay and hydroxyproline assay, which were done using a previously described protocol with minor modifications (Kliment et al., 2011). Briefly, 100 mg of epididymal and inguinal fat pads were sonicated in CHAPS detergent buffer (50mM Tris-HCl, pH7.4, 150mM NaCl, 10mM CHAPS, 3mM EDTA and protease inhibitors). 100 µl of lysate was used for sircol and hydroxyproline assay. 100 mg of epididymal and inguinal fat pads were used to extract DOC-soluble and DOC-insoluble fractions and analyzed using ELISA as previously described (Myneni et al., 2014).

Indirect calorimetric measurements

For indirect calorimetry measurements, animals were individually housed in metabolic chambers maintained at 20 to 22°C on a 12-h/12-h light-dark cycle with lights on at

0700. Metabolic parameters (oxygen consumption, carbon dioxide production, respiratory exchange ratio (RER), and locomotor activity and energy expenditure) were obtained continuously using a TSE system. Mice were provided with the standard chow or HFD diet and water ad libitum. Presented results contain data collected for a period of 5 days following 5 days of adaptation to the metabolic cages.

Statistical analysis

Data are the standard error of the mean. Differences between groups were determined by ANOVA followed by Turkey's post hoc tests or Student's t-test as appropriate. $p<0.05$ was considered significant.

4.5 Results

FXIII-A deficient mice are protected from high-fat diet induced obesity

To determine the potential role of FXIII-A gene on the weight gain, development of obesity and its associated metabolic complications, 4 weeks old, male *F13a1+/+* and *F13a1-/-* mice were fed either regular chow diet or HFD for 20 weeks. During this time, mice on a HFD gained significant weight and developed prediabetic symptoms, which include loss of insulin sensitivity and glucose intolerance, and fatty liver (hepatic steatosis). During the 20 week challenge, body weight was measured weekly. GTT, ITT, food intake, body composition and fat pads weight were measured at the end point 20 weeks. Body weight analysis and food intake of the mice on chow diet showed no significant difference between *F13a1+/+* and *F13a1-/-* mice (**Figure 1A,B**). However, at necropsy *F13a1-/-* mice showed a significant increase in the fat pad's weights compared to *F13a1+/+* mice were: inguinal fat pad (24% higher), inter-scapular (27% higher), mesenteric (39% higher), epididymal (28% higher) (**Figure 1C**), however, this increase did not translate to increased weight of the mouse. Similarly, on HFD diet the body weight gain showed no significant difference between *F13a1+/+* and *F13a1-/-* mice (**Figure 2A**). Food intake was the same in both mice (**Figure 2B**). Fat pad weights after 16-week HFD showed a significant *decrease*, i.e., epididymal fat pad weight was decreased by 20% and mesenteric by 21%, inguinal fat by 18% in *F13a1-/-* mice

compared to *F13a1+/+* mice (**Figure 2C**). Comparison of the total fat mass on chow and HFD showed that HFD feeding resulted in a significant increase of 44% in fat mass in *F13a1+/+* mice, but not a significant increase in the *F13a1-/-* mice (3.4%) compared to chow diet (**Figure 2D**). These results suggest that, although *F13a1-/-* mice are significantly fattier on regular chow diet, they are protected from HFD induced obesity.

FXIII-A deficiency improves insulin sensitivity on HFD

HFD feeding in mice is associated with the development of prediabetes that includes increased in blood glucose and insulin resistance (Surwit et al., 1988). To further explore the effects of FXIII-A deficiency on insulin resistance, we analysed the metabolic parameters in *F13a1-/-* and *F13a1+/+* mice. Analysis of fasting blood glucose levels in *F13a1-/-* and *F13a1+/+* mice on chow and HFD showed no significant differences (**Figure 3A**). Random blood glucose level showed that HFD feeding has caused significantly increased blood glucose levels by 35% in *F13a1+/+* which is a sign of prediabetes. *F13a1-/-* mice showed a 17% reduced blood glucose level in comparison to *F13a1+/+* (**Figure 3B)**. Glucose tolerance test (GTT) was done to assess the pancreatic function. On chow diet, *F13a1-/-* mice showed impaired glucose clearance compared to *F13a1+/+* mice. On HFD, both *F13a1-/-* and *F13a1+/+* mice display similar, but impaired glucose clearance (**Figure 3C,D**), suggesting that FXIII-A might have a role in pancreatic function. Insulin tolerance test (ITT) was done to examine glucose clearance in response to insulin independent of pancreatic function. Data shows that *F13a1+/+* have developed insulin resistance on HFD (significantly increased AUC value), however, *F13a1-/-* mice display the same level of insulin sensitivity on both chow diet and HFD (**Figure 3F,G**). Collectively, this data indicates that *F13a1-/-* mice are protected from developing HFD-induced insulin resistance.

F13a1-/-* mice on HFD show increased insulin sensitivity, i.e., enhanced insulin-induced Akt signalling *in vivo

To explore further the improved systemic insulin sensitivity on HFD, insulin-stimulated glucose disposal rate in peripheral tissues-muscle, AT and liver was assessed. At 20 weeks of age, mice were injected with insulin, peripheral metabolic tissues were

immediately dissected and total protein was extracted and Western blotted for Akt phosphorylation to assess the activation of insulin signalling. In *F13a1-/-* mice, insulin induced a significantly robust increase in Akt Ser-473 phosphorylation without affecting total insulin receptor levels (IRβ). This increase in insulin sensitivity in HFD-fed *F13a1-/-* mice (compared to *F13a1+/+* mice on HFD) was observed in the epididymal fat pad (**Figure 4A**), inguinal fat pad (**Figure 4B**) and skeletal muscle (**Figure 4C**), but not in liver (**Figure 4D**). These results support the observation that *F13a1-/-* were mice resistant to development of insulin resistance on HFD and show increased insulin sensitivity. In summary, these results suggest that increased insulin sensitivity of *F13a1-/-* mice were primarily from the increased insulin responsiveness of AT and muscle.

Increased adipocyte cell size in *F13a1-/-* mice on HFD

Improved insulin sensitivity has been shown to be associated with smaller adipocyte size (Hammarstedt et al., 2012; Salans et al., 1968), however, in some cases the larger adipocyte size also was correlated with improved insulin sensitivity (Khan et al., 2009). Histological examination and frequency distribution of adipocytes in the epidydimal fat pad revealed an increase in small and very large adipocytes in HFD-fed *F13a1-/-* mice compared to HFD-fed *F13a1+/+* mice at 20 weeks of age (**Figure 5A,B**). However, the total number of adipocytes are same in both *F13a1+/+* and *F13a1-/-* mice (**Figure 5C**). The average adipocyte size in *F13a1-/-* mice are significantly increased compared to *F13a1+/+* mice, which might be due to the higher number of adipocytes in the range of 50,000-100,000 µm range in *F13a1-/-* mice (**Figure 5D,E**). This increase in AT cell size also supports increased insulin sensitivity of AT in *F13a1-/-* mice.

Reduced collagen and fibronectin levels in AT of *F13a1-/-* mice on HFD

The presence of larger adipocytes in *F13a1-/-* mice suggest a less restrictive extracellular matrix (ECM) which might also contribute to improved insulin sensitivity. Collagen is a major component of the AT extracellular matrix, and obesity is associated with an overall increase in expression of several collagens. Genetic disruption of type VI collagen results in an improved metabolic phenotype associated with larger adipocytes (Khan et al., 2009). To examine the levels of ECM in AT of *F13a1-/-* mice and *F13a1+/+*

mice, we analyzed total collagen levels in epididymal and inguinal fat pads using sircol and hydroxyproline assays. Analysis of epididymal fat pad shows a trend towards reduced collagen levels in *F13a1-/-* mice compared to *F13a1+/+* mice on HFD, but this was not significant. However, inguinal fat pad shows a significantly reduced collagen levels in *F13a1-/-* mice compared to *F13a1+/+* mice on HFD (**Figure 6A,B**). Collagen assembly in the ECM is regulated by FN (Velling et al., 2002), and our previous work showed that *F13a1* MEFs display reduced FN assembly during adipocyte differentiation (Myneni et al., 2014). Indeed, FXIII-A has been linked to the ECM accumulation in many tissues and cell culture models, particularly plasma fibronectin (pFN)(Bennett et al., 2002; Cui et al., 2014; Moretti et al., 2007). In epididymal fat pad, DOC-soluble of FN showed a trend of reduced FN level in *F13a1-/-* mice compared to *F13a1+/+* mice on HFD, but not in DOC-insoluble fraction. In inguinal fat pad, the FN levels in the DOC-soluble fraction of is significantly reduced. The DOC-insoluble fractions showed a similar trend towards reduced FN levels, but not significant in *F13a1-/-* mice compared to *F13a1+/+* mice on HFD (**Figure 6C,D**). These results suggest that the subcutaneous AT of HDF-fed *F13a1-/-* mice have reduced levels of two major ECM components, FN and collagen, than the *F13a1+/+* mice on HFD.

FXIII-A deficiency decreases macrophage accumulation in AT of HFD

It has been previously shown that increased macrophage accumulation in AT on HFD is linked to development of diet-induced insulin resistance (Weisberg et al., 2003), and FXIII-A was shown to modulate macrophage migration (Sarvary et al., 2004). This prompted us to investigate if macrophage infiltration into AT is altered in *F13a1-/-* mice. Immunohistochemistry shows localized macrophages in the crown like clusters surrounding adipocytes (**Figure 7**). More crown like structures were seen in *F13a1+/+* mice on HFD compared to *F13a1-/-* mice, suggesting decreased macrophage levels in *F13a1-/-* AT. This results suggest that decreased macrophage in AT also contributes to improved metabolic profile of *F13a1-/-* mice on HFD.

Decreased fat in the liver of *F13a1-/-* mice on HFD.

HFD induced insulin resistance is also associated with hepatic steatosis (Perlemuter et al., 2007). Histological analysis of liver show that *F13a1-/-* mice on HFD has reduced lipid accumulation compared to *F13a1+/+* mice, as evident by reduced vacuolation in H&E stained section of the liver (**Figure 8A**). Weights of the livers were not significantly different in *F13a1+/+* mice and *F13a1-/-* mice (**Figure 8B**). Also, the circulating triglyceride levels were significant lower in *F13a1-/-* mice compared to *F13a1+/+* mice suggesting overall healthier lipid metabolism on HFD (**Figure 8C**).

Reduced energy expenditure in *F13a1-/-* mice on HFD

To examine whether the absence of FXIII-A could affect lipid accumulation and fat mass via increasing physical activity and thus energy consumption, mice were placed in metabolic chambers. Physical activity on HFD was not increased, surprisingly, it was significantly reduced in *F13a1-/-* mice during night time compared to *F13a1+/+* mice (**Figure 9A**). The *F13a1-/-* mice show reduced energy expenditure (EE) on HFD both during the day and night compared to *F13a1+/+* mice. On chow diet the *F13a1-/-* mice during night time showed a small but significant increase in EE compared to *F13a1+/+* mice, this increase in EE during the night did not affect the total EE (**Figure 9B**). The changes in energy expenditure on HFD were also reflected by reducing oxygen consumption (VO2) (**Figure 9C**) and carbon dioxide production (VCO2) (**Figure 9D**) in *F13a1-/-* mice compared to *F13a1+/+* mice. The respiratory exchange ratio (RER) was not altered in *F13a1-/-* mice and *F13a1+/+* mice on chow or HFD (**Figure 9E**) suggesting that the substrate utilization (carbohydrates and lipids) was not altered. Together, these data show that *F13a1-/-* mice have reduced energy expenditure accounting for reduced activity on HFD.

4.6 Discussion

F13A1 gene that encodes for FXIII-A transglutaminase was identified as a potential causative gene for obesity in WAT and several SNPs in *F13A1* gene were reported to associate with BMI (Naukkarinen et al., 2010) and insulin resistance (Schweighofer et

al., 2012). How FXIII-A is linked to the development of obesity and its metabolic consequences has remained unknown. To shed light on the role of FXIII-A in energy metabolism, we characterized the metabolic phenotype of *F13a1* deficient mice. We report that global elimination of *F13a1* reduced AT mass on HFD. Although, *F13a1*-/- mice on HFD gained the same level of body weight like their wild type controls, they are resistant to developing diet-induced insulin resistance and exhibit other characteristics of 'metabolically healthy obesity'. These include increased adipocyte size, decreased collagen and FN levels in AT, decreased liver fat and reduced circulating triglycerides and macrophage infiltration to AT. These changes in fat mass were not caused by increased energy expenditure, as the *F13a1*-/- mice showed decreased energy expenditure. Our study is first to bring *in vivo* evidence showing that FXIII-A deficiency can improve metabolic health.

Although *F13a1* gene suggested to be causative gene to obesity, complete absence of *F13a1* gene in mice did not increase weight gain on HFD, but a significant decrease in AT mass. This change in fat mass without altering the body weight was also observed in other mouse models such as osteopontin (OPN) deficient mice (Nomiyama et al., 2007) and osteonectin/SPARC null mice (Bradshaw et al., 2003). It was reported that OPN deficient mice gained the same weight as their wild-type controls on HFD, but also showed improved insulin sensitivity associated with reduced macrophage infiltration of AT. Conditional AT knockout of OPN also resulted in reduced gene expression of collagens *Col1a1, Col6a1* and *Col6a3*, reduced fat cell size, decreased ECM remodelling (Lancha et al., 2014; Nomiyama et al., 2007). Similarly, SPARC-null mice have increased subcutaneous and epididymal fat pads, reduced type I collagen levels in fat pads, increased adipocyte diameter and adipocyte number (Bradshaw et al., 2003). This was consitant with our data of reduced collagen levels and improved insulin sensitivity in fat pads of *F13a1*-/- mice. Interestingly, both SPARC and OPN are transglutaminase substrates in the extracellular space (Facchiano and Facchiano, 2009). Our previous work showed that FXIII-A is the only transglutaminase with crosslinking activity in AT (Myneni et al., 2014) which suggests that in *F13a1*-/- mice may show altered SPARC and OPN functions that may subsequently lead to a similar

matrix related phenotype. The increase in fat mass without having deleterious metabolic effects also was reported in a mouse model that was treated with peroxisome proliferator-activated receptor gamma (PPARγ) agonist (Ferre, 2004) and over expression of adiponectin in *ob/ob* mouse (leptin deficient mouse-obesity mouse model) (Kim et al., 2007). PPARγ mediates adipogenesis and insulin sensitivity. Our previous work we have shown that FXIII-A inhibits adipogenesis and inhibition of FXIII-A activity promotes PPARγ levels and increases insulin sensitivity in 3T3-L1 cells (Myneni et al., 2014), suggesting that this might be one of the downstream mechanisms of improved insulin sensitivity in FXIII-A mice.

Collagen is the major constituent of AT ECM. *F13a1-/-* mice shown a reduced AT collagen content on HFD, which might also contribute to reduced macrophage levels in AT of these mice. Furthermore, extracellular matrix components themselves are linked to the development of insulin resistance. Knocking out of Type VI collagen in *ob/ob* mouse showed an improved metabolic profile and improved insulin sensitivity, which is attributed to the enhanced AT expansion and increase in adipocyte cell size (Khan et al., 2009). Indeed, we also observed an increase in size of adipocytes in AT of *F13a1-/-* mice and the presence of smaller adipocytes along with very large adipocytes. The very large adipocytes might stimulate recruitment and proliferation of an adipocyte precursor, which leads to greater small adipocytes fraction. It has been reported that increased ECM deposition reduces the amount of adipocyte progenitors in WAT and thus contributes to loss of proper function and expansion of AT under need for expansion (Chandler et al., 2011). The presence of both smaller and larger cells was also observed in mice treated with peroxisome proliferator-activated receptor gamma (PPARγ) agonist (Gesta et al., 2007).

A major factor contributing to metabolic failure in obesity is AT inflammation, which is characterized by macrophage infiltration. Macrophages infiltration into AT forms crown-like structures (CLSs) which represent dying adipocytes. The density of CLSs correlates with insulin resistance and proinflammatory environment. Analysis of *F13a1-/-* mice showed decreased levels of macrophages and CLSs in mouse WAT suggesting an

improved inflammatory profile of the tissue and the presence of healthy adipocytes. It is possible that this phenotype results from the combination of lack of FXIII-A in adipocytes, and lack of FXIII-A in macrophages themselves as FXIII-A in macrophages was shown to play a role in migration and phagocytosis (Dardik et al., 2007). In the absence of FXIII-A macrophage function would be expected to be compromised as seen in our study thus contributing to reduced macrophage levels in AT and increased insulin sensitivity. Other factor which might have affected macrophage accumulation is lower levels of ECM in HFD-fed *F13a1-/-* mouse WAT as macrophages generally localized to profibrotic areas (Klingberg et al., 2013).

Skeletal muscle is the major contributor of peripheral insulin sensitivity and HFD causes lipid accumulation in muscle can cause abnormalities in matrix composition that in turn can affect the function of mitochondria and lead to insulin resistance in muscle. Insulin resistance in muscle was associated with the increased hydroxyproline content of the muscle of type 2 diabetic patients (Berria et al., 2006). In *F13a1-/-* mice, muscle also showed increased insulin sensitivity, which might be due to reduced collagen levels.

As discussed above, seven SNPs has been identified in *F13A1* gene in humans that link to BMI. In the light of our findings, these SNPs may influence F13A1 by modulating its expression and thus increasing or decreasing the activity of the enzyme. V34L polymorphism in *F13A1* was shown to increase enzyme activation, but was not associated with obesity. Our results suggest that the enzyme activity may not directly influence weight, but modulate insulin sensitivity and general metabolic health.

In summary, we have found that mice deficient in FXIII-A show characteristics of metabolically healthy obesity, which include lack of insulin resistance, decreased fat in liver and lower circulating triglycerides compared to wild type mice on a same obesity inducing diet. FXIII-A deficient AT shows signs of healthy phenotype on HFD that include reduced macrophage levels, reduced collagen levels and increased adipocyte size in AT. FXIII-A may provide an excellent molecular target to improve the metabolic profile in obesity and to regulate insulin resistance.

4.7 Acknowledgements

We would like to thank Cui Cui for assistance. This study was supported by grants to MTK from the Canadian Institutes of Health Research (CIHR) and the CIHR Institute of Genetics. VDM received stipends from Faculty of Dentistry and the CIHR Systems Biology Training Program.

Conflict of interest

The authors declare no competing financial interest.

4.8 References

Al-Jallad, H.F., Myneni, V.D., Piercy-Kotb, S.A., Chabot, N., Mulani, A., Keillor, J.W., and Kaartinen, M.T. (2011). Plasma membrane factor XIIIA transglutaminase activity regulates osteoblast matrix secretion and deposition by affecting microtubule dynamics. PloS one *6*, e15893.

Al-Jallad, H.F., Nakano, Y., Chen, J.L., McMillan, E., Lefebvre, C., and Kaartinen, M.T. (2006). Transglutaminase activity regulates osteoblast differentiation and matrix mineralization in MC3T3-E1 osteoblast cultures. Matrix biology : journal of the International Society for Matrix Biology *25*, 135-148.

Ariens, R.A., Philippou, H., Nagaswami, C., Weisel, J.W., Lane, D.A., and Grant, P.J. (2000). The factor XIII V34L polymorphism accelerates thrombin activation of factor XIII and affects cross-linked fibrin structure. Blood *96*, 988-995.

Bennett, C.N., Ross, S.E., Longo, K.A., Bajnok, L., Hemati, N., Johnson, K.W., Harrison, S.D., and MacDougald, O.A. (2002). Regulation of Wnt signaling during adipogenesis. The Journal of biological chemistry *277*, 30998-31004.

Berria, R., Wang, L., Richardson, D.K., Finlayson, J., Belfort, R., Pratipanawatr, T., De Filippis, E.A., Kashyap, S., and Mandarino, L.J. (2006). Increased collagen content in insulin-resistant skeletal muscle. American journal of physiology. Endocrinology and metabolism *290*, E560-565.

Borst, S.E. Adipose Tissue and Insulin Resistance. Nutrition and Health: Adipose Tissue and Adipokines in Health and Disease, 281.

Bradshaw, A.D., Graves, D.C., Motamed, K., and Sage, E.H. (2003). SPARC-null mice exhibit increased adiposity without significant differences in overall body weight. Proceedings of the National Academy of Sciences of the United States of America *100*, 6045-6050.

Chandler, E.M., Berglund, C.M., Lee, J.S., Polacheck, W.J., Gleghorn, J.P., Kirby, B.J., and Fischbach, C. (2011). Stiffness of photocrosslinked RGD-alginate gels regulates adipose progenitor cell behavior. Biotechnology and bioengineering *108*, 1683-1692.

Cui, C., Wang, S., Myneni, V.D., Hitomi, K., and Kaartinen, M.T. (2014). Transglutaminase activity arising from Factor XIIIA is required for stabilization and conversion of plasma fibronectin into matrix in osteoblast cultures. Bone *59*, 127-138.

Dardik, R., Krapp, T., Rosenthal, E., Loscalzo, J., and Inbal, A. (2007). Effect of FXIII on monocyte and fibroblast function. Cellular physiology and biochemistry : international journal of experimental cellular physiology, biochemistry, and pharmacology *19*, 113-120.

Dardik, R., Leor, J., Skutelsky, E., Castel, D., Holbova, R., Schiby, G., Shaish, A., Dickneite, G., Loscalzo, J., and Inbal, A. (2006a). Evaluation of the pro-angiogenic effect of factor XIII in heterotopic mouse heart allografts and FXIII-deficient mice. Thrombosis and haemostasis *95*, 546-550.

Dardik, R., Loscalzo, J., and Inbal, A. (2006b). Factor XIII (FXIII) and angiogenesis. Journal of thrombosis and haemostasis : JTH *4*, 19-25.

Despres, J.P., and Lemieux, I. (2006). Abdominal obesity and metabolic syndrome. Nature *444*, 881-887.

Facchiano, A., and Facchiano, F. (2009). Transglutaminases and their substrates in biology and human diseases: 50 years of growing. Amino acids *36*, 599-614.

Ferre, P. (2004). The biology of peroxisome proliferator-activated receptors: relationship with lipid metabolism and insulin sensitivity. Diabetes *53 Suppl 1*, S43-50.

Ferron, M., Wei, J., Yoshizawa, T., Del Fattore, A., DePinho, R.A., Teti, A., Ducy, P., and Karsenty, G. (2010). Insulin signaling in osteoblasts integrates bone remodeling and energy metabolism. Cell *142*, 296-308.

Gesta, S., Tseng, Y.H., and Kahn, C.R. (2007). Developmental origin of fat: tracking obesity to its source. Cell *131*, 242-256.

Hammarstedt, A., Graham, T.E., and Kahn, B.B. (2012). Adipose tissue dysregulation and reduced insulin sensitivity in non-obese individuals with enlarged abdominal adipose cells. Diabetology & metabolic syndrome *4*, 42.

Inbal, A., Lubetsky, A., Krapp, T., Castel, D., Shaish, A., Dickneitte, G., Modis, L., Muszbek, L., and Inbal, A. (2005). Impaired wound healing in factor XIII deficient mice. Thrombosis and haemostasis *94*, 432-437.

Khan, T., Muise, E.S., Iyengar, P., Wang, Z.V., Chandalia, M., Abate, N., Zhang, B.B., Bonaldo, P., Chua, S., and Scherer, P.E. (2009). Metabolic dysregulation and adipose tissue fibrosis: role of collagen VI. Molecular and cellular biology *29*, 1575-1591.

Kim, J.Y., van de Wall, E., Laplante, M., Azzara, A., Trujillo, M.E., Hofmann, S.M., Schraw, T., Durand, J.L., Li, H., Li, G., et al. (2007). Obesity-associated improvements in metabolic profile through expansion of adipose tissue. The Journal of clinical investigation *117*, 2621-2637.

Kliment, C.R., Englert, J.M., Crum, L.P., and Oury, T.D. (2011). A novel method for accurate collagen and biochemical assessment of pulmonary tissue utilizing one animal. International journal of clinical and experimental pathology *4*, 349-355.

Klingberg, F., Hinz, B., and White, E.S. (2013). The myofibroblast matrix: implications for tissue repair and fibrosis. The Journal of pathology *229*, 298-309.

Koseki-Kuno, S., Yamakawa, M., Dickneite, G., and Ichinose, A. (2003). Factor XIII A subunit-deficient mice developed severe uterine bleeding events and subsequent spontaneous miscarriages. Blood *102*, 4410-4412.

Lancha, A., Rodriguez, A., Catalan, V., Becerril, S., Sainz, N., Ramirez, B., Burrell, M.A., Salvador, J., Fruhbeck, G., and Gomez-Ambrosi, J. (2014). Osteopontin deletion prevents the development of obesity and hepatic steatosis via impaired adipose tissue matrix remodeling and reduced inflammation and fibrosis in adipose tissue and liver in mice. PloS one *9*, e98398.

Lauer, P., Metzner, H.J., Zettlmeissl, G., Li, M., Smith, A.G., Lathe, R., and Dickneite, G. (2002). Targeted inactivation of the mouse locus encoding coagulation factor XIII-A: hemostatic abnormalities in mutant mice and characterization of the coagulation deficit. Thrombosis and haemostasis *88*, 967-974.

Maes, H.H., Neale, M.C., and Eaves, L.J. (1997). Genetic and environmental factors in relative body weight and human adiposity. Behavior genetics *27*, 325-351.

Moretti, F.A., Chauhan, A.K., Iaconcig, A., Porro, F., Baralle, F.E., and Muro, A.F. (2007). A major fraction of fibronectin present in the extracellular matrix of tissues is plasma-derived. The Journal of biological chemistry *282*, 28057-28062.

Muszbek, L., Bereczky, Z., Bagoly, Z., Komaromi, I., and Katona, E. (2011). Factor XIII: a coagulation factor with multiple plasmatic and cellular functions. Physiological reviews *91*, 931-972.

Myneni, V.D., Hitomi, K., and Kaartinen, M.T. (2014). Factor XIII-A transglutaminase acts as a switch between preadipocyte proliferation and differentiation. Blood *124*, 1344-1353.

Naukkarinen, J., Surakka, I., Pietilainen, K.H., Rissanen, A., Salomaa, V., Ripatti, S., Yki-Jarvinen, H., van Duijn, C.M., Wichmann, H.E., Kaprio, J., et al. (2010). Use of genome-wide expression data to mine the "Gray Zone" of GWA studies leads to novel candidate obesity genes. PLoS genetics *6*, e1000976.

Nomiyama, T., Perez-Tilve, D., Ogawa, D., Gizard, F., Zhao, Y., Heywood, E.B., Jones, K.L., Kawamori, R., Cassis, L.A., Tschop, M.H., et al. (2007). Osteopontin mediates obesity-induced adipose tissue macrophage infiltration and insulin resistance in mice. The Journal of clinical investigation *117*, 2877-2888.

Perlemuter, G., Bigorgne, A., Cassard-Doulcier, A.M., and Naveau, S. (2007). Nonalcoholic fatty liver disease: from pathogenesis to patient care. Nature clinical practice. Endocrinology & metabolism *3*, 458-469.

Pittas, A.G., Joseph, N.A., and Greenberg, A.S. (2004). Adipocytokines and insulin resistance. The Journal of clinical endocrinology and metabolism *89*, 447-452.

Poon, M.C., Russell, J.A., Low, S., Sinclair, G.D., Jones, A.R., Blahey, W., Ruether, B.A., and Hoar, D.I. (1989). Hemopoietic origin of factor XIII A subunits in platelets, monocytes, and plasma. Evidence from bone marrow transplantation studies. The Journal of clinical investigation *84*, 787-792.

Raghu, H., Cruz, C., Rewerts, C.L., Frederick, M.D., Thornton, S., Mullins, E.S., Schoenecker, J.G., Degen, J.L., and Flick, M.J. (2015). Transglutaminase factor XIII promotes arthritis through mechanisms linked to inflammation and bone erosion. Blood *125*, 427-437.

Salans, L.B., Knittle, J.L., and Hirsch, J. (1968). The role of adipose cell size and adipose tissue insulin sensitivity in the carbohydrate intolerance of human obesity. The Journal of clinical investigation *47*, 153-165.

Sarvary, A., Szucs, S., Balogh, I., Becsky, A., Bardos, H., Kavai, M., Seligsohn, U., Egbring, R., Lopaciuk, S., Muszbek, L., et al. (2004). Possible role of factor XIII subunit A in Fcgamma and complement receptor-mediated phagocytosis. Cellular immunology *228*, 81-90.

Schweighofer, N., Lerchbaum, E., Trummer, O., Schwetz, V., Pilz, S., Pieber, T.R., and Obermayer-Pietsch, B. (2012). Androgen levels and metabolic parameters are associated with a genetic variant of F13A1 in women with polycystic ovary syndrome. Gene *504*, 133-139.

Spalding, K.L., Arner, E., Westermark, P.O., Bernard, S., Buchholz, B.A., Bergmann, O., Blomqvist, L., Hoffstedt, J., Naslund, E., Britton, T., et al. (2008). Dynamics of fat cell turnover in humans. Nature *453*, 783-787.

Surwit, R.S., Kuhn, C.M., Cochrane, C., McCubbin, J.A., and Feinglos, M.N. (1988). Diet-induced type II diabetes in C57BL/6J mice. Diabetes *37*, 1163-1167.

Velling, T., Risteli, J., Wennerberg, K., Mosher, D.F., and Johansson, S. (2002). Polymerization of type I and III collagens is dependent on fibronectin and enhanced by integrins alpha 11beta 1 and alpha 2beta 1. The Journal of biological chemistry *277*, 37377-37381.

Visscher, P.M., Brown, M.A., McCarthy, M.I., and Yang, J. (2012). Five years of GWAS discovery. American journal of human genetics *90*, 7-24.

Weisberg, S.P., McCann, D., Desai, M., Rosenbaum, M., Leibel, R.L., and Ferrante, A.W., Jr. (2003). Obesity is associated with macrophage accumulation in adipose tissue. The Journal of clinical investigation *112*, 1796-1808.

Wolpl, A., Lattke, H., Board, P.G., Arnold, R., Schmeiser, T., Kubanek, B., Robin-Winn, M., Pichelmayr, R., and Goldmann, S.F. (1987). Coagulation factor XIII A and B subunits in bone marrow and liver transplantation. Transplantation *43*, 151-153.

4.9 Figures

Fig.1

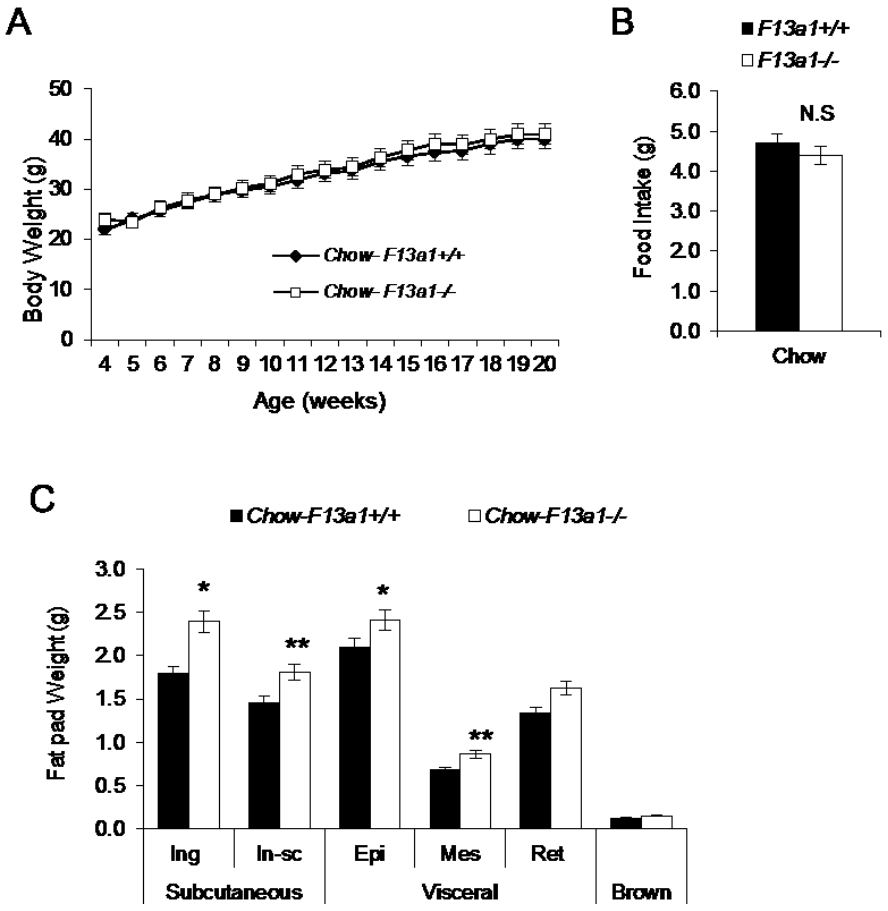

Figure 1. Increased fat pad weighs in *F13a1-/-* mice on chow diet. (A) Body weight was monitored weekly between 4 and 20 weeks of age (n=9-11 mice/group). No change was observed between *F13a1-/-* and *F13a1+/+* mice. **(B)** Food intake measured by metabolic cages over 4 days (n=4 mice/group) showed no changes between *F13a1-/-* and *F13a1+/+* mice. **(C)** Subcutaneous, visceral and brown fat depot weights were analyzed. *F13a1-/-* mice showed increased fat pad weights are; change was seen in inguinal (Ing), inter-scapular (In-sc), epididymal (Epi), and mesenteric (Mes). Retroperitoneal (Ret) and brown fat showed no change between *F13a1-/-* and *F13a1+/+* mice (n=10-16 mice/group). All error bars represent SEM; *p<0.05; **p<0.01; N.S-Not Significant.

Fig.2

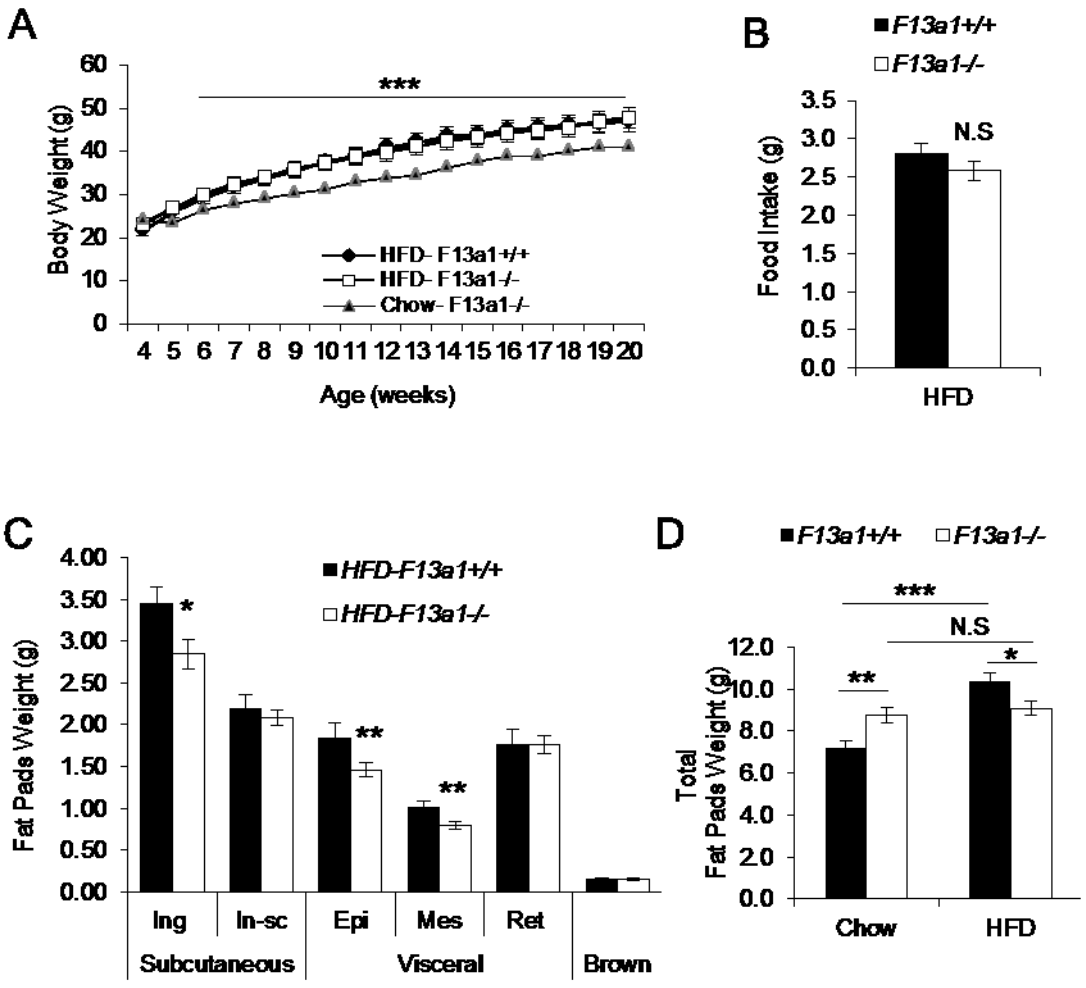

Figure 2. *F13a1-/-* mice on HFD show resistance to fat accumulation to adipose tissue. (A) Body weight was monitored weekly between 4 and 20 weeks. HFD was introduced from 4 weeks on (n=9-11 mice/group) and induced a significant weight gain in both *F13a1-/-* and *F13a1+/+* mice compared to chow. Weight gain in *F13a1-/-* mice were similar to *F13a1+/+* mice on HFD. **(B)** Food intake measured by metabolic cages over 4 days (n=4 mice/group) showed no changes between *F13a1-/-* and *F13a1+/+* mice. **(C)** Subcutaneous, visceral and brown fat depot weights were analyzed. *F13a1-/-* mice showed decreased fat pad weights compared to *F13a1+/+* on HFD; change was seen in inguinal (Ing), epididymal (Epi), and mesenteric (Mes) fat pads. Retroperitoneal

(Ret), inter-scapular (In-sc) and brown fat showed no change between *F13a1-/-* and *F13a1+/+* mice (n=10-16 mice/group). **(D)** Total fat pad weight from *F13a1-/-* and *F13a1+/+* mice on chow and HFD show that *F13a1-/-* mice do not increase fat mass on HDF (data is collected from Figures 1D and 2D). All error bars represent SEM; *p<0.05; **p<0.01; ***p<0.001; N.S-Not Significant.

Fig.3

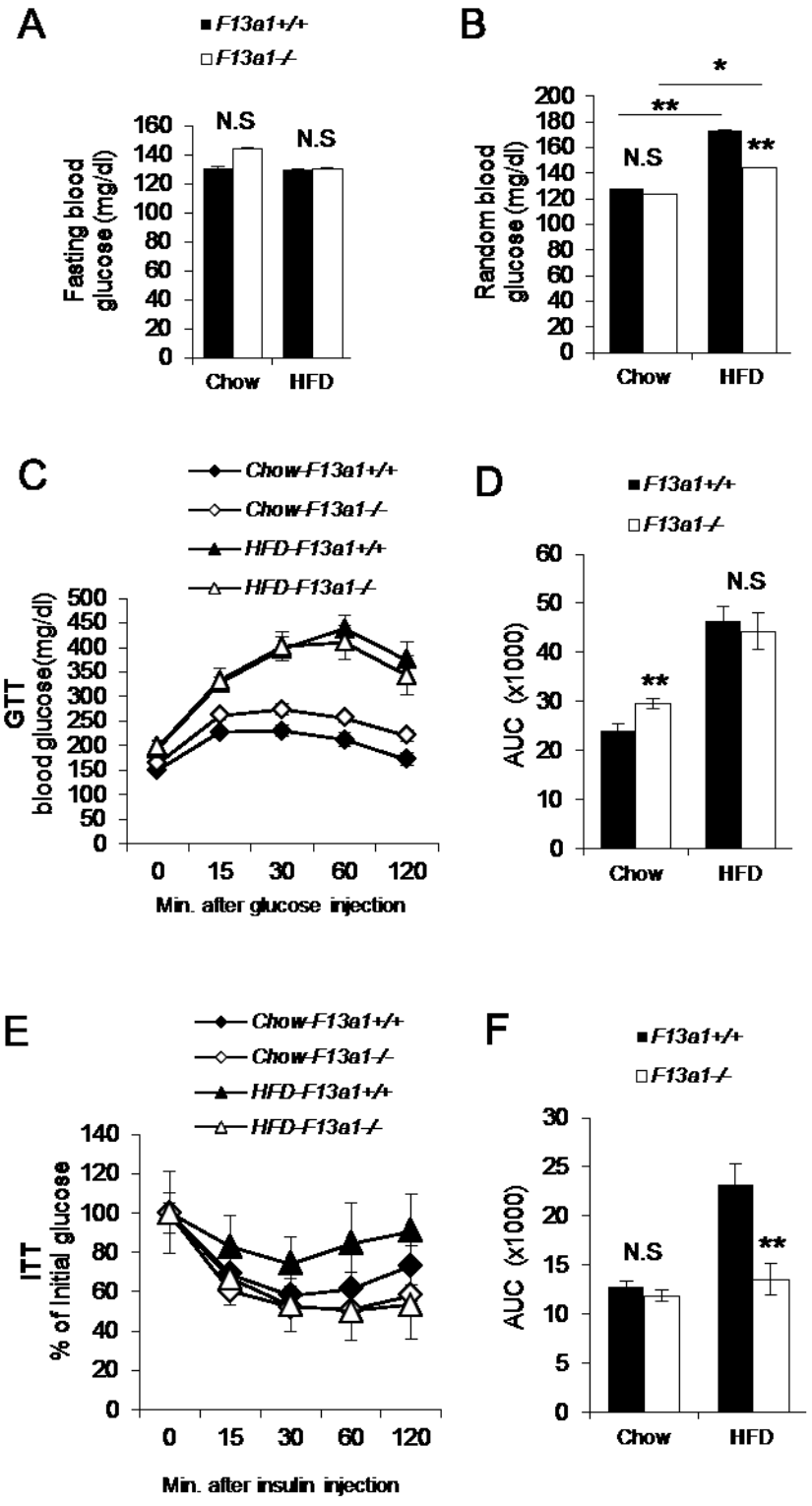
A
F13a1+/+
F13a1-/-
Fasting blood glucose (mg/dl)
N.S
N.S
Chow
HFD
B
Random blood glucose (mg/dl)
*
**
N.S
**
Chow
HFD
C
Chow-F13a1+/+
Chow-F13a1-/-
HFD-F13a1+/+
HFD-F13a1-/-
GTT
blood glucose(mg/dl)
Min. after glucose injection
D
F13a1+/+
F13a1-/-
AUC (x1000)
N.S
**
Chow
HFD
E
Chow-F13a1+/+
Chow-F13a1-/-
HFD-F13a1+/+
HFD-F13a1-/-
ITT
% of Initial glucose
Min. after insulin injection
F
F13a1+/+
F13a1-/-
AUC (x1000)
N.S
**
Chow
HFD

Figure 3. Enhanced insulin sensitivity in *F13a1-/-* mice on HFD. (A) Fasting blood glucose levels measured after 12 h of fasting (n=9-11 mice/group). No change was observed between *F13a1+/+* and *F13a1-/-* mice nor the different diets. **(B)** Measuring random blood glucose levels showed a significant increase in HFD in both mice, however, the blood glucose levels in *F13a1-/-* mice on HFD was significantly lower compared to *F13a1+/+* mice (n=9-11 mice/group). **(C)** Intraperitoneal Glucose Tolerance Test (GTT) after 6 h of fasting/ Glucose of 1 g/kg injection was used and blood glucose levels were monitored for 120 min (n=9-11 mice/group). **(D)** Area under the curve (AUC) from GTT analyses. *F13a1-/-* mice on chow displayed decreased tolerance to glucose challenge (higher AUC value) but on HFD no change was observed. **(E)** Intraperitoneal Insulin tolerance test (ITT) after 6 h of fasting. Glucose of 0.5 U/kg injection was used and blood glucose was monitored for 120 min (n=9-11 mice/group). **(F)** Area under the curve (AUC) for ITT. *F13a1-/-* mice show no difference in values on a chow diet, however, on HFD they show improved insulin sensitivity marked by significantly decreased AUC. All error bars represent SEM; *p<0.05; **p<0.01; ***p<0.001; N.S-Not Significant.

Fig.4

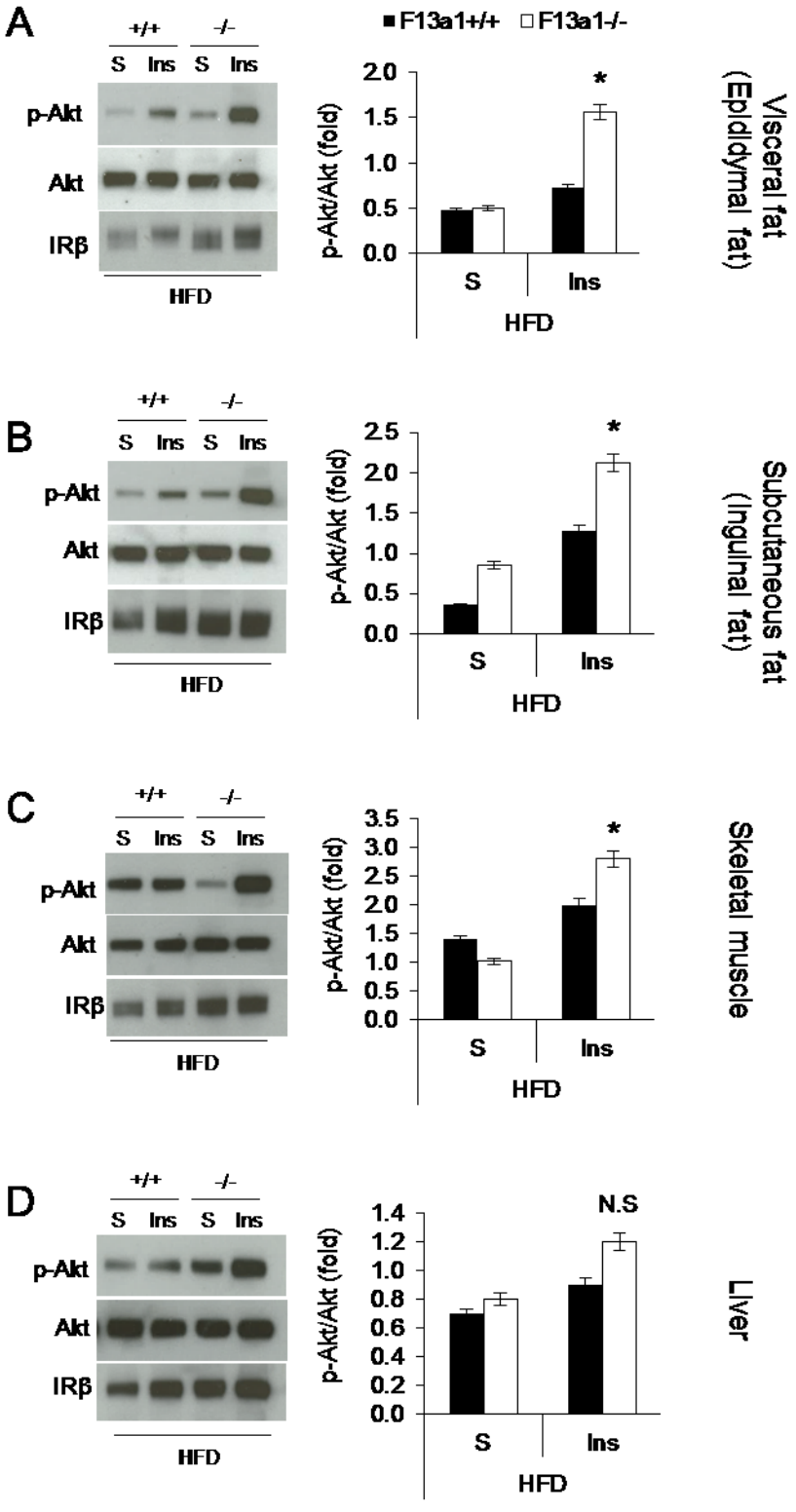
A
+/+
-/-
S Ins S Ins
p-Akt
Akt
IRβ
HFD
■F13a1+/+ □F13a1-/-
p-Akt/Akt (fold)
2.0
1.5
1.0
0.5
0.0
*
S
Ins
HFD
Visceral fat
(Epididymal fat)
B
+/+
-/-
S Ins S Ins
p-Akt
Akt
IRβ
HFD
p-Akt/Akt (fold)
2.5
2.0
1.5
1.0
0.5
0.0
*
S
Ins
HFD
Subcutaneous fat
(Inguinal fat)
C
+/+
-/-
S Ins S Ins
p-Akt
Akt
IRβ
HFD
p-Akt/Akt (fold)
3.5
3.0
2.5
2.0
1.5
1.0
0.5
0.0
*
S
Ins
HFD
Skeletal muscle
D
+/+
-/-
S Ins S Ins
p-Akt
Akt
IRβ
HFD
p-Akt/Akt (fold)
1.4
1.2
1.0
0.8
0.6
0.4
0.2
0.0
N.S
S
Ins
HFD
Liver

Figure 4. Insulin sensitivity and signalling in peripheral tissues *in vivo*. *F13a1-/-* and *F13a1+/+* mice were fasted for 6 h, and injected with saline (S) and insulin (Ins) (2.5 U/kg). Muscle, epididymal, inguinal and liver were dissected, extracted and insulin signalling activation was assessed by measuring p-Akt (S473) and Akt levels and levels of insulin receptor (IRβ) by Western blotting. **(A)** Epididymal fat pad and quantification of the blots showed increased p-Akt (S473) in *F13a1-/-* mice, demonstrating increased insulin sensitivity of the tissue. **(B)** Inguinal fat pad and **(C)** Gastronemius muscle showed a similar increase in p-Akt (S473) levels upon insulin injection in *F13a1-/-* mice. **(D)** Liver did not show activation of insulin signalling pathway. All error bars represent SEM; (n=3 mice/group); *p<0.05; N.S-Not Significant.

Fig.5

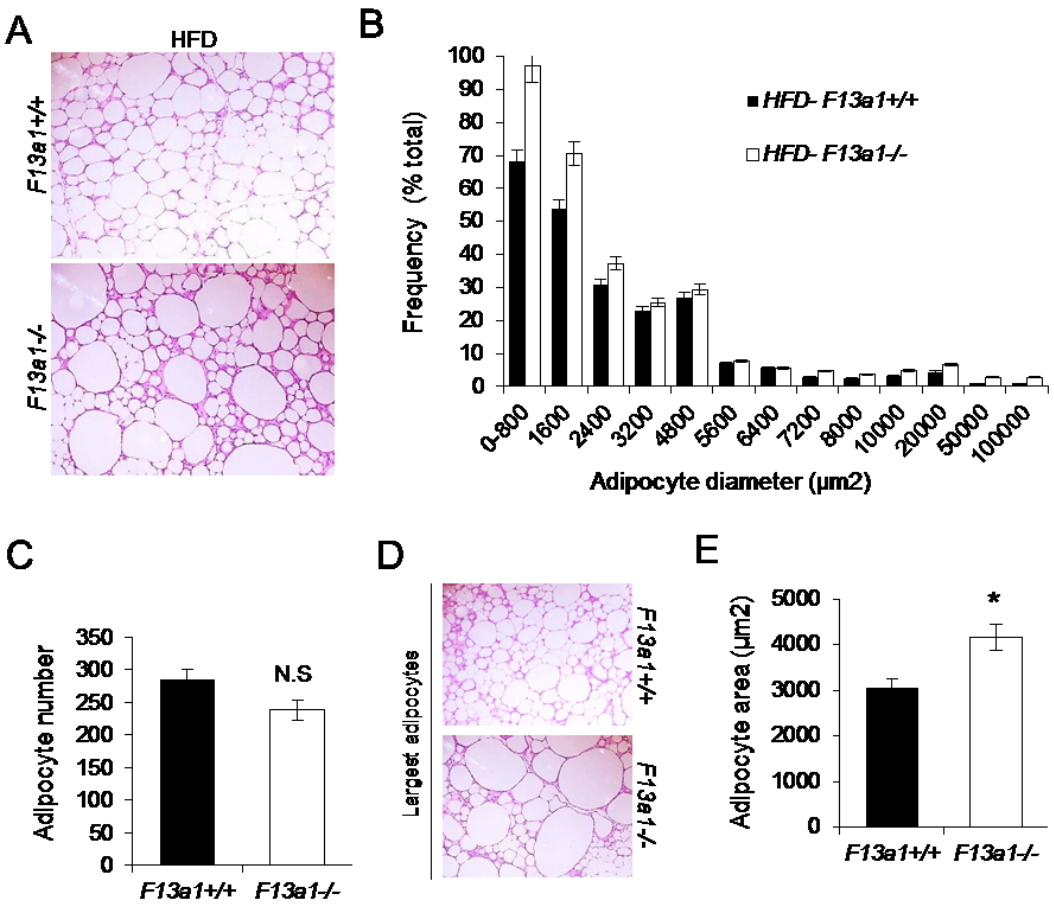

Figure 5. Increased size of adipocytes in *F13a1-/-* mice. (A) H&E stained sections of epididymal fat pads from *F13a1-/-* and *F13a1+/+* mice after 20 weeks of HFD. **(B)** Frequency distribution of adipocytes in mice on HFD diet; the frequency of larger adipocytes was increased in *F13a1-/-* mice. **(C)** Total adipocyte number; No significant difference is observed between *F13a1-/-* and *F13a1+/+* mice on HFD. **(D)** H&E stained sections of some of the largest adipocytes observed in both mice. The adipocytes in the range of 50,000-100,000 diameter are observed in *F13a1-/-* mice. **(E)** Average adipocyte area; A significant increase in the average adipocyte size/area is seen in *F13a1-/-* mice.

Fig.6

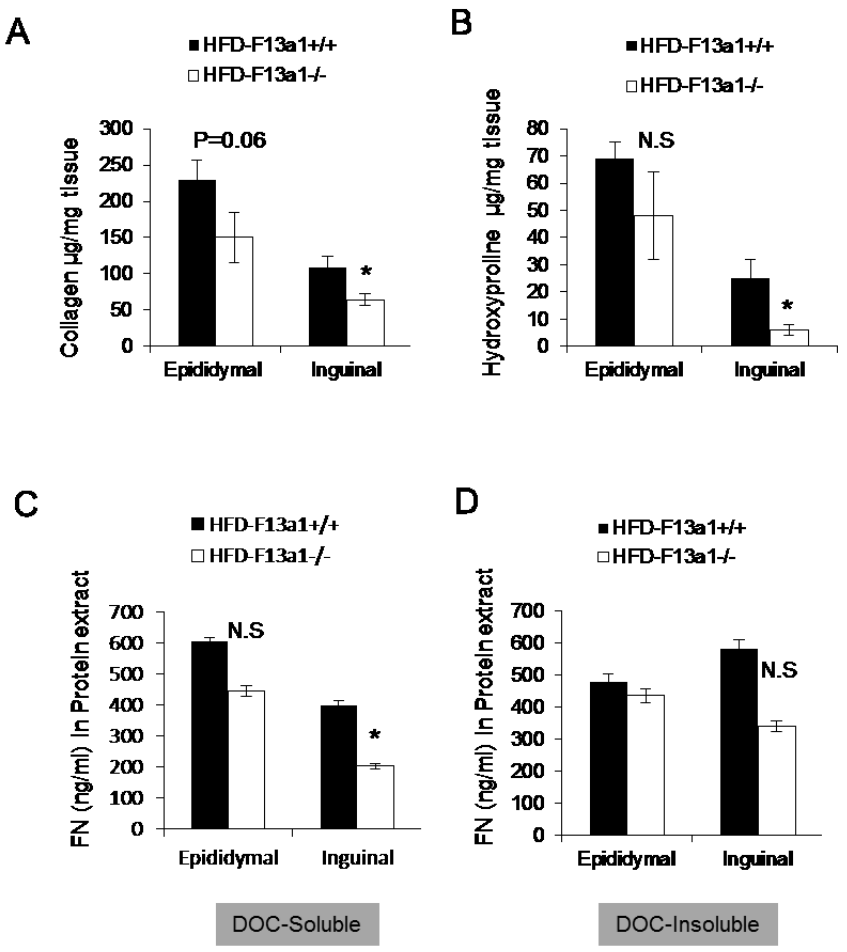

Figure 6. Reduced collagen and fibronectin levels in epididymal and inguinal fat pads in *F13a1-/-* mice on HFD. (A) Collagen levels analyzed by Sircol assay **(B)** Collagen levels analyzed by hydroxyproline content. Analyzed from total extracts of epididymal and inguinal fat pads show reduced collagen levels. Reduction was significant inguinal fat pad. **(C)** FN levels analyzed with ELISA assay in DOC-soluble fraction of epididymal and inguinal fat pads. Significant reduction of DOC-soluble fraction in the inguinal fat pad was observed in *F13a1-/-* mice. **(D)** FN levels analyzed with ELISA assay in DOC-insoluble fraction of epididymal and inguinal fat pads DOC-insoluble fraction. A reduction, however, not significant one in DOC-insoluble fraction was seen. All error bars represent SEM; (n=4 mice/group); *p<0.05; N.S-Not Significant.

Fig.7

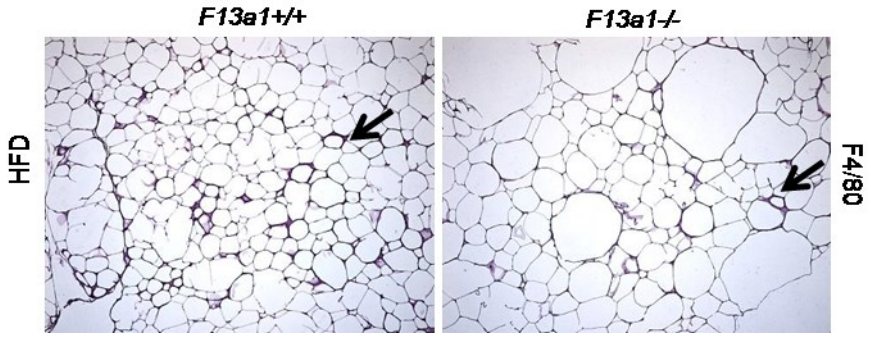

Figure 7. Decreased macrophage level in adipose tissue of *F13a1-/-* mice on HFD. Immunohistochemistry of epididymal fat pads from *F13a1-/-* and *F13a1+/+* mice on HFD at 20 wk of age was analyzed for macrophage levels. Staining with F4/80 antibody in *F13a1-/-* and *F13a1+/+* mice show reduced macrophage levels (brown color) in *F13a1-/-* mice. Arrows indicate crown like structure caused by macrophages.

Fig.8

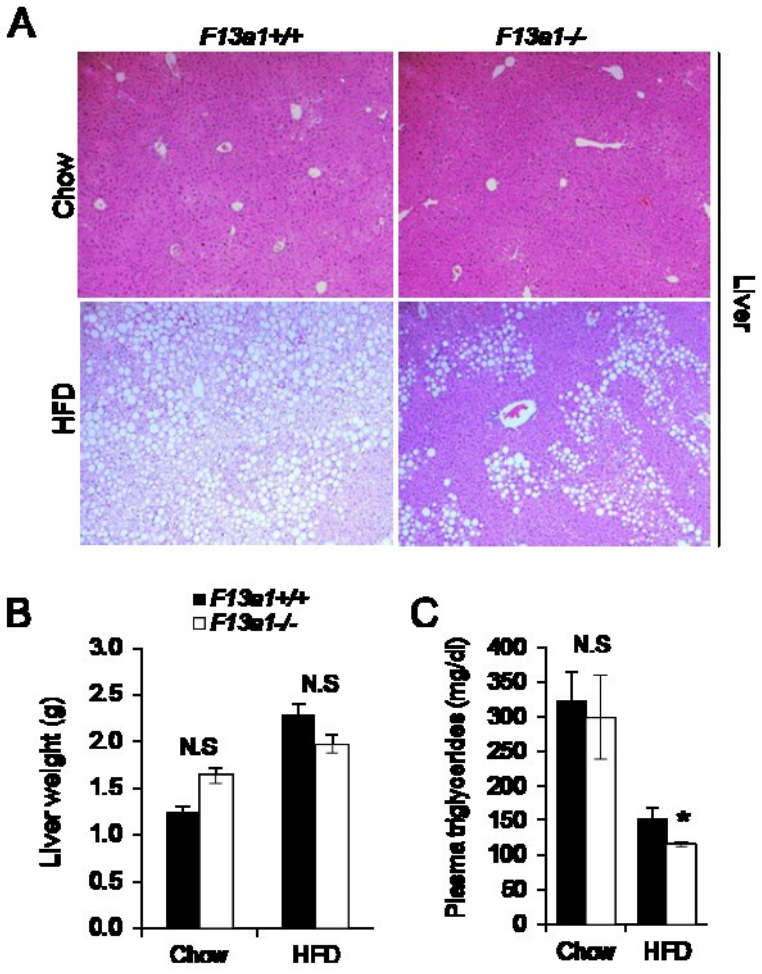

Figure 8. Circulating lipids and accumulation of fat in liver of *F13a1-/-* mice is decreased on HFD. (A) H&E stained sections of *F13a1-/-* and *F13a1+/+* mouse liver on chow and HFD. *F13a1-/-* mice liver showed reduced fat accumulation compared to *F13a1+/+* mice. **(B)** Weights of livers of *F13a1-/-* and *F13a1+/+* mice on chow and HFD. No significant difference in liver weight was observed (n=7-8 mice/group). **(C)** Reduced circulating triglycerides in *F13a1-/-* mice on HFD (n=4 mice/group). All error bars represent SEM. *p<0.05; N.S-Not Significant.

Fig.9

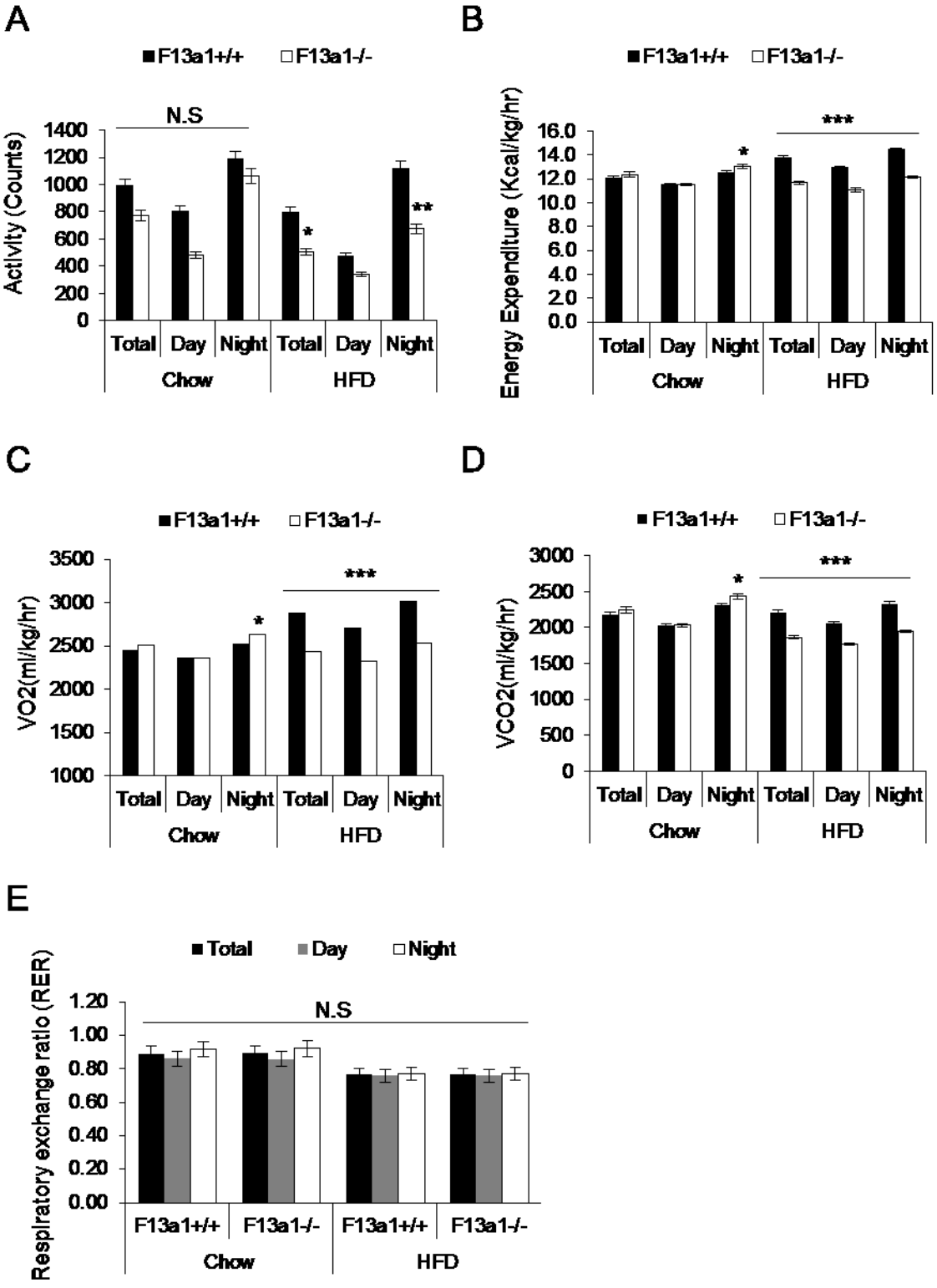
A
F13a1+/+
F13a1-/-
N.S
Activity (Counts)
1400
1200
1000
800
600
400
200
0
*
**
Total
Day
Night
Total
Day
Night
Chow
HFD
B
F13a1+/+
F13a1-/-
Energy Expenditure (Kcal/kg/hr)
16.0
14.0
12.0
10.0
8.0
6.0
4.0
2.0
0.0
*
***
Total
Day
Night
Total
Day
Night
Chow
HFD
C
F13a1+/+
F13a1-/-
VO2(ml/kg/hr)
3500
3000
2500
2000
1500
1000
*
***
Total
Day
Night
Total
Day
Night
Chow
HFD
D
F13a1+/+
F13a1-/-
VCO2(ml/kg/hr)
3000
2500
2000
1500
1000
500
0
*
***
Total
Day
Night
Total
Day
Night
Chow
HFD
E
Total
Day
Night
Respiratory exchange ratio (RER)
1.20
1.00
0.80
0.60
0.40
0.20
0.00
N.S
F13a1+/+
F13a1-/-
F13a1+/+
F13a1-/-
Chow
HFD

Figure 9. Reduced activity and energy expenditure of *F13a1*-/- mice on HFD. Metabolic cage measurements were taken during the day (light) and night (dark) cycles over the course of four days. **(A)** Total activity (ambulatory and rearing) was reduced in *F13a1-/-* mice on HFD. **(B)** Energy expenditure was reduced in *F13a1-/-* mice on HFD**. (C)** Oxygen consumption (VO2) was significantly lower in *F13a1-/-* mice on HFD. **(D)** Carbon dioxide production (VCO2) was significantly lower in *F13a1-/-* mice on HFD. **(E)** Gas exchange data used to calculate the respiratory exchange ratio (RER=VO2/VCO2). No significant change was observed. All error bars represent SEM. (n=4 mice/group) *p<0.05; **p<0.01; ***p<0.001, N.S-Not Significant.

4.10 Ongoing work

- Analysis of *F13a1* expression in epididymal and inguinal fat pads of one and five months on chow diet and HFD in *F13a1+/+* mice to identify if *F13a1* gene and FXIII-A protein expression increases with age or diet, and between fat pads.
- Analysis of *Tgm2* expression in *F13a1-/-* mice to identify for *Tgm2* compensation.
- Analysis of *Mcp-1 and collagen gene* expression in *F13a1+/+* and *F13a1-/-* mice, to confirm the finding of reduced macrophage and collagen levels.
- Immunohistochemistry staining for Mac 2 macrophages.
- Analysis of autophosphorylation site of IRβ in adipose tissue by Western blotting.
- SircoI and Hydroxyproline assay of skeletal muscle extracts to support for the insulin sensitivity.
- Analysis of Ki67 for proliferation and TUNEL assay for apoptosis in epididymal fat pads.

CHAPTER 5 - Summary and Conclusions

Obesity is a growing health problem worldwide, and is associated with the development of insulin resistance, type 2 diabetes, coronary heart disease, hypertension and stroke. FXIII-A transglutaminase was recently identified in genome-wide association studies as a potential causative obesity gene in white adipose tissue of monozygotic twin pairs discordant for BMI. The exact function of FXIII-A or the TG family members in obesity or adipocyte differentiation is not known. The *overall objective* of this PhD thesis was to determine the role of FXIII-A and the other TG enzymes in adipogenesis and whole body energy metabolism. Understanding the importance of FXIII-A and other TG enzymes in adipose tissue biology and whole body energy homeostasis is important for the development of better pharmacological intervention for the treatment of obesity and its co-morbidities.

In Chapter 2, we examined the role of transglutaminase activity in adipogenesis. Mouse WAT and 3T3-L1 preadipocytes showed abundant transglutaminase activity that arose from FXIII-A. FXIII-A was localized to the preadipocyte cell surface and acted as a negative regulator of adipogenesis by promoting the assembly of FN from plasma into preadipocyte extracellular matrix. The assembled FN modulated cytoskeletal dynamics and maintained the preadipocyte state. FXIII-A-assembled plasma fibronectin matrix also promoted preadipocyte proliferation and potentiated the pro-proliferative effects of insulin while suppressing the pro-differentiating, PI3K - Akt insulin signalling. Thus, FXIII-A serves as a preadipocyte-bound proliferation/differentiation switch that mediates the effects of hepatocyte-produced circulating plasma fibronectin.

In Chapter 3, we investigated the function of TG2 during adipocyte differentiation. TG2 deficient MEFs displayed increased and accelerated lipid accumulation, which was associated with increased expression of major adipogenic transcription factors, *PPARγ* and *C/EBPα*. Protein levels of Pref-1/Dlk1, an early negative regulator of adipogenesis, were down regulated in the absence of TG2 during early differentiation. Similarly, TG2 null cells displayed defective canonical Wnt/β-catenin signalling with reduced β-catenin nuclear translocation, reduced ROCK kinase activity and actin stress fiber formation and increased Akt phosphorylation. Addition of exogenous TG2 enzyme to TG2 null and

control cells significantly inhibited lipid accumulation, reduced expression of *PPARγ* and *C/EBPα* and promoted the nuclear accumulation of β-catenin, and recvered Pref-1/Dlk1 protein levels. We concluded that extracellular TG2 is a negative regulator of adipogenesis.

In Chapter 4, we characterized the metabolic phenotype of FXIII-A deficient mice on HFD to understand the direct effect of FXIII-A in the development of obesity and insulin resistance *in vivo*. The absence of FXIII-A decreased fat accumulation to fat tissue on HFD, however, it didn't affect body weight and food intake. FXIII-A deficient mice showed characteristics of 'metabolically healthy obesity'. Primarily, mice were protected from diet induced insulin resistance. An increase in insulin sensitivity is seen in epididymal, inguinal adipose tissue, and muscle. The increase in insulin sensitivity in fat tissue was associated with reduced macrophage infiltration, increased adipocyte size and reduced total collagen and fibronectin levels in fat tissue. The mice also displayed, decreased liver fat accumulation and lower circulating triglycerides on HFD. The data presented in this chapter revealed a novel role for FXIII-A in preventing insulin resistance in diet induced obesity.

In summary, FXIII-A and TG2 present in adipose tissue are inhibitors of adipocyte differentiation, and FXIII-A regulates insulin sensitivity and whole body energy metabolism. The work presented in this thesis represents a significant contribution to knowledge within the field of transglutaminases. Specifically, this work presents the following novel and original contributions.

5.1 Original Contributions

- Identified FXIII-A and TG2 are the only TG family members present in murine AT.
- Demonstrated transglutaminase activity in AT and during adipogenesis.
- Identified Factor XIII-A as the main crosslinking enzyme during adipcyte differentiation.
- FXIII-A is an inhibitor of adipocyte differentiation.

- FXIII-A crosslinks only pFN, but not EDA-FN.
- FXIII-A regulates insulin sensitivity during adipocyte differentiation.
- FXIII-A crossliked PFN promotes insulin, pro-proliferative effect over pro-differentiation.
- Extracellular TG2 is an inhibitor of adipocyte differentiation.
- Extracellular TG2 regulates Pref-1 protein levels, a major inhibitor of adipocyte differentiation.
- FXIII-A null mice are insulin sensitive and show signs of 'metabolically healthy obesity' on obesogenic diet.

5.2 Future Work

- Analyzing *F13a1* gene expression in WAT of metabolically healthy and metabolically sick obese individuals and/or monozygotic twins, as described in studies of Pietilainen group.
- Investigating FXIII-A production in ob/ob mice and how it relates to the development of metabolic disturbances.
- Generation of F131-/-;ob/ob mice to understand if the absence of F13a1 protects from development of metabolic disturbances.
- Generation of adipose tissue specific FXIII-A conditional knockout mice and analyzing the metabolic phenotype on a HFD.
- Generation of macrophage specific FXIII-A conditional knockout mice and analyzing the metabolic phenotype on a HFD.
- Assessing if overexpression of FXIII-A in adipose tissue would promote metabolic problems in obesogenic diet.
- Assessing if circulating FXIII-A contributes to the metabolic disturbances via injecting mice on HFD with recombinant FXIII-A.
- Assessing if insulin regulates *F13a1* gene in cell lines, MEFs and adipose tissue explant culture to give more insight to target FXIII-A in insulin resistance.
- Characterizing TG family members in skeletal muscle, and understating the role of FXIII-A in insulin sensitivity of skeletal muscle.

- Characterizing metabolic phenotype of TG2 knockout mice on a HFD, and investigating FXIII-A production in TG2 knockout mice.
- To asses TG activity in general in FXIII-A knockout mice,TG2 knockout mice and FXIII-A and TG2 double knockout mice to see for compensation from other TG enzymes occurs.
- To identify TG family members and TG activity in BAT, and in BAT differentiation and function.